OPTICAL AND ELECTRICAL PROPERTIES OF CONDUCTING POLYMER FILMS

Thesis
Submitted in partial fulfilment
of the requirements for the degree of
DOCTOR OF PHILOSOPHY

By

MANOJ KUMAR RAM

Under the Supervision of
DR. B.D. MALHOTRA

**BIRLA INSTITUTE OF TECHNOLOGY AND SCIENCE
PILANI (RAJASTHAN) INDIA
1994**

BIRLA INSTITUTE OF TECHNOLOGY AND SCIENCE, PILANI(RAJ.)

RESEARCH & CONSULTANCY DIVISION.

CERTIFICATE

This is to certify that the thesis entitled **"Optical and Electrical properties of Conducting Polymer Films"** submitted by **MANOJ KUMAR RAM**, ID.No. 90PZYF013 for award of Ph.D Degree of the Institute, embodies original work done by him under my supervision.

Dr. B.D. MALHOTRA
Scientist.
BECPRL, National
Physical Laboratory,
New Delhi-110 012,
India.

Date: December 14, 1994.

Dedicated to

sweet   memories   of   my M*other*

ABSTRACT

ABSTRACT

Conducting polymers such as polypyrrole and polyaniline have recently attracted much attention. These interesting molecular electronics materials have been considered to have potential application in electro-optical devices, batteries and molecular electronics etc. It has been thought that the detailed information with regards to the optical and electrical properties holds the key towards the commercialization of those important organic conducting polymers.

Conducting polymer films of polypyrrole films have been prepared by electrochemical techniques. Such polypyrrole films have been characterized using UV-Visible, FTIR, Dielectric relaxation and Cyclic voltammetric technique, respectively. Application of conducting polypyrrole films such as Schottky devices and electrochromic displays have also been demonstrated.

Polyaniline films have also been synthesized using solution casting, vacuum deposition and electrochemical technique respectively. Optical and electrical properties of various polyaniline films have been experimentally investigated. Various junction parameters such as ideality factor, barrier height, carrier concentration etc., of some of the Schottky devices based on semiconducting polypyrrole films have also been determined.

Attempts have also been made to inprove upon the mechanical properties of polypyrrole by copolymerizing it with Napthol and N-phenyl pyrrole respectively. Measurements of electrical conductivity carried out on poly α-Naphthalene oxide pyrrole as a function of temperature bring out the operation of Mott's variable range hopping mechanism in this conducting copolymers.

The Langmuir-Blodgett (LB) filmdeposition technique has been known to be an excellent method for the deposition of ultrathin uniform insulating layers comprising of fatty acids and their salts. This technique has been successfully used to obtain multilayers of polyemeraldine base. Besides this, metal-insulator-semiconductor (MIS) devices have been fabricated by passivation of electrochemically deposited polypyrrole films by Langmuir-Blodgett films of cadmium stearate (CdSt$_2$).

ACKNOWLEDGEMENTS

CONTENTS

CHAPTER V   STUDIES ON CONDUCTING COPOLYMER FILMS

CHAPTER VI STUDIES ON LANGMUIR-BLODGETT FILMS

APPENDIX

Summary
List of publications

CHAPTER I

INTRODUCTION

Rapid progress in the field of conducting polymers in the past about ten years has led to the discovery of new electronic materials, new concepts and development of new technologies [1-3]. A large number of new conducting polymers (also referred to as synthetic metals) such as polyacetylene, polypyrrole, polythiophene, polycarbazole, polyaniline and polyaniline-co-orthoanisidine etc. have been synthesized using chemical and electrochemical techniques [4-6].

Electrical conduction in trans-polyacetylene, whose ground states are energetically degenerate has been understood to originate from the solitonic excitations that arise as a result of disruption in bond conjugation in this interesting conducting polymer. In various other conducting polymers like cis - polyacetylene, poly-p-phenylene and polyisothianaphthene etc., the transport of electrical charge occurs via polarons that have been considered to result from the ground states of neutral and charged solitons [7-8].

With increased concentration of polarons due to doping, formation of bipolarons may occur. Compared to polarons that are both singly charged and carry spins, bipolarons are doubly charged and are spinless [9]. Moreover, the two positive charges of bipolaronic species that also have structural deformations associated with it are similar to Bardeen-Cooper-Schrieffer theory of superconductivity, and hence move as a pair [10].

Non-linear excitations (solitons, polarons and bipolarons) have been found to play important role towards the technical development of non-linear optical devices [11]. The excellent environmental stability of both polypyrroles and polyanilines have led to their potential uses in a number of applications in Schottky devices, electrochromic displays

and light weight batteries etc. [12,13].

There is an increased interest of researchers presently working in diverse disciplines such as physics, chemistry, electronics and biology etc to tailor conducting polymer films having desired electrical and mechanical properties. This has, however, not yet been possible because majority of conducting polymers are not soluble in any of the known organic solvents. Besides this, most of these conducting organic materials degrade when heated beyond 200°C. Processibility is thus a major problem heralding commercialization of conducting polymers [14].

A number of methods such as solution casting, electrochemical, vacuum evaporation and plasma polymerization etc. have been suggested for the preparation of conducting polymer films [15-16]. The solution cast films of poly-p-phenylene sulfide have been prepared. The electrical conductivity of such conducting polymer films measured using four-points-probe technique has been determined as 10^{-4} S/cm [17]. Such a value of electrical conductivity obtained for poly-p-phenylene sulfide is too low for it to be used for any technological application [18]. Semiconductive, conducting and insulating polymer films have been prepared by electrochemical technique [19].

The ease of control of thickness of conducting polymer films ranging from 1 μm to several microns coupled with their electrical and optical properties has resulted in this method being used for several applications such as in surface protection, microelectronics, electrocatalysis and energy storage etc [20]. Numerous investigations conducted on electrochemically polymerized films have indicated the amorphous nature of these films arising due to the presence of cross-links. It may, however, be emphasized that actual structures of such conducting polymer films, both in their doped and undoped states have not yet been determined [21]. Besides this, the degree of polymerization including

2

distribution of dopants in the majority of conducting polymer films have not yet become available [22].

It is often difficult to keep a precise control over the various parameters using both solution casting and electrochemical techniques [23]. Conducting polymer films have recently been obtained using a vacuum deposition process. The vacuum deposited films of conducting polymers (e.g. polyaniline) have been shown to be thermally stable [24]. Such films have been found to contain a number of defects and dangling bonds that make these unsuitable for the fabrication of any solid state electronic devices.

With a view to obtain defect free conducting polymer films, Langmuir - Blodgett film deposition method has recently been employed. Using such a sophisticated technique, metal-insulator-semiconductor devices based on electro-polymerized conducting polypyrrole films and cadmium stearate Langmuir - Blodgett layers have recently been fabricated [25]. Such devices have shown excellent electrical characteristics. However, the major problem that is confronting the active researchers engaged in this highly potential field relates to their poor thermal stability including inferior mechanical properties of conducting polymers [26].

Recent studies have indicated that plasma polymerization of a monomer (e.g. thiophene) can be used to obtain films having thicknesses ranging from 50-100 Å. Compared to Langmuir - Blodgett films, plasma polymerized films have been found to show improved thermal stability [27]. However, careful control of various processing parameters is extremely important to extend the scope of plasma polymerized conducting films to various optical and electrical applications.

Optical properties of conducting polymers have recently attracted much interest. For instance, one of the most important results relates to the optical spectrum obtained

3

in transmission and reflection mode obtained in case of trans and cis-polyacetylene. The observed spectrum for trans-polyacetylene shows a spectrum at 1.8 eV whereas the spectrum for cis - polyacetylene exhibits a peak at 2.1 eV corresponding to the π-π^* transition [28-29]. Similar results have been obtained in case of other conducting polymers. Optical spectroscopy is a very powerful tool for the characterization of electronic processes that occur in conducting polymers in their doped and undoped states, respectively. The changes in the optical absorption spectra bring out important information with regards to both the transport of charge and the phenomenon of doping [30]. The optical studies of conducting polymers are extremely important for understanding the electronic properties of conducting polymers.

Electrical properties of conducting polymers can be considered as a response when an electrical field is applied across it. Compared to metal, these interesting electronic materials exhibit a variety of phenomena such as electrical conduction, polarization [31]. Systematic investigations of electrical characteristics of desired conducting polymers are likely to be very helpful towards a better understanding of these materials at a molecular level. Moreover, such studies will prove valuable for a better understanding of the optical and thermal properties of conducting polymers [32].

1.1 CONDUCTING POLYMERS

Development of the field of conducting polymers can be divided into three categories such as polymers filled with conductive materials such as carbon or graphite, the charge transfer complexes and the polymer with conjugated backbones.

4

1.1.1 POLYMERS WITH CONDUCTIVE FILLERS

The attempts have earlier been made to generate conducting polymers by blending rubber like polyethylene, poly (vinylchloride) (PVC), poly(methylmethacrylate) (PMMA) or styrene acrylonitrile copolymer and butadiene nitrile filled with conductive filler flakes or the powder of metal flakes like nickel, copper, aluminium, iron or graphite powder [33]. The major practical function of the polymer matrix is to hold the conductive elements together dispersed in a solid phase. The interest in such materials derives from low cost, light weight, mechanical durability, and ease of processibility of the polymer component in concert with reasonably good conductivity. But these composites cannot be regarded as conducting polymers because of the insulating nature of matrix polymer, which generates much heat during the passage of electricity [34]. Their conductivities are not very high and applications are restricted to electronic devices against electromagnetic interference. Though the conductive filler polymers have flexibility, mechanical integrity and processibility but have less conductivity (0.1 S/cm) and hence cannot be termed as electronic materials [35]. The other disadvantage of the conductive filler matrix is that its electrical characteristics and optical properties generally depend upon both the shape of the filler and its wettability of the filler by the polymer matrix.

1.1.2 ORGANIC CHARGE TRANSFER COMPLEXES

The past two decades have witnessed unabated interest in the characterization of organic charge - transfer (CT) salts that display unusual solid state properties [36]. Several attempts have been made for the synthesis of charge transfer complexes, whose short intra-stack distance in such complexes permits overlap of π-molecular orbitals on adjustment sites which results in the delocalization of unpaired electrons and in a very

narrow metallic energy band. It has been reported that an unstable perylene -bromide salt is conducting and subsequently many salts of TCNQ have been found to be semiconducting in nature. For example, tetrathiafulvalene (TTF) and tetra-methyl-tetraselenium (TMTSF) form 1:1 donor acceptor molecular complexes with tetracyanoquinodimethane (TCNQ) having conductivity of 500 S/cm or higher at room temperature [37]. The charge transfer complexes between TCNQ and poly (2- vinyl pyridine) and poly[styrene - co - (2-vinyl pyridine)] etc have resulted in moderate to poorly conducting complexes. The electrical conductivity of such a system depends on the ratio [TCNQ]/ [TCNQ$^+$]. Thus, in the absence of neutral TCNQ, electrical conductivity has been found to be less than 10^{-9} S/cm which rises to 10^{-6} and 10^{-2} S/cm at ratios 10:1 and 1.1:1, respectively irrespective of the polymer system (which merely act as supporting / binding agent both for TCNQ molecule and TCNQ $^.$ ion in a regular fashion).

Conducting charge transfer complex salts are composed of highly ordered arrays of donor and acceptor species, one or both of which can be radical ions and are thermodynamically stable. It is necessary for a charge transfer complex to be associated with a proper ratio (acceptor to donor), otherwise it will exhibit poor electrical conductivity and poor surface morphology. Besides this, these materials have higher extinction coefficient, lower refractive index and higher band gap (>4.1 eV) [38]. The structures of some of the charge compounds have been given in fig.1:
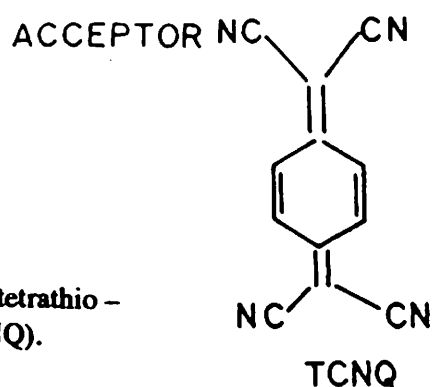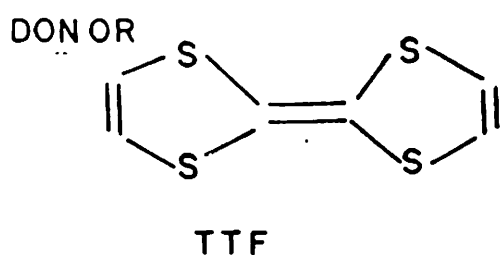
Fig. 1 Structures of some charge transfer Complexes, tetrathio - fulvalene (TTF) and tetracyanoquinodimethane (TCNQ).

1.1.3 POLYMERS WITH CONJUGATED BACKBONES

Electrical conduction in conducting polymers can be understood in terms of delocalization of π - electrons principally along the polymer chains. These are electronically one dimensional [39]. The novel feature of conducting polymer can be defined as the backbones (or pendant group), which are responsible for the generation and propagation of charge carriers and electron delocalization is mainly responsible for very interesting phenomena such as phase transition, charge density waves, metal-to-insulator transition and non-harmonic excitations (solitons,polarons and bipolarons) exhibited by a conducting polymer [40].

The outermost (valence) electrons of a carbon atom occupy two 2s and 2p atomic orbitals. The trigonal sp^2 and linear sp^1 hybrids leave one and two p electrons out of the bond forming hybrid orbitals. The structures of unsaturated carbon compounds can in principle give rise to extended electronic states formed by the overlap of p-electrons. The extended π-electron systems could thus provide a basis for the metallic behaviour in polymer. The fact that conjugated polymers are semiconductors arises from the fact that linear (quasi-one dimensional) chains are unstable against a deformation of carbon skeleton which leads to the localization of π-electrons. This effect is termed as Peierls transition or the bond alternation (fig.2) [41].
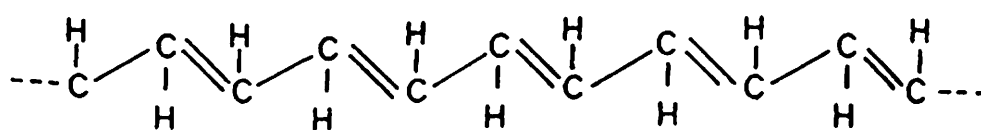
Fig.2 Bond alternation in trans-polyacetylene.

There is tremendous excitement in the possibility of achieving materials which have important electronic and optical properties like semiconductors and metals and also have attractive mechanical properties and processing advantages over the conductive

7

fillers and charge transfer complexes. A new class of electronic materials has recently been proposed with the preparation of polyacetylene [(CH)$_x$] using Ziegler-Natta catalyst by Natta et al [42]. The insoluble powder of (CH)$_x$, synthesized by this method is found to be insoluble in any organic solvent with a conductivity of 10^{-5} S/cm. Later, it has been proposed that the properly substituted polyacetylene molecule cannot only be conducting but also superconducting at room temperature.

Though much theoretical predictions about the nature of (CH)$_x$ have been fore-cast but the real thrust of conducting polymers has begun with the successful synthesis of cis and trans forms of polyacetylene. In the preceding years Shirakawa et al [43] have succeeded in preparing free standing films of (CH)$_x$ by passing pure acelytene gas over Ziegler-Natta catalyst at temperature (195 K). The conductivity of copper coloured cis-PA and silver coloured trans-PA films have been respectively measured as 1.7×10^{-9} and 4.4×10^{-5} S/cm [43]. As soon as these conducting films are exposed to chlorine or bromine gas, there is a tremendous increase in electrical conductivity by 10-12 orders of magnitude. AsF$_5^-$ doped polyacetylene has an electrical conductivity of 10^5 S/cm and activation energy of 0.5 eV [44]. It has been seen that cis-isomer of PA is a stable form at low temperatures whereas trans - isomer is stable at elevated temperatures. The electrical conductivity of polyacetylene is hardly stable in atmosphere and its conductivity decreases drastically when it is exposed to air and this process can be observed following the changes in optical, Raman and ESR spectra, respectively [45]. Numerous theoretical models have been proposed in literature for investigating the mechanism of charge transport in polyacetylene. Efforts to improve upon the stability of the metallic PA in air have not yielded satisfactory results [45].

Poly(p-phenylene) (PPP) and poly (p- phenylene sulphide)(PPS) have been

synthesized by Friedal Craft and coupling reactions, respectively [46]. The chain length of PPP is only 15-20 phenyl units and increases slightly on doping with AsF_5 having conductivity 500 S/cm and band gap of 3.5 eV, but the transport of the charge carriers via short chain is restricted. PPS is thermally processable but its electrical conductivity when exposed to AsF_5 vapours gets lowered. Doping of these conducting polymers (PPP and PPS) results in anisotropic conductivity and consequently anisotropic optical properties [47].

Real thrust in the field of conducting polymers has originated with the synthesis of polyindole, polyfuran, polypyrrole (PPY), polythiophene (PT) etc. which in general have five membered ring structure with one hetroatom X (X = N, O, and S etc.). PPY (of different origin) has been known from for a the long time. The first electrochemical synthesis of a PPY film by Diaz et al [19] has revealed that the possibility of a highly conducting and stable synthetic metal is not too remote. The electrical conductivity of BF_4^- doped PPY film has been measured to be of the order of 100 S/cm with a band gap of 3.2 ev and activation energy of 0.04 eV. Polypyrrole in the doped state has absorption bands at 0.7, 1.4 and 2.1 eV, attributed to the presence of polarons. Polypyrrole consists of very small crystalites and is 95% amorphous [48]. Though, polypyrrole has been used for the fabrication of electronic devices such as Schottky diodes, metal -insulator - semiconductor (MIS) devices, it is not as yet a proccesable polymer. Moreover, it has not been possible to produce conducting PPY with electron -donating species to obtain n-type organic semiconductor.

Polyaromatic compounds such as polyaniline and its derivatives such as poly (1-methoxy aniline), poly(N-acetyl aniline), poly(m - methyl aniline) and poly (N-phenyl aniline) etc. have received a new dimension due to their processibility and
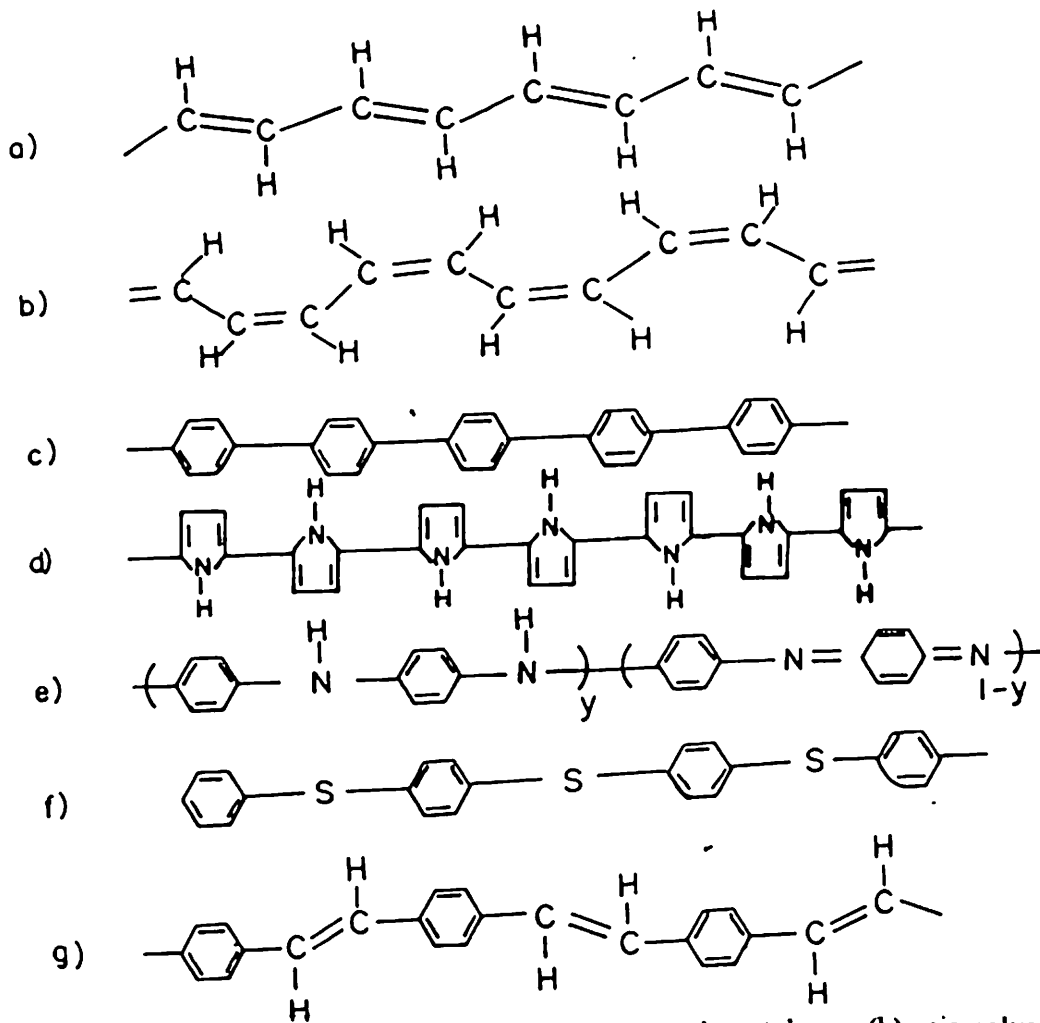
Fig.3 Structures of some conducting polymers: (a) trans-polyacetylene, (b) cis-polyacetylene, (c) poly(para-phenylene), (d) polypyrrole, (e) polyaniline, (f) poly(phenylene sulphide), (g) poly (phenylene vinylene)

1.2 SOME MAJOR PROBLEMS IN CONDUCTING POLYMERS

1.2.1 MECHANISM OF ELECTRICALCONDUCTION

The most carefully prepared conjugated polymers are not perfect and contain a variety of defects known as conjugational defects. These occur due to the two-fold degeneracy. Trans- polyacetylene for example is a Peierls insulator that allows the possibility of non-linear excitations in the form of bond alternation domain walls, each with an associated electronic state at the centre of the gap. Soliton is a topological kink in the electron-lattice system, a domain wall is connected with two phases with opposite bond alternations. Since there is a translational symmetry and the mass is small, the

11

soliton is mobile [56]. The charge of a non-bonding electron sitting on the conjugation

defect is compensated by the nucleonic charge of carbon atom. This type of defect is

neutral (neutral soliton). The competition of the elastic and condensation energies

spreads on the domain wall over a region of about 12-14a , a(Å) is the C-C distance

along the $(CH)_x$ chain. So single soliton defects can exist on imperfect chains. These

electronic states are a solution of the Schrondinger equation in the presence of the

structural domain wall and can therefore accommodate 0,1 or 2 electrons. The neutral

soliton has one electron in the midgap state. Positively and negatively charged solitons

have zero or two electrons respectively in the mid-gap state. The reversed spin-charge

relation exists for the solitons in trans-$(CH)_x$ as charge solitons are non-magnetic,

whereas a neutral soliton has spin 1/2. The charged solitons are formed by electron

transfer onto the polymer chain on doping with electrons or acceptor ions due to a

relation given by Takayama et al [41]. $E_s = \Delta (4/\pi)$ where E_s is the energy for creation

of soliton and Δ is the creation of an electron - hole pair.
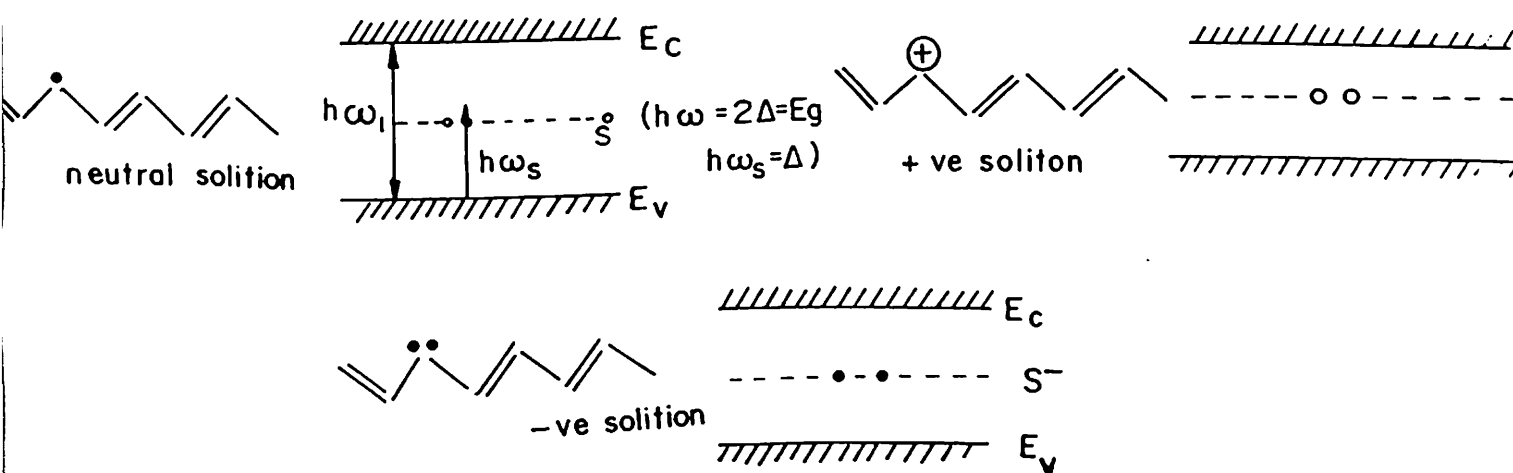
Fig.4 Schematics of solitons in trans -polyacetylene: (a) neutral soliton, (b) negatively charged solitons, (c) positively charged solitons, where E_c, E_v, E_g and hw are the conduction band, valence band, band gap and photon energy, respectively.

Polaron/bipolaron is the simple defect type that occurs in cis-PA, PPY, PT and

PANI etc. These arise due to the reduction in dimerization parameter over a limited

region of chain [12-3]. The ground state is not degenerate. However, the energy difference

per bond $\Delta E/l$ might be expected to be small i.e greater than zero (in cis-$(CH)_x$) but

less than trans-$(CH)_x$. So obvious lack of degeneracy cannot support stable soliton

excitations. Because creating a soliton pair separated by a distance d would use an

energy of about $d(\Delta E/l)$. This linear confinement energy leads to bipolarons as the

lowest energy charge transfer configuration in such a chain, which creates energy

somewhat greater than $(4/\pi)$. The spin charge relationship of such polarons is

traditional. Polaron is a charged electron site (radical cation), plus a lattice relaxation

around the charge [8]. Schematic of polarons and bipolarons formed in PPY are shown

in fig.5:
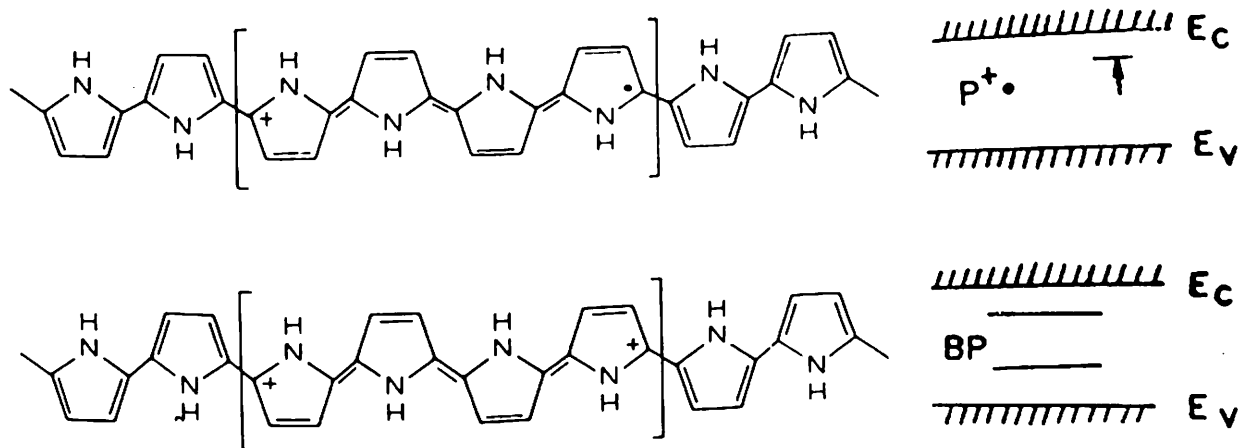
Fig.5 (a) Polarons and (b) bipolarons in conducting polypyrrole.
P^+, BP, charged polarons and bipolarons, E_c and E_v refer to conduction
band and valence bands, respectively.

13

TABLE 1 Some characteristics of solitons, polarons and bipolarons

DEFECT	NATURE	SPIN	CHARGE
Soliton	neutral	$\pm 1/2$	0
Soliton	charged	0	+e or -e
Polaron	charged	1/2	+e or -e
Bipolaron	charged	0	+2e or -2e

In addition to these defects, conducting polymers are likely to contain a variety of other defects such as cross - links, branch points and conformational defects. Such defects may arise due to chemical linking of monomer unit yielding an undesired linkage and breakage of chemical regularity. The cross-linking results in the rubbery nature of a conducting polymer. The defects such as solitons, polarons and bipolarons are the only means to attain the desired electrical conductivity in conducting polymers.

1.2.2 ENVIRONMENTAL STABILITY

Some of the problems that have heralded the applications of conjugated polymers relate to environmental stability and the loss of desirable mechanical properties on doping. It is very important for a conducting polymer film to be stable in doped and undoped states in normal atmospheric conditions. Conducting polyacetylene films have been found to be highly unstable in atmosphere. Moreover, conductivity of I_2 - doped polyacetylene has been reported to be decreased with time on its exposure to air [57-58]. The electrical conductivity of poly(phenylene sulphide) decreases on being treated with

14

moisture [59]. Both the atmospheric oxygen and moisture have been found to affect the electrical characteristics of polypyrrole films. Similarly, electrical conductivity of doped polyaniline increases when subjected to water vapours. It has been reported that redox potential and chemical reactivity of polymer chains are, however, two important parameters to be considered for understanding the stability of conducting polymers [60]. If the reduction potential of a polymer is greater than the reduction potential of oxygen (0.14), such a polymer is stable in air [61]. Thus, PPY oxidizes slowly in air. On the other hand poly(3-methyl thiophene) and polythiophene have their oxidation potential as 0.7 V which is larger than the oxidizing potential of moisture [62]. PPS undergoes reduction due to its oxidation potential (1.6 V) [63]. For instance, in polyacetylene, oxygen causes oxidation of the chain resulting in the shortening of the chain. This greatly influences the electrical and the optical properties of a conducting polymer by interrupting the extended delocalization.

1.2.3 THERMAL STABILITY OF CONDUCTING POLYMERS

The conductivity of polyacetylene decreases with time at room temperature as it reacts with oxygen. Its thermal degradation starts at 593 K [64]. Polyhetrocyclic compounds like polypyrrole, polythiophene and polycarbazole etc. are relatively thermally more stable [65]. Polypyrrole has been found to show particularly good stability and high conductivity over a period of few months in some cases. PPY films with tetra-fluroborate and perchlorate retain their properties over a prolonged time upto about 423 K whereas polythiophene shows similar characteristics upto 473K [66]. The effect of inorganic and organic dopants on electrical properties of PPY films as a function of temperature has also been systematically studied. An ageing effect on electrical and optical properties of

both polyaniline and its salt has been observed.

1.2.4 PROCESSABILITY OF CONDUCTING POLYMERS

Processibility is an important criterion for a desired conducting polymer for its commercial use. Moreover, it is always easy to characterize if conducting polymers can be shaped into desired forms. Conjugation in a polymer should not be disrupted on its being processed. Well-known conducting polymers such as PA, PPY, PPP etc. have been found to be insoluble and infusible. Therefore, the processibility of these conducting polymers is neither possible by solution technique or by the melt processing method. PPS films have been cast from AsF_3 solution and these then become conducting when doped with AsF_5 [67]. Polyaniline has recently been shown to be processable when cast from NMP / THF at high temperature. The Langmuir Blodgett films of PANI have also been prepared due to its solubility in NMP [68].

The copolymerization technique has been used in case of poly (3-methyl thiophene) and poly (methyl methacrylate) with a view to improve upon the processibility of these conducting polymers. Copolymer films cast from THF solution show decreased value of electrical conductivity (10^{-2} S/cm) on being exposed with I_2. The introduction of organic groups such as N-phenyl, N-methyl, octadecyl etc. in a monomer brings about flexibility and enhanced solubility of a polymer. Poly(o-methoxy aniline) films have however, been cast from NMP and THF solutions.

1.3 PREPARATION OF CONDUCTING POLYMER FILMS

Technological development of conducting polymer is possible only when thin to

thick films can be synthesized and characterized exhaustively. It is known that conducting polymer films have very large surface to volume ratio, which consequently influences the film properties over bulk materials. The principle techniques used to synthesize various conducting polymer films have been briefly described as under:

1.3.1 CHAIN POLYMERIZATION

It is an important method wherein all the atoms present in a monomer are incorporated into a desired polymer. A monomer required for the preparation of a polymer film generally depends upon the selection of one or more methods. For example, polyacetylene (PA) is polymerized using a Ziegler - Natta catalyst. Free standing cis - PA (98.1%, cis content) have been prepared by Shirakawa et al [43] by polymerization of pure, dry acetylene gas at 195 K using titanium -tetra buto-oxide triethyl aluminium catalyst system in toluene with Al: Ti in 4:1 ratio [69]. All trans-PA has been obtained by polymerizing polyacetylene at 423 K and using hexadecane as solvent. Polymerization at 291 K results in PA film having about 40.7% trans content. Polyacetylene has been synthesized using tetraethylammonium/ tetrabutoxy titanate Al Et_3/ Ti $(OBu)_4$ catalyst dissolved in silicone oil and treated at 393 K for two hours before use. Polyacetylene films thus obtained are homogeneous, oriented, regular, compact, crystalline and defect free. The films produced in this way range in the thickness from 10^{-5} to 0.05 cm depending upon the physical and chemical parameter of polymerization of acetylene. In this process, the choice of a catalyst and the concentration are often difficult for the fabrication of conducting polymer films. Polyphenyl-acetylene, poly(1-hexyne) and substituted polyacetylene are synthesized etc. by this method (fig.6).

17

$$CH \equiv CH \xrightarrow[\text{AlCl}_3]{\text{Ti(Bu)}_4} \quad -(CH = CH)_n$$
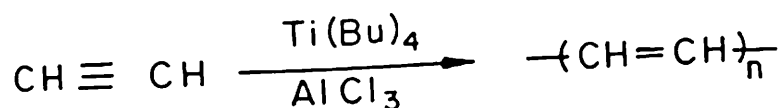
Fig.6 Preparation of a polyacetylene film by chain polymerization

1.3.2 TEMPLATE POLYMERIZATION

Highly oriented fibrillar films of conducting polymers are synthesized using this method where the pores of a porous membrane act as template for a nascent polymer [70]. Nanoscopic polyacetylene fibrils have been synthesized by polymerizing acetylene within the pore of a filtration membrane when pregnated with the solution of a catalyst. Template synthesized polyacetylene films have been found to be preferentially oriented parallel to the fibrillar axis and also possess higher electronic conductivity than polyactylene when synthesized in identical conditions. The derivative of polyactylenes have also been synthesized by this method.

1.3.3 POLYMER PRECURSOR ROUTE

This is an innovative and useful technique to overcome the problem of intractability in conducting polymers. Such a technique involves the synthesis of a highly soluble precursor polymer which is processed and purified in solution and is finally converted to the less tractable polymer film. Polyacetylene, poly(phenylene vinylene) (PPV), poly(arylene vinylene), dialkoxy substituted phenylenes etc. have been synthesized by this method. Poly(p-phenylene vinylene) (PPV) can be prepared in film form by

18

precursor polymer route [71-72].The precursor polymer obtained in aqueous solution forms a bis-sulphonium salt of p-xylene by base initiated polymerization reaction by elimination of halogen acid and dimethyl sulphide from p-xylene-α-dimethyl sulphonium halides [72].

$$X^{\ominus} \; R_2\overset{\oplus}{S} \; (CH)_2 \; -\!\!\langle\bigcirc\rangle\!\!- \; CH_2 \; S\overset{\oplus}{R_2} \; X^{\ominus}$$

$$\xrightarrow{OH^{\ominus}} \; \left[CH_2 \; -\!\!\langle\bigcirc\rangle\!\!- CH \right]\!+ R_2S + HX$$

$$\xrightarrow{\Delta} \; \left. -\!\!\!\left[\!\langle\bigcirc\rangle\!\!- CH = CH \right]\!\!\right.\!- \; + R_2S + HX$$

Fig.7 Preparation of poly(phenylene vinylene) film by precursor route technique; X = Cl⁻ or Br⁻ and R = CH₃ or C₂H₅.

1.3.4 SOLID-STATE POLYMERIZATION:

The conducting sulfur nitride $(SN)_x$ films have been obtained by passing S_4N_4 vapour at 353 K and a pressure of less than 1 μm over silver/wool catalyst. Then it is polymerized by thermal initiation in solid state at 253K. Poly(1-chloro 2-phenyl acetylene), distyryl pyrazine, polypyrrole, polydiacetylene etc. have been polymerized using UV or gamma irradiation to obtain a defect free polymeric film [73-74].

1.3.5 PLASMA POLYMERIZATION

It is a method to prepare ultrathin uniform polymer layers that strongly adhere to an appropriate substrate. Electric glow discharge is used to create low temperature or 'cold' plasma. Thin siloxane polymer film functionalized by sulphonate group, polypyrrole, polythiophene etc. are prepared by this technique [27]. Polymer films of 500-3000 Å can be obtained under the plasma current of 70 -95 $\mu A/$ cm² and a pressure of ≈ 0.2 torr in a dc discharge plasma. This method gives polythiophene films that have

been found to be photoconducting. The advantage of this method is that it eliminates various steps needed for conventional coating process. The film fabrication depends upon the nature of starting material, the reaction condition and the temperature of the substrate.

1.3.6 SOLUTION - CAST METHOD

It is an important method that can be used for fabrication of thin to thick film. This method generally depends upon the solublility of the conducting polymer. At first the polymer is synthesized by chemical synthesis technique and the polymer is made soluble in an organic solvent. The solution is heated under low pressure for the formation of a conducting polymer film. The films of polyaniline, derivatives of polyaniline like poly(o-methoxy aniline), copolymer of poly(aniline-anisidine) etc. can be fabricated by the above method. Poly(o-methoxy aniline) powder is dissolved in N-methyl pyrrolidinone (NMP) in appropriate proportions [75]. The solution is heated in a vacuum oven under a pressure of 10^{-2} torr and at a temperature of 170^0C. The free standing films can thus be formed. The uniformity of film strongly depends upon the low pressure and can be controlled by the evaporation of the organic solvent.

1.3.7 ELECTROCHEMICAL POLYMERIZATION

Electrochemical polymerization is regarded as a simple and novel technique for the preparation of a desired conducting polymer film. Galvanostatic, potentiodynamic or cyclic voltammetry techniques have been respectively used for this purpose. The films are prepared by stoichiometric polymerization of monomer in the presence of a desired electrolyte in a cell consisting of working, counter and reference electrodes, respectively.

20

rocyclic compounds such as polythiophene, polycarbazole, polyfuran, polypyrrole, olymer of pyrrole and polyaniline etc. are synthesized by this technique [76-77]. olythiophene containing BF_4^- ions are obtained by electrolysis of thiophene in aceto- rile containing lithium tetrafluroborate $(LiBF_4)$. Poly(thiethyl pyrrole) a copolymer hiophene and pyrrole have been synthesized using 2-2' thiethyl pyrrole.

In the electrochemical synthesis the electropolymerization is accompanied by iltaneous oxidation. The first step involves the oxidation of monomer to its radical ion. Since electron transfer reaction is faster than the bulk solution and the second ep involves the coupling of two radical cations to produce a dihydrodimer dication which leads to dimer after loss of two protons and rearomatization (fig.8) [78].
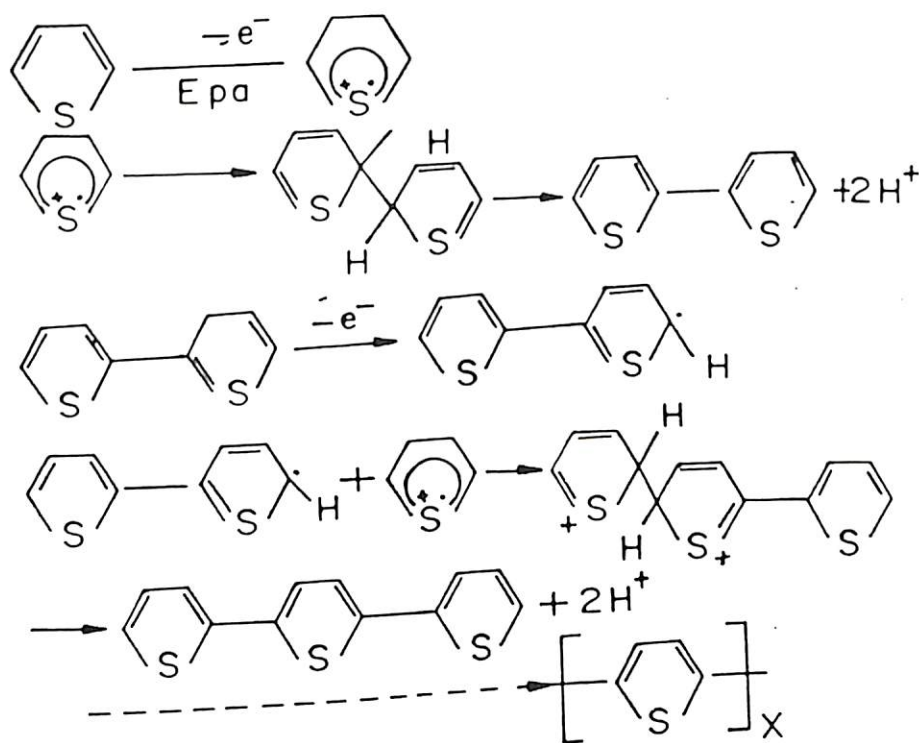
Fig.8 Schematic of electropolymerization of polythiopene, where E_{pa} and e^- are the oxidation potential and electronic charge, respectively.

1.3.8 VACUUM DEPOSITION METHOD

Vacuum deposition is a relatively simple process that makes use of a chamber, a power supply and heating elements capable of heating a material to a temperature at

a required pressure. A vacuum pump system is capable of reducing the pressure sufficiently to allow the evaporation of the coating material and fix it in its position. It has now become possible to produce thin layer deposits of conducting polymer by vacuum deposition techniques. Such experiments have been conducted with terphenyl deposits which can then be dimerized or trimerized in poly(p-phenylene). Salaneck et al [79] have investigated the electrical properties of vacuum deposited polyaniline film. Conducting polymer films formed by this technique are molecularly oriented and are parallel to the substrate. The films of polydiacetylene, polyaniline and polyaniline derivatives etc. have been fabricated by the vacuum deposition technique.

1.3.9 PHOTOCHEMICAL POLYMERIZATION METHOD

Photochemical polymerization has some advantages for the fabrication of a conducting polymer film. Polypyrrole patterns, have been generated using photochemical and photocatalytic polymerizations on some inorganic semiconductors. The photochemical deposition of polypyrrole is performed via the intermediacy of a photosensitive copper (I) complex, [$Cu(dpp)^{+2}$], the excited form of which can be transformed into copper II by reducing p-nitrobenzyl bromide, the resulting copper II complex is then able to oxidize pyrrole into polypyrrole (dpp= 2,9 diphenyl phenanthroline) on semiconductor surface [80]. Ruthenium II tris(bipyridine) has been used as the photosensitive intermediate and a cobalt complex, penta-amino cobalt III chloride, as quencher $[Co(NH_3)_5Cl]Cl_2$ play the role of oxidant (fig.9). The experiment is performed by impregnation of membrane with the result of pyrrole polymerization which occurs according to a predetermined reaction.

$$CO\ (NH_2)_5\ Cl^{2+} \diagdown\diagup \begin{array}{l} \text{Ru }(bPy)_3^{2+} \\ \text{Ru }(bPy)_3^{3+} \end{array} \diagdown\diagup \begin{array}{l} \text{Poly-pyrrole} \\ \text{Pyrrole} \end{array}$$

Decomposition
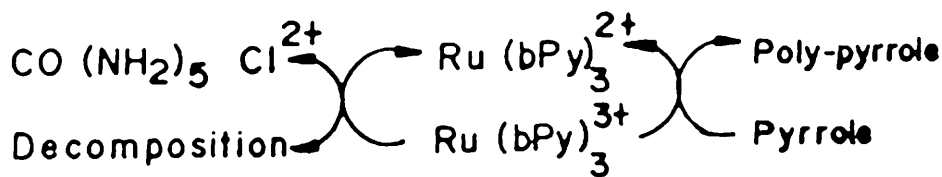
Fig.9 Photochemical deposition of polypyrrole films, where $CO(NH_2)_5Cl^{2+}$, $Ru(bPy)_3^{2+}$, $Ru(bPy)_3^{3+}$ are penta-amino cobalt III chloride, ruthenium II tris (bipyridine) and ruthenium II tris (tripyridine), respectively.

1.3.10 LANGMUIR - BLODGETT FILM DEPOSITION TECHNIQUE

Precise thickness control coupled with the degree of control over the molecular architecture has firmly established a role for Langmuir-Blodgett film in thin film technology [81-82]. Langmuir-Blodgett technique has been applied for preparing organic thin films in which functional parts are arranged in ordered states. The feasibility of locating functional parts at the molecular level alongwith the control of the thickness of resultant film are the novel features of this technique. This technique includes two steps such as the formation of stable monolayer films at air-water interface and subsequent transfer of the film onto a solid substrate.

A typical film forming molecule consists of a hydrophilic part and a hydrophobic part. The former usually contains the functional moiety of the films of an alkyl chain. These built up monolayer assemblies on the substrates are now referred to as Langmuir-Blodgett films whereas the floating monolayer is termed as Langmuir monolayer. The hydrophilicity and hydrophobicity of the molecule play important roles in each step suggesting that the modification of hydrophilic part of the molecule should result in films with different structures and functions even if functional moieties are in isolated form.

23

Conventionally, a lipophilic fatty acid is attached to the monomer to facilitate the deposition of an oriented film. Subsequently, the monomer is polymerized by suitable means. Alternatively, preformed polymers such as alkylthiophene mixed with stearic acid is dissolved in a suitable solvent and deposited. The deposition (PPV) is achieved in three steps as the preparation of monolayers films of the poly(sulphonium salt) onto n appropriate plate and thermal treatment of such multilayer films resulting in the ormation of PPV film.

The LB films of polyaniline and methoxyaniline have recently been prepared with known amount of polymer in N-methyl pyrrolidinone(NMP) /CHCl$_3$ and acetic acid or NMP/CHCl$_3$ solution of polyaniline [83-84]. Polyalkylthiopene and a variety of both alkyl substituted thiopene and pyrrole have been used for fabrication of Langmuir-Blodgett films [85]. For example pyrrole monolayer is polymerized at air-water interface of an LB trough in the presence of an active pyrrole molecule and ferric chloride. LB films have been formed from mixed monolayers comprising of cadmium stearate and a conjugated polymer.

1.4 PROPERTIES OF CONDUCTING POLYMER FILMS

Optical, electrical and structural properties of conducting polymer films can be experimentally investigated using a number of techniques. There is no single experiment which in general is capable of providing the detailed description of the properties of conducting polymer films. It is true that the best insight into the detailed properties of a film is available through a carefully chosen combination of several available techniques. A conducting polymer film has a relative orientation, pseudo-crystalline

structure and peculiar imperfections over the bulk material. Again, these factors change with time as the film grows in different conditions and finally its properties approach to the bulk conducting polymer. The main properties of a conducting film are those that can be repeatedly cycled between the oxidized state and reduced state. Some of these properties of some conducting polymer films have been discussed below.

1.4.1 MECHANICAL PROPERTIES

Diaz et al [80] have shown that the nature of a solvent and also the anions used in the preparation of the conduction polymer film strongly influence both the conductivity and differential mechanical properties such as Young's modulus, the tensile strength and elongation at break etc.. The elastic properties of a conducting polymer depend upon the chain alignment and have been characterized by the Harmans orientation function defined as $f=[3<\cos^2\sigma>-1]/2$ where $<\cos^2\sigma>$ is the average of the square of the cosine angle, (σ) between the chain axis and stretch direction. Chain-alignment in conjugated polymer requires a stage of drawing or stretching polymer at some line in the processing of the polymer. The attachment of flexible size chain to main chain, which provides a reliable means of setting the polymer into solution does not however tend to give good orientation [86].

It has been shown that PPY doped with BF_4^-, ClO_4^- and PTS ions have the Young modulus of 0.16 N/nm^2, indicating good mechanical properties of these conducting polymers. Moreover, PPY is a typical hard and brittle material with a high tensile strength with no yield stress and high Young's modulus.

Mechanical properties of PPY film can be compared to those of polystyrene and nylon. The composite of PVC/PPY also shows the lower modulus , lower tensile strength

and yield which are the characteristics of a soft material. The mechanical properties of PPS decrease, with increased doping (e.g AsF$_5$) concentration due to inhomogenity of surface or chemical and physical alternation of chemical and substantial loss. AsF$_3$ appears to act as solvating agents for the doped polymer, lowering the energy of the doped complex and allowing enhanced diffusion into the interior of PPS film. Films doped in this manner show improved mechanical properties as compared to those prepared with AsF$_5$ alone. The film prepared by dissolving polyaniline in N-methyl pyrridinone (NMP) on heat treatment at glass transition temperature ($\geq 110^{\circ}$C) have been found to be elongated to 400%. Besides this, such films have been found to have anisotropic properties. The films having good mechanical properties are used for the fabrication of electronic devices such as field - effect - transistor (FET).

1.4.2 STRUCTURAL PROPERTIES

The degree of molecular ordering in a conducting polymer is determined by a combination of different techniques such as X-ray scattering, scanning tunneling electron microscopy (STEM), X-ray photoelectron spectroscopy (XPS) etc. The short range order of the double - layered structure in sulphonate doped polypyrrole systems have been speculated by X-ray diffraction. A planer configuration of polypyrrole system has been experimentally performed on polypyrrole/anion system using transmission and reflection X-ray diffraction experiments [87]. The copolymer of pyrrole and N-methyl pyrrole shows a marked variation in structural anisotropy as revealed by X-ray scattering with apparent copolymer content. There is a trend between the observed variation in electrical conductivity and structural anisotropy of this conducting copolymer. Further, it has been shown that polyisothianaphathlene consists of crystalites approximately 20 Å in size.

Poly(3-methyl thiophene) and polypyrrole have crystalline order, possible less then 5%. Cis and trans content in polyacetylene is reported to be in extended chain forms consisting of an irregular matted web of highly crystalline smooth fibrils forming a net sponge. The fibrils ranging from 100 to 400 Å in width have been observed.

The d - spacing in polyaniline has been deduced from the observed peaks, according to Bragg's formula :

$$\lambda = 2d \sin\theta \qquad\qquad \text{Eq.1}$$

using the Scherrer formula

$$L = 0.9 / \Delta (2\theta) \cos\theta \qquad\qquad \text{Eq.2}$$

where λ, d, θ and L are the wavelength, inter spacing distance, angle of the diffracted ray, the crystalline domain size, respectively. The value of L is found to be 30 to 70 Å for conducting polyaniline system. The X-ray diffraction studies conducted on ES-I and E-II show these to be pseudo - orthorombic in structure with different crystalline size. It has been concluded that ES-I and ES-II essentially are amorphous. The inter spacing for NMP cast stretched films of PANI has been found to be 2-5 Å [88].

1.4.3 MORPHOLOGY OF CONDUCTING POLYMER FILMS

Morphology of a conducting polymer film is important property which needs to be carefully investigated because it is now well - established that the fibrillar structure of polyacetylene is often advantageous as it can easily store up to 7% of the available charge. SEM picture of a stretched PA film shows a bundle of fibers with average fiber diameter being around 800Å. SEM studies conducted on polyhetrocyclic compounds such as polypyrrole, polythiophene and poly(3-methyl thiophene) show that the structures are fibrillar, spherical with particle diameter of nearly 100 nm [89]. It has been seen that

polypyrrole films having counter anions such as Br⁻ have dense and homogeneous structures.

Morphological studies carried on the solution and electrochemically prepared polyaniline films have confirmed the existence of clusters (50 - 250 nm in diameter) [90]. The thick films of PANI have been shown to have regular surface morphologies. Scanning tunneling microscope studies carried out on solution cast polyaniline films have revealed granular (5-10 nm in diameter) nuclei having globular or spherical shape [91]. It has been seen that the compact surface of a conducting polymer results in a higher value of electrical conductivity. However, the surface morphology of a conducting polymer film in general is globular with fine grain boundaries.

1.4.4 OPTICAL PROPERTIES OF CONDUCTING POLYMER FILMS

Optical properties of conducting polymer films deal with the electronic excitation, absorption near the infrared, refractive index, extinction coefficient, second harmonic and third harmonic generation etc. As a whole optical properties of conducting polymers are important for understanding the electronic structures of a desired material. In general, an insulating polymer film is transparent (or lightly coloured) whereas on doping a conducting polymer film typically absorbs in the visible region. Poly(isothianaphthene) film however becomes blue black in the undoped state and it becomes transparent yellow in the doped state [92].

π- conjugation in a conducting polymer is indicated by its colour and its electronic spectra. Spectroscopy has become a powerful probe for the characterization of electrical processes that occur in a conducting polymer in its doped and undoped

states including those during insitu doping [93]. The changes of the optical spectra accompanying doping are significant and these spectral changes play a key role in elucidating the mechanism of doping and the nature of charge storage species in a polymer chain. Doping induces additional energy bands (due to solitons, polarons or bipolarons) in the principal energy band of a conducting polymer. The optical spectroscopy is thus a valuable tool for the determination of optical band gap of conducting polymer films. The optical band gap, E_g is an important characteristic whose magnitude governs the electronic and optical properties of a conducting polymer. The existence of a band gap in a conducting polymer is considered to originate principally from bond alternation.

Trans-PA shows a strong absorption peak at 1.8-1.9 eV but on doping with I_2 (or AsF$_5$), new absorption peaks appear at 0.65 - 0.7 eV and at 1.9 eV in the observed optical spectra [94]. The midgap absorption gives a direct evidence for charged solitons in the doped PA. In trans-PA the degree of the bond alternation r, the difference between the length of carbon-carbon double bond ($r_{C=C}$ = 1.346 Å) and that of single bond (r_{C-} = 1.446 Å) is experimentally observed to be of the order of 0.08-0.1Å. It has been shown that in the case of insitu doping of trans-PA, the mid - gap absorption intensity increases monotonically in proportion to the dopant concentration. The independent evidence has been obtained from the doping induced modes that appear in the mid-infrared associated with local vibrational modes of charges in conducting polymers [95].

The infrared studies conducted on PA reveal new absorption peaks at 900 cm^{-1} and 1370^{-1} identified with two internal modes of a kink soliton arising due to the π - electron. 1290 cm^{-1} and 1400 cm^{-1} peaks have been associated with internal vibrations and are found to be unchanged in the low doping level of PA. The non-linear optical

29

properties of PA have been recently studied. The stronger resonance enhancement of $X^{(3)}$ at 0.59 eV having a value of 10^{-8} esu (after) has been measured in this conducting polymer. The remarkable oscillator strength associated with doping - induced spectroscopic feature arises directly from the spatial extent of the charge storage state of PA and its derivative. The existence of solitons has been proved unambiguously through a series of photo-induced absorption and photo-induced ESR measurements in PA. The values of refractive indices in PA and its class such as polydiacetylene at 480 nm have been measured to be 1.5 and 2.1 which are close to the value found for the other polymeric systems.

Polyhetrocyclic conducting polymer such as polypyrrole has been found to be susceptible to air and moisture. The absorption spectra of neutral PPY has absorption bands at 3.2 eV and 1.3 eV, respectively, when it is exposed to air. Further, the height of the 3.2 eV absorption peak decreases whereas that of the 1.3 eV peak increases due to oxidation by oxygen. The absorption spectra for oxidized PPY films show broad bands near 1.0 eV arising due to conduction electrons and the observed absorption peaks near 3.0 eV have been associated with an inter band transition derived from the π-π^* transition in the polypyrrole film. Strongly oxidized PPY is not a metal, but has two narrow bands in the gap which can be assigned to bipolarons. The optical dielectric constant of a PPY film at low energy (0.1 eV) has been measured to be 2.5 which is typical for a polymer. The results of ellipsometric measurements conducted on PPY fibrils are in agreement with the spectroscopic measurement [96].

In non-degenerate doped conducting polymers like polythiopene, poly(2,2´ bithiophene) or poly(3-methyl thiopene), more than one peak has been observed in the UV-visible absorption spectrum. The absorption peaks have been attributed to the π-π^*

transition. The intensity of the absorption with interband transition gradually decreases on doping. Besides this, various absorption peaks have been found to be shifted to higher energies. Band gap of poly(isothianaphthalene) (PITN) has been calculated as 1.0 eV indicating that it is half of the parent polythiopene. It can be further seen (Table 2) that reduction of the band gap is directly related to the value of the electrical conductivity of poly(3-octyl thiopene) and PITN films, respectively. It is interesting to note that electrochemically prepared films and solution cast films of poly(3-methyl thiophene) have the same UV - absorption spectra. The doping of polythiophene results in significant changes in its structure.

Optical properties of polyaniline have been extensively studied in using the UV - visible absorption spectroscopy. There is no charge conjugation symmetry in polyaniline because the Fermi level and band gap are not formed in the centre of the π-band. Hence, the valence and conduction bands are asymmetric. Spectroscopic measurements have provided important information on the electronic structure of the insulating emeraldine base including the evolution of the electronic structure as a function of the degree of protonation. Interestingly, the absorption peak at 2.1 eV in emeraldine base disappears whereas two new absorption peaks centered at 1.5 and 2.9 eV appear as a result of protonation. In conducting polyemeraldine base film the absorption peaks at 1.0, 1.5 and 3.0 eV demonstrate the interchain coupling [97]. Ellipsometric studies have been used to obtain values of refractive index and extinction coefficient as 1.5002 and 1.8 respectively. The optical properties of some of the conducting polymers have been given in Table 2.

TABLE 2: Optical parameters of some conducting polymers.

SYSTEM	DOPANT	ABSORPTION E_{max}(eV)	IONIZATION POTENTIAL (eV)	WIDTH OF HIGHEST OCCUPIED π BAND(eV)	BAND GAP (ev)
Trans-PA	neutral	1.9	4.7	6.5	1.4
Trans-PA	I_2, AsF_5	0.7, 0.9	4.7	.5	1.4
Cis-transoid	neutral	1.5	4.8	6.4	1.5
trans-cisoid	neutral	-	4.7	6.5	1.3
Polythiophene	neutral	2.6	4.5	7.01	2.6
Polythiophene	BF_4^-	0.7, 1.7, 2.6	4.5	7.01	2.6
Polydi-acetylene	-	2.1	5.1	3.9	2.1
Poly(p-phenylene)	-	3.2	5.5	3.9	3.2
Poly(m-Phenylene)	-	4.5	6.1	0.7	4.5
Poly(p-phenylene vinylene)	-	2.5	5.1	2.8	2.5
Polybenzyl	-	5.9	6.5	0.6	-
Polypyrrole	neutral	3.2	-	-	3.2
Polypyrrole	doped	3.0	3.8	0.8	3.0
Polyaniline	undoped	2.0, 3.8	-	-	3.0
Polyaniline	doped	1.5, 2.9, 3.8	-	-	3.8
Poly(p-phenylene xylidiene)	-	-	6.5	2.5	3.4

1.4.5 ELECTRICAL PROPERTIES OF CONDUCTING POLYMERS

Electrical properties of conducting polymers, are the responses arising due to application of an electric field. The response of a conducting polymer to an electric field can be sensed as conductivity (dc/ac), dielectric relaxation, space charge polarization,

dielectric constant and Hall effect (charge mobility) etc. Moreover, electrical characteristics of conducting polymers films can be helpful towards their respective morphological and chemical behaviours.

A conjugated polymer becomes electrically conducting when it is treated with a strong oxidizing agent. Although, the charge species are incorporated by doping. The electrical conductivity is not ionic but electronic as is evident from the fact that no significant charge alternation in conductivity occurs after passage of more than sufficient current for complete polarization. The electrical conductivity of a conducting polymer depends upon the nature of chemical reactivity of the dopant, process of doping, doping level, method and condition of polymer complexes, processing of polymers and degree of crystallinity [98].

The dc conductivity is governed by the concentration of dopant ions in a conjugated polymer. Naarman et al [99] have obtained the conductivity of highly oriented anisotripic film of polyacetylene to be $10^5 \, \Omega^{-1} \, cm^{-1}$. I_2 doping of PA can result in increased electrical conductivity by 13 orders of magnitude. However, I_2 is too weak to get oxidized in the poly(phenylene sulphide) or poly(paraphenylene). The doping of PA, polythiophene and poly(3-methyl thiopene), polypyrrole and polyaniline by I_2 results in higher values of electrical conductivity of each of these respective conducting polymers [100].The electrical conductivity depends upon both the nature of dopant and the process of doping. Polypyrrole films when treated with two different dopant ions such as ClO_4^- and BF_4^- differ in conductivity. The ClO_4^- doped poly(3- methyl thiophene) has electrical conductivity of 10 -30 S/cm. On being doped with oxygen and moisture, the conductivity rises to 750 S/cm. The sharp change in dc conductivity of polymer in case of poly(3-methyl thiophene) on ITO and platinum surface arises due to the ordered or

defect free polymer chain. The activation energies of PA, PPY and polyaniline have been estimated to be 0.3, 0.041 and 0.03 eV respectively in their respective doped states.

The transport of electrical charge at low temperature leads to temperature dependent characteristics of electrical conductivity (Table 3) obeying the Mott's law of variable range hopping in three dimensions:

$$\sigma_{dc} = \sigma_o \exp[(-T_o/T)^{1/4}] \qquad Eq.3$$

where the symbols have their usual meanings. It shows that the charge transport in lightly doped PPY, PA, PT and PANI etc. is similar to that of amorphous semiconductors of tetrahedral type [101]. In interpreting conductivity versus temperature curves, most reports deal with a resonance fit resulting in the variable range hopping. At higher concentration level, the change in electrical conductivity of PPY may either be via diffusion or through the hopping of charges via bipolaron sites. In polyacetylene the conductivity is dominated by the energy required to produce a pair of neutral grains and the probability of a carrier tunneling between the grains. This leads to a temperature dependence of the form:

$$\sigma_{dc} = \sigma_o \exp[(-T_o/T)^{1/2}] \qquad Eq.4$$

Such behaviour has been observed in the granular materials at low fields. At high fields, non-ohmic behaviour has been predicted by granular model. This model can be applied to doped conducting polymers.

The space charge polarization phenomena resulting from the distribution and alignment of molecules under the influence of applied field with blocking contacts have been studied in PA, PPY and PANI, respectively. The values of carrier mobility for each of these conducting polymers has been calculated to be of the order of 10^{-5} cm^2/V.sec . The value of dielectric constants of polyacetylene and polypyrrole have been estimated to be of the order of 50-130 and 25-100, respectively.

The frequency $(10^3 - 10^7)$ and dielectric relaxation measurements have been shown to yield valuable information pertaining to the conduction mechanism since solitons, polarons and bipolarons have a major effect on the electronic states accessible to electrons traversing a sample. In dc conductivity σ_{dc} studies, the net charge which traverses the entire sample is measured. In contrast in ac conduction measurement the electrical conductivity is measured as a function of frequency of an alternating electric field. The difference occurs due to the motion of charge carriers in the extended region and the total conductivity can be expressed as: [102]:

$$\sigma_{tot} = \sigma_{dc}(T) + \sigma_{ac}(f, T) \qquad \text{Eq.5}$$

$$\sigma_{dc} = 0.39[\, N(E_f)/\alpha \ k_B \ T]^{1/2} \ v_0 \ e^2 \ exp \ [(-T_0 \ /T)^{1/4}] \qquad \text{Eq.6}$$

$$T_0 = 16 \ \alpha^3 \ /K_B \ N(E_f) \qquad \text{Eq.7}$$

$$\sigma_{ac} = 2 \ (\pi^2/3) \ e^2 \ K_B \ T \ N^2(E_F) \ \alpha^{-5} \ f[\ln (v_o/2\pi f)]^4 \qquad \text{Eq.8}$$

where $N(E_F)$ is the carrier concentration at Fermi level, V_o is the hopping frequency and α is the localization length. The Mott's variable range hopping model has been used to estimate charge transport parameters in a number of conducting polymers. The value of phonon frequency, v_o for a given conducting polymer (e.g PPY) has been estimated to be 10^{13} Hz at 10^5 K (temperature constant). The density of states in PPY system ranges from 7×10^{33} to 3×10^{46} states /eV cm^3 and the localization lengths to 10^4 for the undoped system and the doped system have been estimated to be 10^4 and 0.3 Å, respectively. The

35

frequency dependent conductivity measurements of partly protonated emeraldine have been conducted to support the presence of inter-polaron hopping mechanism similar to intersoliton hopping proposed by Kivelson. Compared to polaron, bipolaron in polyaniline has been shown to be an unstable entity. Besides this, the thermoelectric power decreases from 90 mV/K to 10 μV/K for the undoped trans - PA at a concentration above metallic region.

For fabrication of a solid state device based on conducting polymers the electrical properties of a semiconducting polymer /metal are very important and hence are being extensively investigated. The metals having lower and higher work function make a rectifying or an ohmic contact. When a metal is brought into contact with another phase (semiconductor) with different electrochemical potential, charge flows across the semiconductor/ metal junction. The total charge flux can be readily related to the initial difference in Fermi level between the two phases. The magnitude and direction of the initial charge transfer will therefore determine the electrical properties of the resulting schottky device. Table 3 contains the values of the various electrical conductivity measurements pertaining to a number of conducting polymers.

TABLE 3 : Values of electrical conductivity of some conducting polymers.

SYSTEM	METHODS	DOPANTS	CONDUCTIVITY (S/cm)
Polyacetylene	Chemical, Electrochemical	AsF_5^-, I^-, Li, K, $AgSO_4^-$	500-2000
Polyprrole	Electrochemical	ClO_4^-, BF_4^-, H_2SO_4, NO_3^-, AsF_5^-, PF_4^-,	10-600
Poly(N-methyl Pyrrole)	Electrochemical	BF_4^-, ClO_4^-	10^3
Poly(N-phenyl pyrrole)	Electrochemical	BF_4^-	10^3
Polythiophene	Electrochemical	BF_4^-, AsF_5^-, ClO_4^-	10^2 - 100
Poly(3-methyl thiophene)	Electrochemical	CF_3^-, SO_4^-, HSO_4^-	10^2 - 50
Polyfuran	Electrochemical	BF_4^-	80-100
Poly(para-phenylene)	Electrochemical	AsF_6^-, AsF_5^-, I^-, Li	3-100
Polyindole	Electrochemical	ClO_4^-	10^3 - 10^2
Polycarbazole	Electrochemical	ClO_4^-	10^3
Polypyrene	Electrochemical	ClO_4^-	0.1 - 1
Poly(para-phenylene - sulphide)	Electrochemical	AsF_6^-, AsF_5^-, I^-, K	3 - 10^2
Poly(p-pheneylene vinylene)	Electrochemical, Vacuum, Photo-chemical polymerization	AsF_5^-, AsF_6^-	1 - 3
Polyaniline	Electrochemical, Solution casting, Spin coating, Chemical	HCl, $HClO_4$, H_2SO_4 etc.	1 - 200
Poly(pyrrole)-poly(N-methyl pyrrole)	Electrochemical	BF_4^-, ClO_4^-	10^3

1.5 APPLICATIONS OF CONDUCTIVE POLYMER FILMS

Conducting polymers have been utilized a for fabrication of Schottky diode, metal-insulator-semiconductor (MIS) diode and heterojunction devices etc.. Most studies have been made with PA, PPY, PT and PANI since the absorption spectra of these conducting polymers make them good candidates for direct conversion of solar radiation into electrical energy. In this context, solar cells fabricated using metal/polyacetylene have been found to have efficiencies of only 0.3%. Recently, P-N diode has been fabricated by sequential polymerization of pyrrole and thiophene on a platinum substrate and controlled electrochemical doping of PPY largely by p-type dopant (PF_6^-) and a polythiophene layer by n-type dopant $((CH)_3)_4$ n^{+4} doped) [105]. The Schottky diodes of PPY and PT, poly(N-methyl pyrrole-pyrrole) with Al and In have been shown to have ideality factors ranging from 1 to 4 and barrier heights of 0.2-0.6eV.

Field- effect - transistor based on semiconducting PT as semiconductor and conducting PPY (p-toluene sulphonate doped) as source, drain electrode has been recently demonstrated. The device shows an easily detected variation in drain current for flow of only 10^{-12} C in gate circuit. The advantage with conducting polymer for the fabrication of a transistor is that narrower electrode spacing is needed and hence smaller polymer volume means that molecule based transistor requires less energy for switching and hence can be switched more rapidly.

It should be interesting to fabricate Schottky diodes using the para toluene sulphonate (PTS) doped PPY film obtained by electrochemical deposition technique. It may be mentioned that metal-insulator-semiconductor (MIS) devices based on LB films

as insulators have not as yet been fabricated. Such devices can be used as memory elements. It may be mentioned that Schottky diodes using vacuum evaporated polyaniline films have not as yet been studied at length.

Since doping in conducting polymers is a reversible phenomenon and can be electrochemically carried out, doped conducting polymers thus appear to be very promising as electrode materials for the fabrication of rechargeable batteries. PA-lithium battery is in no way inferior to the very limited capacity of accepting injected charge (on doping) and above all its sensitivity to normal environment is restricted for commercialization [106]. The polyaniline -lithium battery commercialized by Bridgestone Corporation in Japan is 0.4 -1.7 gm in weight, has a life cycle (> 1000 cycles), a long sheet life (>5 years) and a high storage reliability. Improvements are being made for an all - polymeric solid state rechargeable battery based on conductive polymers and alkali metal alloys with a view to obtain high efficiency.

Electrochromism is the property of a material or a system to change colour reversibly in response to an applied potential. Polythiopene, PPY, poly (1-methyl aniline) and polyaniline etc. have been suggested for such applications [107]. Owing to their electrochemical oxidation-reduction capabilities which have been associated with colours, PPY/PT composites show red colour to fade yellow to colourless between -0.6 V to 0.2 V in the presence of Cl⁻ ions. Life cycle test of the PANI film in protonic acid shows that switching potential can be varied from 0.2 - 0.4 volts to 0.2 vs 0.8V vs SCE, with life of about 10^5 cycles. Polyisothianaphthene (PITN) has been found to have shorter response time (about 10 milli seconds) and short colour contrast than most other conducting polymers. In its conducting state, it does not absorb much in the infrared region of the spectrum. During day time PITN windows permit visible light to enter and infrared

radiation to heat the room. At night, the conducting polymer changes to its coloured insulating state which absorbs extensively in infrared, thus preventing heat loss.

Most electrochromic devices have far been studied in solution state. It is preferable to employ solid state materials in order to minimize the problems of sealing in hazardous liquids. EC devices are usually required to have a thin layer configuration. With these considerations, experiments with thin layer cells of polyaniline with semi-solid electrolytes are likely to results in its application as the electrochromic.

Conducting polymer (e.g polydiacetylene, polyacetylene and polyaniline) molecules possess large second harmonic as well as third harmonic non-linearity that may be used for the fabrication of electro-optical devices. More important from the electrochemical point of view is the fact that polarization is predominantly electronic with virtually no nuclear motion. This leads to low dispersion in the polarizability of these materials from optical frequencies to dc which in turn results to a low value of dielectric constant (ϵ') resulting in its ability to create very high speed electro-optical devices.

Attempts are being made when the nurses in an operating theatre may be wearing conductive polymer fibers in the form of antistatic clothing. One of the most exciting application foreseen is the use of conducting polymers to deliver or release drugs directly into a patient's skin over weeks or months. Conducting polymers such as poly(3 methyl thiophene), polyaniline thus can be designed in such a way that these release drug ions when an electric current passes through them. The use of conducting polymers as an antistatic clothing is needed by operating personnel to eliminate static discharges that can confuse sensitive electrical monitors or even heart surgery.

It is apparent from the above discussion that a large number of investigations pertaining to conducting polymers especially with regards to the optical and electrical

roperties have been conducted. The field however, has not as yet been exhausted. Keeping this in view, a programme of detailed research pertaining to optical and electrical studies carried out on polypyrrole, polyaniline and a few conducting copolymers has been undertaken. Next Chapter gives a brief description of the various experimental techniques utilized for the preparation, characterization and applications of these conducting polymer films [32].

1.6 REFERENCES

1. A. J. Heeger, P.Smith, A. Fizazi, J. Moulion, K. Pakbaz and S.Rughooputh, *Synth. Metals*, **41-43** (1991) 1027.

2. B. D. Malhotra, N. Kumar and S. Chandra, *Prog. Poly. Sci.* **12** (1986) 179.

3. A. G. MacDiarmid, *Synth. Metals* **21** (1987)

4. M. S. Springborg, *J. Phys.: Condens Matter* **4** (1992) 101.

5. S. Hino, K. Iwasaki and K. Matsumoto, *Synth. Metals* **64** (1994) 259.

6. M. K. Ram, R. Mehrotra, S. S. Pandey and B. D. Malhotra, *J. Phys. : Condens. Matter* **6** (1994) 8913.

7. B.D. Malhotra, *Bull. Mater. Sci.* **10** (1988) 85.

8. M. Kobayashi, N. Colaneri, M. Boysel, F. Wudl, A. J. Heeger, *J. Chem. Phys.* **82** (1985) 5717.

9. M. Nechtschein, J. M. Pernaut and E. Genies, *Synth. Metals* **15** (1986) 59.

10. P. Pincas, P.M. Chaikin and C. Coll, *Solid State Commun.* **12** (1973) 1265.

11. S. Stafstrom, *Phy. Rev. B* **43** (1991) 9158; D. J. William, *Angew. Chem. Int. Engl.* **23** (1984) 690 ; D.J. William, *Non-linear Properties of Organic and Polymeric Materials, ACS Symp. Ser.* No. **233** Washington DC (1983).

12. R. Gupta, S.C.K. Misra, B.D. Malhotra, N. N. Beladakere and S. Chandra., *Appl. Phys. Lett.* **58** (1991) 51.

13. D. N. Batchelder, *Contemp. Physics* **29** (1988) 3.

14. R. Erlandsson, O Inganas, I. Lundstrom and W.R. Salaneck, *Synth. Metals* **10** (1985) 303.

15. Y. Cao, G. M. Treacy, P. Smith and A. J. Heeger, *Appl. Phys. Lett.* **60** (1992) 2711.

16. S.C.K. Misra, M.K. Ram, S. S. Pandey, B. D. Malhotra and S. Chandra, *Appl. Phys. Lett.* **61** (1992) 1219 ; T. Kanetake, K. Ishikawa and T. Koda, *Appl. Phys. Lett.* **51** (1987) 1957.

17. L. W. Shacklett, R. L. Esenbaumer, R.R. Chance, H. Eckhardt, J. E. Frommer and R.H. Baughman, *Synth. Metals* **75** (1980) 1919.

18. *Handbook of Conducting Polymers*, Vol 1 (eds) T.A. Skotheim, Marcel Dekker INC., (1986) New York, 494.

19. A. F. Diaz and K.K. Kanazawa, In Extended Linear Chain Compounds (J.S. Miller, eds.) Plenum, New York, 1982, 417.

20. G. Gustafsson, Y. Cao, G. M. Treacy, F. Klavetter, N. Colaneri and A. J. Heeger, *Nature* 357 (1992) 477.

21. M. Rolland, P. Bernier, S. Lefrant and M. Aldissi, *Polymer* 21 (1980) 1111.

22. W. Deits, P. Cukor, M. Rubner and H. Japson, *Polm. Prepr. Am. Chem. Div. Polym. Chem.* 22 (1981) 197.

23. Y. Cao, P. Smith and A. J. Heeger, *Synth. Metals* 49 (1992) 91.

24. P. Dannetun and K. Uvdal, *Chemtronics* 5 (1991) 173.

25. M. K. Ram, S Annapoorni and B. D. Malhotra, *Appl. Phys. Lett.* (communicated).

26. M. Schmelzer, S. Roth, P. Bauerle and R. Li, *Thin Solid Films* 229 (1993) 255.

27. B. Thomas, M.G. Krishna Pillai and S.Jaylekshi, *J. Phys D: Appl. Phys.* 21 (1988) 503.

28. N. Suzuki, M. Ozaki, S. Etmad, A. J. Heeger and A. G. MacDiarmid, *Phys. Rev. Lett.* 45 (1980) 1209.

29. T. C. Chung, A. Feldblum, A. J. Heeger and A. G. MacDiarmid, *J. Chem. Phys.* 74 (1981) 5504.

30. R. H. Friend, J. V. Acrivos (eds) *Physics and Chemistry of electrons and ions in Condensed Matter*, (1984) by D. Reidel Publishing Comapany, 625.

31. N. N. Beladakere, S. C. K. Misra, M. K. Ram, D. K. Rout, R. Gupta, B. D. Malhotra and S. Chandra, *J. Phys. : Condensed Matter* 4 (1992) 5747.

32. S. C. K. Misra, N. N. Beladakere, S. S. Pandey, M. K. Ram, T. P. Sharma, B. D. Malhotra and S. Chandra, *J. Appl. Poly. Sci.* 50 (1993) 411.

33. E. K. Sichel (ed.), *Carbon Black Polymer Composites*, Marcel Dekker, New York (1982).

34. R. P. Kusy and D. T. Turner, *J. Appl, Polym. Sci.* 17 (1973) 1631.

35. A. Malliaris and D. T. Turner, *J. Appl. Phys.* 42 (1971) 614.

36. E.M. Engler, *Chemtech.* 6 (1975) 667.

37. J.H. Perlstein, *Angew Chem. Int. Eds.*, **16** (1975) 667.

38. W.R. Hertler, *J. Org. Chem.*, **41** (1976) 1412.

39. D. Baeriswyl, *Proc. 3rd General Conf. Cond. Matter Division* EPS (Lausanne 1983) 639.

40. S. Roth, Proct. Inst. Autumn School on *"Electrochem. Conducting Polymers"*, Kazimierz, Poland, September **21** (1987) 1.

41. *Handbook of Conducting Polymers* " eds. T. A. Skotheim, Marcel Dekker (New York and Basel) Vol. 1, 1986.

42. G. Natta, G. Mazzanti and P. Corradini, *Atti Acca Nazl Linca Rend Classe Sci. Fis Mat e Nat* **25** (1958), 3 Chem. Abst. **53** (1959) 13985.

43. H. Shirakawa, and S. Ikeda, *Poly. J.* **2** (1971) 231.

44. C. K. Chiang, C. R. Fincher Jr., Y. W. Park, A.J. Heeger, H. Shirakawa, E. J. Louis, S.C.Gau and A. G. MacDiarmid, *Phys. Rev. Lett.* **39** (1977) 1098.

45. L. D. Kispert, *Radical ionic systems* by L. Lund and Shiotani (eds) Kluwer Academic Publishers, printed in the Netherlands (1991) 463- 478.

46. R. R. Chance, L. W. Shacklette, G. G. Miller, D. M. Ivory, J.M. Sowa, R. L. Elsenbaumer, R.H. Baughman, *J. Chem. Soc. Chem. Commun.* (1980) 347.

47. D. M. Ivory, G. G. Miller, J.M. Sowa, L. W. Shacklette, R.R. Chance and R.H. Baughman, *J. Chem. Phys.* **17** (1979) 1506.

48. A. F. Diaz, K. K. Kanazawa and G. P. Gardini, *J. Chem. Soc. Chem. Commun.* **1** (1979) 635.

49. J. L. Langer, *Synth. Metal* **35** (1990) 301.

50. H. Letheby, *J. Chem. Soc.* **15** (1862) 161.

51. A. G. Green and A.G Woodhead, *J. Chem. Soc. Trans.* **97** (1910) 2388; A. G. Green and A.E. Woodhead, *J. Chem. Soc. Trans.* **101** (1912) 1117.

52. J.R. Renolds, P.A. Proropatic and R.L. Toyooka, *Macromolecules* **20** (1987) 958.

53. G.B. Street, S.E. Lindsey, A.I. Nazzal and K. J. Wanne, *Mol. Cryst. Liq. Cryst.* **118** (1985) 137.

54. A. I. Nazzal, G.B. Street and K.J. Waynne, *Mol. Cryst. Liq. Cryst.* **125** (1985) 303.

55. N. S. Saricifti, M. Mehring, K.U. Gaudl, P. Bauerle, H. Neugebauer and A. Neckel, *J. Chem. Phys.* **96** (1992) 7164. C.F. Shu and M.S. Wrighton, *J. Phys. Chem.* **92** (1988) 5211.

56. K.K. Kanazawa, A.F. Diaz, G.P. Gardini, W.D. Gill, P.M. Grant, J.F. Kwak and G.B. Street, *Synth. Metals* **1** (1980) 329.

57. G. M. Holob. and P. Ehrlich, *J. Poly. Sci. Poly. Phys.* Eds. **15** (1977) 627.

58. M. Aldissi, *Synth. Metals*, **9** (1984) 131.

59. L. W. Shacklette, R.L. Elsenbaumer, R.R. Chance, H. Eckhardt, J.E. Frommer and R.H. Baughmann, *J. Chem. Phys.* **75** (1981) 1919.

60. M. Angelopous, A. Ray, A. G. MacDiarmid and A.J. Epstein, *Synth. Metals* **21** (1987) 21.

61. G. Tourillon and F. Garnier, *J. Electrochem. Soc.* **130** (1983) 2042.

62. H.W. Gibson and J.M. Pochan, *Macromolecules* **15** (1982) 242.

63. A. F. Diaz, J. Crowley, J. Barbon, G. P. Gardini and J. B. Torrance, *J. Electroanal. Chem.* **121** (1981) 355.

64. N.C. Billingham, P.D. Calvert, P.J.S. Foot, *Polymer Degradation and stability* **19** (1987) 323.

65. Y. Wei and K. Hsueh, *J. Polym. Sci., Pt A* **27** (1989) 4351

66. R.J. Waltman, A. F. Diaz and J. Bargon, *J. Electrochem. Soc.* **131** (1984) 1452.

67. J. E. Frommer, R.L. Elsenbaumer and R.R. Chance, *Org. Coat. Appl. Polym. Sci. Proc.* **48** (1983) 552.

68. J.H. Cheung, E. Punkka, M. Rikukawa, R.B. Rosner, A.T. Roappa and M. F. Rubner, *Polym. Mater. Sci. Engg.* **64** (1991) 263.

69. T. Ito, H. Shirawaka, S.Ikeda, *J.Poly.Sci. Poly. Chem.* Ed. **12** (1974) 11.

70. G. Liesser, G. Wagner, W. Muller, V. Enkelmann and W.H. Mayer, *Makromol Chem. Per. Commun.* **1** (1980) 627.

71. M. Seki, S. Isada, T. Mori and H. Inochi, *Solid State Commun.* **74** (1990) 677.

72. I. Murase, T. Ohnishi, T. Noguchi, T. Noguchi and H. Hirooka, *Poly. Commun.* **25** (1984) 327.

73. A.F. Shepard and B. F. Dunnels, *J. Poly. Sci.* **4** (1966) 511.

74. K. K. Kanazawa, A. F. Diaz, G. P. Gardini, W.D. Gill, P.M. Grant, J. F. Kwak and G.B. Street, *Synth. Metals* **1** (1980) 329.

75. A.P. Monkman and P.Adams, *Solid State Commun.* **78** (1991) 29.

76. R. Qian, J. Qiu and D. Shen, *Synth. Metals* **18** (1987) 13.

77. S. Hotta, *Synth. Metals* **22** (1988) 103.

78. G. Kossmehl and G. Chatzitheodorou, *Makromol. Chem. Rap. Commun.*, **2** (1981) 551. ; G. Kossmehl and G. Chatzitheodorou, *Mol. Cryst. Liq. Cryst.* **83** (1982) 291.

79. W. R. Salaneck, I. Lundstrom, B. Liedberg, M. A. Hasan, R. Erlandsson, P. Konradsson, A. G. MacDiarmid and N.L.D. Somasiri, in *"Electronic properties of Conjugated Polymers and Related Compounds*, H.Kuzmany, M. Mehring and S. Roth, Eds. (Springer-Verlag, Berlin), **63** (1985) 218.

80. H. Segawa, T. Shimidzu and K. Honda, *J. Chem. Soc. Chem. Commun.* (1989) 132; G. G. Roberts, *Contemp. Phys.* **25** (1994) 109.

81. V. K. Agarwal, *Physics Today* June (1988) 40; G.G. Roberts, *Sensors and Actuators* **4** (1975) 1380.

82. M. K. Ram, N.S. Sundaresan and B. D. Malhotra, *J. Phys. Chem. Lett.* **97** (1993) 1158.

83. N. E. Agbor, M. C. Petty, A.P. Monkman and M. Harris, *Synth. Metals* **55-57** (1993) 3789.

84. J. H. Cheung, R.B. Rosner, I. Watanabe and M.F. Rubner, *Mol. Cryst. Liquid Cryst.* **190** (1990) 133.

85. D. Macinnes Jr. and B.L. Funt, *Synth Metals* **25** (1988) 242.

86. M. L. Digar, S. N. Bhattacharyya and B. M. Mandal, *J. Chem. Soc. Chem. Commun.* (1992) 21.

88. M. Laridjani, J.P. Pouget, A.G. MacDiarmid and A.J. Epstein, *J. Phys.:1 France* **2** (1992) 1003.

89. J.M. Ko, H.W. Rhee, S. M. Park and C.Y. Kim, *J. Electrochem. Soc.* **137** (1990) 905.

90. A.J. Epstein and A.G. MacDiarmid, *Synth. Metals* **41** (1991) 601.

91. C. Bai, C. Zhu, G.Huang, J. Yang and M. Wan, *UltraMicroscopy* **42** (1992) 1079.

92. F. Wudl, M. Kobayashi and A. J. Heeger, *J. Org. Chem.*, **49** (1984) 3382.

93. M. Springborg, *J Phys: Condens. Matter* **4** (1992) 101.

94. C.R. Fincher, D.L. Peebles, A.J. Heeger, M.A. Druy, Y. Matsumura, A.G. MacDiarmid, H. Shirakawa and S. Ikeda, *Solid State Commun.* **27** (1978) 489.

95. N. Suzuki, M. Ozaki, S. Etemad, A.J. Heeger and A.G. MacDiarmid *Phys. Rev. Lett.* **45** (1980) 1209.

96. Y. Yakushi, L. J. Lauchlan, T. C. Clarke and G.B. Street, *J. Chem. Phys.* **79** (1983) 4774.

97. A. J. Epstein, J. M. Ginder, M. G. Roe, T. L. Gustafson, M. Angelopoulos and A.G. MacDiarmid, Proc. Symp. on Non-linear optical Properties of Polymers, Mat. Res. Soc. Mtg. Boston 11/30-12/5/8 (1987).

98. J. Tsukamoto, A Takahashi, K. Kawasaki, *Jpn. J. Appl. Phys.* **29** (1990) 125.

99. H. Naarman, *Electronic properties of conjugated polymers* (Eds. H. Kuzmany, M. Mehring and S. Roth), Springer Series in Solid State Sciences, Springer Heidelberg, 1987.

100. P.J. Cui, *Science in China (series A)*, **34** (1991) 61.

101. J. M. Ribo, C. Acero, M.C. Anglada, A. Dicko and J.M. Tura, *Bull. Soc. Cat. Cien.*, **XIII** (1992) 335.

102. S. Kivelson, *Phys. Rev. B* **25** (1982) 3798.

103. A. Boyle, E. M. Genies and M. Lapkoski, *Synth. Metals* **28** (1989) C 769.

104. R. A. Pethrick, *Interdisciplinary Science Reviews* **12** (1987) 278.

105. P.M. Grant, T. Tani, W. D. Gill, M. Krounbi and T.C. Clarke, *J. Appl. Phys.* **52** (1980) 869.

106. J. Meyer, *Polymer Engg. Sci.* **6** (1973) 462.

107. M. A. Habib, *Langmuir*, **4** (1988) 1302.

CHAPTER II

EXPERIMENTAL

2.1 MATERIALS

Pyrrole: Fluka; Aniline : Fisher; Ammonia solution: Sarabhai Chemicals; Hydrochloric acid (HCl): E. Merck; Sulphuric acid (H$_2$SO$_4$): E. Merck; Perchloric acid (HClO$_4$): E. Merck; NMP (N-methyl pyrrolidinone): E. Merck; DMF (Dimethyl formamids): E. Merck; THF (Tetra hydrofuran): Ranbaxy; Acetone: Qualigens; Methanol : E. Merck; N-phenyl pyrrole : Aldrich Chemical Co.; α - napthol: E. Merck; tetra-ethyl-ammonium-tetrafluorobarate (TEATFB) : Aldrich chemical Co.; Sodium salt of Paratoluene sulphonic acid (PTS): Aldrich chemical Co.; potassium chloride : aratuluene sulphonic acid Merck; Chromium trichloride: Merck; Phosphorous pentachloride : 99% anhydrous; Poly(ethylene oxide) : Sigma; Polyvinyl chloride : Aldrich chemical Co., Poly (ethylene oxide) (PEO): TCI Japan; Glycerol : Qualigens; Urea : Merck; Indium-tin-oxide (ITO) conducting glass plate: Platinum foil (Johnson - Mathey Co.); Lithium perchlorate (LiClO$_4$): Wilson Laboratories; Metals: Gold (Au), Silver (Ag) and Lead (Pb): E. Merck,

2.2 INTRODUCTION

As mentioned in the previous chapter, morphology of a conducting polymer film is dependent on the various conditions under which such a film is prepared. Prior to the

development of soluble and fusible conducting polymers, thin films of polyacetylene (PA), polypyrrole (PPY) and polythiophene (PT) have been fabricated by thermal and electrochemical techniques, respectively [1,3]. However, free standing films of conducting polymers are difficult to prepare having a controlled thickness using these techniques, because these have to be peeled off from the walls or electrode surface. A significant advantage of electrochemical polymerization methods lies in the ability to control the degree of doping without the need to make the films conducting by exposing these to dopant in the vapor or in solution [4].

Free standing films of PA, PPV, poly(p-phenylene) (PPP) and polyaniline can be prepared by casting these from precursor solution and then converting these films to the desired form for example by heat treatment and doping [5]. However, all these techniques are less utilized compared with the most technologically oriented preparation of poly(3-alkylthiophene), polyaniline etc, which can be conveniently cast from solution or heat pressed from a melt [6]. Free standing films are relatively thick, the thickness typically ranging from a few micrometers to millimeters. Such conducting polymer films are useful for electrical conductivity measurements because these can be easily handled and the measurement signal is larger than in the case of thinner films. Anisotropic conductivity studies are usually performed on the stretched free standing films. These films are also useful for infrared, thermal, dielectric and structure studies.

The crystallinity studies of conducting polymer films have been experimentally investigated on vacuum deposited conducting polymer films [7]. In spite of fragmented chain lengths of most of such conducting polymer films, these have been found to be useful for investigation of optical properties.

The Langmuir-Blodgett (LB) technique is the most sophisticated deposition

method for obtaining conducting polymer films. The multilayer samples, as well as alternating layers of functionally different molecules with precise control of film thickness and architecture can be realized[8]. The long entangled chains of conducting polymer LB films are usually not as ordered as pure surface active molecule aggregates and bundles of polymer chains are formed. Oligomeric LB films on the other hand have been shown to form ordered structures. It may be remarked that solution doping typically destroys the ordered structure of an LB film, whereas subphase (water containing protonic acid or salt) significantly alters the molecular morphologies of LB films[9] . After a conducting film is prepared by any of the available techniques, it needs to be characterized exhaustively before undertaking any application. There is presently no single characterization technique which provides a detailed information on the properties of the material. It means that the true insight into the detailed properties of a film is available through a carefully chosen combination of several available techniques. FTIR, UV - visible, ellipsometry etc. techniques have been used for the characterization of optical properties of a number of conducting polymer films. Electrical conductivity (ac/dc) studies can be carried out to study the electrical properties of a desired conducting polymer. Atomic force microscopy (AFM), scanning tunneling electron microscopy (STEM), scanning electron microscopy (SEM), etc., can be used for investigating the surface morphology of conducting polymer films.

The present chapter deals with the different techniques of preparation of conducting polymer films and various methods of characterization of conducting polymer films based on polypyrrole, polyaniline and some conducting polymers etc. Some of these conducting polymer films have been used for the fabrication of Schottky diode, metal-insulator-semiconductor (MIS) and electrochromic displays.

2.3 PREPARATION OF CONDUCTING POLYMER FILMS

2.3.1 SOLUTION CAST METHOD

Free standing conducting polymer films of varying thickness can be prepared by solution cast technique. Conducting polymers (e.g polyaniline) can first be synthesized using chemical oxidative polymerization in powder form that can be undoped in aqueous ammonia. A conducting polymer is made soluble in an organic solvent. Such a conducting polymer can be cast into film form when heated at low pressure (10^{-2} - 10^{-3} torr). Polydiacetylene, polyaniline and its derivatives like (o- methoxy aniline), copolymer of aniline and o-anisidine etc. have been prepared by this technique [10]. For example, 1 gm. of poly(2-methyl aniline) when dissolved in 100ml of NMP and continuously stirred for 1 hour, filtered twice and spread on the glass plates in a vacuum oven (10^{-2} torr) at about 170°C for two hours results in (10 - 15 μm) poly(2- methyl aniline) films. The conducting films can be removed from the glass when dipped in boiling water. Polyaniline films formed by this technique have elongation of about 400% and are suitable for electrical measurements. If the temperature and pressure are not maintained properly, such films are likely to contain wrinkles on the surface due to the entrapment of the used solvent[111]. It has been revealed that solvent acts as a plasticizer. The detailed information regarding electrical properties on some of the solution cast conducting films have been given in Table I.

TABLE I: Electrical, mechanical and surface properties of some of the solution cast conducting polymer films

SYSTEM	Conductivity S/cm	% Elongation (strain)	Surface structure
Polydiacetylene	10^{-4}	120	homogeneous
Polyaniline	30	400	smooth
Poly(aniline-o-anisidine)	10^{-2}	-	smooth
Poly(hexyl thiophene)	10^{-1}	-	smooth

2.3.2 ELECTROCHEMICAL SYNTHESIS

Electrochemical polymerization is regarded as a novel and simple technique that involves simultaneous oxidation of monomer. A significant advantage of this technique is that polymerization in suitable electrolytic medium gives directly the desired doped polymer as a flexible free standing film. In this method, conducting polymer films are produced on the surface by oxidative coupling and hence electrochemical stoichiometry is maintained. Each conducting polymer film has a different stoichiometry that results from the degree of oxidation of the polymer.

The electrochemical polymerization involves three techniques such as potentiostatic, galvanostatic and potentiodynamic (cyclic voltammetry). For the electrochemical polymerization technique two or three electrodes cell with properly connected power supply or current source are required. In the potentiostatic method constant potential is applied between the two electrodes of a given cell. The charge consumption which accompanies the rate of polymer formation is linearly dependent on the time and has been found to be independent of the concentration of monomer for constant potential electrolysis. Under steady - state conditions, the coupling reaction also

52

occurs between the radical cations of the oligomers, since the dimers, trimers and polymers are more easily oxidized than the monomers. The current depends on the rate of diffusion of pyrrole to the region of the electrode. The constant potential in case of polyaniline produces a powder which adheres poorly to the electrodes.

In the galvanostatic mode the constant current is applied between the counter and the working electrodes. Polyhetrocyclic conducting polymer films have been prepared by this technique. In such a method the resistance of the cell always changes under the constant current maintained between the electrodes. Smooth conducting polymer films have been obtained using such a technique[12].
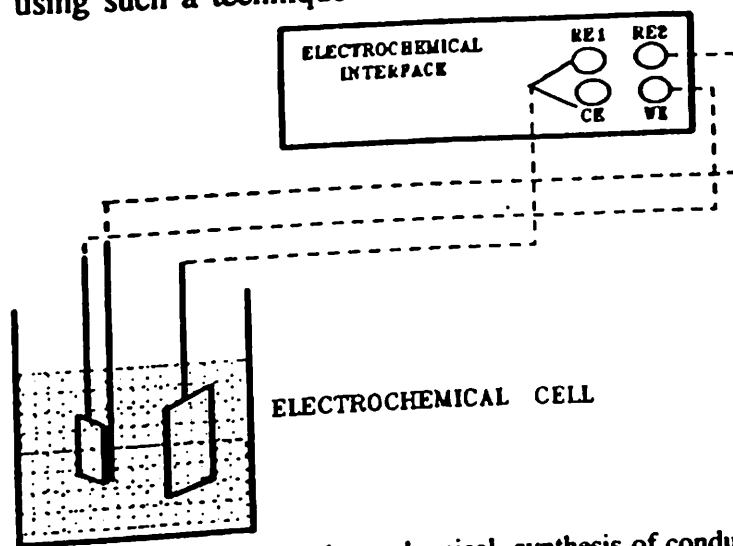
Fig.1 A schematic of a three electrodes cell for electrochemical synthesis of conducting polymer films

The potentiodynamic method is another versatile technique for the formation of conducting polymer films. The controlled potential that acts as an excitation signal between working and counter electrode with respect to reference electrode. The current at the working electrode during the cyclic voltammetry is measured during the potential scan between the two fixed potentials. Electro-oxidation of aniline by continuously cycling the potential - 0.2 and 0.8V (vs SSCE) produces an even film which adheres strongly on the electrode surface[13] . The films are electroactive and the oxidation reaction is chemically reversible. Moreover, conducting polymer films obtained by potentiodynamic

53

technique are smooth and can be used for electroanalytic studies. Polypyrrole and polyaniline films prepared using this technique have been used as smart windows.

2.3.3 VACUUM EVAPORATION TECHNIQUE

Vacuum evaporation technique is comparatively an easier technique for obtaining molecularly oriented films on a desired substrate. The conducting polymer powder is heated in a boat of tungsten or quartz at a pressure of 10^{-6} torr at a high temperature. This technique involves the use of power supply, diffusion pump, rotary pump and a heating element. The diffusion pump is used to reduce the pressure sufficiently to allow evaporation of the coating material inside the chamber. Polytoluidine powder when heated (800°C) in vacuum (10^{-6} torr) results in the deposition of polytoluidine film. Besides this, conducting polymer films of poly-p-phenylene, polydiacetylene, polyaniline and its derivatives have been fabricated by this technique [14]. These films obtained by this technique are smooth and have been used for a number of electronic applications such as Schottky diode, light emitting diode as indicated in table II.

TABLE II: Characteristics of some vacuum deposited conducting polymer films

Conducting Polymer	Conductivity S/cm	Nature of Film	Application
Polydiacetylene	1	Smooth	SD
Poly(phenylene) Vinylene	10^{-4}	Smooth	LED
Polyaniline	0.1	Smooth	SD

2.3.4 LANGMUIR-BLODGETT TECHNIQUE:

Langmuir - Blodgett technique denotes the transfer of monolayers/multilayers from the water - air interface (or liquid - gas interface) onto a solid substrate. The molecular film at the water - air interface is known as a Langmuir film [15]. This technique has been used for preparing organic thin films in which the functional parts are arranged in ordered states. The preparation of monolayers at the water - air interface generally starts with the Langmuir trough. The trough should be so designed that films can be deposited in the temperature range from near freezing to near boiling point of subphase.

The Langmuir-Blodgett deposition system generally compprises of a Langmuir trough, controlled movable barrier, Whilhemy plate (for measuring pressure), Wilhemy balance, comparator and substrate holder with controlled motor speed. A schematic of an LB is system shown in fig.2:
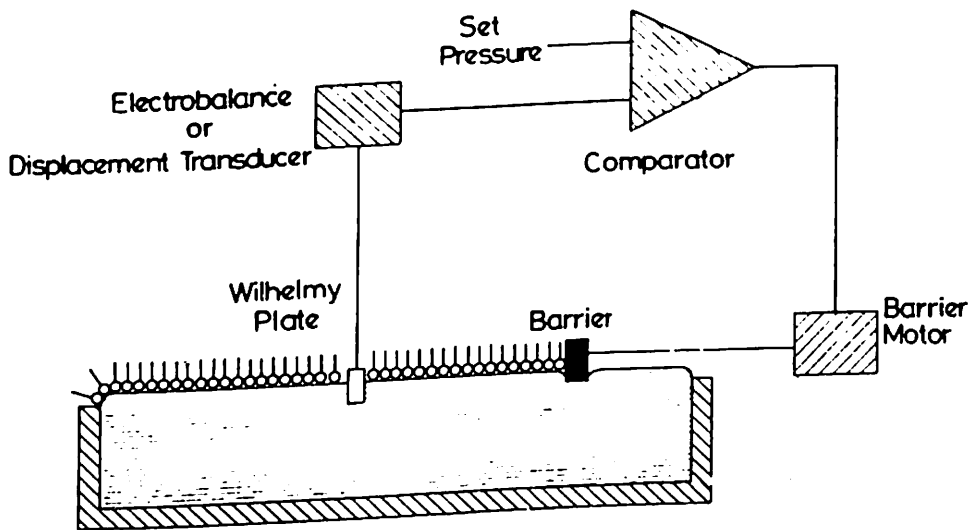

Fig.2   Schematic of a Langmuir-Blodgett system to control surface pressure of a monolayer

The fabrication of multilayers by the LB method is not a very straight forward technique. There are some important technical issues such as the environment, the

subphase, the substrate, the amphiphiles, the cleaning between experiment and the controlled dipping substrate holder relating to deposition of Langmuir-Blodgett films. The most commonly used subphase is water, although mercury as well as glycerol have been used. It is recommended that deionized water having surface tension of 72 mN/m at 25°C may be used. LB films can be deposited on many substrates such as plane glass, quartz, silicon wafer and optical glass plates, etc., respectively. The hydrophilic clean substrate generally used for the LB film deposition shows minimum contact angle with the subphase system. The purity of both amphiphiles and solvent used for depositing molecules are of great importance, otherwise impurities may be incorporated in the monolayers. It is emphasized that the desired surface should be free from any surface - active materials. Besides this, pH and temperature of subphase play an important role for the stabilization of the Langmuir monolayer.

The single most important indicator of the monolayer properties of a material is given by a plot of surface pressure as a function of area of water surface, available to each molecule at constant temperature. Such a curve is known as surface pressure (π) - area (A) isotherm. The behaviour of water, insoluble amphiphile at an air - water interface is usually monitored by the Langmuir trough. In the LB system the area of water of surface can be precisely controlled by the movement of a barrier while the surface pressure of a monolayer, on the water surface can be measured accurately. As soon the barrier in the trough is compressed the effective surface area of the molecules is reduced from the large initial area and there is a gradual onset of pressure until an approximately horizontal region is reached. The pressure - area isotherm has been defined by a parameter, C (compressibility of the barrier) defined as [16]:

$$C = -1/A \left(\delta A / \delta \pi \right)_{T, P, n_i} \qquad \text{Eq.1}$$

where δA is the change of area with change of pressure ($\delta\pi$), at constant temperature (T_i), pressure (P_i) and constant molecular composition (n_i), respectively. The value of solid phase, liquid phase and gaseous phase of the molecules on the surface depends upon the value of compressibility [8].

A molecular ensemble can be considered as a gaseous phase initially after the solvent evaporates and the molecules lie on the subphase as gaseous molecules. Such a behaviour can be represented by the gas equation:

$$\pi A = k_B T \qquad\qquad \text{Eq.2}$$

where k_B is the Boltzmann constant, A is the mean area available per surface active molecule at any instant of time and T is the temperature. At higher values of π, A tends to zero. However, long chain hydrocarbons have a limiting area of $20A°^2$. Thus, at high π values, eq.2 is not adequate to explain the isotherm behavior of the monolayer. Langmuir has re-defined the equation taking this factor into consideration :

$$\pi = k_B T / A\text{-}w \qquad\qquad \text{Eq.3}$$

where w is the limiting area of a given molecule. Again, Eq.3 cannot explain the experimental isotherm behaviour since it does not take care of the contribution of the activity of the molecules at air - water interface. Moreover, the charge on the molecule increases the intermolecular interaction. Taking this into account the molecular activity at the air - water interface and the ionic contribution of the molecule, the isotherm equation can be further modified as

$$\pi = K_B T / w [\ln (1 - n w_1/ (A - w_2)] \qquad\qquad \text{Eq.4}$$

where w_1 and w_2 are the limiting molecular areas of water and the amphiphilic molecule respectively, w_1 has been approximated to $9.1 A°^2$ (from the 2/3 power of the volume of water molecules), f is the activity coefficient of the molecule and is close to unity for very

dilute concentration and n is the total number of ions formed per molecule at the water surface. Pressure vs area isotherm (both numerical and experimental) can be obtained using Eq.4.
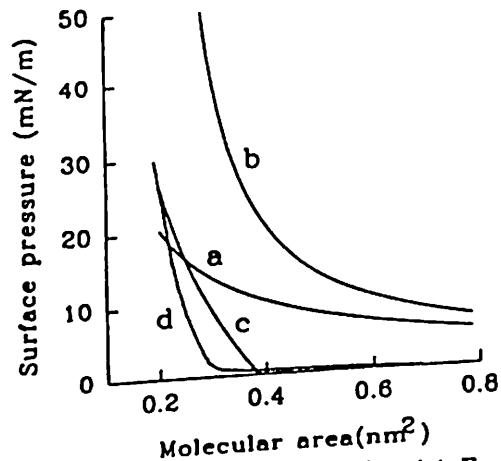

Fig.3   Pressure-area isotherms for stearic acid calculated using (a) Eq.(2), (b) Eq.(3), (c) Eq.(4) and (d) experimentally observed pressure - area isotherm curve.

Feedback loop to control monolayer surface pressure has been shown in fig.2. The area per molecule at the solid phase is calculated for the solid phase condensation of the monolayer molecules on the subphase. The constant pressure is maintained through the barrier compression rate. The solid support is vertically dipped and raised, keeping the surface film at a constant pressure in order to keep the monolayer intact. If the even number of monolayers are deposited on the substrate with continuous insertion/ withdrawal, Y -type LB films are formed. If the monolayers are deposited by inserting the substrate, X- type LB films are produced. If deposition occurs while substrate is taken out of water, Z- type LB films are formed. It can be characterized by the deposition ratio defined as [17]:

$$\phi = A_S / A_L \qquad \text{Eq.5}$$

where A_L is the area occupied by the molecules on the water surface and A_S is the area transferred to the solid substrate. The type of a film simply depends upon the value of AL/AS. If $\phi = 1, 0$ and ∞, the LB films formed are either Y type or X type or Z type, respectively. However, both X type or Z type structures can also be obtained by moving

the substrates in one direction through the floating monolayers and in the opposite direction through the clean water surface. In some cases, Z type deposition has been achieved by decompression of a monolayer during the down strokes.
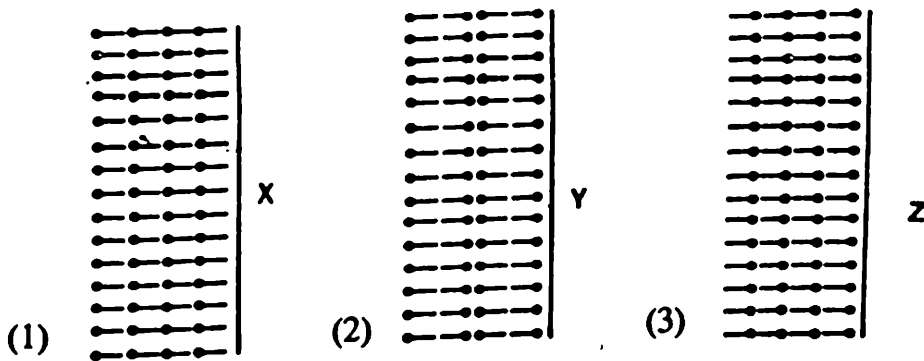

Fig.4 Structures of (1) X, (2) Y and (3) Z type multilayers of Langmuir-Blodgett films.

It may be mentioned that the deposition of an LB film is dependent upon the principles of ionic equilibrium, pH of the subphase, the distribution of cationic and anions between the bulk of the subphase of the monolayers.

2.4 DOPING AND UNDOPING OF CONDUCTING

Doped and undoped states are related to the number of anions or cations present in a conducting polymer. The presence of a dopant results in the change in electrical conductivity of a conducting polymer film due to the redox nature of neutral (undoped) and doped (oxidized) states. In the electrochemical polymerization (for example polypyrrole, polythiophene) simultaneous doping occurs while the films grow. When the films are made by solution casting, LB technique or vacuum deposition, vapour exposure or solution dipping techniques are employed for the doping process. For example, solution cast films of polyaniline when dipped for about 48 hours in 1M HCl, 1M H_2SO_4, 1M $HClO_4$, etc., become doped. The complete undoping of conducting polymer film is generally done in an aqueous NH_3, phenyl hydrazine etc. for a fixed number of hours [18].

Polypyrrole when undoped in aqueous NH$_3$ for 24 hours results in the neutral PPY film. Doping and undoping of a conducting polymer result not only in changes in the electrical conductivity but also brings about changes in its structural, optical and morphological properties, respectively.

2.5 MOLECULAR WEIGHT DETERMINATION BY GEL PERMEATION CHROMATOGRAPHY

The molecular weight of a conducting polymer differs with the structure of its repeat unit. The longer the repeat unit, the higher the molecular weight of a conducting polymer. Extent of conjugation of conducting polymer depends on the effective molecular weight and its distribution. A number of techniques such as intrinsic viscosity measurement (M_v), light scattering (z- average), end group analysis (M_n) and gel-permeation chromatography (GPC) etc. have been used for the determination of molecular weight of a conducting polymer. Amongst these, GPC is the most versatile which is based on the separation of sample molecules by differences in molecular size in a solution. Separation is accomplished by injecting the polymer solution into a continuously flowing stream of a solvent which passes through highly porous, rigid gel particles, closely packed together in a column . The pore sizes of the gel particles may vary from a small to very large. As the solution flows through the gel particles, molecules with small effective sizes penetrate more pores than molecules with larger effective sizes and therefore take no longer to emerge than do the larger sizes and gel molecules. If the gel covers the right range of molecular sizes, the result will be a size separation with the largest molecules leaving the column first. GPC technique yields information on the weight average molecular weight, number average molecular weight and polydispersity

index of conducting polymer.

For an ideal conducting polymer polydispersity should lie between 1 and 1.5. Higher polydispersity leads to the inconsistency in the physical and chemical properties of the film. Poly(3-methylthiopene) has been found to have a molecular weight of about 43000 [19]. Polyaniline has been shown to have molecular weight from 20,000 to 200,000 obtained by using different methods of preparations. The higher molecular weights have been found for polyanilines synthesized at low temperatures.

2.6 THERMAL CHARACTERIZATION

Thermal analysis is a generic term that encompasses several analytical methods such as thermo mechanical-analysis (TMA), thermogravimetric analysis (TGA), differential scanning calorimetry (DSC). DSC and TGA can be respectively used for studying specific heat of a given material and loss of weight of the sample as a function of temperature or time.

DSC is an important experimental tool to study the specific heat of a given material at different temperatures. Specific heat functions generally vary slowly with temperature, high resolution condition including the small sample sizes, slow scanning rates, high instrument sensitivity are required. DSC makes use of two - flow detecting methods such as power compensation method and the heat flux method. It measures the difference in the heat flow between the sample to be tested and a known standard. The samples are kept at the same temperature through the use of an automatic compensator that senses any difference in temperature and makes appropriate adjustment [20]. The heat compensation value is recorded as a function of the thermal flow rate. A cooling

apparatus is used when making low temperature DSC measurements.

The DSC measurement of some conducing polymer films have been performed by heating the sample in an aluminium sample holder with the scanning rate of 10° C/min. Perkin Elmer (model DSC-7) has been used at a heating rate of 10 deg/min. for the recording various thermograms. Conducting polymer films of approximately 10 mg each are used. The nitrogen flow rate of 75 ml/min. is used. Good specific heat data requires maximum care in reproducing instrument conditions from base line to sample run.

2.7 ELECTROCHEMICAL CHARACTERIZATION BY CYCLIC VOLTAMMETRY

Cyclic voltammetry (CV) is perhaps the most versatile electroanalytical technique to study the electroactive species. CV consists of cycling the potential of an electrode which is immersed in an unstirred solution and it involves the measurement of the resulting current. The controlled potential which is applied between the working and counter electrodes can be considered as an excitation signal. The excitation signal for a CV is a linear potential scan with a triangular shape. The triangular potential that sweeps the potential of the electrode between two fixed values is called the switching potential. The measured current at the working electrode during potential scan arises due to the excitation signal. The detailed understanding using cyclic voltammetry technique can be gained by considering the Nerst's equation and the changes in concentration that occur in solution adjacent to the electrode during electrolysis. The proper equilibrium ratio in reversible system, at a given potential is determined by the Nerst equation:

$$E = E^0 - RT/nF \ \ln \ ([R]\ /[0])$$

<div align="right">Eq.6</div>

where O = oxidized form and R = reduced form of a conducting polymer, respectively.

A characteristic of a reversible system for which the experiments have been performed on some of the conducting polymer films pertain to the dependence of the current peak height on the square root of scan rate using the Randles-Sevcik equation for the forward and reverse cycles [21,22] given as under:

$$I_p \ = \ (2.69 \times 10^5) \ n^{3/2} \ A \ D_o^{1/2} \ V^{1/2} \ C_0^{\bullet}$$

<div align="right">Eq.7</div>

where Ip is peak current (A), n in the electron stoichiometry, A is the electrode area (cm^2), D_0 is diffusion coefficient (cm^2/S), $C_0^{\bullet}$ is the concentration (mol/cm^3), V is scan rate (V/S). For an identical system, i_{pa}/i_{pc} = 1.

Schlumberger 1286 Electrochemical Interface, coupled with a plotter has been used to study the cyclic voltammetry of some of conducting polymers such as polypyrrole and polyaniline films etc. The typical arrangement of the cyclic voltammetry studies has been given in fig.5:
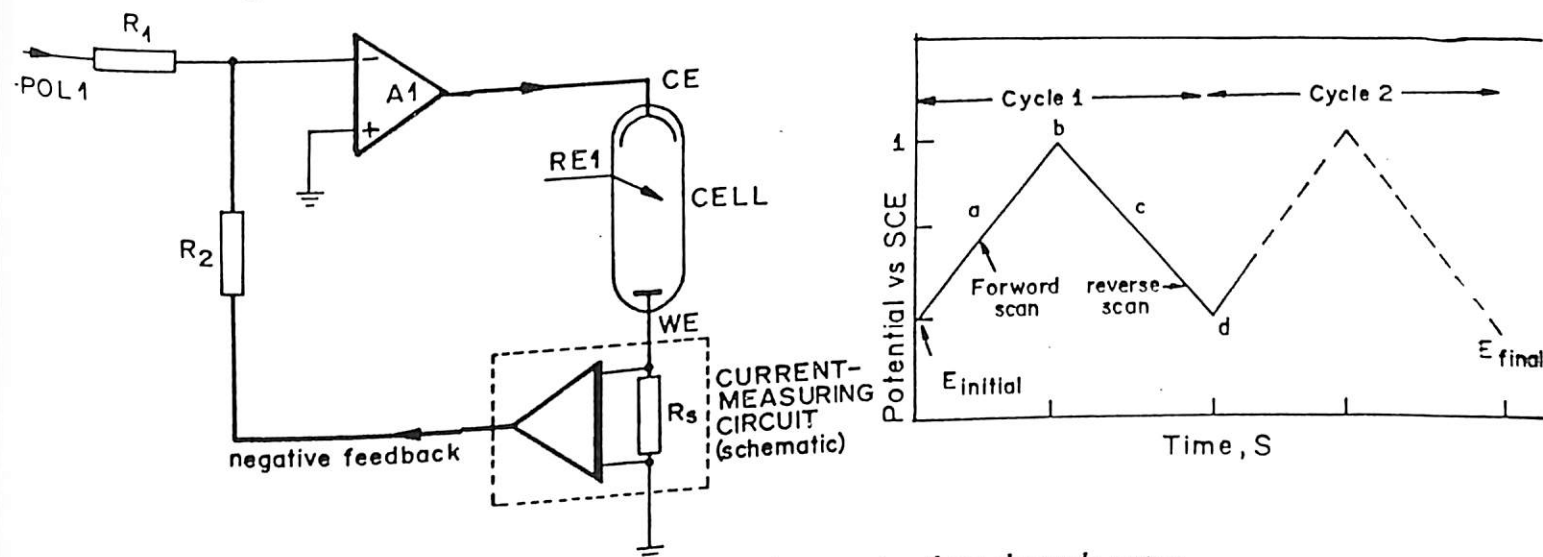

Fig.5   (a) Block diagram of an Electrochemical Set-up based on a using three electrode system, (b) Sweeping potential various from $E_{initial}$ (volts) to E_{final} (volts).

2.8 SCANNING ELECTRON MICROSCOPY (SEM)

SEM technique uses the intensity of secondary emissions (usually abroad energy distribution) of secondary electron. Some of these electrons that recombine with ions at the surface are the basis for the SEM imaging capabilities. The contrast in the image is a result of differences in scattering from different surface areas as a result of geometrical differences. SEM has been widely used for the visualization of organic surfaces, especially in the study of surface morphology, domains, pinhole defects and patterns [23]. Thin film of some of conducting polymers prepared during the course of the Ph D programme have been investigated using this technique. The (model Joel 35 CF) scanning electron microscope has been used for obtaining the a SEM pictures. The block diagram of a scanning electron microscope has been shown in fig.6.

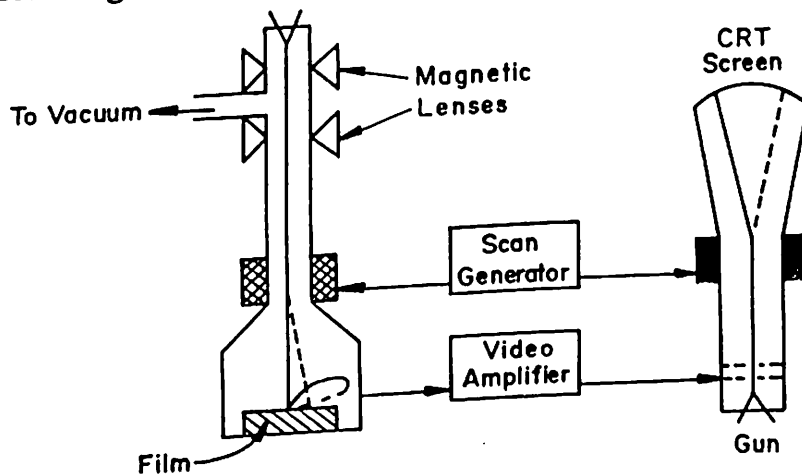Fig.6 Schematic arrangement of scanning electron microscope

2.9 OPTICAL CHARACTERIZATION OF CONDUCTING POLYMER FILMS

2.9.1 FOURIER TRANSFORM INFRARED SPECTROSCOPY

Infrared radiation is defined as the electromagnetic radiation whose frequency

varies between 14300 cm⁻¹ to 20 cm⁻¹ (0.7 -500 μm). Within this region of the electromagnetic spectrum, chemical compounds absorb IR radiation provided there is a change in dipole moment during a normal molecular vibration, molecular orientation, molecular rotation or from a combination of difference in overtones of the normal vibration. The frequencies and intensities of IR band exhibited by a chemical compound uniquely characterize the material and its IR spectrum can be used to identify and also quantify a particular substance in an unknown group[24].

FTIR technique presents a suitable solution that has found extensive application in material science. It converts the information from infrared frequencies, where specific detectors are unavoidable to audio frequencies and are able to track both frequency and intensity. An FTIR spectrometer makes use of three components such as a source, a Michelson Interferometer and a detector. It works on the collimated radiation from the broad band infrared source as shown in Fig.8.

The true transmittance obtained from the FTIR spectrophotometer is defined as:

$$T = (I_s/I_0)_v \qquad \text{Eq.8}$$

where I_s is the instrument response function (single beam spectrum) with the sample, I_0 is the response function without the sample and v is the frequency. If the sample is totally absorbing, no energy passes to the detector and the transmittance value is zero. The absorptivity of a substance being analyzed at the frequency v is a measure of the substance ability to absorb infrared at that frequency and translate it into molecular vibration energy.
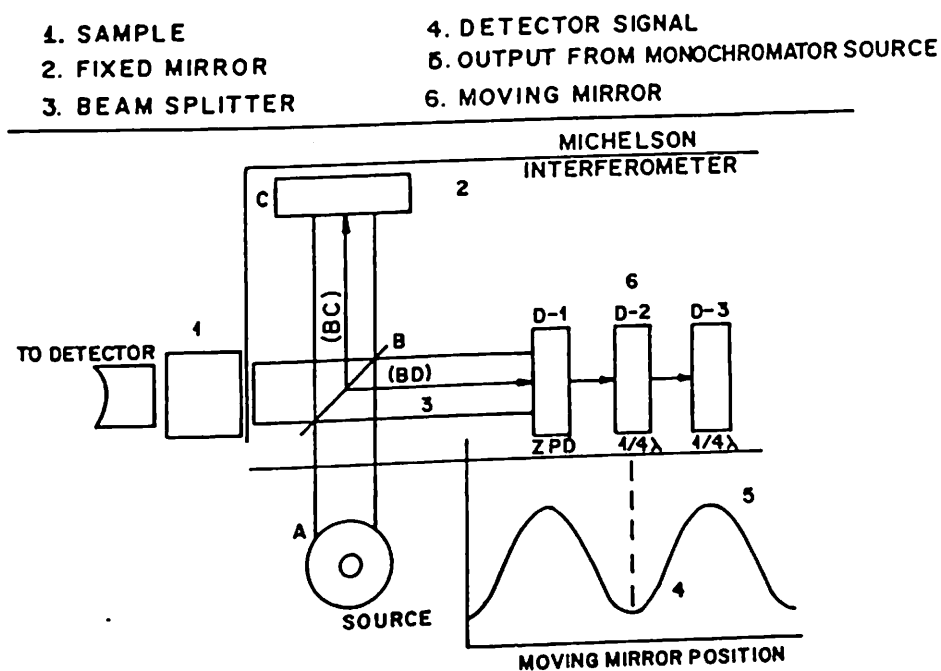
Fig.7 Schematic of an optical arrangement of a FTIR spectrophotometer

The conducting polymer films (for example PPY, PT or polyaniline etc.) have been investigated through appropriate subtraction of background and reference in reflection mode using a Nicolet FTIR spectrophotometer (model 510 P). Prior to the characterization of desired PPY , PANI and copolymer films, the FTIR spectrum (fig.8) of polycarbozole has been recorded [25-27]. The peak at 1230 cm^{-1} is due to dopant ions in polycarbozole. A broad peak at 3400 cm^{-1} occurs as a results of presence of N-H vibration. Interestingly, the FTIR spectrum is similar to that reported in literature.
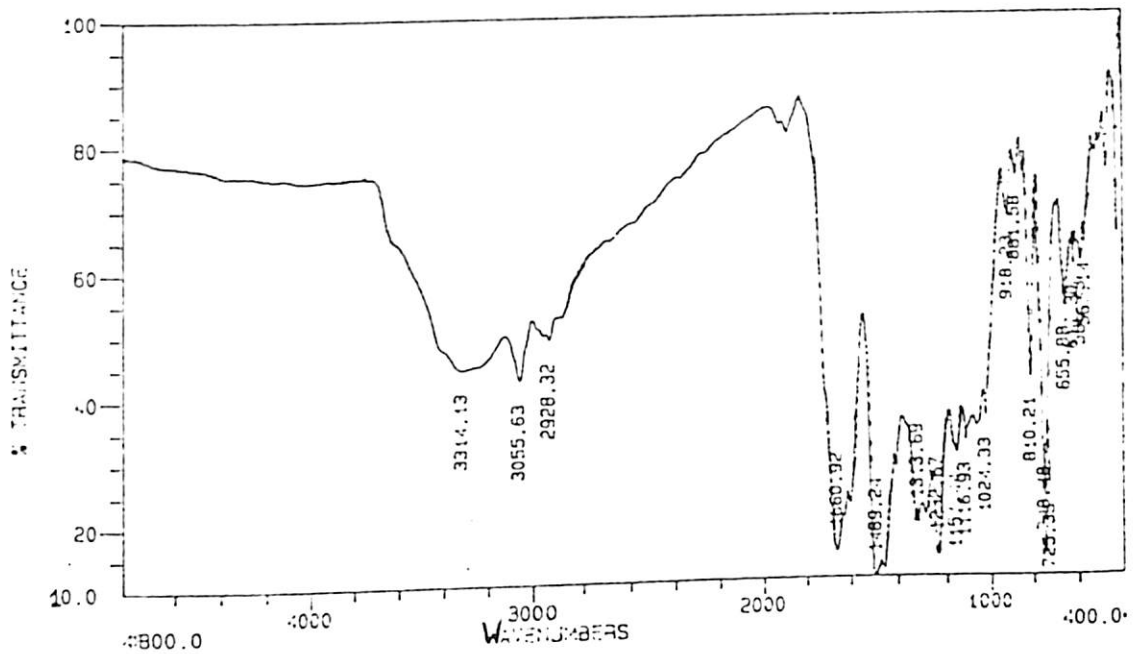
Fig.8 FTIR spectrum of BF$_4$ doped polycabozole film.

2.9.2 UV - Visible spectroscopy

Each crystalline amorphous semiconductor has characteristics of minimum photon energy for the direct interband transition. A semiconductor with a small number of free charge carriers results in the direct interband absorption and has thus been associated with electron transition from a filled band to an empty band. The minimum energy for such a transition is located at a critical point (M_0). If the matrix element (n, $M_{i,j}$) is non-zero at the critical point, the transition is allowed and the optical conductivity results. The ability to calculate electronic transition is given by Beer's law [27]:

$$I/I_o = e^{-\alpha .d} \qquad \text{Eq.9}$$

here I_o = incident light on the sample, I = amount of light that passes through the sample and strikes the detector, α = absorption coefficient for the specific sample at a specific wavelength.

$$\log I/I_o = \alpha .d \qquad \text{Eq.10}$$

where absorbance (ABS) = $\alpha .d$. As can be seen by the equation, the absorption of a

67

sample is directly proportional to the sample's thickness.

D$_2$: Deuterium lamp   W: Window plate

· WI: Halogen lamp   M$_1$–M$_5$: Mirrors, M$_3$ is a half-mirror

F: Filter   L: Lens

G: Grating   Sam: Sample cell

S$_1$: Entrance Slit   Ref.: Reference cell
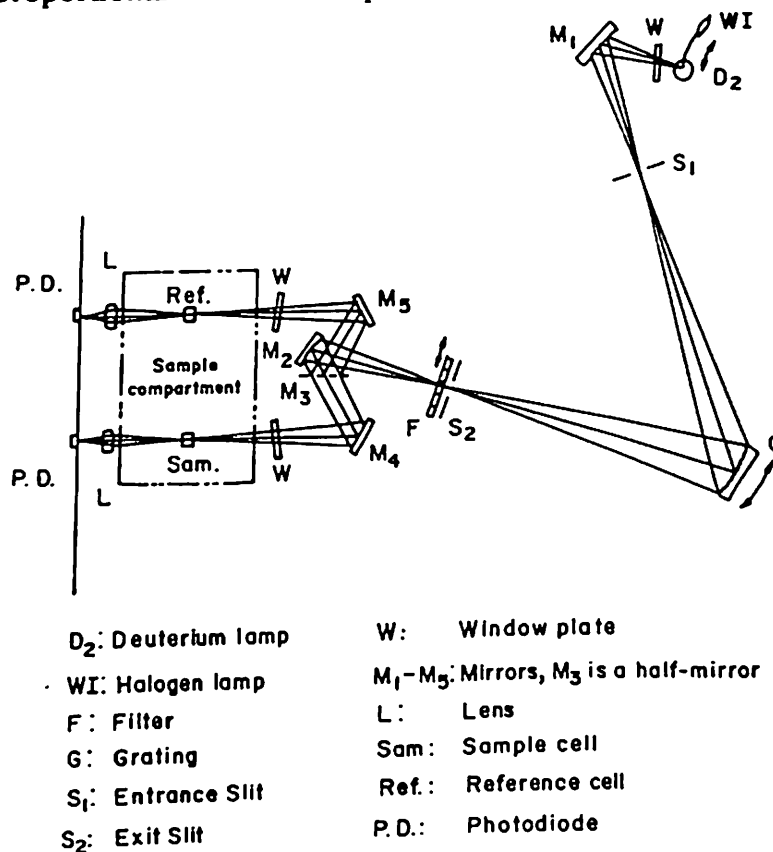
S$_2$: Exit Slit   P.D.: Photodiode

Fig.9   Schematic of an optical arrangement in UV-visible spectrophotometer.

The UV - visible spectra of various conducting polymer films prepared during operation of the Ph. D. programme have been measured by Shimadzu spectrophotometer (model 160 A). The sample and reference beams are detected by the photodiode detector, and are logarithmically converted. The difference is obtained by a differential amplifier and optical absorption signal is read by a central processing unit CPU. The full scale of A/D converter of 5 ABS to cover the measuring range of ± 2.5 A has been used in the Shimadzu UV - visible spectrophotometer. Schematic of an optical arrangement used in a UV - visible spectrophotometer has been shown in fig.9:

A UV - visible absorption curve obtained for polythiophene has been given in fig.10. It can be seen that this spectrum shows peaks at 480nm (2. eV) which is the characteristic of π - π^* interband transition. The peaks seen at 0.65 eV and 1.5 eV have been ascribed to the dopant induced levels that exit in the middle of the band gap [28].
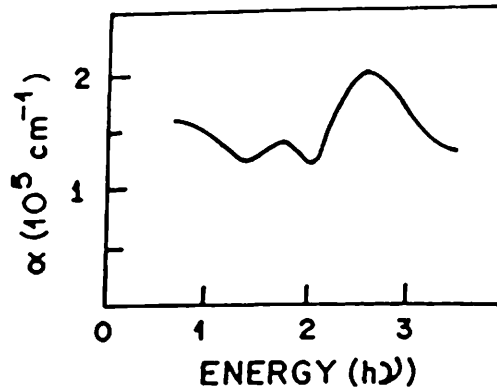
68

Fig.10 UV-visible spectrum of a polythiophene sample.

The optical absorption, $\alpha.d$ in a conducting polymer is proportional to $(h\nu - E_g)^{-1/2}$ as these are one dimensional lattices where $h\nu$ is the incident photon energy and E_g is the energy band gap. The density of states $(g_{n1}(E))$ indicates that $(\alpha . h\nu)$ is proportional to $1/(h\nu - E_g)^{1/2}$ hence can be written as:

and

$$g_{n1}(E) = L/\pi \ (\nu/2)^{1/2} \ (\ 1/(h\nu - E_g)^{1/2})$$ Eq.11

An estmate for E_g can be obtained by plotting $1/(\alpha . h\nu)^2$ vs the photon energy $(h\nu)$. A strong singularity occurs around the band gap E_g [29].
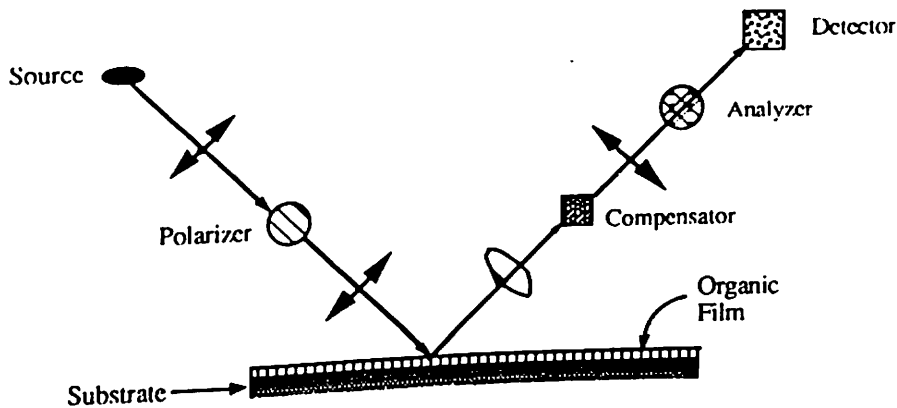
2.9.3 ELLIPSOMETRIC STUDIES

Fig.11 Schematic of an Ellipsometer

69

Ellipsometry is the common optical technique for the determination of the thickness, refractive index and optical dielectric constants of thin conducting polymer film. When a plane - polarized light interacts with a surface at some angle, it is resolved into its parallel and perpendicular components (S- and P- polarized, respectively). These components are reflected from the surface of a conducting polymer film such a way that the amplitude and phase of both components are changed. When S- and P- beams (polarized and reflected) are combined, the result is elliptically polarized light (fig.11) [30]. Ellipsometry uses this phenomenon to estimate the thickness of a conducting polymer film in air by measuring the ratio between r_p and r_s, the reflection coefficient of the P- and S- polarized light, respectively.

In a typical ellipsometer a monochromatic light (He - Ne) is plane polarized (p - angle of polarization) and impinges on the surface. A compensator changes the reflected beam that is elliptically polarized to plane polarized (a = angle of polariza-tion). The analyzer then determines angles by which the compensator polarizes the beam.

The two angles (p and a) give the phase shift between parallel and perpendicular components (Δ), the change in the ratio of the amplitudes of two components (tan ψ) can be expressed as under :

Eq.12

$$e^i \tan \psi = \{(E_{reflected}^{(p)}/E_{reflected}^{(s)})$$

$$/(E_{incidence}^{(p)}/E_{incidence}^{(s)}\}$$

where $\Delta = 2p + \pi/2$ and $\psi = a$. For a clean surface, Δ and ψ are directly related to complex index of refraction of the surface.

Eq.13

$$n^{\wedge s} = n^s (1 - i k^s)$$

where n^s is the ordinary refraction index and k^s is the extinction coefficient. The compensator is set at an azimuth angle of $70°$ and the experimental data are expressed

as $\delta\Delta = \Delta_o - \Delta$ and $\delta\psi = \psi_o - \psi$ and are the ellipsometric angles characteristic of the clean substrate Δ and ψ are measured for the substrate containing conducting polymer film. The refractive index, extinction coefficient, real and imaginary optical dielectric constant of both electrochemical Langmuir-Blodgett deposited films of polyaniline have been measured using ellipsometry technique.

2.10 ELECTRICAL CHARACTERIZATION

Electrical conductivity in general reflects, the net charge motion brought about by an electric field E. The value of electrical conductivity, σ can be expressed as:

$$\sigma = J / E = nq\mu$$

Eq.14

where J is the current density and E is the electric field, n is the carrier concentration of charge carriers (solitons, polarons or bipolarons) and μ is the mobility. It is necessary for a conducting polymer to contain an overlapping set of molecular orbits to provide reasonable carrier mobility along the polymer chain. DC conductivity (σ_{dc}) and ac conductivity (σ_{ac}) of a conducting polymer can be experimentally measured. DC conductivity (σ_{dc}) refers to the net charge which traverses the entire conducting polymer film. On the other hand, σ_{ac} is measured as a function of an alternating electric field. A difference in the behaviour of σ_{ac} is expected when conduction occurs by the motion of charge carriers in the extended states by hopping among localized states (such as solitons, polarons and bipolarons) or by transport between the metal particles embedded in host particles [31].

2.10.1 DC Conductivity

DC conductivity (σ_{dc}) depends upon the net charge flowing in the sample. σ_{dc} of a conducting polymer film can either be measured using two points probes or four-points-probe techniques described below:

(i) TWO POINTS-PROBE METHOD:

It is the simplest method for determination of σ_{dc} conductivity of doped conducting polymer films. The ohmic contacts desired such conducting polymer films can be made by vacuum evaporation of silver or gold. Electrical conductivity, σ_{dc}, can be estimated using the Eq. 15.

$$\sigma_{dc} = (a \,/\, t).(1/\,\rho) \qquad \text{Eq. 15}$$

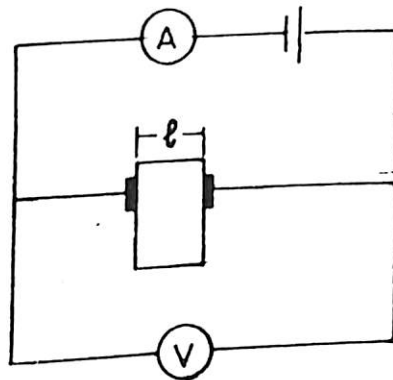where a is the area, t is the thickness and ρ is the specific resistance, respectively.

Fig. 12 Schematic arrangement for electrical conductivity measurements by the two points probe technique

(ii) FOUR -IN - LINE PROBE

The four - in - line probe is often used for the determination of conductivity of doped conducting polymer films or pressed pellets. It makes use of a special probe head which contains four equally spaced spring - loaded electrodes. The head is lowered into the sample until the four-points-probe makes good contact with the sample (fig. 13). A

72

constant current source is used to pass a steady current through the two outermost probes and the voltage drops across inner two are measured. The conductivity, σ_{dc}, of the sample can be calculated using the following relation.

$$\sigma_{dc} = (1 / 2\pi S).(I / V) \qquad\qquad \text{Eq.16}$$

where S is spacing between the probes (usually 0.1 cm), I is the current passing through outer probes and V is the voltage across inner probes. This formula is useful only when the sample thickness is made greater than the spacing between the probes. Further, it is assumed that conductive material is completely space filled. Since one often works with pellets made of compacted powder which contains void space, measured values of conductivities generally represent lower limits. Conductivity values thus determined on contacted powder pellets of polycrystalline materials can be as much as a factor of 10^2 less than that of completely space filled - single polycrystalline materials [31].

(iii) VAN DER PAUW METHOD

It is a technique used for measuring the conductivity of flat and thin samples of conducting polymers. Here four contacts, usually, equally spaced on the periphery of the sample using a conductive paste such as electrodag are made (fig.14). Four wires can be embedded into the periphery of the sample. Current is passed through two adjacent contacts while the voltage drop is measured across the other two. The Van der Pauw technique makes use of the following formula:

$$\sigma = (\ln 2 / \pi t).(I/V) \qquad\qquad \text{Eq.17}$$

where t is the thickness of the sample. The Van der Pauw formula can be used when the sample thickness is less than or comparable to the probe spacing [31].
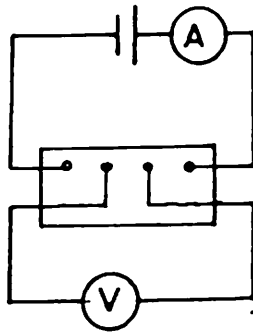
Fig. 13 Schematic diagram of four-
line-in probe for electri
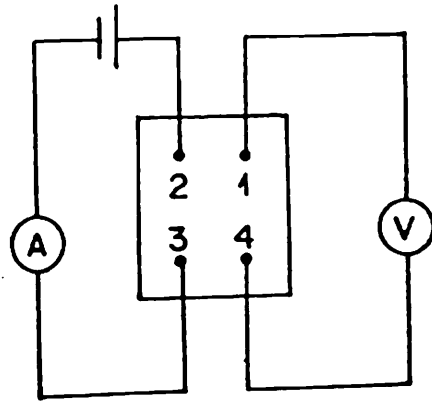-cal conductivity measurements

Fig. 14 Schematic diagram
for Van der pauw method
for electrical conductiv
-ity measurements.

2.10.2 AC CONDUCTIVITY MEASUREMENTS

When an electric field is applied across a given range, the latter dissipates a certain quantity of electric energy that transforms into heat energy. This phenomenon normally occurs at the expense or loss of power, meaning an average electric power (0.3) is dissipated in matter during a certain interval of time. The amount of power loss in a dielectric under the action of the voltage applied to it is commonly known as dielectric loss. The tangent of the loss angle is the ratio between the real dielectric constant(ϵ') and the imaginary dielectric constant (ϵ''). The complex dielectric constant can be expressed as:

$$\epsilon(w) = \epsilon'(w) - i \, \epsilon''(w)$$

Eq. 17

which is a function of radian frequency, $w = 2\pi f$ and loss factor, $(\tan\delta)$.

$$\tan\delta = \epsilon''(w)/\epsilon'(w)$$

Eq. 18

The strong dispersion can be repfresented in the form of:

$$\epsilon^{\bullet} = \epsilon_{-} + \epsilon_0 (\, \epsilon'(w) - i \, \epsilon''(w)$$

Eq. 19

$\epsilon'(w)$ can be calculated using:

$$\epsilon'(w) = C / C_0 = C / (\epsilon_0 \, A/d)$$

Eq. 20

74

where ϵ_0 is the space permitivity, A and d are the area and thickness of the sample. C is the measured capacitance at each frequency [32].

$$\epsilon''(w) = \epsilon'(w) \times \tan\delta \qquad \text{Eq.21}$$

The value of capacitance (C) and loss factor ($\tan\delta$) are measured at each frequency, f, from the impedance analyzer. The value of $\epsilon''(w)$ and $\epsilon'(w)$ are calculated using the Eq.20 and Eq.21, respectively.

A schematic of the measuring circuit integral impedance analyzer (HP 4192 A) is conceptually divided into three sub-sections: (1) the signal source, comprising of a reference frequency generator and an A4 tractional N-loop (2) the auto - balance bridge, comprising of the A1 range resistor/null detector and the A12 modulator (3) the vector ratio detector (VRD), comprising of the A2 phase detector/A-D converter and an all phase amplifier (fig.15). The instrument measures the capacitance as a function of frequency in the range of 5 Hz to 13 MHz. The voltage range for the application of bias varies from the -30V to +30V.
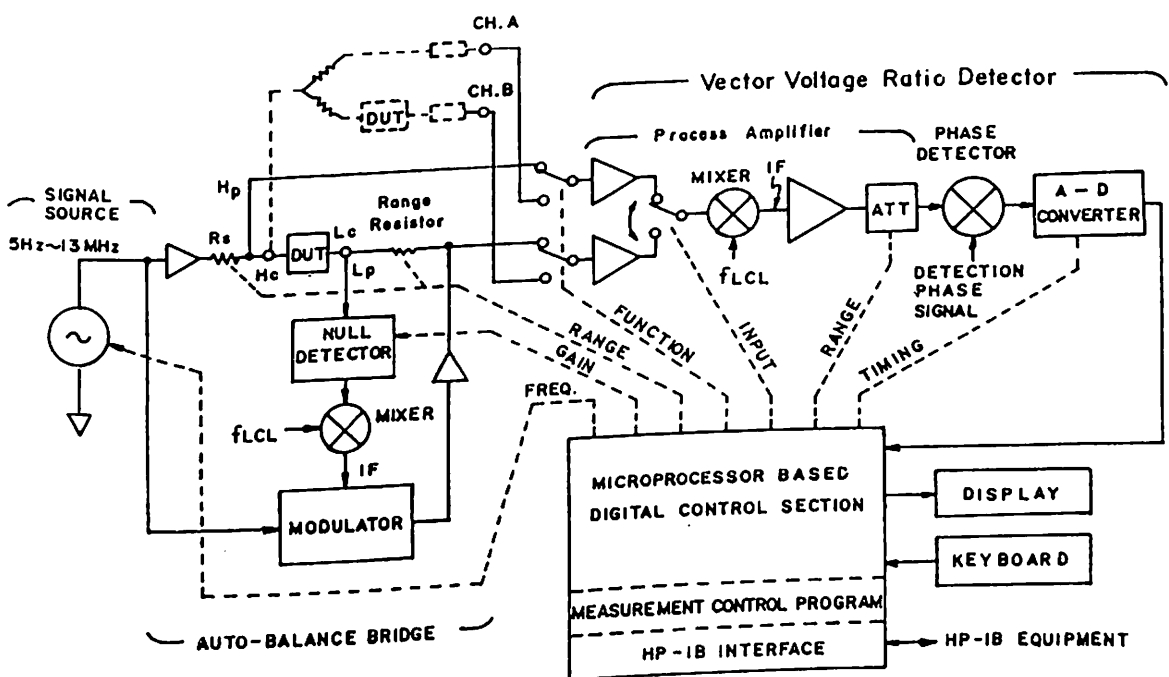

Fig.15 A schematic of a measuring circuit used for capacitance measurements as a function of frequency.

AC conductivity (σ_{ac}), has been measured as a function of frequency using the following relation :

$$\sigma_{ac} = \sigma_m - \sigma_{dc} = B \, w^s \qquad \text{Eq.22}$$

where σ_m is the measured conductivity, σ_{dc} is the conductivity of a desired conducting polymer sample, B is a constant and s is a constant lying between 0.5 to 1. DC conductivity (σ_{dc}) arises due to various band processes arising due to localized states within the gap. The measured conductivity can be calculated using the following formula [33]:

$$\sigma_m = 2 \pi \epsilon_0 \epsilon' \tan\delta \, f \qquad \text{Eq.23}$$

where ϵ_0, ϵ', $\tan\delta$ and f are space charge permitivity, real dielectric constant and loss factor obtained at a desired frequency (f). Eq. 23 has been used for an estimation of electrical conductivities of various conducting polymer films.

2.11 APPLICATIONS OF CONDUCTING POLYMER FILMS

2.11.1 SCHOTTKY DIODE

When a metal and a polymeric semiconductor with different work functions are brought into contact, a re-adjustment of charges takes place in order to establish thermal equilibrium and a potential barrier occurs in the interfacial region. This potential barrier is influenced by various phenomena such as formation of an interfacial layer or surface trapping centers at the interface. The potential barrier at a clean and ideal metal -

76

semiconductor contacts should be determined by the work function difference. The metal with lower work function such as Al, In and Pb etc., when brought in contact with p - type semiconductor eg BF₄ polypyrrole with a higher work function makes a Schottky diode [14]. The effective potential barrier seen by the holes in a p - type semiconductor with metal in contact is governed by the following Eq.24:—

$$\Phi_{bp} = E_g - (\Phi_m - \Phi_{sp})$$ Eq.24

Where Φ_{bp}, E_g, Φ_m and Φ_{sp} are as indicated in fig.16.

$$\Phi_m < \Phi_{sp}$$
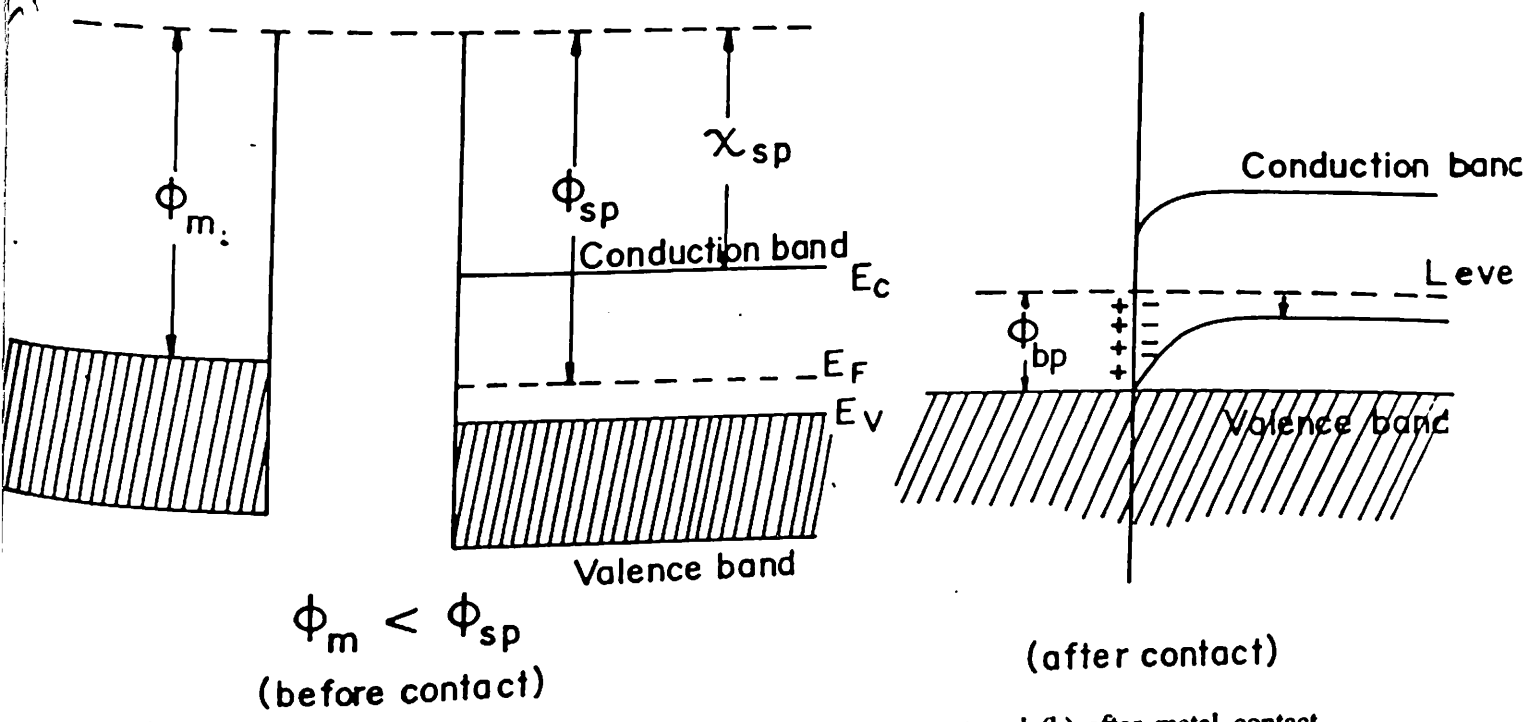(before contact)

(after contact)

Fig.16 Band diagram of a metal/semiconductor interface (a) before contact and (b) after metal contact.

X_{sp} is the electron affinity of given semiconductor given by:

$$X_{sp} = \Phi_{sp} + (E_v - E_F) - E_g$$ Eq.25

$$q V_c = \Phi_{sp} - \Phi_{sp}$$ Eq.26

$$q V_c = \Phi_{bp} - (E_v - E_F)$$ Eq.27

where V_c is the contact potential and Φ_{bp} is the potential barrier or barrier height. The value of the potential barrier can be obtained by current - voltage and capacitance - voltage characteristics including the temperature dependence of the saturation current.

Current - voltage characteristics of most semiconductor contacts can be described by the Richardson - Schottky equation:

$$J = j_0[(-qV/nK_BT - 1)]$$ Eq.28

J is the total current density, J_0 is the value of the reverse saturation current density, V is the applied voltage, n is the ideality factor or diode quality factor. K_B and T are Boltzmann constant and temperature. Such types of device display an exponentially increasing currents when the applied bias voltage is of the opposite polarity (reverse bias). The better rectification properties therefore correspond to a decrease in the value of the reverse saturation current density (J). For a semiconductor, J_0 can be readily correlated with the thermodynamic property of the interface and the barrier height of the junction. From the thermionic emission /diffusion theory, one can express J_0 as:

$$J_0 = A^{**} T^2 exp [(q\phi_b/ KT)]$$

The exp[-{ $q\phi_b$/ KT}], represents the Boltzmann factor relating the electron concentration at the semiconducting surface. A^{**} takes into account the effective density of states in the conduction band and the effective mass of the electron in the semiconductor, phonon scattering of the electrons between the top of the barrier and the metal surface as well as the quantum mechanical reflection at the semiconducting /metal interface. The electronic parameters that decide the performance of such devices are calculated by plotting lnJ vs V. The slope of these curves can be used to obtain the ideality factor (n), The barrier height (ϕ_b) can be calculated using the value of lnJ_0 obtained as an intercept.

The capacitance-voltage measurements on Schottky devices can be used to calculate the value of dopant concentration in a conducting polymer. This procedure is known as Mott -Schottky method[35].

$$1 \, / \, C^2_{diff} = 2 \, (V_C - V) \, /q \, A_0^2 \, \epsilon_0 \, \epsilon \, N_d \qquad \qquad Eq.30$$

where $A_\bullet$ is the differential cross - sectional area of the device, ϵ is the dielectric constant of the semiconductor, N_d is the dopant density and V_C is the contact potential. For simplicity it can be written as:

$$N_d = 2 \, A_0^{-2} \, / \, [\, e \, \epsilon \, \epsilon_0 \, \{ \, dV \, / \, d(1/C^2) \}] \qquad \qquad Eq.31$$

The slope of $1/C^2$ vs V plot gives the value of carrier concentration in a given conducting polymer film. The Schottky diode have been fabricated by the vacuum deposition of various metals onto a number of conducting polymer films.

2.11.2 METAL - INSULATOR - SEMICONDUCTOR DEVICES

Metal - insulator - semiconductor (MIS) diode is one of the most useful devices in the studies on semiconductor surfaces. Since the reliability and stability of most semiconductor devices are intimately related to their surface conditions. An understanding of the surface physics with the help of an MIS diode is of great importance for operation of a semiconducting device. MIS is also called the variable voltage capacitor or charge coupled device (CCD) and it works on the principle that the application of proper sequence (clock voltage pulses). A CCD can move quantities of electrical charge in a controlled manner across a semiconductor substrate. Using this basic mechanism, CCD can perform a wide range of electronic functions, including image sensing data storage, signal processing and logic operations [36].

For an ideal MIS diode energy difference between the metal work function ϕ_m and the semiconductor work function ϕ_s can be defined as:

$$\phi_{ms} = \phi_m - (X + E_s/2q + \Psi_B) = 0 \qquad \qquad Eq.32$$

where ϕ_m is the metal work function, X is the semiconductor electron affinity, X_i is the

insulator electron affinity, E_g the band gap, Φ_B the potential barrier between the metal and the insulator, Ψ_B the potential difference between the Fermi level E_F and the intrinsic Fermi level E_i. In other words, the band is flat (flat band condition) when there is no applied biasing conditions and those in the semiconductor and those with the equal but opposite sign on the metal surface adjacent to the semiconductor. There is no carrier transport through the insulator under dc biasing conditions or the resistivity of the insulator is infinity. MIS devices based on semiconducting polymers have been fabricated by the thermal evaporation of metals on Langmuir - Blodgett film of cadmium stearate. The capacitance- voltage measurements obtained as a function of frequency show that the flat band voltage condition and the accumulation to depletion and inversion regions by measurement of capacitance as a function voltage can be observed.

The energy - band diagrams of an ideal MIS have been shown in fig. 17 and 18:
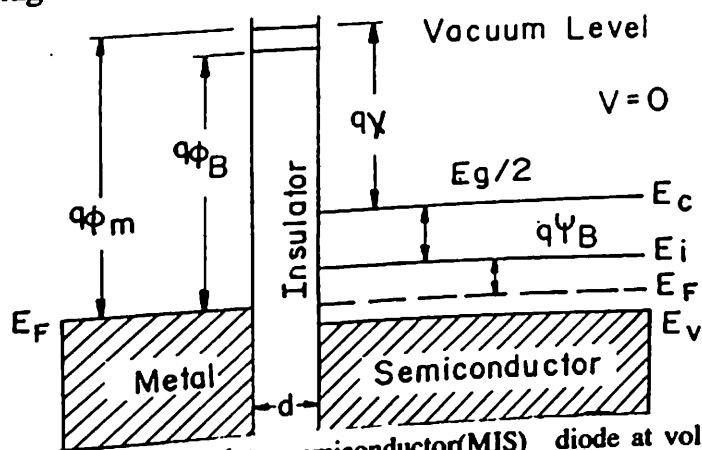

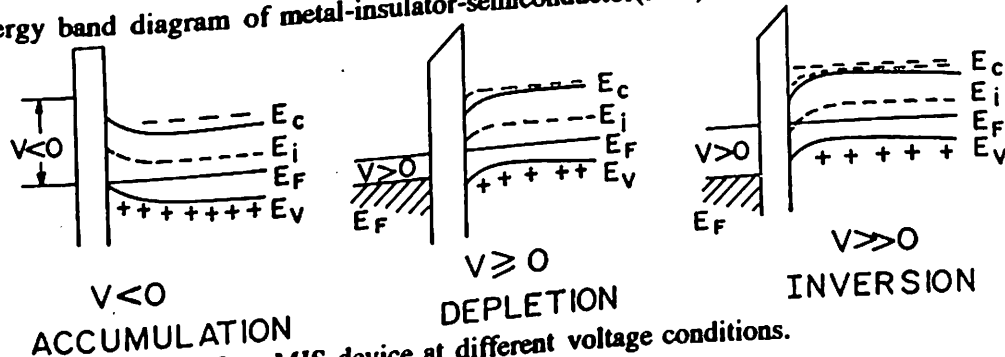Fig.17 Energy band diagram of metal-insulator-semiconductor(MIS) diode at voltage, V = 0V

V<0
ACCUMULATION

V $\geqslant$ 0
DEPLETION

V>>0
INVERSION

Fig.18.   Band diagram of an MIS device at different voltage conditions.

2.11.3 ELECTROCHROMISM

Electrochromism is the property of a material or a system to change color reversibly in response to an applied potential. The color contrast $[(I/I_0(D))]$ of an electrochromic device is characterized by change in electrically induced optical density in EC medium. The optical density change (ΔoD) arises due to an induced absorption usually as a broad band in the visible wavelength region [37]:

$$ I = I_0 = \exp(-\alpha(\lambda)) = \exp(-\Delta oD) \qquad \text{Eq.33} $$

The absorption coefficient $\alpha(\lambda)$ or absorbivity of EC medium can be very high. High color contrast can be achieved with on EC medium of small thickness (d). The electrochromism is based on the method of preparation technique, composition, stoichiometry morphology and structure. The control kinetics of coloration depends on the charge transport across the electrolyte/electrode interface. The barrier controlled process leading to the current voltage behaviour is governed by Bulffer-Volmer equation. If the diffusion in the electrolyte is the dominant process, the current density J can be expressed as :

$$ J = \pi^{1/2} \, n \, F \, D_0^{1/2} \, C_0 \, t^{-1/2} \qquad \text{Eq.34} $$

where n is the number of electrons participating in the reaction, F is the Faraday constant, D_0 is the diffusion coefficient, C_0^* is the concentration of redox species.

The semi-solid electrocromic cells based on PPY and polyaniline in glass / ITO / conducting polymer film / electrolytes/ ITO / glass configuration have been fabricated [35].A schematic arrangement for the measurement of transient current and photocurrent of conducting polymer films has been shown in fig. 19:
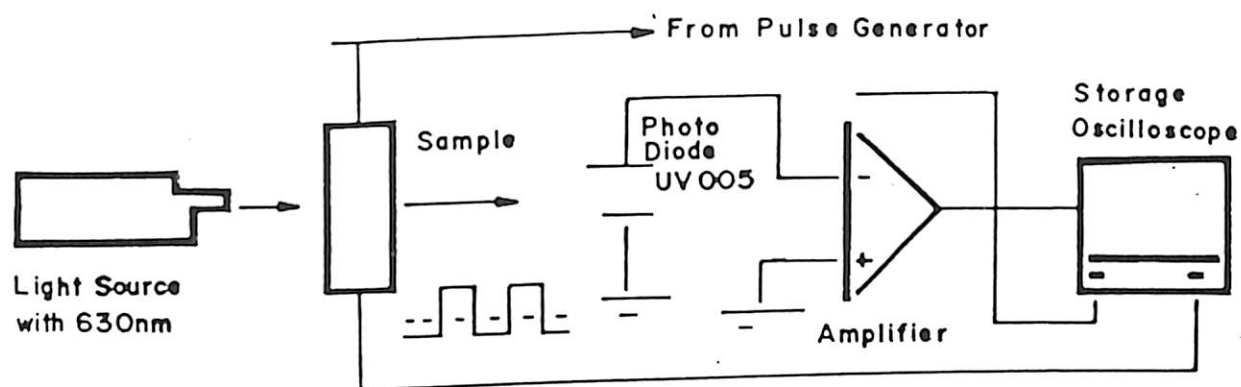
81

Fig. 19. Schematic of set up used for measurement of current transient of electrochromic cells based on conducting polymer films.

The next chapter describes the results of systematic studies in relation to preparation, characterization and applications of conducting polypyrrole films.

REFERENCES

1. G.B. Street, T.C. Clarke, K. Krounbi, P. Fluger, J.F. Rabolt and R.H. Geiss, *Polym. Prep. (Am. Chem. Soc. Div. Polym. Chem.)* **23** (1982) 117.

2. R. Qian, J. Qui, D. Shen, *Synth. Metals* **18** (1987) 13.

3. M. Springborg, *J. Phys. Conden. Matter* **4** (1992) 101.

4. J.C. Chiang, A.G. MacDiarmid, *Synth. Metals* **13** (1986) 193.

5. K. Seki, S. Asada, T. Mori, H. Tnokuchi, I. Murase, T. Ohnishi and T. Noguchi, *Solid State Commun.* **74** (1990) 677.

6. E.M. Genies, New J. Chem. **15** (1991) 5, K. Yoshino, K. Sawada and M. Onoda, *Jap. J. Appl. Phys.* **28** (1989) L1029.

7. K. Uvdal, L Logdlund, P. Dannetun, L. Bertilsson, S. Stafstorm, W.R. Salaneck, A.G. MacDiarmid, A. Ray, E. M. Scherr, T. Hjertberg and A.J. Epstein, *Synth. Metals* **29** (1989) E451.

8. R.A. Hann, In G.G. Roberts, (eds.), *Langmuir - Blodgett Films*, New York: Plenum (1990) pp 17-92.

9. M. Schmelzer, M. Burghard, P. Bauerl and S. Roth, *Synth. Metals* **61** (1993) 97.

10. Y. Cao, G.M. Treacy, P. Smith and A.J. Hegeer, *Appl. Phys. Lett.* **60** (1992) 2711.

11. A.P. Monkman and P. Adams, *Solid State Commun.* **78** (1991) 63.

12. A.F. Diaz, K. Kanazawa and G.P. Gardini, *J. Chem. Soc. Chem. Commun.* (1979) 635.

13. B. Speiser, A. Rieker and S. Pons, *J. Electrochem. Chem.* **159** (1983) 63; S.H. Glarum and J.H. Marshall, *J. Electrochem. Soc. Electrochemical Science & Tech.*, **134** (1987) 2160.

14. T. Kanetake, K. Ishikawa, T.Koda, Y.Tokura and K. Takeda, *Appl. Phys. Lett.* **51** (1987) 1957.

15. M.C. Petty, *J. Biomed. Eng.* **13** (1991) 209.

16. R.A. Hann, *Phili. Trans. R. Soc. Lond. A* **330** (1990) 141

17. G.L. Gaines, Jr. *Insoluble Monolayers at Liquid-Gas Interface*; New York; Wiley Interscience; 1966.

18. D.J. Walton, C.E. Hall and A. Chyla, *Analyst*, **117** (1992) 1305; D.S. Boudreaux, R.R. Chance, J.F. Wolf, L.W. Shacklett, J.L. Bredas, B. Themans, J.M. Andre and R. Silbey, *J. Chem. Phys.* **85** (1986) 4584.

19. M. Abe, O. Ohtani, Y. Umemoto, S. Akizuki, M. Ezoe, H. Higuchi, K. Nakamoto, A. Okuno and Y. Noda, *J. Chem. Soc. Chem. Commun.* (1989) 1736.

20. H.S.O. Chan, S.C. Ng, S.H. Seow, W.S. Sim, T.S.A. Hor, *J. Thermal Analysis* **39** (1993) 177.

21. A.J. Bard and L. R. Faulker, *Electrochemical Method: Fundamentals and Applications*, John Wiley and Son INC, (New York) (1980) pp 142.

22. R.N. Adams, *Electrochemistry at Solid Electrodes*, Marcel Dekker, New York, 1969.

23. A.P. Jansen, P. Akhter, C.J. Harland and J.A. Venables, *Surf. Sci.* **93** (1980) 453.

24. C.L. Ptzig, M.A. Leugers, M.L. Mackelvy, E.E. Mitchell, R.A. Nyquist, *Analytical Chemistry*, **64** (1992) 270.

25. G. Mengoli, M.M. Musiani and B. Schreck, *J. Electroanal. Chem.* **246** (1988) 73.

26. A. T. Efremova and L.D. Arsov, *J. Serb. Chem. Soc.* **57** (1992) 127.

27. H.H. Williard, L.L. Merriff Jr., J.H. Dean, F.A. Settle Jr. (ed), *Instrumental methods of Analysis* (sixth eds) CBS Publishers and Distributors, Jain Bhawan, Delhi (INDIA) pp: 10.

28. A.O. Patil, A.J. Heeger and F. Wudl, *Chem. Rev.* **88** (1988) 183; J.C. Chung, J.H. Kaufman, A.J. Heeger and F. Wudl, *Phys. Rev. B* **30** (1984) 702.

29. A.J. Heeger, S. Kivelson and J.R. Schrieffer, *Reviews of Modern Phys.* **60** (1980) 781.

30. R.M.A. Azzam, N.M. Bashara, *Ellipsometry and Polarized Light*; North - Holland Publishing company, Amsterdam (1977); J.O. Birzer, H.J. Schulzer, *J. Colloid Polymer. Sci.* **264** (1986) 642.

31. R.L. Elsenbaumer and L. Shacklette, (ed. T.A. Skotheim), *Hand Book of Conducting Polymer*, **Vol. I** , (Marcel Dekker, NC), New York (1986) pp: 213.

32. N.F. Mott and E.A. Davis, *Electronic Process in Non- Linear Crystalline Materials*, 2nd Edn., Clarendon press, Oxford, 1979.

33. W. Rehwald, H. Keiss and B. Binbbali, *Z. Phys. B* **68** (1987) 143.

34.   S.M. Sze, *Physics of Semiconductor Devices*, 1st and 2nd Edn, Wiley, New York, 1969 and 1981.

35.   E. H. Phoderick and R. H. Williams, *Metal/ Semiconductor Contacts contacts, Metal/ Semiconductor Contacts*, Clarendon Press, Oxford, 1988.

36.   J.H. Burroughes, C.A. Jones and R.H. Frind, *Nature*, **335** (1988) 137.

37.   B.P. Jelle, G. Hagen, S. Sonde and R. Oxford, *Synth. Metals* **54** (1993) 315.

CHAPTER III

both good thermal and mechanical properties with air and water stability [10]. The availability of unique electrochemical synthesis for the preparation of polypyrrole films by Diaz et al [11] have provided access to a variety of electrical and modern analytical tests that are well known chemical oxidation products of pyrrole, namely, the amorphous, insoluble polypyrrole black films [12]. Besides this, polypyrrole has been extensively used for a variety of applications owing to its stability and superiority in redox process [13].

Polypyrrole films are generally obtained by electrochemical polymerization of pyrrole monomer. The polymerization reaction proceeds via radical cation intermediates. It has been shown a such, that reaction is sensitive to the nucleophilicity of the environment in the region near the electrode surface [14]. This then places some limitations on the choice of the solvent and electrolyte. Many of the reported studies have been performed in aprotic solvents which are poor nucleophilics. Among these, acetonitrile, propylene carbonate, methylene chloride, tetra hydro furan (THF), methanol etc. have been used for the preparation of conducting polypyrrole films [15]. Polypyrrole films have also been synthesized in nucleophilic solvents such as dimethyl formamide and dimethyl sulfoxide etc with the addition of pyrotic acids which decreases the nucleophilicity of the solvents. The electropolymerization of polypyrrole has also been carried out in aqueous media. The polypyrrole films so obtained are however, of poorer quality with lower conductivity. Later, these have been electrochemically synthesized by a mixture of water and aprotic solvents such as alcohol and have been found to possess intermediate electrical conductivity and good mechanical strength [16]. From time to time the solvent has been changed for obtaining polypyrrole films by varying mechanical, electrical and optical properties. The thick polypyrrole films obtained by A. F. Diaz et al [16] have been prepared in aqueous acetonitrile solvent mixture.

87

The conductivity of such polypyrrole films has been found to lie from 100 to 0.5 S/cm and has been seen to depend upon the anion content (1% to 33%) [17]. The polypyrrole films containing with 1% water and 99% acetonitrile are found to be seven times stronger than those obtained using a mixture of 25% water and 75% acetonitrile [18]. The band gap and mechanical strengths of various polypyrrole films have been found to be decreased and are seen to depend upon the nature of solvent such as ethylene glycol, acetonitrile and water [17]. The conductivity of polypyrrole films synthesized in propylene carbonate with tetraethyl ammonium tetrafluoroborate (TEATFB) and para-toluene sulphonate (PTS) electrolytes have been found to have excellent electrical conductivity and optical properties [19].

When polypyrrole films are in conducting forms, the anions which are affiliated with the cationically charged polymer chains have been found to be 10 - 35% by weight. The anions such as tetrafluroborate, hexafluroarsenate, perchlorate, hydrogen sulphate, p-toluene sulphonate etc. are poorly nucleophilic and permit the formation of good quality films. The level of oxidation of pyrrole is 0.25 - 0.32 per pyrrole unit, corresponding to one anion for every 3 - 4 units [17]. It can be remembered that an intrinsic characteristic of the polymer of the anion. The successive use of different anions such as p-toluene sulphonate, perchlorate and fluroborate etc. not only affect the electrical properties but also the structural characteristics of polypyrrole films. G. R. Mitchell [20] has investigated the role of counter - ion which influences the molecular order in conducting films of polypyrrole films including the chain configuration. The anion influences both the electronegativity and the electrical conductivity of the polypyrrole films.

In the present thesis conducting polypyrole films both in aqueous and

non-aqueous media have been respectively prepared. The thermal, electrochemical, structural, optical and electrical properties of these polypyrrole films have been systematically investigated.

3.2 GENERAL PROPERTIES OF POLYPYRROLE (PPY) FILMS

Polypyrrole has generally been considered to belong to the class 1- dimensional polymers having a polyene backbone. In the electronic structure of polypyrrole, π -band is delocalized along the chain with equidistant carbon positions, a metallic behaviour is thus expected. This behaviour is overcome by the stabilization of the chain in dimerized form [19]. Due to the dimerization and symmetry breaking caused by the presence of nitrogen atom, the uppermost π- band is back folded and a gap of about 3.0 eV is opened [21]. Excited states of this system are believed to be polaronic. Polaron with a relaxation of the structural geometry of the polymers towards a quinoid form extend over four pyrolytic rings. The polarons (spin 1/2) are situated at 0.54 eV from the band edges [22]. Theoretical calculations have demonstrated that the formation of a polaron is most favorable energetically in conducting polypyrrole. This type of electronic structure is representative of a 1 - dimensional polymer with a non-degenerate ground state.

When a second electron is removed from the polymer chain, a bipolaron is formed which can be defined as a pair of like charges associated with a strong localized distortion which again extends over four pyrolytic rings. ESR studies by F. Genoud et al [23] have shown the existence of bipolarons in a PPY film. It basically arises due to the apparent lack of correlation between the spin characteristics and the conductivity

wherein it has been concluded that the species responsible for conductivity do not have spin. The formation of a bipolaron is also supported by the calculation which shows that the formation of a bipolaron is thermodynamically more stable than two separated polarons, despite the coulombic repulsion between the two charges defined in the same site. Because of the strong electron - phonon coupling the charge carriers that are produced on the polymer chain by doping takes place the form of polarons/bipolarons [24]. ESR and optical measurements have shown that doping initially creates polarons but as the doping level increases polarons combine to form more stable bipolarons.

Insolubility of polypyrrole in organic solvents has demonstrated that it is not a processable polymer. Films of conducting polypyrrole have a high electrical conductivity varying between 10 to 100 S/cm^{-1} and are black in colour. Raman and IR spectroscopy studies have confirmed the presence of pyrrole ring in the structure. Solid state ^{13}C NMR studies indicate α -α' coupling. The values of ESR line width H_{pp} in case of undoped polypyrrole have been found to vary from 0.2 to 0.3G. The ESR spectra of neutral polypyrrole presents two distinct lines such as a narrow peak with $H_{pp} \approx 0.4$ G and a broad band width $DH_{pp} \approx 2.8G$. The total intensity of about 10^{20} spins per gram has been observed. The perchlorate doped polypyrrole ($\sigma \approx 1$-20 S/cm) exhibits a strong ESR intensity of 5×10^{20} spins per gram and narrow ($DH_{pp} \approx 0.39$ G) ESR signal. These results imply that the ESR signal does not arise from the same species which carries the electric current [25]. The concentration of charge carriers is unrelated to the esr intensity and its correlation unrelated to the linewidth and the value of the carrier mobility has been obtained. This has been interpreted in terms of the formation of bipolarons upon doping, which can carry current by hopping but are diamagnetic. It has been concluded

that esr spectra of these systems are due to neutral radicals and reveal little about the intrinsic processes of conduction in doped polypyrrole system.

The thermal ageing of polypyrrole films at different temperatures has been studied from time to time. The conductivity of polypyrole/ p-toluene sulphonate film has been found to decrease with increasing temperature. The anions like BF_4, ClO_4 are found to be poorly nucleophilic and permits the formation of a good quality polypyrrole film. Due to the hygroscopic nature of polypyrrole film, 5 - 7% of moisture is removed when dried at 110°C [26]. At this juncture the conductivity of polypyrrole film also decreases. It has been shown that the persistent structural disorder in polypyrrole results in both the metallic and semiconducting behaviour of this interesting material. It is hoped that the work described in the present chapter of the thesis will lead to an understanding of the mechanism of conduction processes including structural, electrical and optical properties of polypyrrole that may perhaps be useful in improving its stability. Besides this, the results of these systematic studies may lead to the potential application in the conducting polypyrrole films [27].

3.2.1 OPTICAL PROPERTIES OF PPY FILMS

The optical properties of conducting polypyrrole are strongly influenced by the presence of anions in the polymer matrix. The optical absorption of the neutral PPY has bands at 3.2 eV and 1.3 eV, respectively. When it is exposed to air, the peak height of 3.2 eV peak decreases and the absorption peak at 1.3 eV increases due to its oxidation by oxygen. The absorption spectrum of oxidized polypyrrole film shows broad bands near 1.0 eV attributed to the conduction electrons. The peak near 3.0 eV is associated with an interband transition derived from the $\pi - \pi^*$ transition in polypyrrole [28].

91

The optical absorption studies of polypyrrole doped with perchlorate (ClO_4^-), tetrafluroborate(BF_4^-), hydrogen sulphate (HSO_4^-) and arsenic hexafluoride (AsF_6^-) etc., have been conducted. As-grown perchlorate doped polypyrrole films have absorption bands at 1.0 eV, 2.7 eV and a weak shoulder at 3.6 eV. The most strong reduced polypyrole has a band at 3.2 eV and a shoulder at 4.5 eV. The red shift of the 2.7 eV peak to 3.2 eV is also seen due to a more facile reduction of polypyrrole films. The optical absorption peaks obtained at 0.7 eV and 2.1 eV in polypyrrole have been attributed to the presence of polarons whereas the peak at 1.4 eV is related to the presence of bipolarons. With higher doping level it has been seen that 1.0 eV and 2.7 eV peaks arise due to the formation of two bipolaron bands [29-30]. It has been shown by J. H. Kaufman et al [31] in their insitu electrochemical optical absorption studies of polypyrrole that the recombination of polarons results into formation of bipolarons. High - energy - loss spectroscopy studies have shown that bipolaron model can be used to explain the electron band structure as a function of oxidation [32]. The values of optical dielectric constant at low energy (0.1 eV) has been measured to be 2.5 which is typical for a polymer. The optical dielectric data obtained by ellipsometric measurements of polypyrrole fibrils are in agreement with the spectroscopic measurements.

The insitu polymerization of polypyrrole can be studied through UV - visible spectroscopic studies [3]. The optical properties of conducting polypyrrole depend upon the processing parameters, the type of dopant and the annealing temperature etc.. For the fabrication of any device, the energy band gap, resistivity and structure of a polymer (polypyrrole) should remain constant in different ambients and should not show any significant variation with time.

3.2.2 ELECTRICAL PROPERTIES OF PPY FILMS

The effect of doping on polypyrrole film has been carried on the electrical properties of this conducting polymer. The electrical conductivity σ, of polypyrrole increases slowly upto about 1% of doping with an increase in ESR signal after which its value shows a continuous increase until it has accepted about 2.5% of available charge. The decrease in the intensity of ESR signal with an increase in the doping level of polypyrrole beyond 2.5% cannot be correlated with the corresponding large increase in the value of electrical conductivity. These results cannot be explained on the basis of conventional band theory of solids. It has been shown that difference in the conductivity arising due to the number of sulphonate groups in a dopant molecule has been attributed to the low concentration of polarons in the films. At high doping levels (5%), the evolution of bipolarons occurs and the transport of electrical charge in conducting polypyrole may either be via diffusion of the bipolarons or through the hopping of charge carriers in the bipolaron sites[34].

Like most non-degenerate ground state polymers, bipolarons appear to play significant role in the observed metal - insulator transition in PPY film. DC conductivity measurements have been conducted in both undoped and doped polypyrrole films at low temperatures. The observed phenomenon has been described to the hopping of charge carriers via bipolarons[35]. It should be interesting to experimentally determine the value of dc conductivity (σ_{dc}) of highly doped and lightly doped polypyrrole films with tetrafluroborate radical ions. The exact charge transport mechanism in conducting polypyrrole is still being actively investigated by researchers engaged in this field.

AC conductivity (σ_{ac}) data obtained in the lightly doped polypyrrole has been interpreted using Kivelson's model. In lightly doped polypyrrole, the electric conduction

process is dominated by the phonon assisted electron hopping between polarons and bipolarons states [136]. Extensive theoretical and experimental studies have shown that doping of polypyrrole leads to the formation of localized charged defects on the chains, bipolarons being favoured over single polarons. It has been revealed that p-toluene sulphonate doped polypyrrole films show 2-dimensional variable range hopping between polaron and bipolaron states [20,37]. It has also been shown that p-toluene sulphonate doped polypyrrole films exhibit 2D variable-range hopping model $(T^{-1/3})$ instead of variable range hopping $(T^{-1/4})$ law. It has been brought out that any variation in the fabrication of a polypyrrole film results in variation in the value of the electrical conductivity including the mechanism of charge transport. The total measured electrical conductivity of lightly doped polypyrrole film has been seen to exhibit two types of relaxation mechanisms dependent upon both frequency (100 KHz to 10 MHz) and temperature (77K to 350K) [138].

Charge transport in polypyrrole is not yet completely understood as it possesses a high degree of disorder and exhibits both semiconducting and metallic behaviour. Extensive theoretical and experimental studies show that doping of polypyrrole leads to the formation of localized charged defects on the chains, bipolarons being favoured over single polarons.

3.3 APPLICATIONS OF POLYPYRROLE FILMS

Polypyrrole finds a variety of applications such as in rechargeable batteries, electrochromic displays, gas sensors, Schottky diode, PN diode, etc. The use of the conducting polypyrrole as gas - sensing elements has been reported for detection of ammonia (NH_3), nitrogen dioxide (NO_2) and alcohol [39, 40]. As already mentioned,

94

polymerization of polypyrrole can be achieved in aqueous solution at pH level that do not damage biological materials. This allows use of polypyrrole as an entrapment medium for the fabrication of biosensors. This has been applied in particular to the glucose sensors based on glucose - oxidase (an enzyme). The secondary battery using PPY as cathode material and lithium as an anode electrode has been marketed by - Bridgestone and Allied signal, respectively. The electrolytic capacitors based on polypyrrole films are essential component in most areas of electronics. The solid electrolyte condenser based on PPY has also been fabricated.

With this as a motivation, the experiment pertaining to the studies on the e of annealing, and resistance, surface morphology and optical studies on BF$_4^-$ doped polypyrrole films have been carried out and described in this chapter. It should thusinteresting to investigate the charge conduction mechanism in the BF$_4^-$ doped polypyrrole films. Space charge relaxation stim polypyrrole film may be useful in delineating the motion of charge carriers. The Schottky devices based on PPY doped with BF$_4^-$ have been reported [28]. An attempt has been made towards the fabrication of metal / semiconductor device using the electrochemically deposited polypyrrole in aqueous medium. Besides this, fabrication of electrochromic displays based on PPY in organic medium has been undertaken.

3.4 ELECTROCHEMICAL SYNTHESIS OF POLYPYRROLE FILMS IN NON-AQUEOUS AND AQUEOUS MEDIA :

Polypyrrole films have been electrochemically synthesized using galvanostatic method in a vessel consisting of a three electrode cell comprising of an indium - tin -

oxide (ITO) electrode (resistivity ≈ 10 Ω.cm) as an anode, a platinum foil as a cathode and Ag/ Ag⁺ as a reference electrode. Ultra pure reagents, pyrrole(0.1 M) as a monomer, tetra - ethyl ammonium tetra fluroborate (0.1 M) as supporting electrolyte in 30 ml of propylene carbonate have been used for the electrochemical synthesis [41]. All chemicals have been procured as described in sec.2.1 of the Chapter II. Current density of 0.3 - 0.5 mA/cm² for 30 to 45 minutes has been used during the electrodeposition for 30 to 45 minutes for obtaining self supporting polypyrrole films.

For measurements of UV-visible absorption spectra, PPY on ITO glass has been deposited by varying the time period from 30 sec. to 2 minutes. The thickness (2 to 40μm) of polypyrrole film is dependent on the amount of charge passed during electro-polymerization.

The same set of electrodes has been used for electrochemically prepared PTS-doped polypyrrole films using 0.1 M of sodium salt of p-toluene sulphonic acid, 0.1 M pyrrole and 30 ml of deionized water. The current density of 0.3 mA/cm² has been used for 30 to 45 minutes for obtaining free standing films of polypyrrole. It may be mentioned that the temperature of the cell has been maintained at 4-5 °C. Polypyrrole films when treated with aqueous ammonia (NH₃) for 24 hours results in their being undoped.

3.4.1 MECHANISM OF ELECTROCHEMICAL POLYMERIZATION OF POLYPYRROLE FILMS

The mechanism of electrochemical polymerization of pyrrole in general, consists of the following steps as represented (fig.1) [14].

96

STEP 1.

STEP 2.

STEP 3.

STEP 4.

STEP 5.
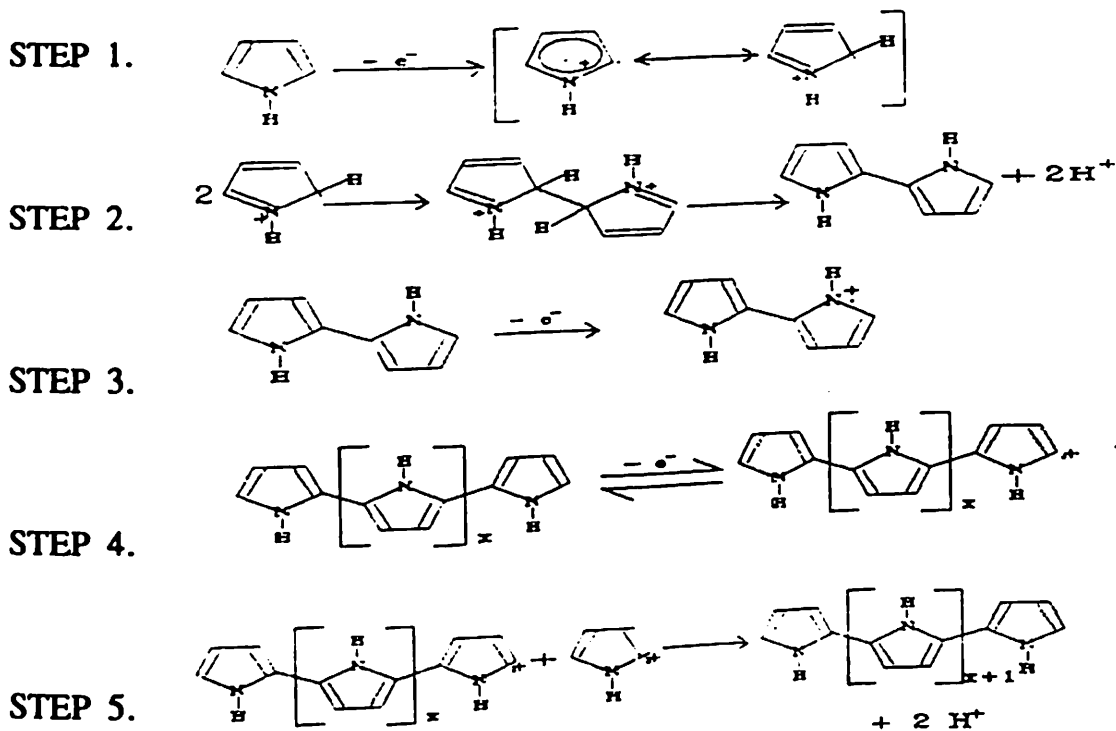
Fig. 1 Mechanism of electrochemical polymerization of polypyrrole

Step 1 relates to the oxidation of the monomer to a radical cation. In step 2 dimerization of the radical cations followed by a proton loss yield's a neutral dimer. Next oxidation of dimer to its radical cation (step 3). Step 4 shows the oxidation of radical cation with another cation. In step 5, the formation of polypyrrole results as a consequence of more repeating successive unit.

Under steady - state conditions, the coupling reaction occurs between the radical cations of pyrrole and the radical cations of the oligomer. Compared to the dimer, trimer and the polymer states, the polymers are more easily oxidized than monomers. Therefore, these will also be present in the oxidized states and not in the neutral form during the polymerization reaction. In such conditions, the current depends upon the rate of diffusion of pyrrole to the region of the electrode. With regards to the subsequent

97

aromatization reaction, the various steps leading to the formation of polypyrrole moieties are not as yet known.

The oxidation and reduction reactions can be studied by cyclic voltammetry. Cyclic voltammetry is an electroanalytical technique used to delineate the cause of electroactivity and the electrochemical properties of polypyrrole films because it can better describe the characteristics of electrochemical switching behaviour. Fig.2 shows the cyclic voltammogram of a 0.3 μm thick film of PPY that has been obtained at a scan rate of 20 mV/sec in propylene carbonate solution with 0.1M tetra ethylammonium fluoroborate (TEATFB). Initially, -0.8 volt has been applied with reference to Ag/Agcl for the complete reduction of a such polypyrrole film and then cycled between -0.8 to 0.6 V. The oxidation potential of tetra eltylammonium tetra fluoroborate has been determined as -0.2 V for a PPY film. The reduction reaction occurs at -0.3V in the cathodic sweep, suggesting that the kinetics of the two reactions are different. It has been further seen that the oxidative and reductive changes of a PPY films are independent of scan rate [42]. The cathodic peaks are significantly broader than the anodic peaks. It has been revealed that PPY is completely reduced at -0.8 V and is subsequently oxidized at 0.4V. It may be mentioned that the shape of the cyclic voltammogram has been found to be dependent on the nature of BF_4^- ions in the electrolyte which suggests that the kinetics of the electron transfer process is primarily limited by diffusion of counter ion in the polypyrrole film. The doping and undoping effect can further be studied by using the optical measurements on PPY films [43].
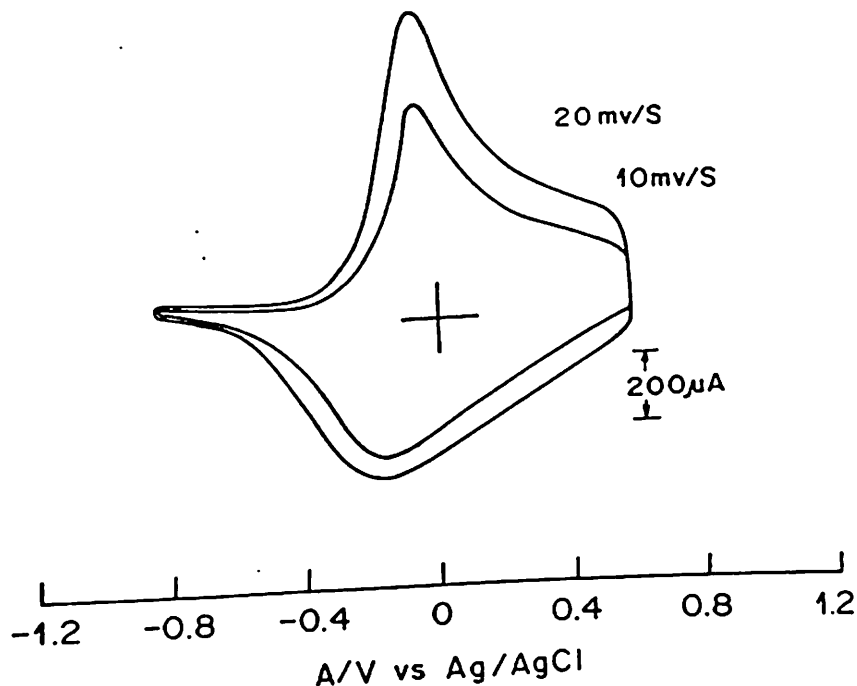
Fig.2 Cyclic voltammogram of 0.3 µm thick polypyrrole film, scan rate 10 and 20 mV/s in 0.1M TEATFB in propylene carbonate.

3.5 OPTICAL PROPERTIES OF POLYPYRROLE FILMS :

3.5.1 FTIR STUDIES

Fourier-transform infra-red (FTIR) and UV-visible spectroscopy studies have been performed to characterize both the conducting and neutral states of polypyrrole films. FTIR provides in details the molecular properties of pristine and doped polypyrrole films. FTIR spectra of polypyrrole not only reveal the structural evidence but also the mechanistic view related to the process of conduction.

FTIR studies of various polypyrrole film have been conducted using Nicolet FTIR (model 510 P) spectrophotometer. Various spectra of PTS and BF$_4^-$ doped and undoped polypyrrole films have been recorded following the standard method mentioned in literature [29,31].
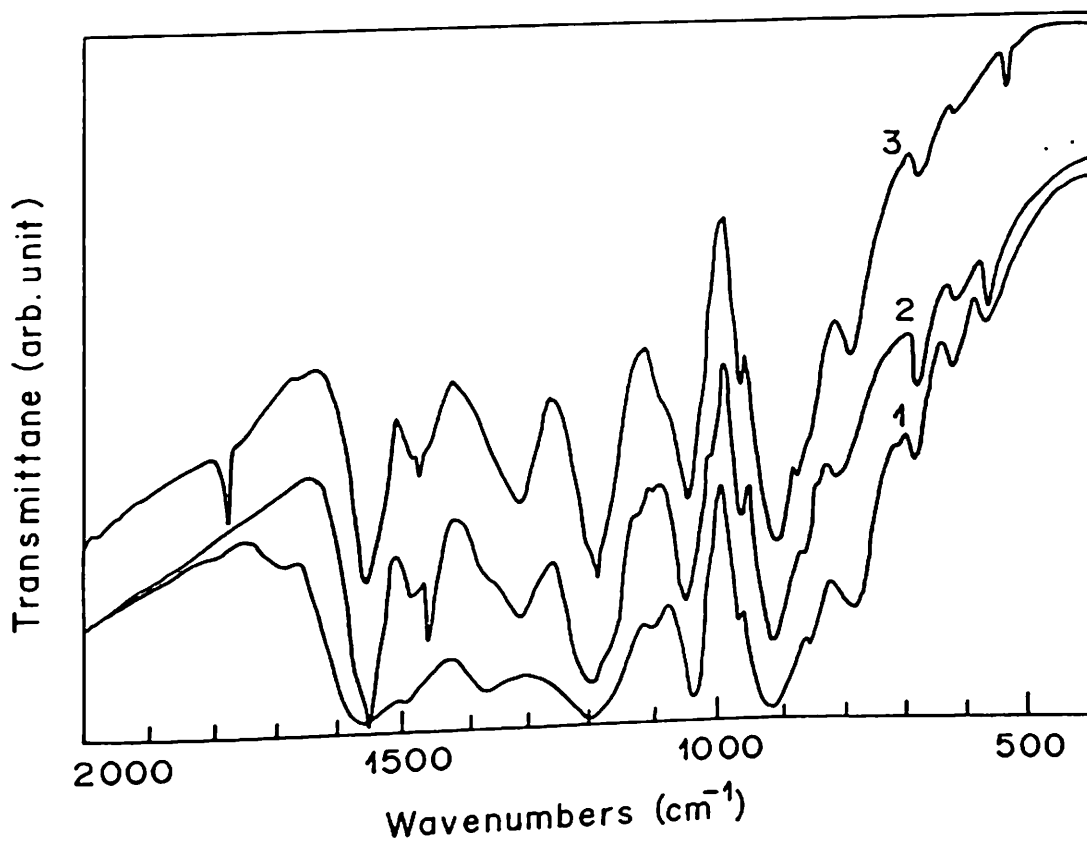
Fig.3   FTIR spectra of polypyrrole films (1) undoped polypyrrole;
(2) PTS doped polypyrrole; (3) BF₄⁻ doped polypyrrole films

Fig. 3 shows the results of FTIR spectra of polypyrrole films doped with BF_4^- ion (curve 1), PTS ion (curve 2) and of undoped polypyrrole (curve 3) film. Principal transmission bands corresponding to polypyrrole are observed at 1550, 1474 , 1448, 1324 and 1200 cm⁻¹, respectively. The band seen at 1550 cm⁻¹ is due to C=C stretching. Whereas 1474, 1448 and 1324 cm⁻¹ are respectively, due to the existence of C-C and C-N vibrations stretching in the pyrrole ring. Moreover, 1200 and 1050 cm⁻¹ peaks are due to the presence of C-N (def). The 975 cm⁻¹ peak is due to ring breathing in polypyrrole. The band at 875 cm⁻¹ is due to the pyrrole ring (def). The peaks at 575 and 625 cm⁻¹ are due to the pyrrole ring (torr). When a polypyrrole film is undoped in aqueous ammonia the 1324 cm⁻¹ peak is lost (curve 3, fig.3) and a new peak appears at 1374 cm⁻¹. Further, the at 1550 cm⁻¹ peak is shifted to 1575 cm⁻¹ due to the presence of ammonia. This shift indicates the conversion of benzoid structure to quinoid structure. Another important feature is the compensated reaction of NH_3 with (BF_4^- doped) polypyrrole resulting in the loss of 962 cm⁻¹ peak [44,45].

100

Results of this measurement clearly demonstrate the presence characteristic vibrational bands of polypyrole moieties. Besides this, undoping with NH_3 does not lead to the loss of any structure of various polypyrrole films

3.5.2 UV -VISIBLE STUDIES

The UV- visible spectroscopy is performed to understand the basic electronic structure of a desired organic material. It is a powerful tool for characterization of electronic processes that occur in the doped and undoped states of a conducting polypyrrole film. Moreover, the UV - visible studies are likely to unravel the semiconducting nature of polypyrrole. Besides this, these studies have been used to determine the thickness of polypyrrole film provided it transmits more than 50% of UV-visible radiation. The insitu polymerization studies can also be carried out with the help of UV-visible technique.
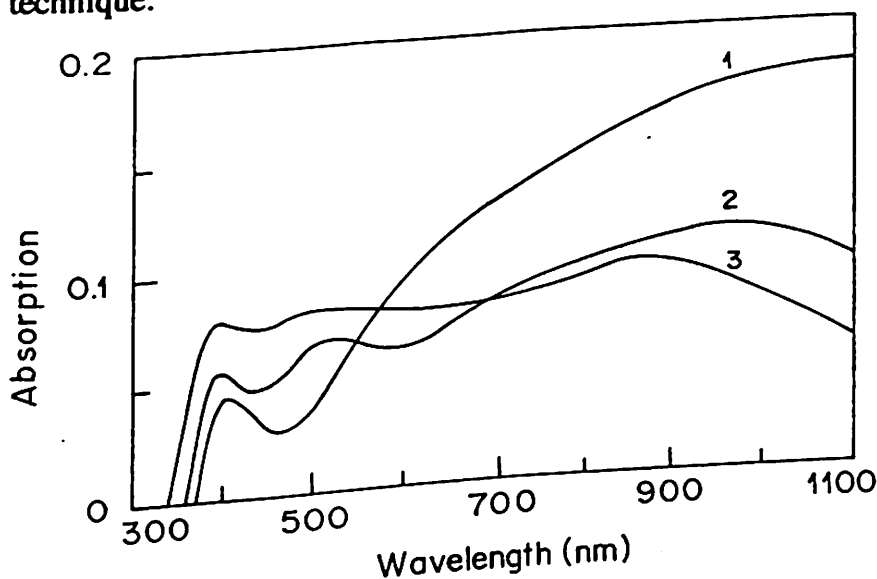
Fig.4   UV-visible spectra of undoped polypyrrole (curve 1),
PTS -ion doped polypyrrole (curve 2) and
BF_4^- ion doped polypyrrole (curve 3) films.

Fig.4 shows the UV-visible spectra of undoped polypyrrole (curve 1), PTS-doped polypyrrole (curve 2) and BF_4^- doped polypyrrole (curve 3) film, respectively. The peak

101

at 410nm (3.0 eV) has been attributed to interband transition derived from the $\pi - \pi^*$ transition of PPY moiety. The peak at 990 nm (1.25 eV), 530 nm (2.3 eV) and 435 nm (2.85 eV) have been observed for the doped polypyrole films. The peaks at 530 nm (2.3 eV) peak is due to the doping of polypyrrole films with BF_4^- and PTS ions, respectively. The knowledge of optical properties of conducting polymers are important to understand the basis of electronic structure of PPY which is implied by its colour and electronic spectra.
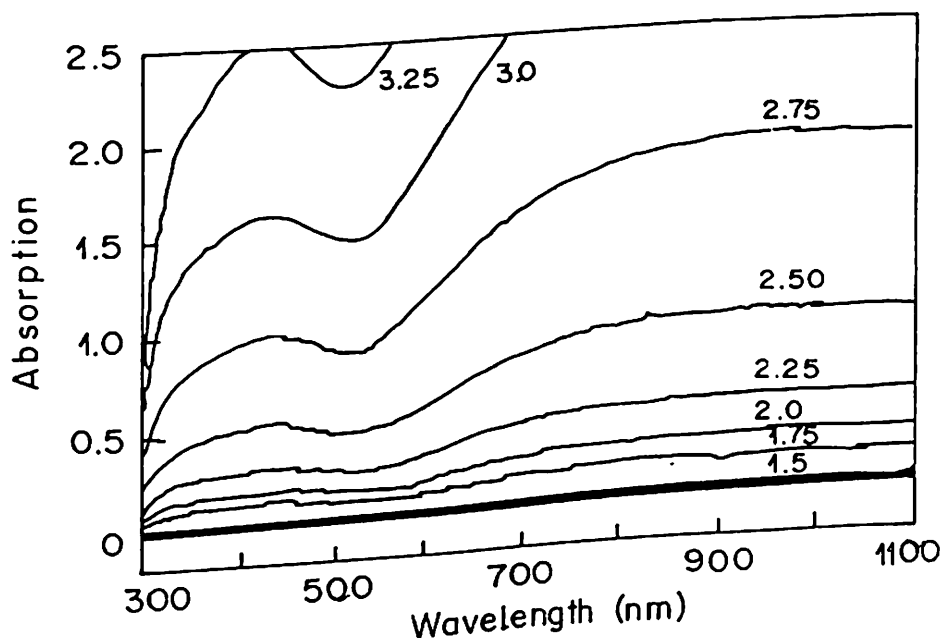
Fig.5   The insitu UV-visible absorption spectra as a function of voltage (V) for the growth of polypyrrole films.

Fig. 5 shows the results of insitu optical absorption measurements carried out on BF_4^- doped polypyrrole films, electrochemically deposited on ITO glass as anode and platinum as a counter electrode in a cuvette containing propylene carbonate. It has been observed that polypyrrole films start growing at 1.0 V. The $\pi - \pi^*$ transition peak appears

at 3.1 eV and n - π^* transition at 2.1 eV for doped PPY, respectively. Further, as the voltage increases the polypyrrole film becomes thicker at about 3.25 V absorbing the UV - visible radiation completely. The changes in the magnitude of absorption unravel the role of polymerization of pyrrole resulting in the formation of PPY film.
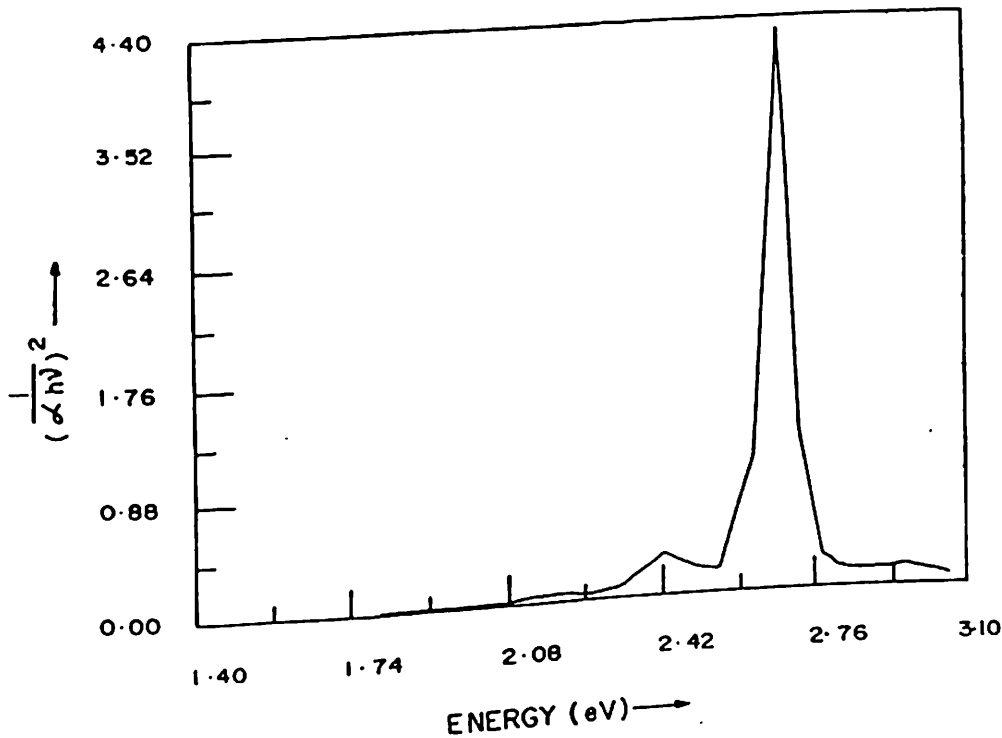

Fig.6   Plot of $(\alpha.h\nu)^{1/2}$ vs photon energy for unannealed BF$_4^-$ doped PPY films in the range of 1.4 - 3.1 eV.

Fig.6 has been obtained by plotting $1/(\alpha\ h\nu)^2$ vs hv (photon energy) for the unannealed BF$_4^-$ doped PPY. The optical absorption edge as determined from this figure is seen to be around 2.7 eV. The optical energy band gap (E_g) has been estimated to be about 3.0 eV. It can be seen that band edges are not very sharp and energy gap can be assumed to be an apparent band gap. The absence of crystallinity results in the band edges being blunt. As in the case of amorphous semiconductor, band edges contain tails

with reasonable density of states. The observed energy band gap (3.0 eV) is well within the region of other doped polypyrrole systems. It has been reported that the band gap of PPY lies in the range of 1.4 - 6.0 eV depending upon the preparation of the films and type of dopants. It has also been seen that the undoped PPY have a band gap of 3.2 eV.
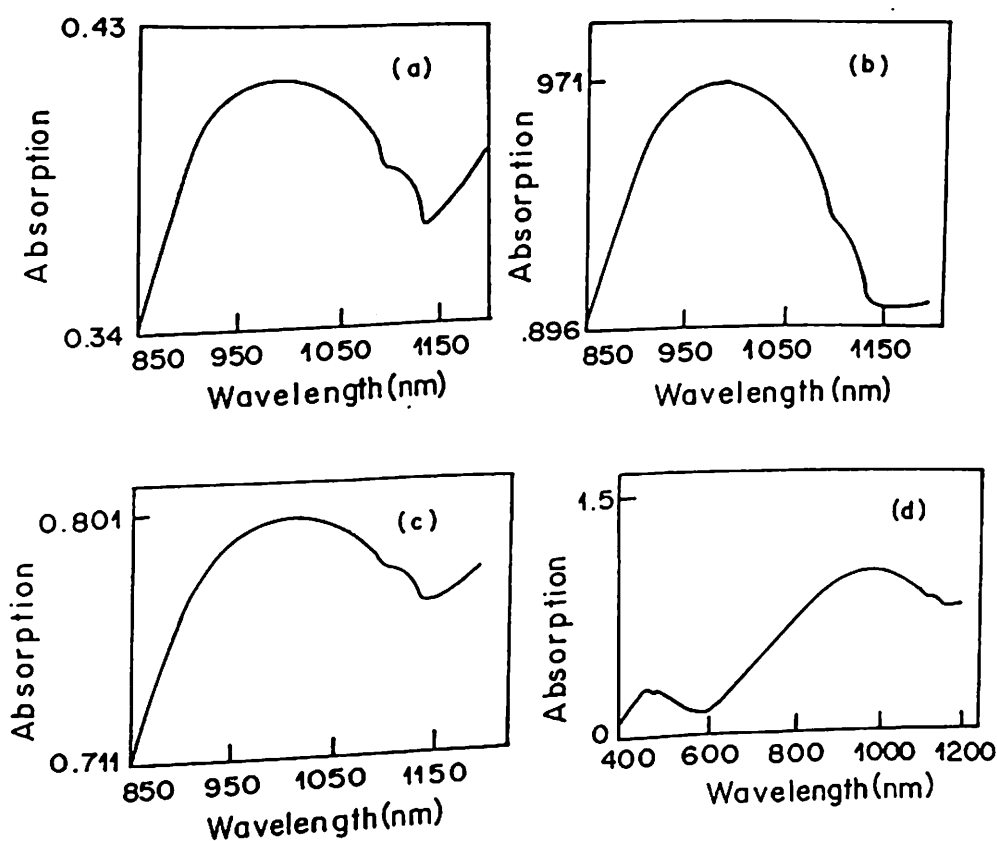

fig.7   Optical absorption of BF$_4^-$ doped PPY films in the range of 400 - 1200 nm, (a) unannealed, (b) annealed for 40 hours, (c) annealed for 70 hours, (d) annealed for 100 hours.

Fig. 7 (a, b, c and d) shows the optical spectra of BF$_4^-$ doped PPY films that have been annealed at 70°C for various durations such as 20, 40, 70 and 100 hours, respectively. It can be seen that optical absorption spectra of BF$_4^-$ doped PPY film are

modified as a consequence of annealing. This is expected for an amorphous solid. Apart from the observed annealing effect, there is clearly a significant change in the optical spectra arising as a result of dopants. The peaks in the region of 1000 - 2600 nm are usually attributed to the polaron defect levels and determine the conductivity properties of PPY films.

3.6 SCANNING ELECTRON MICROSCOPE (SEM) STUDIES:

The surface characterization is very helpful for the determination of operational characteristics of a device based on polypyrrole. The quality of polypyrrole films depends upon the type of dopant ions, quality of solvent used, temperature of the electrochemical cell, magnitude of current density and the polymerization conditions etc.. The surface characterization of the various BF_4^- doped polypyrole films have been experimentally
A complex 1-a
investigated through scanning electron microscope technique [46].

Fig.8 (a,b,c and d) shows the SEM pictures of doped polypyrrole films. The SEM micrograph (fig. 8a) of a polypyrrole film shows a continuous and uniform surface. It can be clearly seen that the SEM pictures reveal the restructuring molecules in various of the polypyrrole films. Further, a large number of pores and voids are observed after it is annealed (70° C) for 15 hours (fig.8b). Further, when these polypyrrole films are annealed (70°C) for 40 hours, uniform structures containing no voids and pores are clearly visible in fig.8C, The continuous and uniform structure of BF_4^- doped PPY film perhaps yields a minimum value of resistance. Fig.8d exhibits the surface morphology of a doped BF_4^- PPY film after it is annealed for about 100 hours. It can be seen that even though the resistance of polypyrrole film has considerably stabilized, the surface

105

morphology no longer remain smooth. Such polypyrrole films have used for the fabrication of metal - insulator - semiconducting (PPY) devices described in Chapter VI.
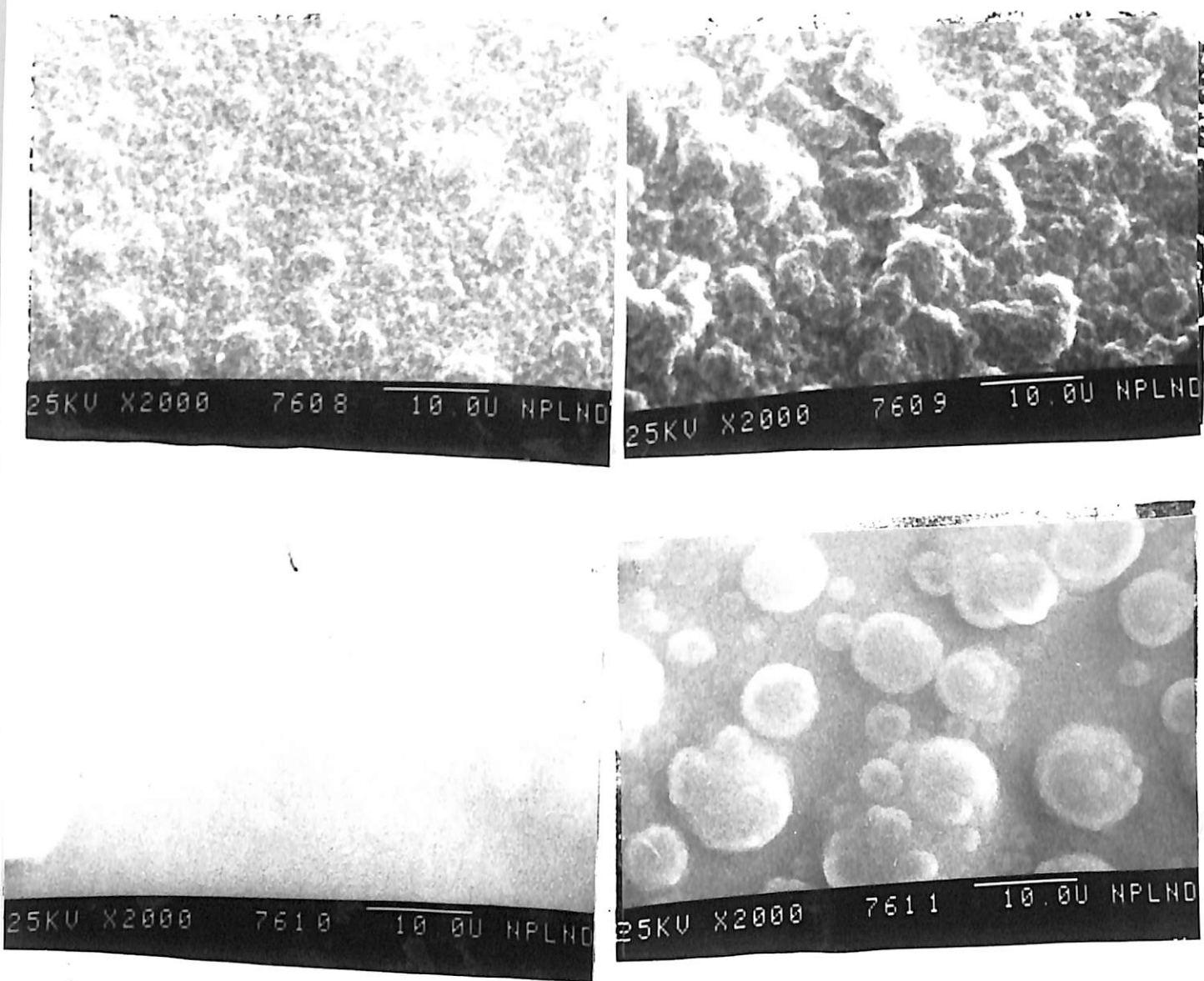

Fig.8 Scanning electron microscographs of doped PPY film
(a) unannealed, (b) annealed for 15 hours (c) annealed for
40 hours and (d) annealed for 100 hours, annealing temperature 70°C.

The value of energy band gap (3.0 eV) depends upon the carrier concentration in the conducting polypyrrole. After 40 hours of annealing the structure of polypyrrole has considerably smoothened. For further processing of polypyrrole films, the studies relating to electrical properties described in the next section have been systematically

3.7 ELECTRICAL PROPERTIES OF POLYPYRROLE FILMS

3.7.1 DC CONDUCTIVITY STUDIES

It is known the polypyrrole films prepared by electrolytic polymerization of pyrrole show high electrical conductivity. The mechanism of such a high value of conductivity has been widely investigated using optical and ESR studies. It has been revealed that polarons and bipolarons in the polypyrole films serve as positive charge carriers [47]. In addition much attention has been paid to a variety. of factors which control the conductivity of polypyrrole films. Importance of electrical properties of polypyrrole films has recently stressed [46]. Hence various experiments pertaining to different dopant anions such as BF_4^-, PTS , ClO_4^- and Cl^- in corporated in various polypyrrole films have been systematically conducted. The electrical conductivity measurements have also been carried out as a function of temperature on polypyrrole with a view to understand the charge transport mechanism. The electrical conductivity of various polypyrrole films measured by four points probe method vary from 100 to 0.2×10^{-8} S/cm (Table I).

TABLE I: Conductivity and nature of polypyrrole films

System	Conductivity S/cm	% of dopant	Nature of Film
PPY-neutral	0.2	-	Smooth
PPY-BF_4^-	20	32	Smooth
PPY-PTS	100	33	Smooth
PPY-ClO_4^-	4	25	Granular
PPY-Cl	4	22	Rough

Films thickness measured as 5 - 10 μm.

At room temperature, electrical conductivity of various PPY films varies from 20 - 100 S/cm. The conductivity of the BF_4^- doped PPY and PTS doped PPY films has been found to be 20 and 100 S/cm, respectively. The higher value of electrical conductivity of PTS doped PPY film may perhaps be due to in oxidation with water which creates intrinsic dipoles in the PPY matrix. The charge conduction mechanism in PTS doped PPY film depends upon the molecular oxygen and water, which probably affect the charge transfer interaction with the π - electrons or nitrogen atoms in the PPY system.

(i) EFFECT OF TEMPERATURE:

Mechanism of charge conduction in doped PPY films with BF_4^- or PTS-ions has been of interest since it is the p-type semiconductor. The presence of localized electronic states of energies less than the band gap arising as a result of changes in local band order, including the formation of polarons and bipolarons have lead to the possibility of new types of charge carriers present in the PPY matrix. The temperature variation of (σ_{dc}) conductivity has been experimentally studied on lightly doped and heavily doped (BF_4^-) polypyrrole films. Fig.9 a and fig. 10 show the variation of $\log\sigma_{dc}$ of electrical conductivity ($\log \sigma_{dc}$) as a function of $10^3/T$ both for lightly doped and heavily doped BF_4^- doped polypyrrole films, respectively. The absence of a linear fit in polypyrrole (fig.9 and fig.10) indicates that the electrical phenomenon is perhaps not governed by the transport of the charge carriers via extended wave phenomenon.
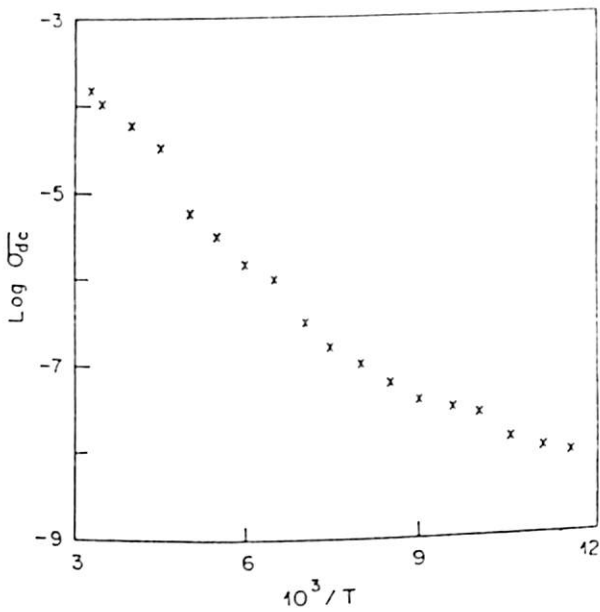
108

Fig.9 Variation of $\log\sigma_{dc}$ vs $10^3/T$ for lightly doped BF_4^- polypyrrole films
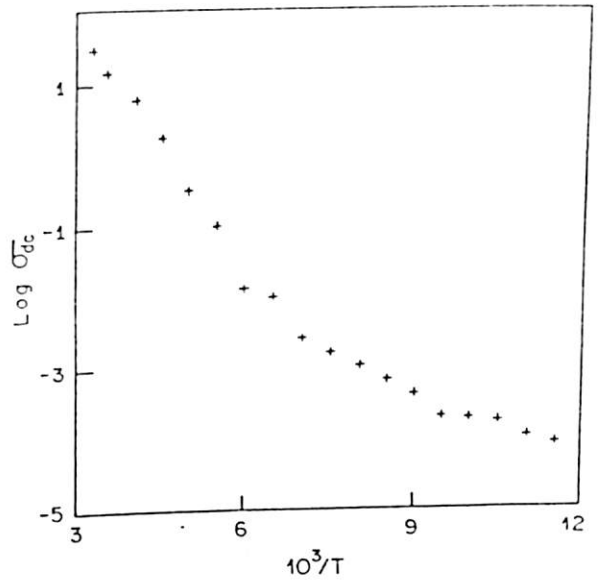

Fig.10 Variation of $\log\sigma_{dc}$ vs $10^3/T$ for heavily doped BF_4^- polypyrrole films

Fig. 11 shows the plot of $\log\sigma_{dc}$ vs $10^3/T^{1/4}$ for lightly doped (BF_4^-) PPY film indicating a linear fit. Fig.12 shows a linear fit for electrical conductivity data obtained for highly doped polypyrrole as a function of at $10^3/T^{1/3}$. These results demonstrate that hopping of charge carriers perhaps plays an important role towards the transport of charge via hopping resulting either from the deep trapped states or localized states. Since in the case of lightly doped sample the trapped sites are larger in number, the theory predicts that $T^{-1/2}$ will be the dominant factor, which in the present context has been found to vary as $T^{-1/3}$ because of the interplay between $T^{-1/2}$ and $T^{-1/4}$. In a lightly doped PPY film, electrical conduction is due the to hopping of a fewer number of charges trapped at various sites in the polypyrrole films [37].
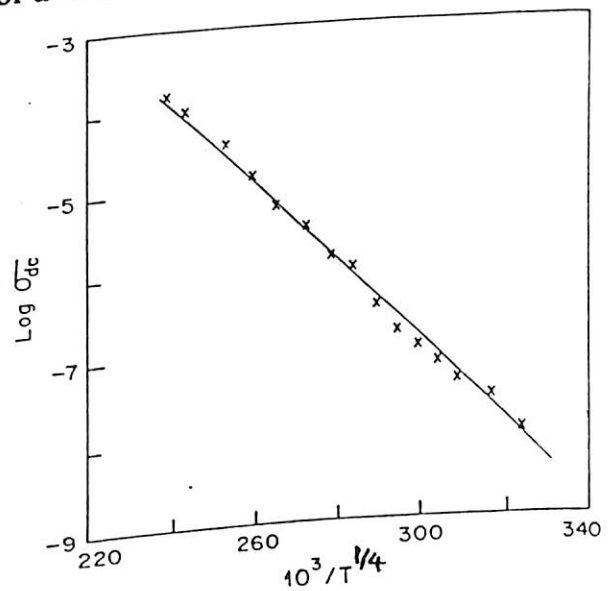
Fig.11 Variation of $\log\sigma_{dc}$ as a function of $10^3/T^{1/4}$ for lightly doped BF_4^- polypyrrole films
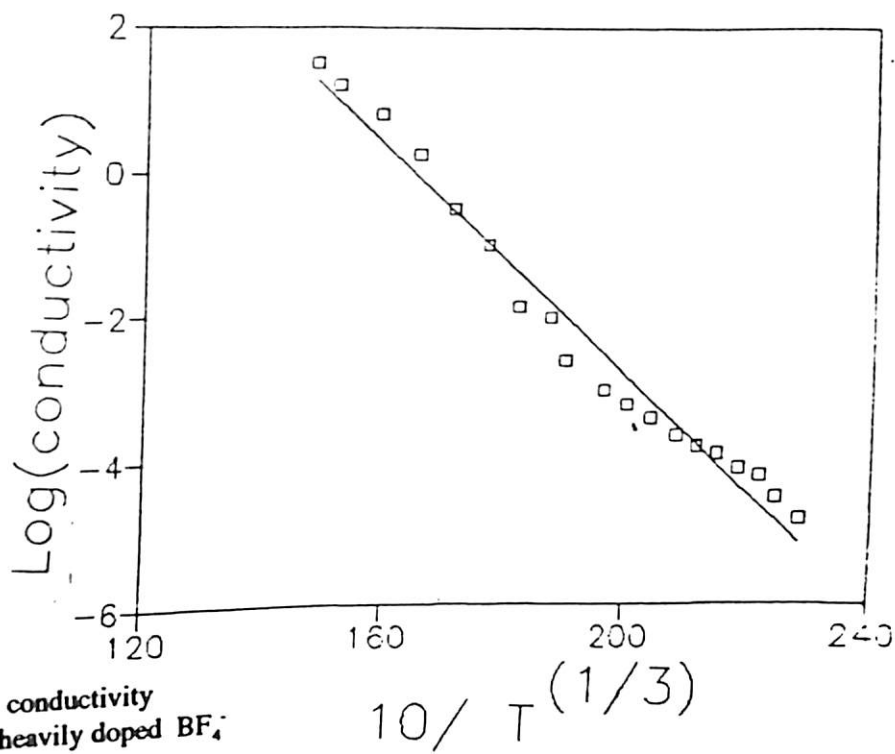
109

Fig.12 Variation of logarithmic of electrical conductivity (log σ_{dc}) as a function of $10^3/T^{1/3}$ for heavily doped BF_4^- polypyrrole films

Some of the electrical parameters obtained in case of lightly doped polypyrrole have been calculated using ~~the clarify~~ the Mott variable range hopping eq.1 [38]:

$$\sigma_{dc} = 2[9\,\alpha\,N_0 / 8\,\pi\,K_B\,T]^{1/2}\,v_{ph}\,exp\,[(T_0/T)]^{1/4} \qquad Eq.1$$

where $T_0 = 16/K_B\,N_0\,\alpha^3$ and N_0 is the density of states at Fermi level, v_{ph} is phonon attempt frequency and α is a three dimensionality averaged characteristic decay length for localized sites involved in the variable range hopping. To facilitate comparison, the dc conductivity data of various polypyrrole films has been plotted against $10^3/T^{1/4}$ (fig. 11). The linear curves indicate a good fit to the data with a composition dependence.

The conductivity of lightly doped (BF_4^-) PPY has been measured to be 1.58×10^{-4} S/cm which is 10^6 orders less in magnitude with respect to doped PPY films. The localization length varies between 1 to 10 A^0 and a hopping distance has been found to be 0.607 - 2.6 eV. The carrier density of states decreases from 3.22×10^{22} to 3.21×10^{19} $cm^{-3}\,eV^{-1}$. The hopping length frequency has been calculated for the lightly doped poly-pyrrole system to be 1.754×10^{12} Hz. The results of temperature dependence of the conductivity in the oxidized PPY suggest that variable range hopping model based on polarons quantatively explains the observed conductivity data. It has been suggested that

110

for an ordered material having polaronic conduction processes, the jump frequency of the polaron is due to single optical phonon absorption and emission. It indicates that the polaronic hopping conduction can give rise to temperature independent activation energy. Table II shows the various electrical parameters for the lightly doped PPY films, that have been obtained by the Mott variable hopping conduction mechanism:

TABLE II: Electrical conductivity parameters for lightly doped polypyrrole films for σ_{dc} at 300 K = 1.58 x 10^{-4} Ω^{-1} cm^{-1}

Temperature $T_o(K)$ x 10^6	Activation energy $W(eV)$	Localization length α^{-1} Å	Hopping distance R	$N(E_F)$ $cm^{-3}eV^{-1}$ x 10^{22}	Hopping frequency $\nu_{ph}(Hz)$ x 10^{12}
5.761	0.049	1	0.607	3.22	1.75
5.761	0.049	1.5	0.781	0.37	1.75
5.761	0.049	5	1.928	0.10	1.75
5.761	0.049	10	2.562	0.003	1.75

(ii) EFFECT OF ANNEALING :

Fig. 13 shows the variation of resistance for BF_4^- doped PPY films annealed at 70°C for various duration of time. The resistance of the BF_4^- doped PPY increases sharply with time within the initial 15 hours of annealing reaching a peak value of 56 Ω and it decreases to a value about 12 Ω after being annealed for about 30 hours. Further annealing of these PPY samples does not result in any significant change in the resistance of the doped PPY film that may perhaps be caused by the evaporation of the solvent during the annealing process. Due to the complex structure of the polymeric chains in electrochemically deposited PPY films, polymeric molecules are locked in the resulting structure. This re-constructuring of PPY films leaves voids and pores that act as resistive paths. This process is completed within 15 hours of annealing . Annealing

beyond 15 hours results in the restructuring of PPY films eliminating the persistent voids and pores, which in turn result in the increase of resistance. After annealing for 40 hours, the resistance attains a stable value. This indicates that a complete ordering of the polymeric chains has occurred leading to a stabilized polypyrrole structure [28].
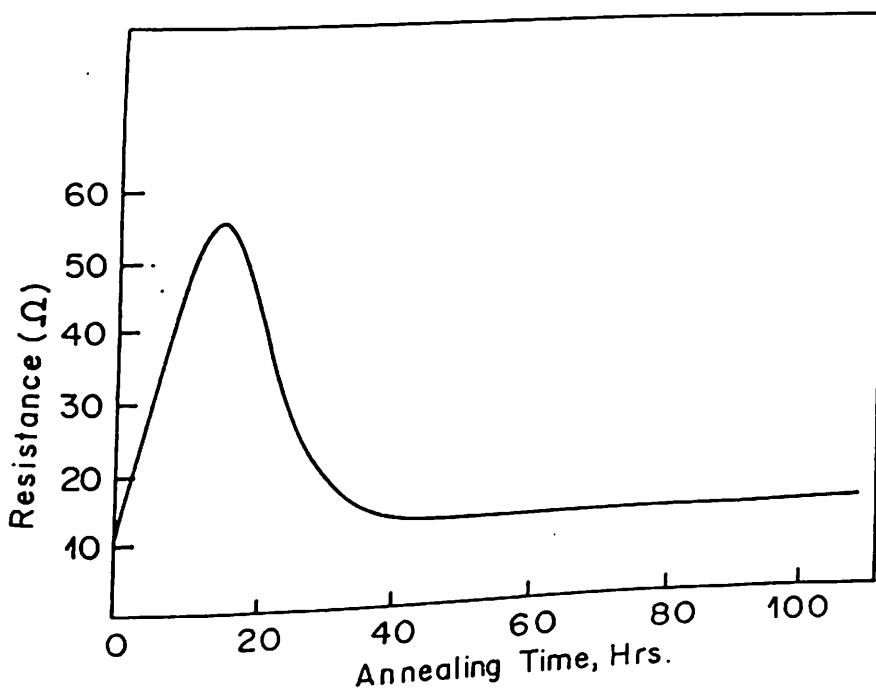

Fig. 13 Plot of resistance vs annealing time for BF_4^-
doped PPY films; annealing temperature 70°C

3.7.2 AC CONDUCTIVITY STUDIES OF PPY FILMS :

Charge transport in conducting polypyrrole has attracted a great deal of interest in recent years. A number of experimental techniques such as optical, NMR, ESR and also XPS have been used to determine the nature of charge carriers in this non - degenerate conducting polymer. It is believed that polarons and bipolorans are perhaps responsible for the observed electrical behaviour. It must, however, be remarked that the exact mechanism relating to the origin of electrical conduction in this molecular electronic (natural) has not yet been clearly established. As in the case of inorganic, semi-conductors, dielectric relaxation studies have recently been shown to be extremely

112

valuable towards delineating the phenomenon of conduction in various conducting polymer films. In this context, ac conductivity studies with gold contacts in lightly doped polypyrrole films has recently been reported. The observed ac conductivity in polypyrrole films has been explained on the basis of available of conduction mechanism.

Polypyrrole doped with BF_4^- ions is known to be a p- type semi-conductor. Such a doped polypyrrole film forms a rectifying or blocking contact with a metal having a lower work function than that of PPY system. It will thus be interesting to experimentally investigate the phenomenon through dielectric measurements. Al-PPY-Al structure has been fabricated for studying the charge transport in polypyrrole film. This section deals with the systematic investigation of dielectric relaxation and ac conductivity of undoped and BF_4^- doped polypyrrole films [48].

Blocking contacts have been made by depositing aluminium (Al) on electrochemically prepared BF_4^- PPY films by vacuum evaporation (10^{-6} torr). DC conductivity measurements have been carried out using HP 4192-A impedance analyzer. Fig. 14 shows the variation of capacitance as a function of frequency for aluminium (Al) - undoped PPY - aluminium (Al) capacitors at room temperature (290K). There is a decrease of capacitance from 20Hz to 100Hz but the marked peak at 200 Hz clearly indicates the entreatment of propylene carbonate (solvent). This has been assigned to the presence of or Max-Wagner polarization arising due to contact effect. The decrease of capacitance from 200Hz to 10KHz clearly shows the presence of interfacial polarization at the electrode.
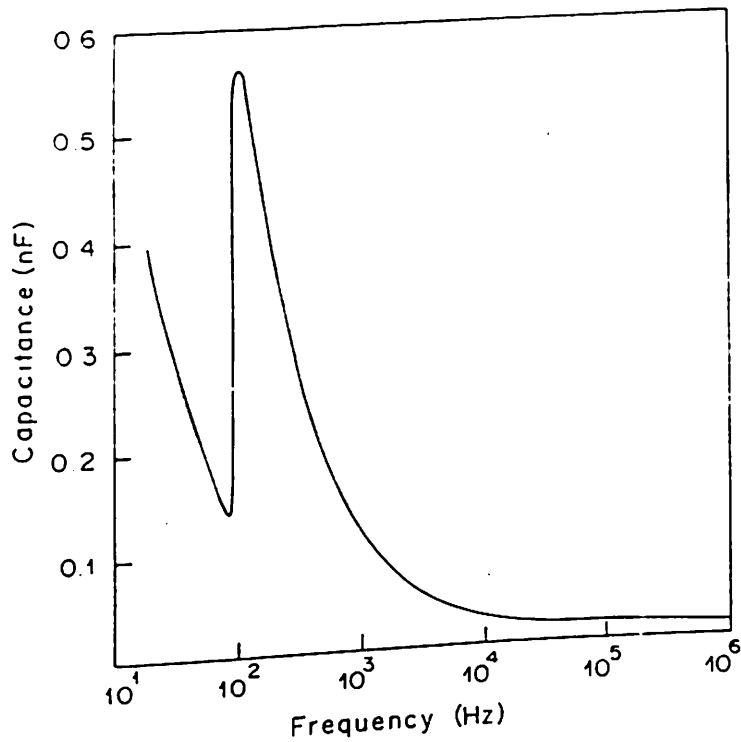
113

Fig.14 Variation of capacitance as a function of frequency for Al-undoped PPY-Al capacitor.
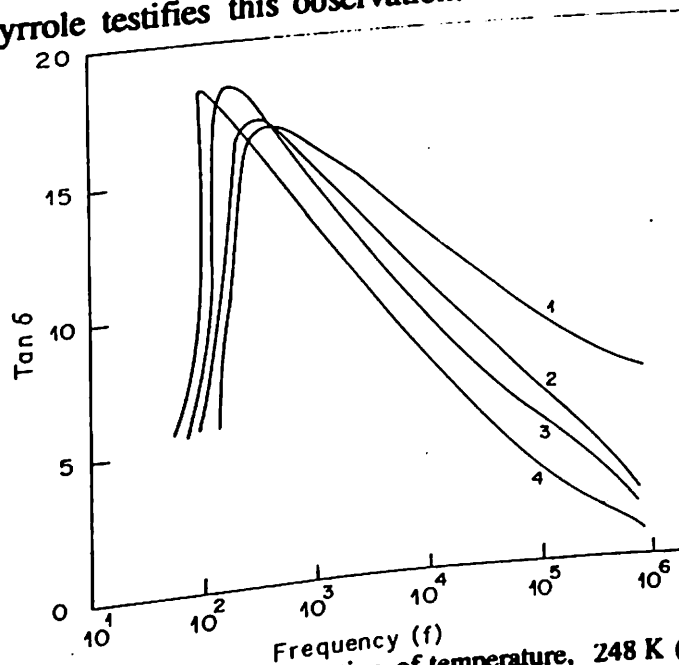
Fig.15 shows the variation of dielectric loss factor vs frequency as a function of temperature, 248 K (curve 1), 290 K (curve 2), 310 K (curve 3) and 400 K (curve 4), respectively. The clear shift of the loss factor (tan δ) peaks at around 200Hz to 100KHz demonstrates the orientation of the entrapped solvent molecules in the PPY matrix. The presence of C=O vibrational peak (1700 cm^{-1}) peak present in the FTIR spectra (fig.3) of undoped polypyrrole testifies this observation.

Fig.15 Variation of tan δ vs frequency as a function of temperature, 248 K (curve 1), 290 K (curve 2), 310 K (curve 3) and 400 K (curve 4)

Fig. 16 shows the variation of observed capacitance and loss factor (tan δ) in Al-PPY (BF₄⁻)-Al structure obtained as a function of frequency. The rise in frequency indicates the interfacial polarization arising due to the formation of space charges near the electrode. The dielectric loss factor decreases with increase in the frequency and is maximum at a frequency at around 800KHz. The variation of capacitance shows a strong resonance at about the same frequency. Clearly, the resonance is due to the formation of dipoles in thin PPY film when blocking contacts are made.
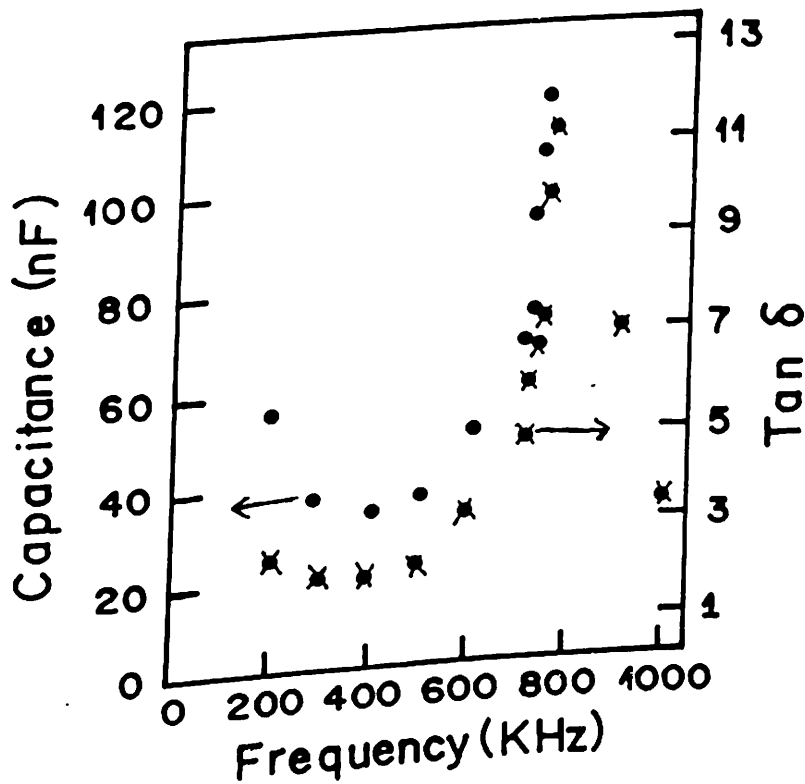
Fig. 16 Variation in differential capacitance and loss factor (tan δ) in Al-PPY(BF₄⁻)-Al structure as a function of frequency at zero bias.

Fig. 17 is obtained by plotting log ϵ'' vs logw. It shows two relaxation times 0.25 μs to 0.03 μs, respectively. The origin of these relaxation times is the fact that polypyrrole is a highly disordered material and the charge transport occurs both along the chain. The Cole- Cole plot (Fig.18) also shows the distribution of relaxation times which has been obtained by plotting C(pF) tanδ vs Capacitance. The deviation from the semicircular graph is clearly due to the presence of charge carriers and their observed conductivity and accordingly the complex permitivity ϵ'' can be written as [48]:

$$\epsilon^* = \epsilon_- + (\epsilon_s - \epsilon_-) / (1 + iw\tau) \qquad Eq.2$$

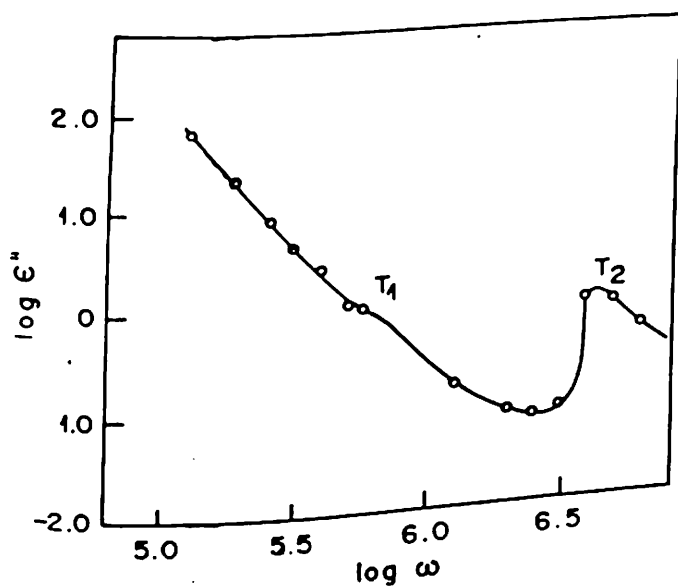where ϵ_s is the static dielectric constant and τ is the relaxation time.

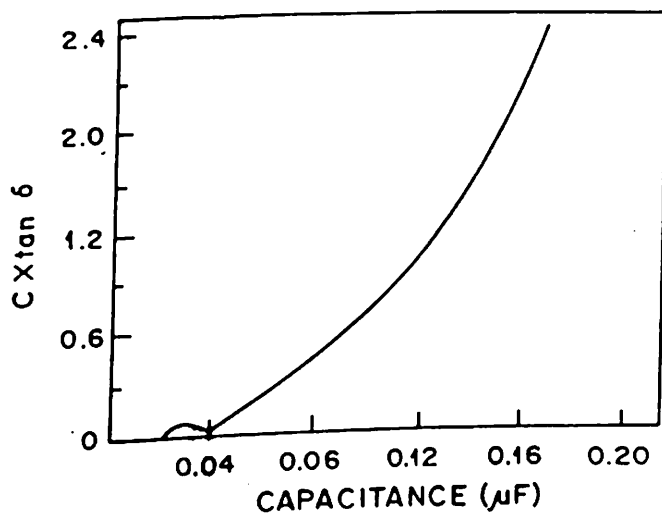Fig. 17 logw vs loge" for BF$_4^-$ doped PPY film at 290K
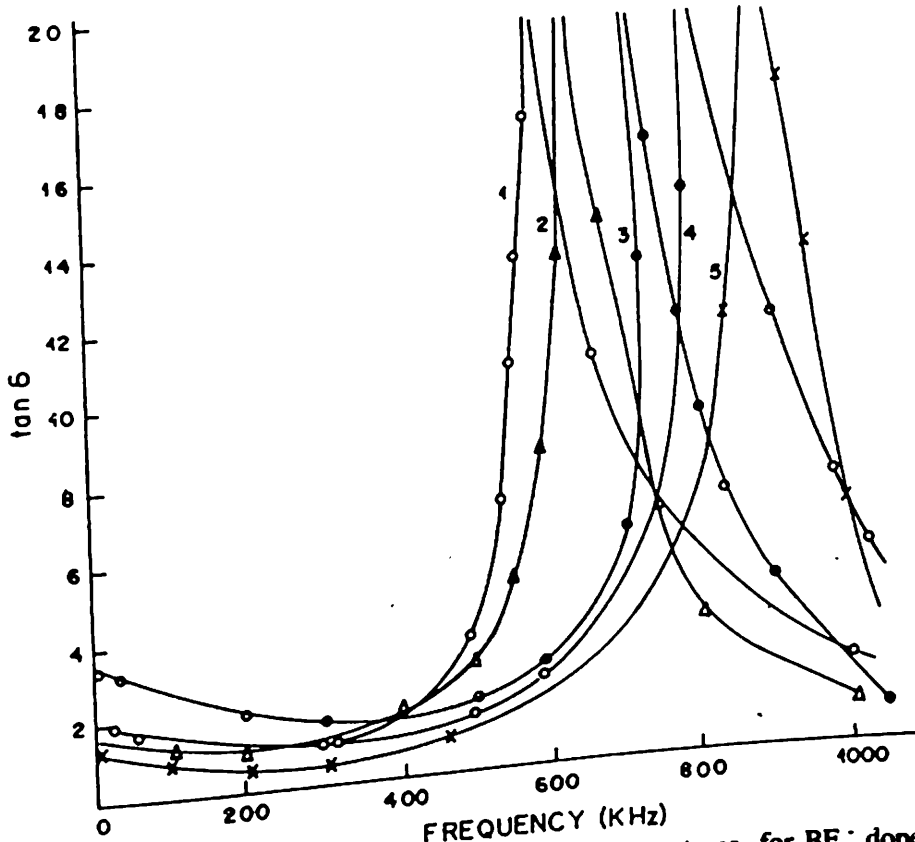
Fig.18 Cole - Cole plot for PPY at 290K

Fig.19 Variation in loss factor with frequency at different temperatures for BF$_4^-$ doped PPY at 100 mV static bias curve 1, 400K; curve 2, 310 K; curve 3, 290 K; curve 4, 248 K; curve 5, 210 K
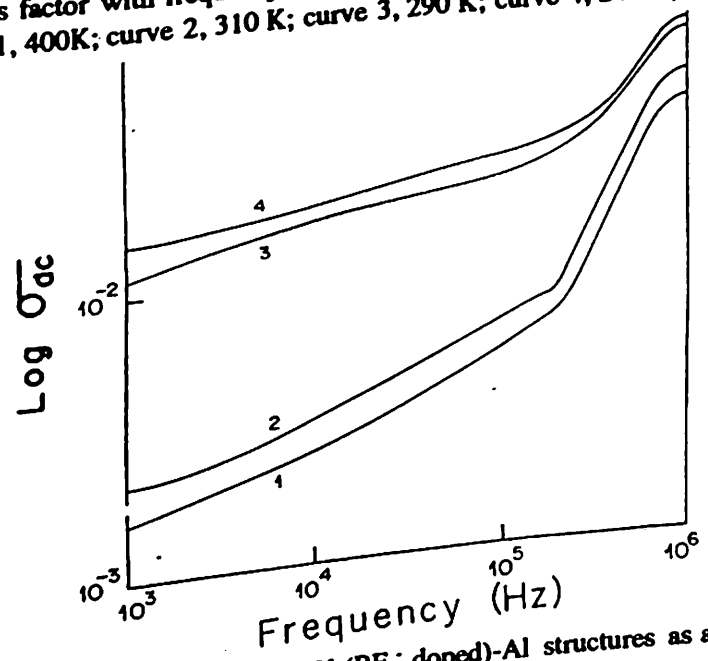

Fig.20 Variation of logσ_{ac} vs frequency of Al-PPY (BF$_4^-$ doped)-Al structures as a function of temperature curve 1, 248K; curve 2, 290K; curve 3, 350K and curve 4, 400K
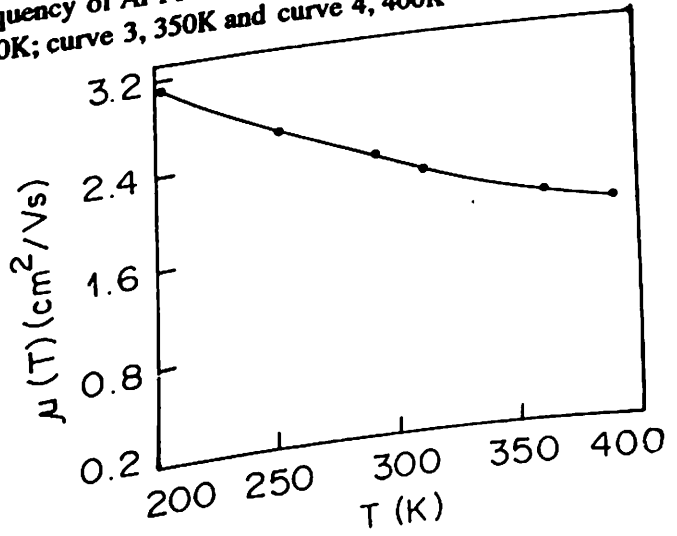

Fig.21 Variation in mobility with temperature.

117

The mobility of the charge carriers has been computed using the following equation [48]:

$$\mu = (w_m^4 \, \epsilon^3 \, \epsilon_0^3 L^2 / \, n^3 \, e^3 \, V_s)^{1/4} \qquad \text{Eq.3}$$

where w_m is the frequency at which the dielectric loss is maximum and V_s is the static bias across the film, $n = 10^{18}/ \, cm^3$ is the carrier concentration, $\epsilon = 100$ and ϵ_0 is the permitivity of space charge. Fig.21 shows the variation of mobility as a function of temperature. This needs further elucidation as the negative temperature coefficient can be understood only in the light of structural properties and conduction mechanisms proposed for the transport of charge carriers in PPY films. Interestingly, the investigations show multiple relaxation times. Although, a distribution between the types of charge carrier or transport is not possible at this stage. The charge carriers are polarons or bipolarons as compared to earlier results obtained (as) using Boltzmann transport equation. The temperature dependent mobility found in Al- PPY (BF$_4^-$ doped) - Al structure is consistent with their results. This suggests that scattering due to phonon is dominant in PPY is perhaps the reason for the observed negative temperature coefficient. Much higher temperature inhibits the information of kink states which results in diminished mobility. The negative temperature coefficient for mobility is also observed in many organic conductors.

3.8 ELECTROCROMIC DISPLAY BASED ON PPY FILMS

Polypyrrole is an important member of an emerging family of electrochemically conductive polymers which can be electrochemically switched between oxidized (conducting) and the neutral (insulating) states, respectively. This characteristic has been

used for the fabrication and characterization of display based on polypyrrole using required electrolytes. However, the application of electrochromic materials in display devices requires many properties such as low voltage, low power, good colour contrast, low switching time and long life time [51,52].

PPY films have been prepared as discussed in sec. 3.4 of this chapter. The films are washed with acetone and dried in a desiccator for two hours. The electrochromic window consisting of PPY in ITO glass plate is sandwiched with other ITO glass plate having the semi-solid electrolyte resulting in the semisolid configuration, as glass/ITO/ PPY / electrolyte / ITO /glass. The electrolytes used for the present studies are HCl +PEO, PEO+LICIO$_4$, PTS+urea+glycerol, PEO+PTS, and PTS+ glycerol + PEO, respectively. The electrical contacts have been made with alligator clips after ensuring that there is a minimum contact resistance. The cell is placed in Shimadzu (model 160 A) spectrophotometer and the spectra are recorded for different electrolytes at various voltage. The cell is mounted in an optical bench and has been illuminated at 500 nm with a tungsten halogen lamp through a monochromator. The spectra has been recorded as discussed in Sec.2.11.3 of Chapter II.

Fig.22 shows the visible absorption spectra of PPY film in glycerol + urea + PTS electrolytes at various voltages. The colour of the film changes from violet (blue) to yellow which are diffusing in or coming (of from) the film. The oxidized PPY has a broad spectrum at > 540 nm. The reduced PPY has a sharp peak at around 410 nm. When the films are reduced it has been seen that the intensity of 410 nm peak increases and the peaks at 540 nm gradually decreases. At the complete reduction the peak at about 1010 nm disappears (in curve 5 (fig.22)). The similar change has been observed with all the other electrolytes used for the semisolid cell configuration based on PPY films. The bias

119

potential used in semisolid cell are higher than the that of liquid cell which indicating that cell shows higher resistance perhaps due to the presence of semi solid electrolytes.
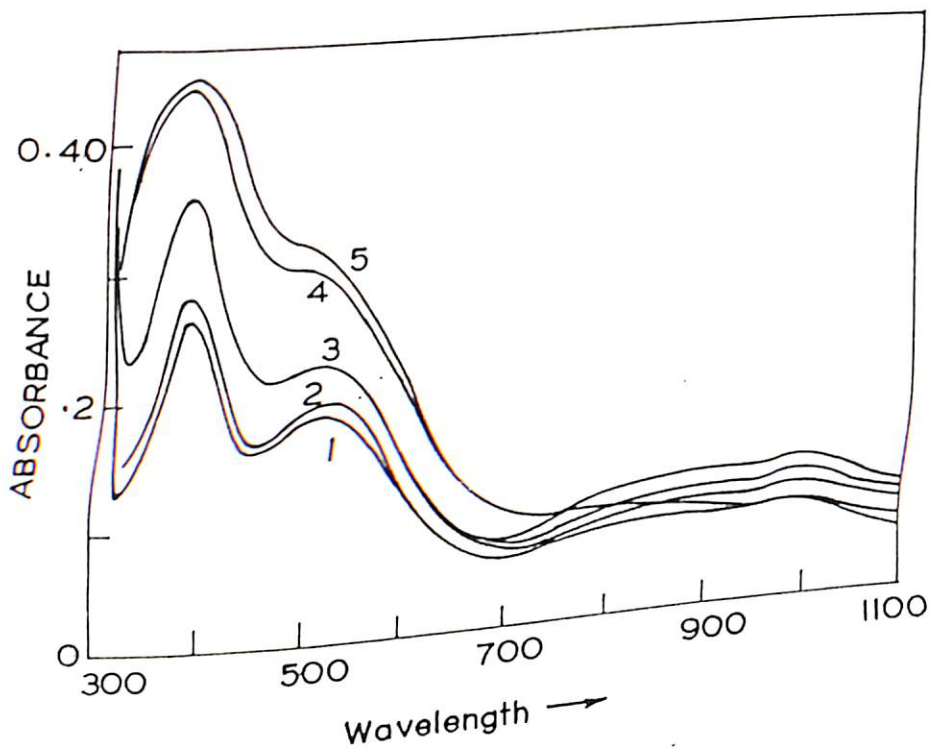

Fig.22 Variation of absorption vs frequency as a function of voltage curve 1 (1 V), curve 2 (0.6V), curve 3(0.2 V), curve 4 (0.0V) and Curve 5 (-0.4V)

Fig. 23 shows the variation of electrochemical decay current as a function of time for different electrolytes used in semisolid configuration of electrochromic devices based on PPY. It can be seen that the doping and undoping process in PPY containing PEO based polymeric electrolyte at room temperature occurs mainly through (on) anion transport. PPY may be effectively doped by ClO$_4$-ions upto a high value of 30%

120

monomeric unit when the semisolid configuration is used with LiClO$_4$ and PEO electrolytes. The electrochemical current decays in the same way as obtained using LiClO$_4$ dissolved in propylene carbonate. It is seen (fig.23) that in the presence of glycerol the decay current is less than that of the PEO+ LiClO$_4$ and HCl+PEO, respectively. The rates of doping and undoping processes are considerably lower in semi-solid cells and have been attributed to the slow ion diffusion both in the electrodes and the electrolyte material. This somewhat limits the application of PPY to low rate limited capacity devices.
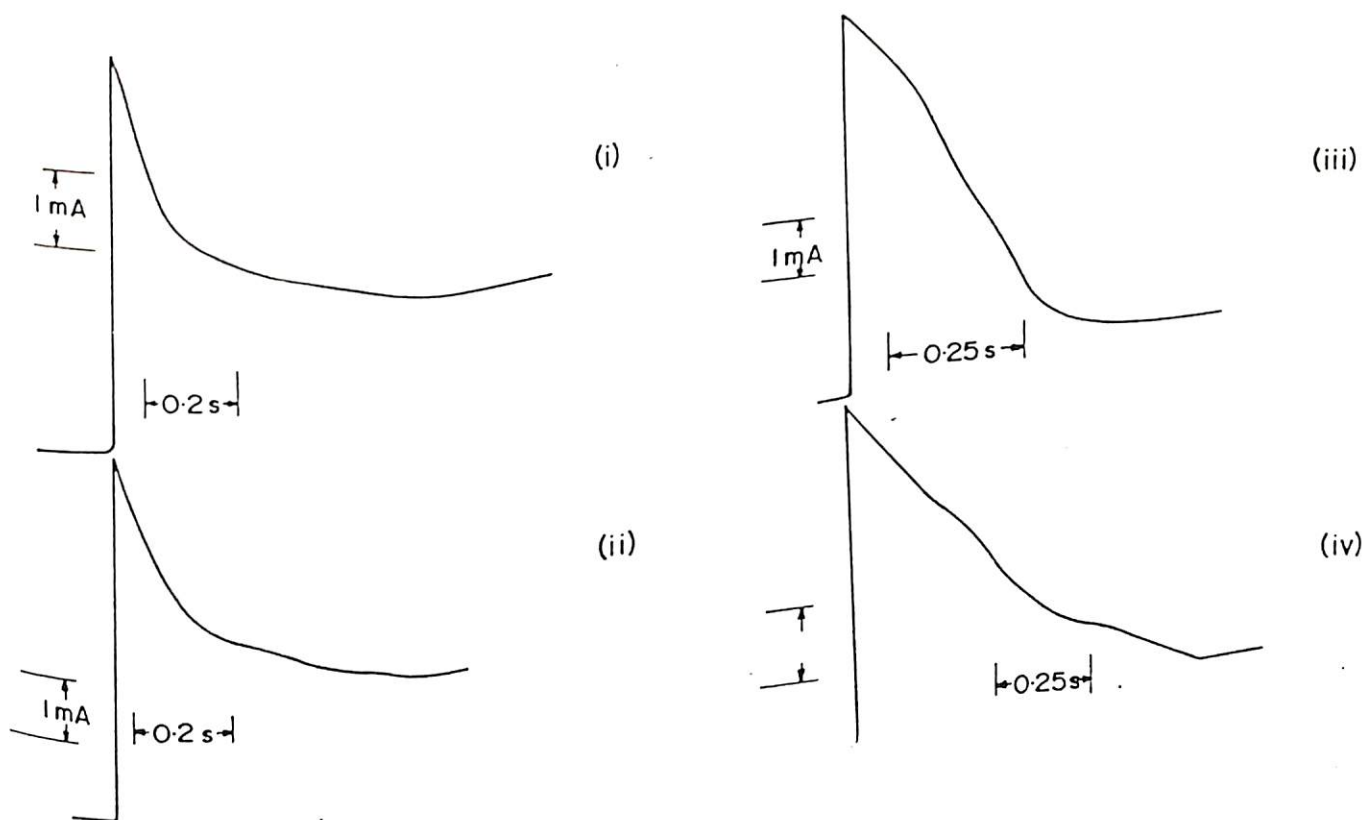

Fig.23 Analysis of current transients for PPY film in (i) PEO + LiClO$_4$, (ii) PEO +HCl (iii) PTS+glecerol+PEO and (iv) PTS + glycerol + Urea, systems.

Fig.24 exhibits the change in optical transmittance for different electrolytes used for the semisolid cell configuration. The half time for colour change related with electrochemical current transient obtained for each system has been calculated to evaluate the switching speed of the film. It has been generally noted that the values are in the neighborhood of 0.2 sec. to 1.5 sec for all the cells studied.
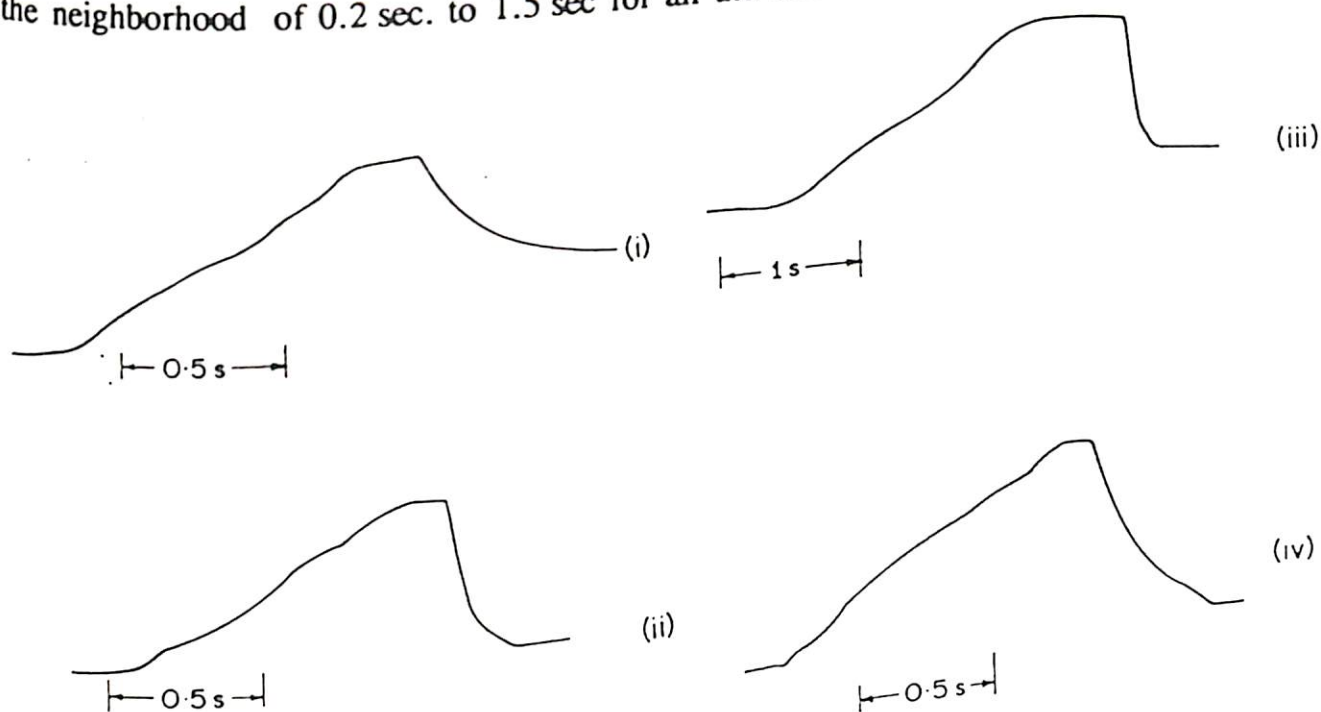

Fig.24 Optical transmittance vs time for cells listed for colour switching of PPY film (1) PEO+LiClO₄, systems (ii) HCl + PEO (iii) PTS+glycerol+PEO, systems (iv) PEO+PTS+glycerol,systems

The kinetics of the process may become diffusion controlled for PEO + PTS, HCl + PEO, PEO + LiClO₄, PEO + LiClO₄ + Glycerol but in PTS + glycerol + Urea the current decay is exponential (fig.25) contrary to expectation. It may be controlled either by proton movement into and out of the PPY film or by the counter ion motion. Due to the presence of PEO there is a slight slow diffusion due to the solid electrolyte, hence much slower diffusion of the ion cancels out the thin layer effect. The diffusion coefficients have been calculated for all the system and are given in Table 4.

The diffusion coefficient of cyclic voltammogram can be calculated by Randles-

Sevics equation as described in Chapter II (Sec.2.7). The redox couples whose peak shifts on further apart with increasing scan rate have been categorized as quasi - reversible. Having obtained these results, a test of reversibility of the system is to check whether a plot of I_p as a function of $V^{1/2}$ is linear. It must be emphasized that a reversible cyclic voltammogram can only be observed if both oxidation (O) and reduction (R) process are stable and the kinetics of the electron transfer process on the surface is in equilibrium so that the equation follows Nerst equation [53].
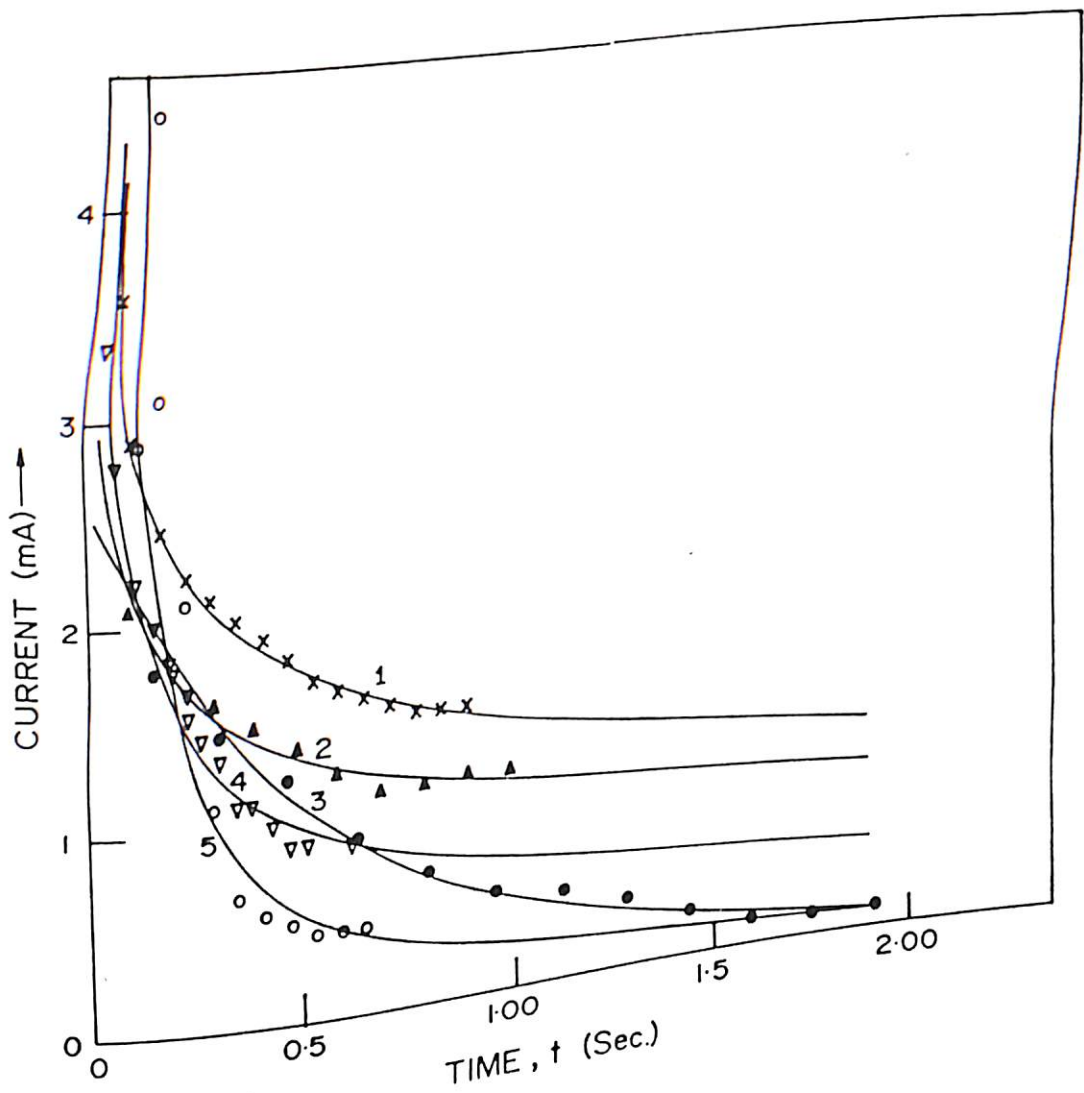

Fig. 25 Electrochemical current transient for the colour switching of PPY film (i)HCl +PEO systems (ii) PEO + LiClO$_4$ systems (iii) PTS+urea+glycerol systems (iv) PEO+PTS and (v) PTS+glycerol+PEO systems
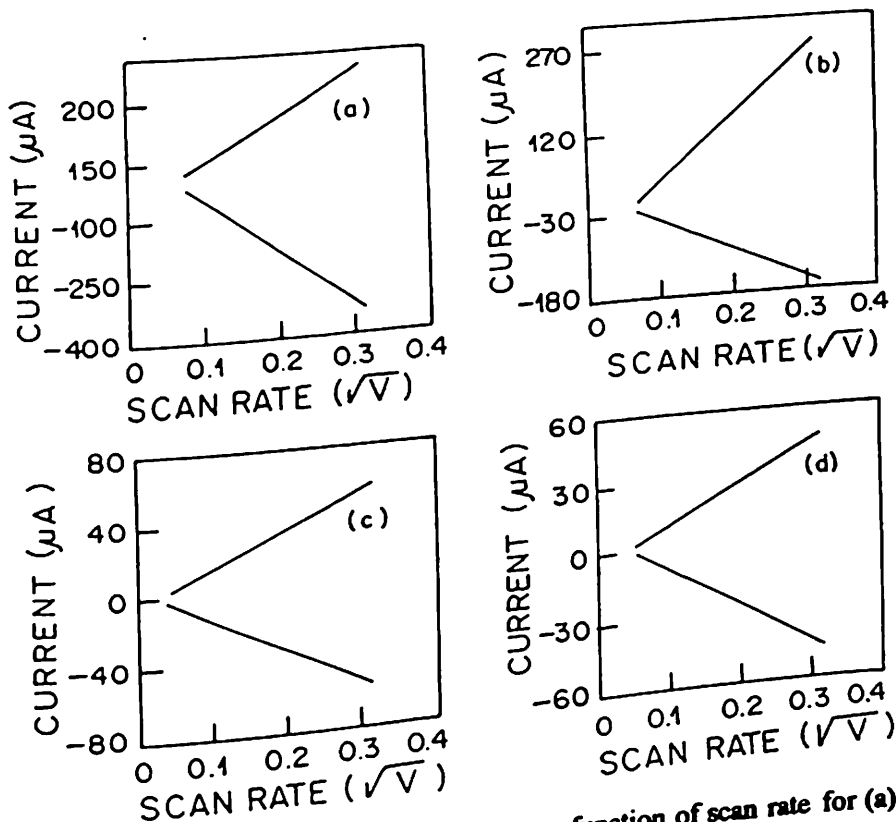
Fig. 26 Plot of oxidation and reduction peak current as a function of scan rate for (a) PEO + PTS, (b) HCl + PEO, PEO + LiClO₄, (c) and (d) PEO + LiClO₄ + Glycerol

TABLE 3: Parameters governing the performance of electrochromic cells

System of Cells	Half life $t_{1/2}$(sec)	Voltage (V)	Diffusion Coeff. D_f $10^{-10} cm^2/s$	Cycle life time	Comment (Process)
ITO/PPY/HCl+ PEO/ITO	0.224	-2 to 2	0.162	$> 10^3$	Diffusion
ITO/PPY/PEO+ LiClO₄/ITO	0.95	-1.2 to 1	0.113	$> 10^3$	Diffusion
ITO/PPY/PTS+ Urea+Glycerol/ ITO	1.20	-2 to 2	-	$> 10^3$	Exponential
ITO/PPY/PEO+ PTS/ITO	0.36	-2 to 2	0.060	$> 10^3$	Diffusion
ITO/PPY/PTS+ Glycerol+PEO/ ITO	0.42	-3 to 2	0.003	$> 10^3$	Diffusion

124

TABLE 4: *Electrochromic cell parameterss calculated using the cyclic voltammogram study*

System of Cells	Slope I_p /$V^{1/2}$x 10^{-6} amp/(V/s)$^{1/2}$	Slope I_c /$V^{1/2}$x 10^{-6} amp/(V/s)$^{1/2}$	Anodic Diffusion Coeff. D_f 10^{-10}cm^2/s	Cathodic Diffusion Coeff. D_f 10^{-10}cm^2/s	Current Transient 10^{-10}cm^2/s
HCl+PEO	1077	1362	0.129	0.206	0.162
PEO+LiClO$_4$	579	1170	0.037	0.152	0.122
PTS+Urea+Glycerol	164	174	0.004	0.003	-
PEO+PTS+Glycerol	174	169	0.003	0.0034	0.003
PTS+PEO	299	209	0.090	0.044	0.060

3.9 SCHOTTKY DIODES BASED ON PPY FILMS

Schottky diodes based on electrochemically deposited PPY and desired metal (Sn, Al and In) have been shown to exhibit interesting electrical characteristics. Such devices have been reported to have ideality factors ranging from 10.11 to 10.67 as calculated by R. Gupta et al [54]. Schottky devices based on PTS doped PPY films have been studied. Current - voltage measurements have been undertaken on such Schottky diodes.

Schottky diodes have been fabricated by thermally evaporating pure (99.99%) metals (Sn, Al and In) on BF$_4^-$ doped semiconducting PPY film. The effective junction area in each device is about 10^{-3} cm^2. Gold contacts are made after carefully removing the PPY film from ITO glass plate. Current (I) - voltage (V) measurement of the each of Schottky devices are conducted using Keithley electrometer (model 610).
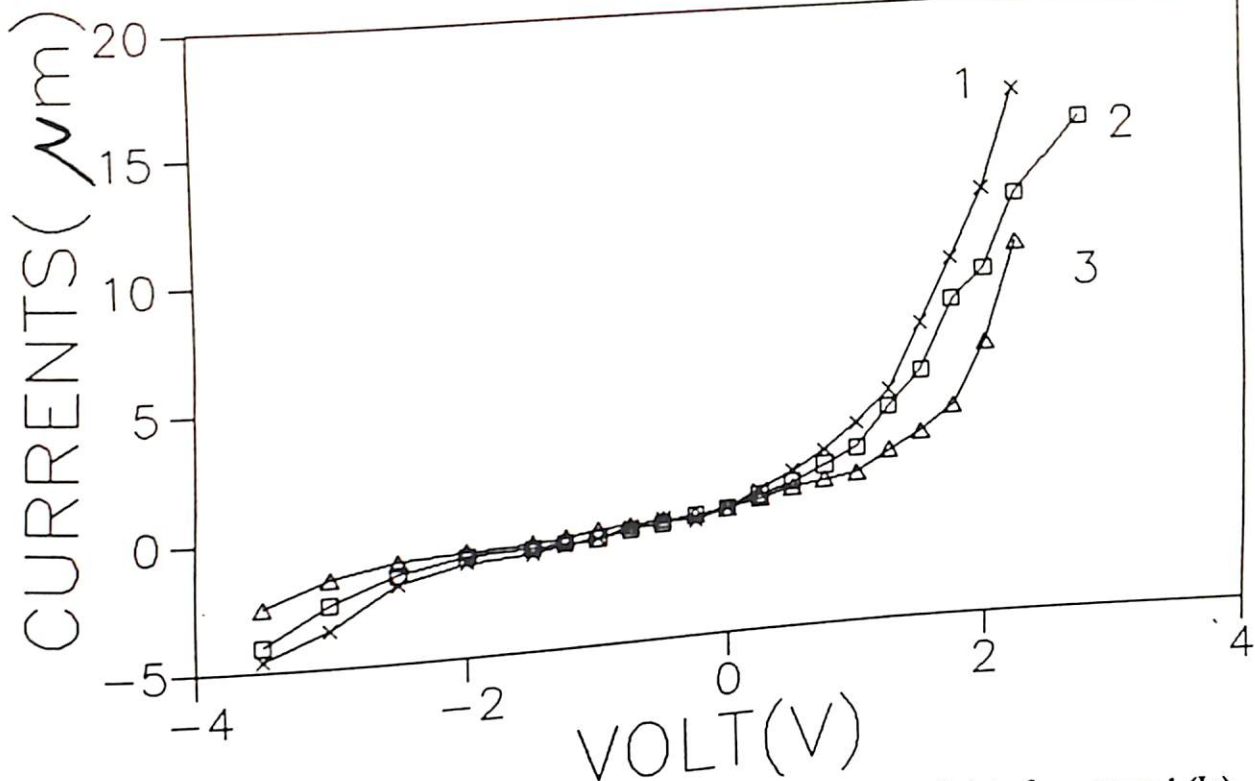
Fig.27 Variation of current (I) vs voltage (V) for various metal /PPY (PTS doped) interface, curve 1 (In), curve 2 (Al) and curve 3 (Sn).

Fig.27 shows the results of various Schottky diodes containing indium (curve 1), aluminium (curve 2), tin (curve 3), respectively. Interestingly, I-V characteristics of both Al/PPY and In/PPY devices are identical to those observed for BF_4^- doped PPY/metal interface. The rectification ratios for Al/PPY and In/PPY have been found to be 9 and 7, respectively. I-V characteristics for Sn/PPY are found to as good as those obtained with Al and In. The various junction parameters have been calculated using Schottky equation as discussed in sec.2.11.1 of Chapter II.

Table 5 shows the values of ideality factors and barrier heights calculated from logJ vs logV plots for various structures. The values of barrier height X_b determined for In/PPY interfaces is lower than that of Al/PPY interface. It can be tentatively concluded that Al makes the excellent Schottky diode with PPY film. It has been further observed that Al undergoes oxidation process and changes the interface properties. The carrier concentration of doped polypyrrole films has been found to be 3×10^{10} cm^{-3} using the Schottky - Richardson equation. The values of various junction parameters have been given in Table 5.

126

TABLE 5: Calculated electronic parameters of Schottky diode based on polypyrrole films:

Metal	Work Function eV	Barrier Height X_b	Ideality Factor (n)
Sn	4.42	0.37	8.85
Al	4.28	0.39	8.82
In	4.12	0.39	8.00

3.10 CONCLUSIONS:

It has been seen that anion influences the electrical and optical properties of PPY films. Mott variable range hopping conduction mechanism prevails for the undoped and lightly doped PPY film whereas $T^{-1/3}$ law holds good for the heavily doped PPY films.

The optical peak absorption is observed at about nm. The energy band gap determined by the optical absorption studies has been found to be $E_g = 3.0$ eV. The value of the energy band gap depends upon the carrier concentration in conducting polymer, which in the case of PPY has been found to be of the order of $10^{20}/$ cm^3. The resistance of the BF$_4^-$ doped PPY films exhibits a transition during annealing at 70^0 C. It has been attributed to the structural changes in the PPY films as is revealed by SEM studies. The structural changes are perhaps caused by the evaporation of the solvent from the film resulting in the creation of voids and pores. The annealing triggers the process of filling of such voids and pores. These studies have established that the PPY film becomes electrically stable. The modification of optical properties of polypyrrole film upon annealing is also observed.

Dielectric relaxation studies conducted on Al-PPY-Al capacitors have revealed many interesting structural and transport properties of charge carriers in PPY. Space charge polarization has been observed in the above system and a simple analysis of this

phenomenon on the basis of space-charge theories further, has helped to understand the charge transport mechanisms. The movement of charge carriers inside the PPY under the influence of an external field and the consequent creation of space charge has been seen to give rise to interfacial polarization. Approximations to space-charge theories are useful both in understanding the dielectric phenomenon and in estimating the mobility of charge carriers. This study indicates that dielectric spectroscopy can be of great use in delineating the charge transport phenomena in conducting polymers. Although, in principle, the effects of diffusion have to be taken into account for the best estimates of the values of mobility, the qualitative nature is apparent. However, it would be interesting to include the diffusion effects in the equations of motion of the space-charge boundary, and hence in the complex permitivity.

Semisolid electrochromic display has been fabricated using polypyrrole film. It has been shown that kinetics of the process is controlled by ionic diffusion for PEO containing electrolytes whereas the PTS+ $LiClO_4$ +Urea, the current decay has been shown by proton movement and into the film or the counter ion motion. It has been shown that improvements in the practical realization of polymer/electrolyte interface will depress the contact resistance with immediate improvement in the output of the devices.

It has been shown that schottky devices can be fabricated by thermal evaporation of metal (Ag/Sn/Ag/In) on electrochemically prepared PPY films. Such devices have been found to exhibit improved values of various junction parameters.

The next chapter describes the results of similar studies carried on polyaniline film prepared using solution cast, electrochemical and vacuum deposition techniques, respectively.

3.11 REFERENCES

1. M. Fukuyama, Y. Kudoh, N. Nanai and S. Yoshimura, *Mol. Cryst. Liq. Cryst.* **224** (1993) 61.

2. G.R. Mitchell and A. Geri, *J. Phys. D: Appl. Phys.* **20** (1987) 1346.

3. B. Sun, J.J. Jones, R.P. Burford and M. Skyllas - Kazacos, *J. Electrochem. Soc.* **130** (1989) 678.

4. J.M. Ribo, C. Acero, M.C. Anglada, A. Dicko, J.M. Tura, *Bull. Soc. Cien* **XIII** (1992) 335.

5. M. Takakubo, *Synth. Metals* **18** (1987) 53.

6. Y. Nogami, J.P. Pouget and T. Ishigura, *Synth. Metals* **62** (1994) 257.

7. R. McNeill, R. Siudak, J.H. Wardlow and D.E. Weiss, *Aust. J. Chem.* **16** (1963) 1056; B.A. Bolto, R. McNeill and D.E. Weiss, *ibid* **16** (1963) 1076.

8. A. Dall'Olio, Y. Dascola, V. Varacco and V. Bocchi, *C.R. Acad. Sci. Ser C* **267** (1968) 433.

9. H. Shirakawa, T. Ito and S. Ikeda, *Polym. J.* **2** (1971) 231.

10. A.F. Diaz, K.K. Kanazawa and G.P. Gardini, *Chem. Commun.* (1979) 635.

11. L.J. Bukley, D.K. Roylance and G. E. Wnek, *J. Polym. Sci. Part B: Polym Physics* **25** (1987) 2179.

12. M. Salmon, A.F. Diaz, A.J. Logan, M. Krounbi and J. Bargon, *Mol. Cryst. Liq. Cryst.* **83** (1982) 265.

13. C.S.C. Bose, S. Basak and K. Rajeshwar, *J. Phys. Chem.* **96** (1992) 9899.

14. G. Bidan, *Mater. Sci. Forum* **21** (1987) 21.

15. J.M. Ko, H. W. Rhee, S.M. Park and Y. Y. Kim, *J. Electrochem. Soc.* **137** (1990) 905.

16. A. F. Diaz, R. Hernandez, R. J. Waltman and J. Barbon, *J. Phys. Chem.* **88** (1984) 3333.

17. M. Salmon, A. F. Diaz, A.J. Logan, M. Krounbi and J. Bargon, *Mol. Cryst. Liq. Cryst.* **83** (1983) 1297; K. Imanishi, M. Satoh, Y. Yasuda, R. Tsushima and S. Aoki, *J. Electroanal. Chem.* **242** (1988) 203.

18. A.F. Diaz and B. Hall, *IBM J. Res. Dev.* **27** (1983) 342.

19. P. Batz, D. Schmeißer and W. Gopel, *Solid State Commun.* **74** (1990) 461.

20. G.R. Mitchell and A. Geri, *J. Phys. D: Appl. Phys.* **20** (1987) 1346.

21. M. Nechtschein, F. Devreux , F. Genoud, E. Vieil, J. M. Pernaut and E. Genies, *Synth. Metals* **15** (1986) 59.

22. B. D. Malhotra, N. Kumar and S. Chandra, *Prog. Polym. Sci.* **12** (1986) 179.

23. F. Genoud, M. Guglielmi, M. Nechtschein, E. Genies and M. Salmon, *Phys. Rev. Lett.* **55** (1985) 118.

24. J.C. Scott, J.L. Bredas, K. Yakushi, P.Pfluger and G.B. Street, *Synth. Metals* **9** (1984) 165.

25. J.C. Scott, P.Pfluger M. T. Krounbi and G.B. Street, *Phys. Rev. B* **28** (1983) 2140.

26. R. Erlandsson, O. Inganas, I. Lundstrom and W.R. Salaneck, *Synth. Metals* **10** (1985) 303.

27. K. Yakushi, L.J. Lauchlan, T.C. Clarke and G.B. Street, *J. Chem. Phys.* **79** (1983) 4774.

28. S.C.K.Misra, N.N.Beladakere, S.S.Pandey, M.K.Ram, T.P.Sharma, B. D. Malhotra and S. Chandra, *J. Appl. Polym. Sci* **50** (1993) 411.

29. J.L.Bredas, R.R. Chance and R. Silbey, *Mol. Cryst. Liq. Cryst.* **77** (1981) 319.

30. J.L.Bredas, J.C. Scott, K. Yakushi and G.B. Street, *Phys. Rev. B* **30** (1984) 1023.

31. J. H. Kaufman, N. Colaneri, J. C. Scott, G.B. Street, *Phys. Rev. Lett.* **53** (1984) 1005.

32. F. Martin, A.C. Prieto, J.A. Saja and R. Aroca, *J. Mol. Struc.*, **174** (1988) 363.

33. A.O. Patil, A.J. Heeger and W. Wudl, *Chem. Rev.* **88** (1988) 183.

34. G. B. Street, in eds. T. A. SKotheim, *Handbook of Conducting Polymer Vol.1 (Marcell Dekker, INC, New York)* (1986) pp: 265.

35. J. M. Ribo, C. Acero, M. C. Anglada, A. Dicko, J. M. Tura, N. Ferrer-Anglada and A. Albaredam, *Bull. Soc. Cat. Cien* **XIIII** (1992) 335.

36. D. Emin and K.L. Ngai, *J. Phys. (Paris) Colloq.* **44** (1983) C3 - 471.

37. G.R. Mitchell, R. Cywinski, S. Mondal and S.J. Sulton, *J. Phys. D: Appl. Phys.* **22** (1983) 1231.

38. R. Singh, R. P. Tandon, V. S. Panwar and S. Chandra, *J. Appl. Phys.* **69** (1991) 2504.

39. M. Aizawa, T. Yamada, H. Shinohara, K. Akagi and H. Shirakawa, *J. Chem. Soc. Chem. Commun.* (1986) 1315.

40. T. Hanawa, S. Kuwabata and H. Yoneyam, *J. Chem. Soc., Faraday Trans. 1* **84** (1988) 1587.

41. A. F. Diaz, A. Martinez and K. K. Kanazawa, *J. Electroanal. Chem.* **130** (1981) 181.

42. J. M. Ko, H. W. Rhee, S. M. Park and C. Y. Kim, *J. Electrochem. Soc.* **137** (1990) 905.

43. C. M. Elliott, A. B. Kobelove, W. J. Albery and Z. Chem, *J. Phys. Chem.* **95** (1991) 1743.

44. P. Novak, B. Rasch and W. Vielstich, *J. Electrochem. Soc.* **138** (1991) 3300.

45. B. Tian anf G. Zerbi, *J. Chem. Phys.* **92** (1990) 3892.

46. S. Tokito, T. Tsutsui and S. Saito, *Chemistry Lett.* (1985)) 531.

47. F. Genoud, M. Guglielmi, M. Nechtschein, E. Genies and M. Salmon, *Phys. Rev. Lett.* **55** (1985) 118.

48. N. N. Beladakere, S. C. K. Misra, M. K. Ram, D. K. Rout, R. Gupta, B. D. Malhotra and S. Chandra, *J. Phys. : Condens. Matter* **4** (1992) 5747.

49. M. Gamoudi, J. J. Andre, B. Francois and M. Maitrot, *J. Phys. Paris* **43** (1982) 953.

50. M. K. Ram, R. Mehrotra, S. S. Pandey and B. D. Malhotra, *J. Phys.: Condens. Matter* **6** (1994) 8913.

51. K. Hyodo and M. Omae, *J. Electroanal. Chem.* **292** (1990) 93.

52. A. Watanabe, K. Mori, Y. Iwasaki, Y. Nakamura and S. Niizuma, *Macromolecules* **20** (1987) 1793.

53. M. K. Ram, N. S. Sundaresan and B. D. Malhotra, *J. Mat. Sci. Lett.* **13** (1994) 1490.

54. R. Gupta, S. C. K. Misra, B. D. Malhotra, N. N. Beladakere and S. Chandra, *Appl. Phys. Lett.* **58** (1991) 51.

CHAPTER IV

STUDIES ON CONDUCTING POLYANILINE FILMS

4.1 INTRODUCTION

Polyaniline is the oldest organic synthetic metal, known till date [1,2]. Until recently, it has been considered as the most ill-defined class of materials, which can be obtained by the chemical oxidative polymerization of aniline [2-4]. In the late fifties, Mohilner et al [5] have proposed new methodologies for the synthesis of polyaniline [6]. The current phase of polyaniline research has been existing since 1980. Polyaniline has been considered to be a novel electronic material for electronic devices [7]. Though polyaniline is not soluble in most organic solvents, it can however be made processable under specific conditions.

Polyaniline refers to a class of polymers, which consists of upto 1000 or more repeat units of aniline. It can exist in four oxidation states ranging from completely oxidized state (pernigraniline) to (reduced form) (leucoemeraldine) [8]. The structure of polyaniline has been given in fig. 1:
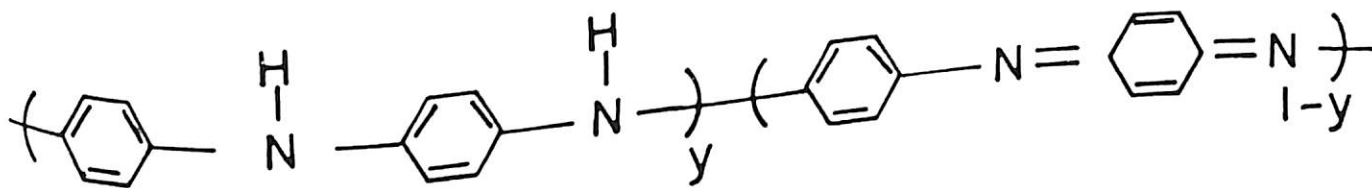

Fig.1 Structure of polyaniline.

In fig. 1, the values of y = 1, 0.5 and 0 result in leucoemeraldine, emeraldine and pernigraniline states respectively. The various structures of polyaniline have been shown in fig. 2:
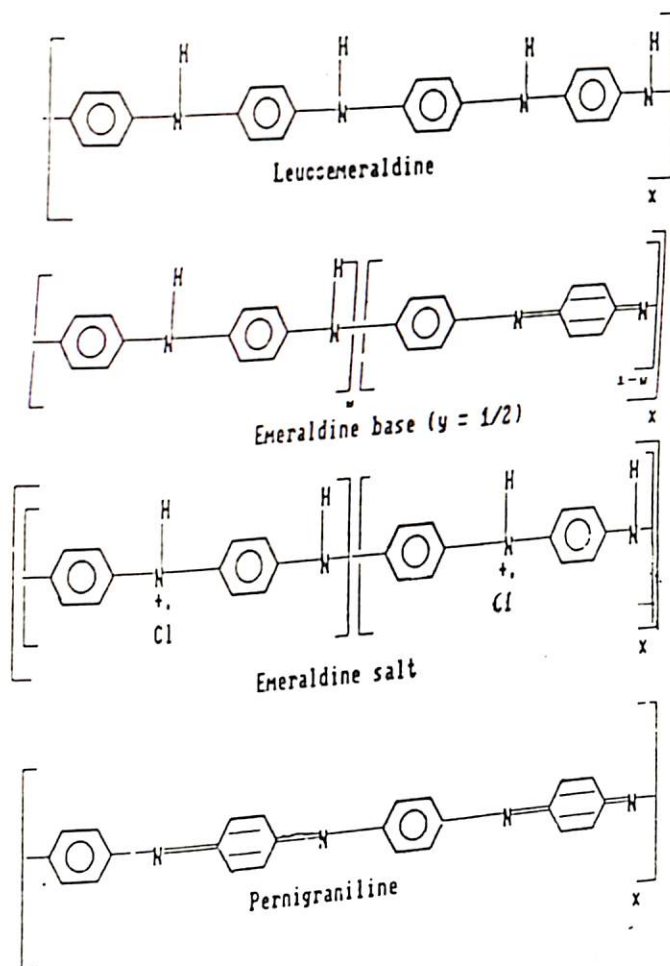

Fig.2 Structures of various forms of polyaniline.

The emeraldine (0.5) oxidation state of polyaniline exhibits the highest level of conductivity upon protonation reaching its value to 5 S/cm with 50% protonation [9]. Emeraldine base (EB) and its salt are two distinct classes of emeraldine base (EB I) and its HCl salt present in ES I exhibit partial crystalline structures. Partly protonated polyaniline (ES-I) can be synthesized easily by the oxidative polymerization of aniline in aqueous acid media by a variety of oxidizing agents; the most commonly used being

ammonium peroxydisulphate, $(NH_4)S_2O_8$, in aqueous HCl. The black green partial crystalline powder is classified as emeraldine salt ES I. ES I contains only 42% of protonation level [10]. This polymer can be deprotonated by aqueous ammonium hydroxide or aqueous NH_3 to give black blue amorphous powder which is classified as emeraldine base I ie EB - I.

Exhaustive extraction at room temperature under nitrogen of as - synthesized emeraldine first with tetrahydrofuran (THF), then with N-methyl pyrrolidinone (NMP) results in the removal of 20% (weight percentage) of oligomeric material and impurities. The resulting emeraldine base powder is classified as EB II and it is found to be crystalline upto doping level of 50% (pseudo-orthorombic). The emeraldine hydrochloric salt ES II, obtained by doping of the EB II powder with 1M HCl is partly crystalline and has a crystal structure different from that of ES-I [10]. It has higher value of electrical conductivity than ES-I obtained by protonation of as - synthesized emeraldine base powder from which EB-II is derived.[13] CNMR studies reveal information the structural properties of as synthesized Polyaniline obtained by oxidative coupling for EB -I and EB-II, respectively.

Thin polyaniline films can be fabricated by solution casting, spin casting, vacuum deposition, Langmuir-Blodgett and electrochemical techniques, respectively [11-15]. Thick Polyaniline films are generally formed by the solution cast method. The spin and solution cast polyaniline films have been used for spectroscopic studies of polyaniline by Cao et al [16] whereas optical and electrochemical characterization of Langmuir-Blodgett films of polyaniline has been extensively studied by Agbor et al [17] and Ram et al. [14]. The insitu polymerization, spectrochemical studies have been carried out on the electrochemically synthesized polyaniline film [18]. The excellent electronic parameters such as rectification

ratio, barrier height, work function of vacuum deposited polyaniline / interface have been experimentally determined [13].

Solution cast, vacuum deposition, electrochemical techniques have been used for the fabrication of desired polyaniline film. Optical, electrical, surface and thermal properties of these films have been experimentally investigated [13].

4.1.1 GENERAL PROPERTIES OF POLYANILINE

The emeraldine base form of polyaniline differs substantially from earlier polymers like polypyrrole, polythiophene etc. in several aspects. Firstly, it is not charge conjugation symmetric and its Fermi level is not exactly at the center of the band gap so that the valence and conduction bands are highly very asymmetric [19]. Consequently, the energy level position of the doping induced and photo-induced absorption spectra differ substantially from those in charge - conjugation symmetric conducting polymers (e.g trans-polyacetylene) [20-21]. Secondly, both carbon rings and nitrogen atoms are within the conjugation path forming a generalized AB polymer [22]. Thus, the emeraldine polymer differs substantially from polypyrrole and polythiophene whose heteroatoms do not contribute significantly to π - band formation. Thirdly, the emeraldine base can be converted from an insulating state ($\sigma_{dc} \approx 10^{-11}$ S/cm) to metallic state ($\sigma_{dc} \approx 10$ S/cm) at room temperature, if protons are added to -N= sites while the number of electrons in the chains are held constant [23].

When polyaniline is doped with protonic acids, a broad polaron band appears in a gap instead of two and a second band appears deep in the gap with a very narrow band near conduction edge. The polaron metal band model has been proposed for polyaniline [24]. The

detailed analysis of electronic structure calculation is supported by the experimental evidence produced by UV-visible spectroscopy, ESR and XPS studies, respectively. The metal-to-insulator transitions of polyaniline strongly effect the chemical structure and the electronic band structure of polyaniline. At all doping levels, the nitrogen atoms can be protonated and deprotonated depending on the pH of the medium.

X-ray spectroscopic analysis of oligomeric polyaniline shows an angular rotation of adjacent rings relative to zigzag chains of the nitrogen atoms in accordance with theoretical predictions in polyaniline.

The electronic band structure of PANI exhibits in the intermediate and fully oxidized forms, polaronic and bipolaronic defects in the band gap. The conducting form of polyaniline is suggested to be a polaron metal where the defects are delocalized over the whole undisturbed conjugation length in semi-quinoid distortions for all the ring structure (polaron lattice). Traditionally, halogens such as chloride, iodine and bromide have been used to enhance the electrical conductivity of the emeraldine base. The charge transfer interaction with halogens results in a decrease in imine repeating unit in the case of emeraldine base. This phenomenon has been extensively studied by Tang et al [25].

4.1.2 OPTICAL PROPERTIES OF POLYANILINE

Optical spectroscopic measurements of polyaniline films have so far provided information on the electronic structure of insulating emeraldine base (EB) form of polyaniline and also the band structure as a function of the degree of protonation. Upon protonation, the absorption at 2.1 eV in EB polymer disappears. In the solution cast film

of ES, three characteristic absorption peaks have been observed at 1.0, 1.5 and 3.0 eV, respectively [26]. In a fully oxidized polyaniline film (doped with conc. H_2SO_4), absorption peak at 2.2 eV along with weak absorption has been reported [16]. It has been proposed that transformation to the metallic state is due to the formation of a polaron lattice in this conducting polymer.

In IR measurement absorption centered at 0.5 eV has been attributed to the presence of charge carriers in polyaniline Kuzmany et al. [27] have suggested that this perhaps results in the observed metal-to-insulator transition. FTIR spectra of polyaniline obtained as a function of the oxidation state in the aqueous acidic medium with pH 3.0 shows maximum intensity at 1375 cm^{-1} indicating the presence of charge carriers in PANI. FTIR absorption studies conducted by Sariciftci et al [24] on polyaniline (in fully oxidized) support the applicability of free carrier model. The values of various optical parameters such as refractive index (n) and dielectric constant (ϵ') obtained for this conducting polymer show reasonable agreement with those obtained for other conjugated polymers. A.J. Epstein et al [28] have reported an unusually high value of non-linear optical susceptibility (X^3) in polyaniline film.

4.1.3 ELECTRICAL PROPERTIES OF POLYANILINE

The highest value of dc conductivity, σ_{dc}, so far obtained for the stretched polyaniline film is about 20 S/cm. Polyaniline films fabricated by solution cast, spin casting and electrochemical techniques show dc conductivity in the range of 1 - 20 S/cm. Mechanism of charge conduction in polyaniline has been of interest for many years.

For example, exposure of the emeraldine base polymer to a protonic acid (HCl) causes a transformation to the emeraldine salt (ES) form of polyaniline. The salt form of PANI exhibits metallic properties including Pauli susceptibility and a free - carrier absorption typical of a metal. It has been revealed that there is a linear increase of susceptibility with increasing level of protonation. Partial protonation leads to the phase segregation between protonated and unprotonated regions, especially for doping level greater than one. Zuo et al [29] have proposed through charge transport measurements carried out in emeraldine salt that conduction occurs via charging - energy limited tunneling among the small granular polymeric grains.

Measurements of temperature dependence of both electrical conductivity σ_{dc}, and thermo-power as a function of protonation level have established the first systematic evidence relating to formation of granular metallic islands in polyaniline. DC conductivity (σ_{dc}) of the metallic emeraldine salt polymer has been found to be very sensitive to the environmental humidity. Frequency (10^1 to 10^{10} Hz) dependent conductivity studies have demonstrated that the primary effect of moisture is on the barrier between the small polymer grains.

A model based on partly protonated polyaniline has been proposed to support the presence of an interpolaron hopping by Kivelson [30]. In a temperature dependence study of polyaniline having protonated ion level in the range between 0 to 0.08, it has been shown that charge transport in this material is similar to that observed in the case of insulating materials. It has been proposed that the charge conduction is due to the hopping of charges among the fixed polaron sites. Ram et al [31] have recently suggested two relaxation

138

mechanisms operating in the emeraldine base.

Most investigations pertaining to electrical conduction mechanism have been experimentally performed with ohmic contact such as gold and silver in pellet or film form of polyaniline. Aluminium (Al) having a lower work function makes a rectifying contact with polyaniline.

4.1.4 APPLICATIONS OF POLYANILINE

Excellent stability of conducting polyaniline films in air as well as water including the ease of transition between insulating and conducting states with voltage has prompted researchers to use it in electrochromic displays, as ion-exchangers and also various microelectronic devices. Other perspective applications of polyaniline include Schottky diodes, cable shielding, electrochromic cells, light emitting diode, photo cells and glucose sensor etc.[32-34].

Most conducting polymers suitable for device can be prepared from wet, solution cast and electrochemical techniques. In such a process, it is difficult to keep a precise control over the parameter, requisite quality and characteristic properties of conducting polyaniline films. Vacuum deposited thin polyaniline films can be helpful towards the fabrication of desired devices.

Keeping this in view detailed experiments pertaining to the doping effect on polyaniline have been conducted. Optical constants of polyaniline films have been calculated using UV-visible and ellipsometric measurements. Besides this, various experiments pertaining to the role of aluminium contact with a view to delineate charge conduction

mechanism in polyaniline films. The space charge relaxation studies including DC electrical conductivity (σ_{dc}) on HCl doped polyaniline films have been systematically conducted. Dielectric relaxation studies have been systematically carried out on aluminum-polyaniline (emeraldine salt)-aluminium (Al-PANI-Al) capacitor configuration both as a function of frequency and temperature, respectively. The analysis of the results obtained for such a configuration has been shown and the value of mobility has been compared with the value obtained by other methods shown in literature [34]. Schottky diodes with both solution cast as well as vacuum deposited polyaniline films have been fabricated. The different electronic parameters have been experimentally determined. Besides this, the semisolid electrochromic cell with different semisolid electrolytes have been fabricated.

4.2 STUDIES ON SOLUTION CAST POLYANILINE FILMS

Polyaniline has been categorized as an intractable material. It has been reported that the films obtained by dissolving emeraldine base powder in N-methylpyrrolidinone (NMP) does not change the basic structure of polyaniline, when emeraldine base film is doped with different protonic acids, the resulting films (emeraldine salt) after processing are found to have higher values of electrical conductivity [12].

An attempt has therefore been made to prepare solution cast films of polyaniline and its properties have been investigated using FTIR, UV-visible and electrical conductivity

measurements. The effect of doping on polyemeraldine base form has been systematically examined.

4.2.1 PREPARATION OF SOLUTION CAST POLYANILINE FILMS

Polyaniline has been chemically synthesized by polymerization of aniline (Merck) using ammonium peroxy disulphate $[(NH_4)_2S_2O_8]$ as an oxidant. 0.219 mole of distilled polyaniline (20 ml) is dissolved in a 200 ml solution of 0.05M (11.5 gram) ammonium peroxydisulphate precooled to 0-5°C. 1M HCl is slowly added to the above solution and the reaction allowed to continue for 4 hours [35]. The dark green precipitate of polyaniline recovered from the reaction vessel is filtered and washed with 1M HCl. This precipitate is further extracted with tetra hydrofuran using soxhlet extractor and is dried under dynamic vacuum. The emeraldine salt powder is again filtered and washed with deionized water as well as acetone for removal of any oligomers. It is then undoped using aqueous ammonia at pH 12.0 for 12 hours and is dried under dynamic vacuum for 24 hours. The blue powder thus obtained is emeraldine base.

The emeraldine base powder so obtained is used for the solution casting of polyemeraldine film. 1 gm of the emeraldine base is stirred magnetically in the 250 ml NMP (b.p. 202°C) at room temperature for eight hours and the blue solution is filtered through a buchnner funnel. This solution is used to cast emeraldine base films on glass plates and is heat treated at 160 to 170°C for obtaining the free standing films of emeraldine base. These films are washed with acetone and are protonated by immersing these in 1M HCl, 1MHNO$_3$, 1M HClO$_4$ and 1M H$_2$SO$_4$ under dynamic vacuum for 24 hours, respectively.

The films of various thicknesses (10 to 150 μm) of emeraldine salt can thus be obtained when heated at 150°C (for removal of any moisture).

4.2.2 FTIR STUDIES ON SOLUTION CAST POLYANILINE FILMS

The FTIR analysis of emeraldine base film shows characteristic peaks at 3400, 2900, 1625 and 1175 cm^{-1} (fig.3). The peak at 3400 cm^{-1} is due to secondary amine (N-H) stretching vibration. The peak at 2900 cm^{-1} is due (C-H) stretching vibration, while 1625 cm^{-1} is attributed to aromatic C=N bond (quinoid). The strong band at 1300 cm^{-1} has been attributed to the combination of several stretching and bending vibrations involving emanating from C-N bonds. The peak assigned at 823 cm^{-1} is due to C-H stretching for emeraldine base.
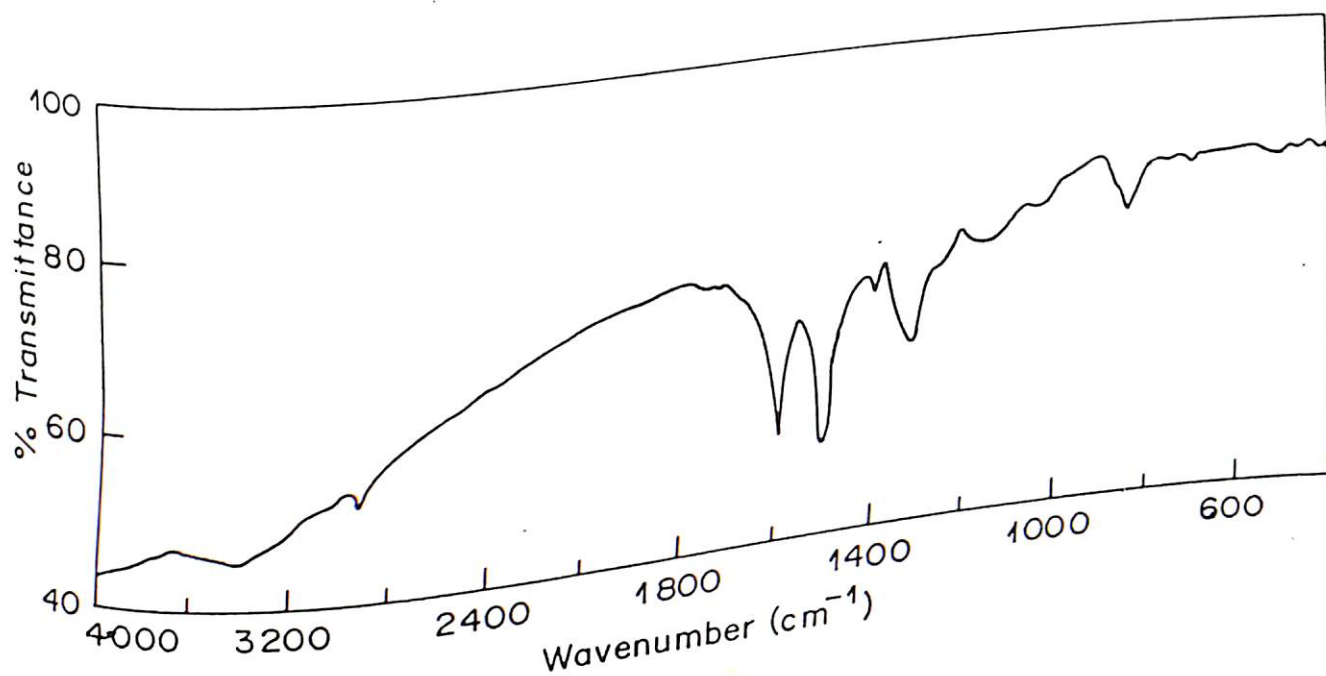
Fig.3 FTIR spectrum of a solution cast emeraldine base film

142

Fig.4 shows FTIR spectra of polyaniline doped with different protonic acids. Curve 1 (fig.4) shows the FTIR spectrum of $HClO_4$ doped polyaniline film. The band at 1375 cm^{-1} appears to be due to the oxidation of polyemeraldine base film suggesting the metallic state of PANI. The intensity of 1500 cm^{-1} peak decreases whereas 1590 cm^{-1} peak increases with doping . Incidentally, both these peaks have been assigned to the benzoid ring. The frequency at 843 cm^{-1} shifts to a higher value with increase in degree of doping. The strong characteristic peaks at 1100 cm^{-1} and 640 cm^{-1} pertaining to ClO_4^- ions in polyaniline matrix can be clearly seen in this fig. 4 (curve 1). There is also an increase in the intensities of 1300 and 1140 cm^{-1} bands due to enhanced doping. However, there is no change in the intensity of 3425 cm^{-1} absorption which arises due to N-H vibrations. The band observed at around 1100 cm^{-1} originates not only from δ -C-H of the rings but also from ClO_4^- vibration. 1140 cm^{-1} band corresponds to the Raman active ring δ-C-H vibration mode.

Curve 2 (fig.4) shows the FTIR spectrum for the H_2SO_4 doped polyaniline film. It exhibits peaks at 1375 and 983 cm^{-1} assigned to the presence of HSO_4^- ions. The peak at 1175 cm^{-1} indicates the presence of Cl^- ion in polyaniline film as shown in the FTIR spectra of HCl doped polyaniline (curve 3, fig.4). Curve 4 (fig.4) exhibits the effect of higher doping with HNO_3 on polyaniline film. The strong band observed at 1375 cm^{-1} has been attributed to the higher doping in PANI film. Besides this, another strong band at 1175 cm^{-1} in emeraldine base film has been observed. The band noticed at 1629 cm^{-1} has been attributed to the emeraldine base film (curve 5, fig.4). The positions of the peaks around 800 cm^{-1} which appears for the polyemeraldine base shifts as a result of the protonic acid doping.
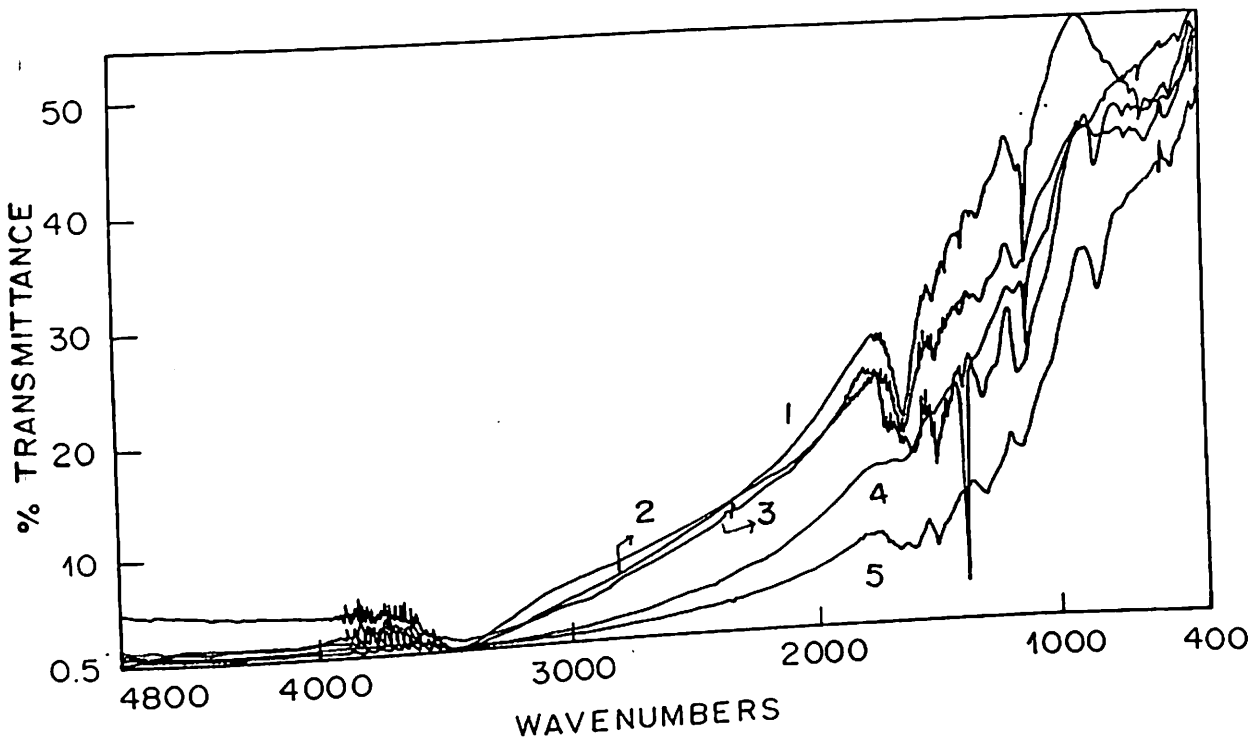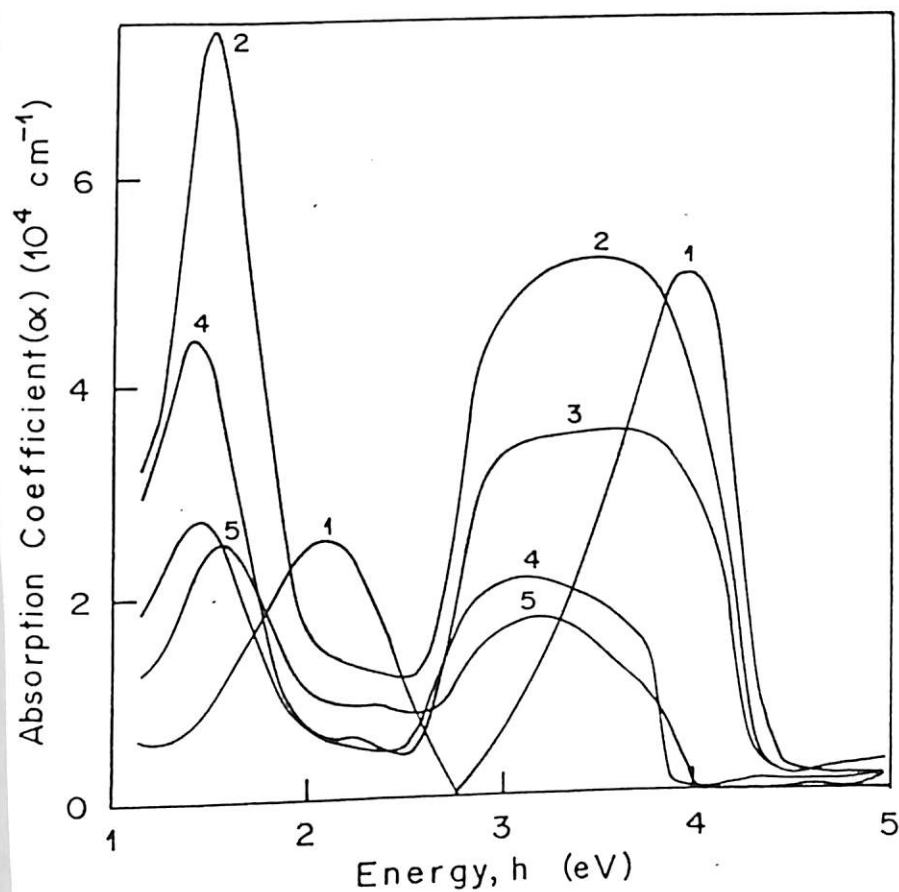
Fig.4 FTIR spectra of some solution cast polyaniline films doped with different protonic acid: curve 1 (HClO₄), curve 2 (H₂SO₄), curve 3 (HCl), curve 4 (HNO₃) and curve 5 (polyemeraldine base)

4.2.3 UV-VISIBLE STUDIES OF SOLUTION CAST FILMS OF POLYANILINE

The effect of both change in the oxidation level and also the protonation level on the electronic structure of polyaniline are presently some of the most important issues. The resulting spectral changes have been extensively studied in recent years. The protonic acid doping in polyaniline changes the number of electrons in the valence band or into conduction band and moves the Fermi level. The maximum doping level in emeraldine base is about 50% with protonic acid whereas the dications are formed near the quinoid ring. However, the extensive observations and other studies have shown that the protonated

144

mer results via polysemiquinine radical cations and the resonance forms consists of sepa-

polarons. The sequential change of polyaniline with protonic acid is given in fig.5

-visible spectra of some polyaniline solution cast film, Curve 1 (undoped polyaniline), curve 2 (H_2SO_4
lyaniline), curve 3 ($HClO_4$ doped polyaniline), curve 4 (HCl doped polyaniline) and curve 5 (HNO_3
e).

he optical absorption spectra of protonated polyaniline films have been shown in

ig.5 shows the absorption bands at 1.4-1.5, 2.3 and 3.3-3.6 eV for each of the

. It is interesting to see that the polaron bands observed at 1.4 eV and 1.5 eV have

signed to the presence of HNO_3 and HCl in polyaniline, respectively. It can be seen

· π^* transition is not so sharp in the doped polyaniline [37].

145
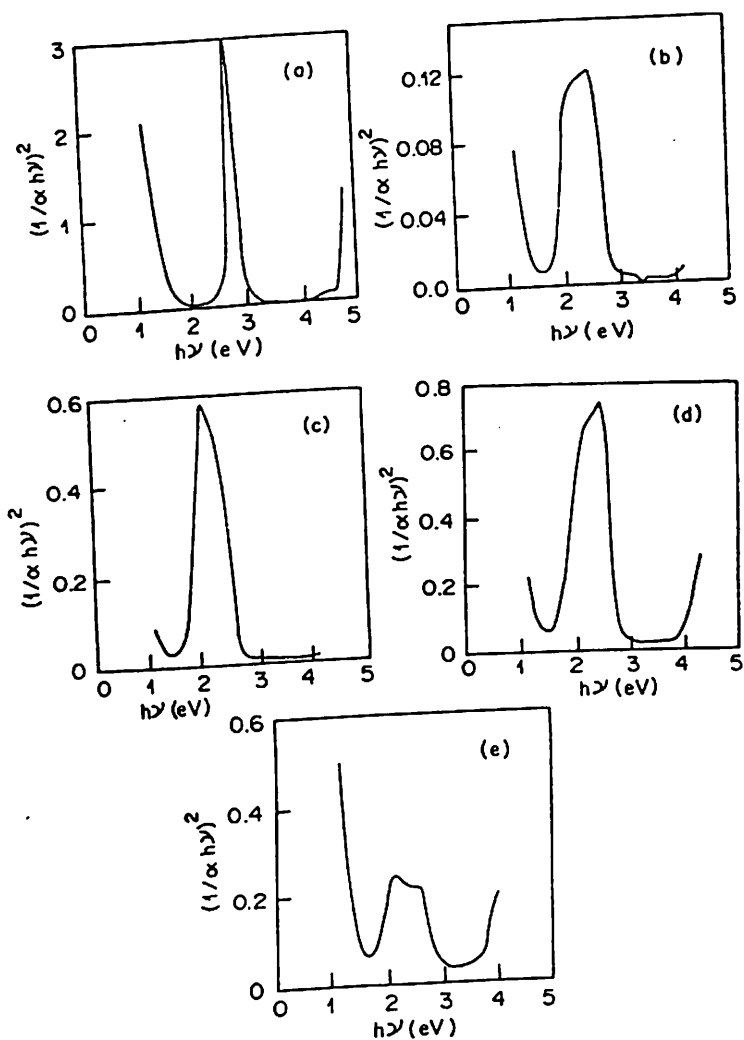
Fig. 6 Plot of $(1/h \nu . \alpha)^2$ vs photon energy $(h\nu)$ for some solution cast films; undoped polyaniline and with various protonic acids such as (b) H_2SO_4 doped (c) HNO_3 doped (d) HCl doped (e) $HClO_4$ doped polyaniline respectively

Fig. 6(a to e) shows the plots of $(1/\alpha . h \nu)^2$ vs photon energy $(h\nu)$ for polyaniline films such as emeraldine base obtained as a consequence of doping with different protonic acids. The band gap obtained for the undoped polyaniline has been calculated to be 3.6 eV. The values of band gaps of various doped polyaniline film lie in the range from 3.25 to 3.3 eV. These values are in agreement with the data obtained for vacuum deposited polyaniline

films.

4.2.4 THERMAL STUDIES OF SOLUTION CAST POLYANILINE FILMS
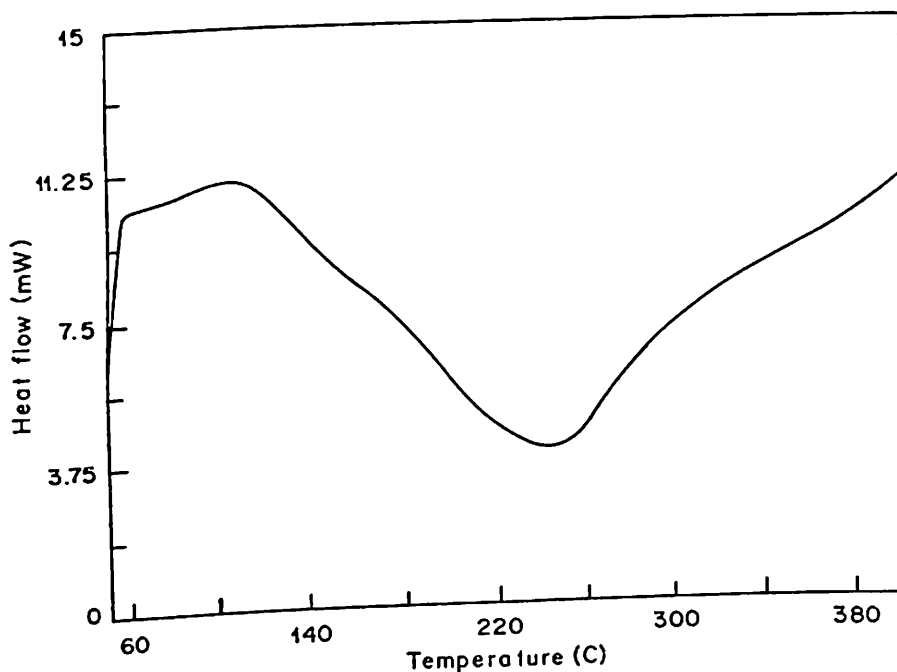
Fig. 7 DSC thermogram of a solution cast polyaniline (emeraldine base) film.

Thermal analysis is known to give useful information in relation to the stability of conducting polymer. In this context. differential scanning calorimetric studies have been performed on some solution cast polyaniline films. Fig. 7 shows the DSC thermogram of this conducting polymer. The observed endotherm at 100°C can be attributed to the presence of intrinsic water (H_2O) in the polyanline matrix. The observed endothermic peak can be attributed to the loss of weight of polyaniline arising due to the release of water molecule. The endothermic enthalphy change from 140 to 300°C is due to the presence of cross-links in the polyaniline chain. The broad exothermic peak at about 250°C occurs due to the loss of weight (7-10%) of polyaniline films [38].

147

2.5 ELECTRICAL CONDUCTIVITY STUDIES OF SOLUTION CAST POLYANILINE FILMS

The electrical conductivity of metallic emeraldine salt polymer has been found to be sensitive to humidity. A conduction mechanism based on electron - hopping between localized states, known as a proton-exchange-assisted conduction of electrons (PEACE) has recently been proposed. Such a behaviour has been understood on the basis of quasi - one dimensional variable range hopping model. However, no unified model presently exits that can explain the observed electrical phenomenon over the entire temperature range. DC conductivity (σ_{dc}), studies on HCl doped polyaniline films have been experimentally performed on some solution cast films. The ohmic contacts have been obtained by vacuum deposition of silver onto polyaniline films.

Fig.8 shows variation of σ_{dc} obtained for HCl doped polyaniline has been plotted as a function of $10^3/T$, indicating a poor fit. These results suggest that electrical conduction in HCl doped PANI is predominantly via hopping of charge carriers. The plot of $\log\sigma_{dc}$ vs $T^{-1/4}$ (fig.9) does not once again yield a linear fit suggesting that the variable range hopping conduction mechanism is perhaps not predominant in this temperature region.
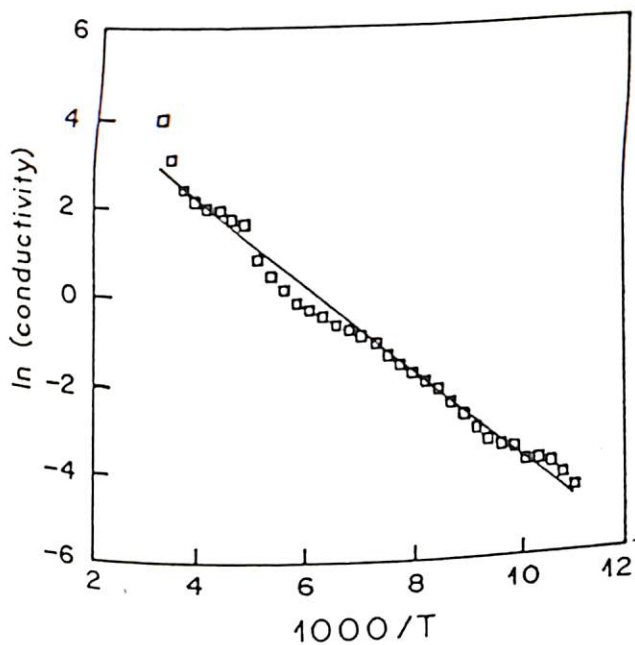
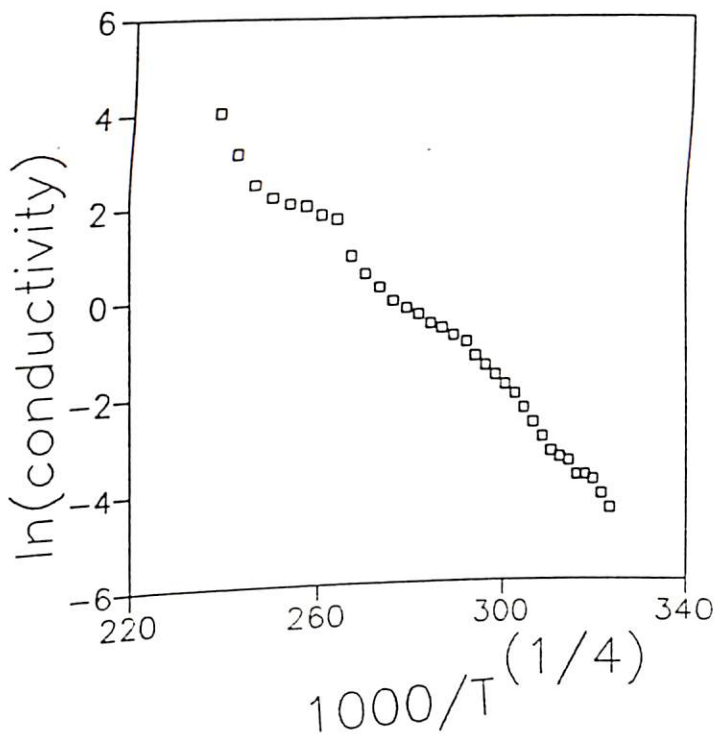Fig.8 Variation of ln σ_{dc} vs $10^3/T$ of solution a HCl doped polyaniline film

Fig.9 Variation of ln σ_{dc} vs $10^3/T^{1/4}$ of a solution cast polyaniline film

Plot of logσ_{ac} vs $10^3/T^{1/2}$ (fig.10) has been attempted [39]. A linear fit can be clearly seen (fig.10). It appears that a quasi 1 D-variable range hopping conduction phenomenon in which charges are transported effectively along one dimension is perhaps operative in this conducting polymer. The temperature dependence measurements of electrical conductivity in polyaniline suggest a cigar shaped metallic region. These polyaniline chains are assumed

149

to have finite length and are perhaps packed parallel into bundles. If the disorder is weak ie $E_F \, \tau_i/h >> 1$, there exists a threshold value of interchain transition rate w_c, below which $(w < w_c)$ the electron states are localized and above which $(w > w_c)$, these are extended over several chains. Thus there exists a fairly high temperature below which the quasi 1D-VRH model is applicable.

The electrical conduction along the polyaniline can hence be expressed as [40,41]:

$$\sigma = \sigma_0 \exp[- (T_0/T)^{1/2}] \qquad \text{Eq.1}$$

$$\sigma_0 = e^2 \, \mathbf{v}_{ph}/\alpha K_B TA \qquad \text{Eq.2}$$

and

$$T_0 = 8\alpha/g(E_F \, K_B) \qquad \text{Eq.3}$$

where $\mathbf{v}_{ph}$ is the attempting frequency, K_B is the Boltzmann's constant, $g(E_F)$ is the density of states with the sign of spin, A is the average cross-sectional length.

The value for T_0 for the emeraldine salt has been found to be 1370K which is in close agreement with the calculated value by Zuo et al [29]. Moreover, value of T_0 is nearly of the same order as deduced from the charging - energy - limited tunneling model proposed granular metal. The value of density of states $g(E_F)$ in this conducting polymer has been obtained as 4.2×10^{28} J^{-1} cm^{-1}. The hopping localization length has been taken as 10 Å.
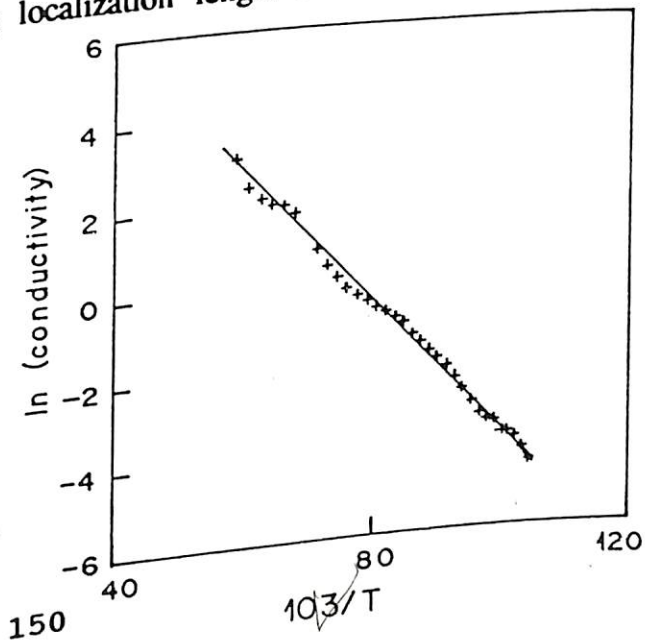

Fig.10 Variation of $\log \sigma_{dc}$ vs $10^3/T^{1/2}$ for a solution cast HCl doped polyaniline film

150

4.2.6 DIELECTRIC RELAXATION STUDIES ON SOLUTION CAST POLYANILINE FILMS

Charge transport mechanism in conducting polymers has been investigated in recent years using a number of experimental methods such as dielectric relaxation, ac conductivity and photoconductivity etc [30]. It has been proposed that non-linear excitations such as solitons and polarons play an important role in the transport of electric charge in conducting polymers. Dielectric spectroscopy has been found to be one of the valuable experimental tools for understanding the phenomenon of charge transport in conducting polymers.

Philip et al [39]. have proposed a random dimer model that explains the observed electrical conductivity of leucoemeraldine as a function of oxidation. Javadi et al. [44] have experimentally shown that a model based on granular polymeric metal particles and localization within metallic islands plays an important role in the frequency and temperature dependence of dielectric constant of polyaniline. Further, the barriers present among the granular polymeric metal particles of emeraldine salt form of polyaniline have been suggested to arise from the presence of cross-links, chain ends and protonated amine groups (NH^{2+}) etc.

Similarly, Zuo et al [29] have carried out various studies relating to both temperature and electric field dependence of σ and thermopower as a function of protonation level of polyaniline. These studies have brought out that the charge transport in emeraldine base is polyaniline. These studies have brought out that the charge transport in emeraldine base is dominated by phase segregation with protonated and unprotonated regions pointing out to the operation of charging energy limited tunneling mechanism in this system.

Space charge relaxation studies have been used to experimentally determine the mobility of charge carriers in thin films of organic conducting polymer [42]. During the preparation of the Ph.D. programme, dielectric studies have been carried out on aluminium(Al) -polyaniline- aluminium(Al) capacitor configuration in the frequency region from 10^3 to 10^7 Hz using blocking contacts on thin films of polyaniline. The Al-PANI-Al capacitor configuration wherein Al and PANI have work functions as 3.74 eV and 4.12-4.28 eV, respectively, is known to exhibit interesting space charge polarization near the electrodes under the static bias across the sample. No injection or extraction of charge occurs from polyaniline as the electrodes (Al) are blocking and the charges align towards their respective electrodes. The results of the present investigations conducted on Al-PANI-Al structure yield valuable information on the mobility of charge carriers on polyaniline. The effect of both temperature and thickness of polyaniline on the mobility of charge carriers has been systematically investigated.

Al-PANI-Al capacitor configuration used for dielectric measurement have been fabricated by vacuum deposition (10^{-6} torr) of aluminium (99.99%). I-V characteristics of Al/PANI/graphite and Al-PANI-Al capacitor configuration are experimentally determined using Keithley (617) electrometer. Both the dielectric and capacitance measurements are performed on various Al-PANI-Al configuration having different thicknesses of polyaniline at a signal voltage of 0.1 V, with 0 mV, 50 mV, 100 mV and 200 mV dc bias using a HP 4192A impedance analyzer operating in the frequency range 5 Hz to 13 MHz.

Fig. 11a shows the results of current(I)-voltage(V) measurements on Al-PANI-graphite and Al-polyaniline-Al configurations fabricated using a desired thickness

(30 μm) of polyaniline. From this figure, one can clearly see that Al makes a Schottky contact with polyaniline (curve 1), whereas it forms rectifying contacts on both sides of Al/polyaniline/Al configuration. In the light of this result, I-V measurements on Al-polyaniline-Al configurations have been carried out for various thicknesses of polyaniline such as 15, 32, 45, 54 and 145 μm, respectively at room temperature. From these results, it can perhaps be concluded that Al shows the rectifying behaviour in all Al-PANI-Al configurations.

Fig. 12 gives the variation of capacitance with frequency measured for a number of Al-PANI-Al structures with varying thickness of polyaniline at room temperature at 100 mV dc bias. The value of the capacitance gradually decreases with increase in frequency resulting into a resonance behaviour at 680 kHz for all Al-PANI-Al structures. Fig. 13 shows the result of the capacitance and dielectric loss measurements conducted on desired Al-PANI-Al configuration at 0 V bias fabricated using polyaniline film having respective thickness from 26 to 30 μm. The slow decrease of capacitance with frequency coupled with the observed resonance at 680 kHz (Fig.12 and 13) indicates the presence of space charge polarization in the above Al-PANI-Al configurations [43].
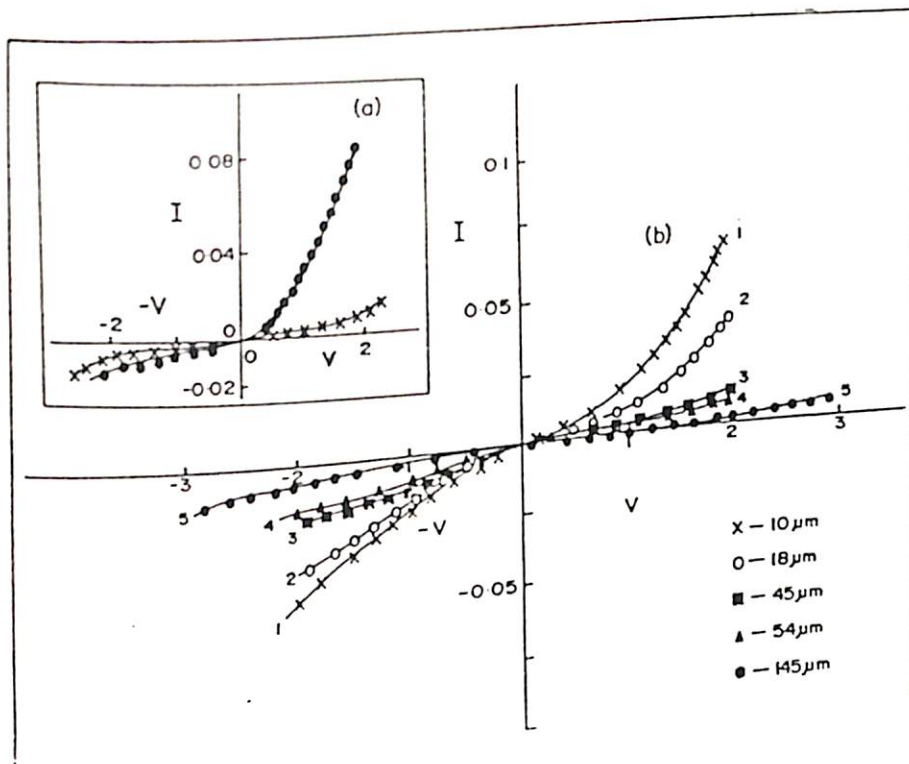
Fig.11 (a) variation of current, I (mA) - voltage, V (volts) for Al-PANI (emeraldine salt)-graphite and (x) Al-PANI (emeraldine salt)-Al configurations. (b) Variation of current I (mA) -voltage, V (volts) characteristics in Al-PANI (emeraldine salt)-Al configuration as a function of thickness: curve 1(10μm), curve 2 (18μm), curve 3 (45μm), curve 4 (54μm), curve 5 (145μm).
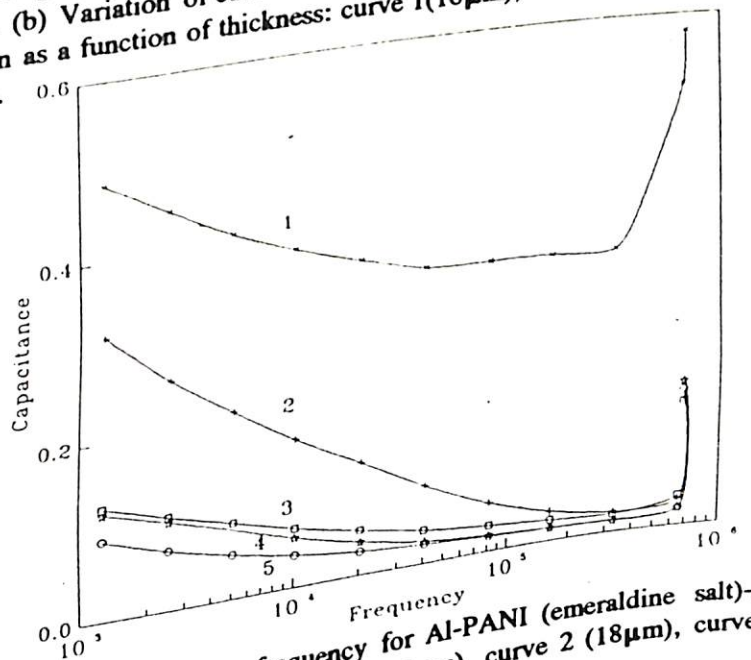
Fig.12 Variation of differential capacitance (μF) with logarithm frequency for Al-PANI (emeraldine salt)-Al configuration at static bias of 100mV as a function of thickness curve 1 (10μm), curve 2 (18μm), curve 3 (45μm), curve 4 (54μm), curve 5 (145μm).

154
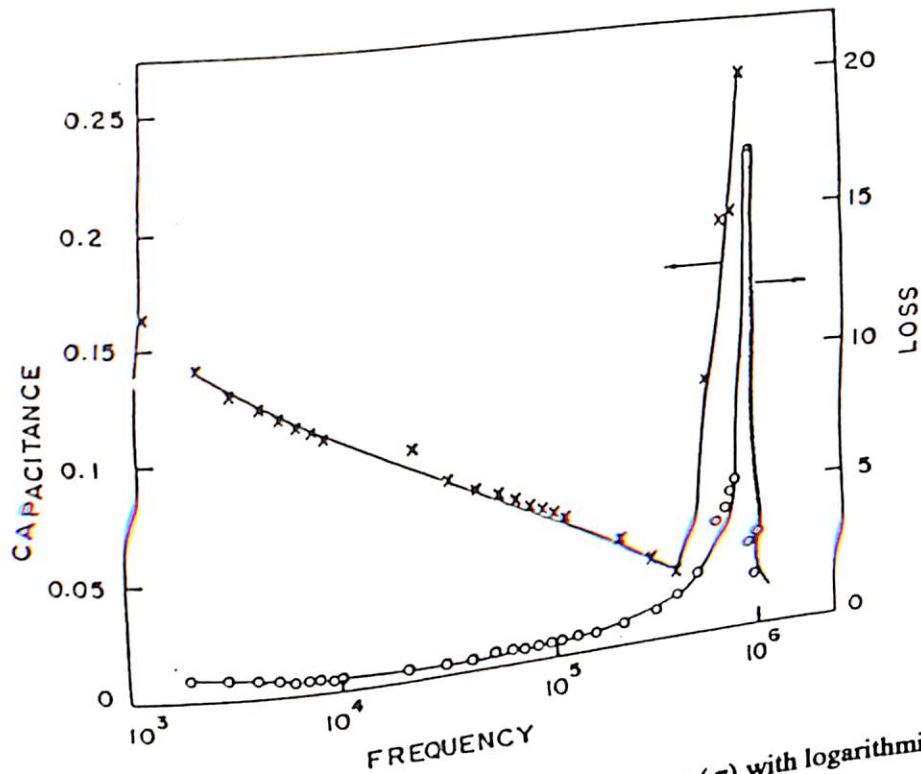
Fig.13 Variation of differential capacitance (μm) (x) and dielectric loss (σ) with logarithmic frequency at 0 bias.
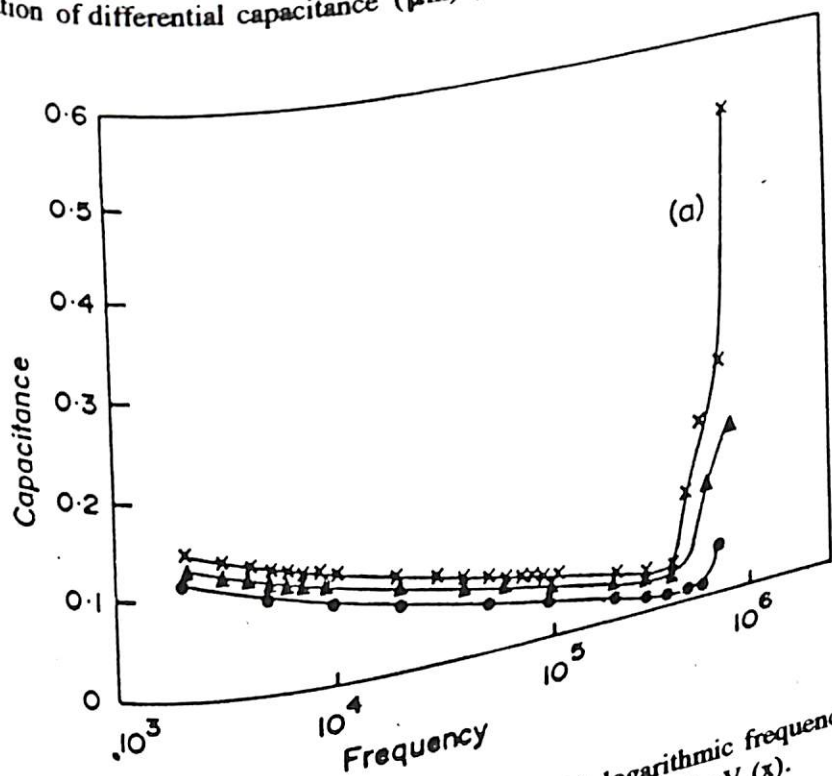

Fig.14(a) Variation of differential capacitance (μF) with logarithmic frequency (Hz) for Al-PANI (emeraldine salt)-Al at various bias voltages, 50mV (o) , 100mV (?) and 200mV (x).
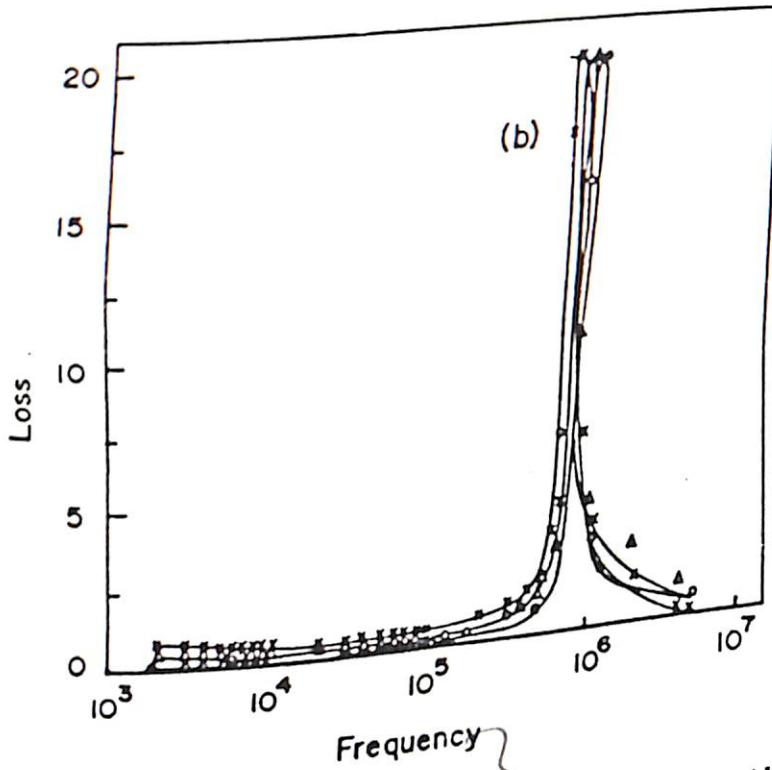
155

Fig.15(b) Variation of dielectric loss with logarithmic frequency (Hz) for the Al-PANI (Emeraldine salt)-Al at various bias voltage 50mV (o), 100mV (?) and 200 mV (x).

Fig.14 and fig.15 exhibit the results of systematic studies carried out on a given Al-PANI-Al structure relating to both dielectric loss and capacitance as a function of frequency at various bias voltages such as 50, 100 and 200 mV, respectively. The observed increase in the value of both capacitance (Fig. 14) and dielectric loss (Fig. 15) with bias voltage indicates the increased density of charge carriers in the space charge region of Al-PANI-Al configuration. Interestingly, the resonance occurs at the same frequency (Fig. 14 and fig.15) as observed earlier in (Fig.13).

Fig.16a shows the variation of imaginary part of the dielectric constant ϵ'' as a function of w. In this figure, one can clearly see the presence of two relaxation times in polyaniline. The values of these relaxation times have been calculated and are found to

156

be 1 μs and 0.3 μs, respectively.

Fig. 16b is the Cole-Cole plot obtained as a result of the present measurements for various temperatures such as 120, 290, 323 and 373.6 K, respectively. The marked deviation (scew type) from semi-circular arc as seen in this Fig. 15b. points out to the operation of a complex relaxation behaviour in this typical system arising due to presence of charge carriers and their conductivity. Consequently, one can express complex permitivity, as

$$\epsilon^{\cdot} = \epsilon_{\alpha} + [(\epsilon_0 - \epsilon_{\alpha}) / 1 + i\tau w)] - i \sigma w \qquad Eq.4$$

where ϵ_0 is the static dielectric constant, τ is the relaxation time and ϵ_{α} is the instantaneous dielectric permitivity, σ is the conductivity of the medium and w is the angular frequency. The observed scew type behaviour (Fig. 16b) can be understood to arise both from the conduction of various charge carriers (presumably polarons/bipolarons) and their resulting dipoles [30].
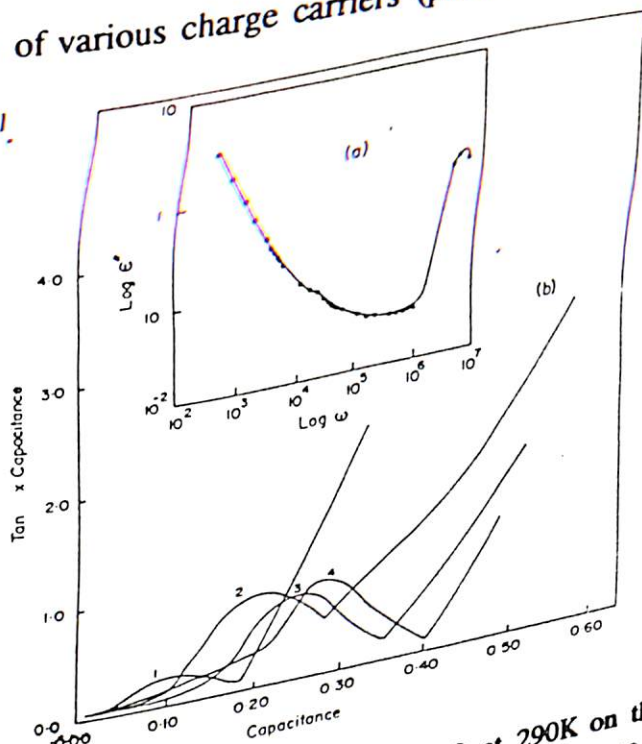

Fig. 16 (a) Variation of imaginary part of ϵ'' as a function w (=$2\pi f$) at 290K on the logarithmic scale (b) Cole-Cole plots for Al-PANI (emeraldine salt)-Al as a function of temperature: curve 1 (120K), curve 2 (290K), curve 3 (323K) , curve 4 (373.6K).

157

The nature of semi-circle (i.e. scew type) indicates the presence of different relaxation rates. Further, the relaxation time obtained from the Cole-Cole plot is found to be dependent on temperature and obeys the following Arrehenious equation [30]:

$$\tau = \tau_0 \exp[E_a' / k_B T] \qquad \text{Eq.5}$$

where E_a' is the activation energy, k_B is the Boltzmann constant. The activation energies E_a' of conduction have been calculated to be 0.042 eV and 0.028 eV, respectively. The observed shift of the Cole-Cole plot with the increase in temperature indicates the presence of multiple relaxation in the given Al-PANI-Al configuration. Moreover, the departure from scew behaviour beyond 0.3 μF curve 2, (Fig. 16b) seen in the Cole-Cole plot signifies the contribution originating from the contact (Al) of the given Al-PANI-Al configuration. Similar behaviour in the various other Cole-Cole plots (Fig. 16b) can also be seen. The contact effect may perhaps arise due to the Schottky junction found as a result of thermal evaporation of aluminium on polyaniline films.

Fig. 17a exhibits the variation of dielectric loss as a function of frequency at different temperatures. The relaxation observed here is typical of relaxation expected for the damping of dipole oscillators. Although, the shapes of loss profiles are similar, the shift in the frequency at which the dielectric loss maximum occurs can perhaps be attributed to the change in the value of the mobility of charge carriers. At a higher temperature, the shift of the dielectric loss peak is probably due to the increased number of induced dipoles in Al-PANI-Al configuration. Moreover, the induced dipoles are likely to be oriented in the direction of the applied electric field at higher frequency.

An attempt has been made to compute the magnitude of mobility of charge carriers

using the following relation [43] :

$$\mu = [w_m^4 \, \epsilon_0^3 \, L^2 \, / \, n^3 \, e^3 \, V_s]^{1/4}$$

where w_m is the angular frequency at which there is a maximum dielectric loss, V_s is the static bias (0.1V), n is the carrier concentration, $\epsilon = 100$ and ϵ_0 is the permitivity of space charge. Fig.17b shows the plot of $1/C^2$ against applied voltage. The slope of the observed curve can be used to calculate the magnitude of carrier concentration, that has been found as $n = 10^{18}$ cm^{-3}).
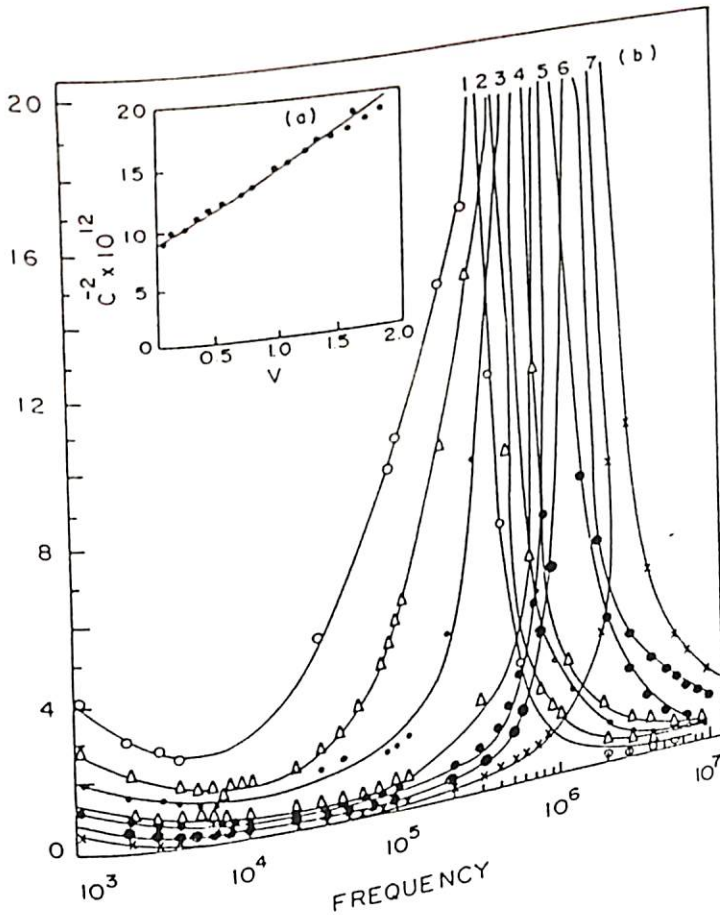
Fig. 17(a) Variation of dielectric loss with logarithmic frequency (Hz) at different temperatures for Al-PANI(emeraldine salt)-Al at static bias (100mV) curve 1 (120K), curve 2 (133K),curve 3 (213K), curve 4 (290K), curve 5 (323K), curve 6 (363K), curve 7 (373.6K). (b) Variation of $1/C^2(F^{-2})$ of Al-PANI-(emeraldine salt) -Al configuration as function of applied voltage (volts)

Fig. 18a exhibits the variation of mobility as a function of temperature. This figure indicates that the value of mobility increases slowly upto 300k after which we notice a sharp and sudden increase at about 340k. It appears that polyaniline undergoes a phase transition at this temperature. Such a behaviour points to the occurrence of a glass - rubber transition in polyaniline films. The value of mobility μ, calculated at 300k has been found to be 9.6 $\times 10^{-6}$ cm^2/V.sec. The value of mobility μ calculated as a function of thickness of polyaniline film has been shown in Fig. 18b. The value of slope obtained as ≤ 2 confirms the presence of space charge polarization.
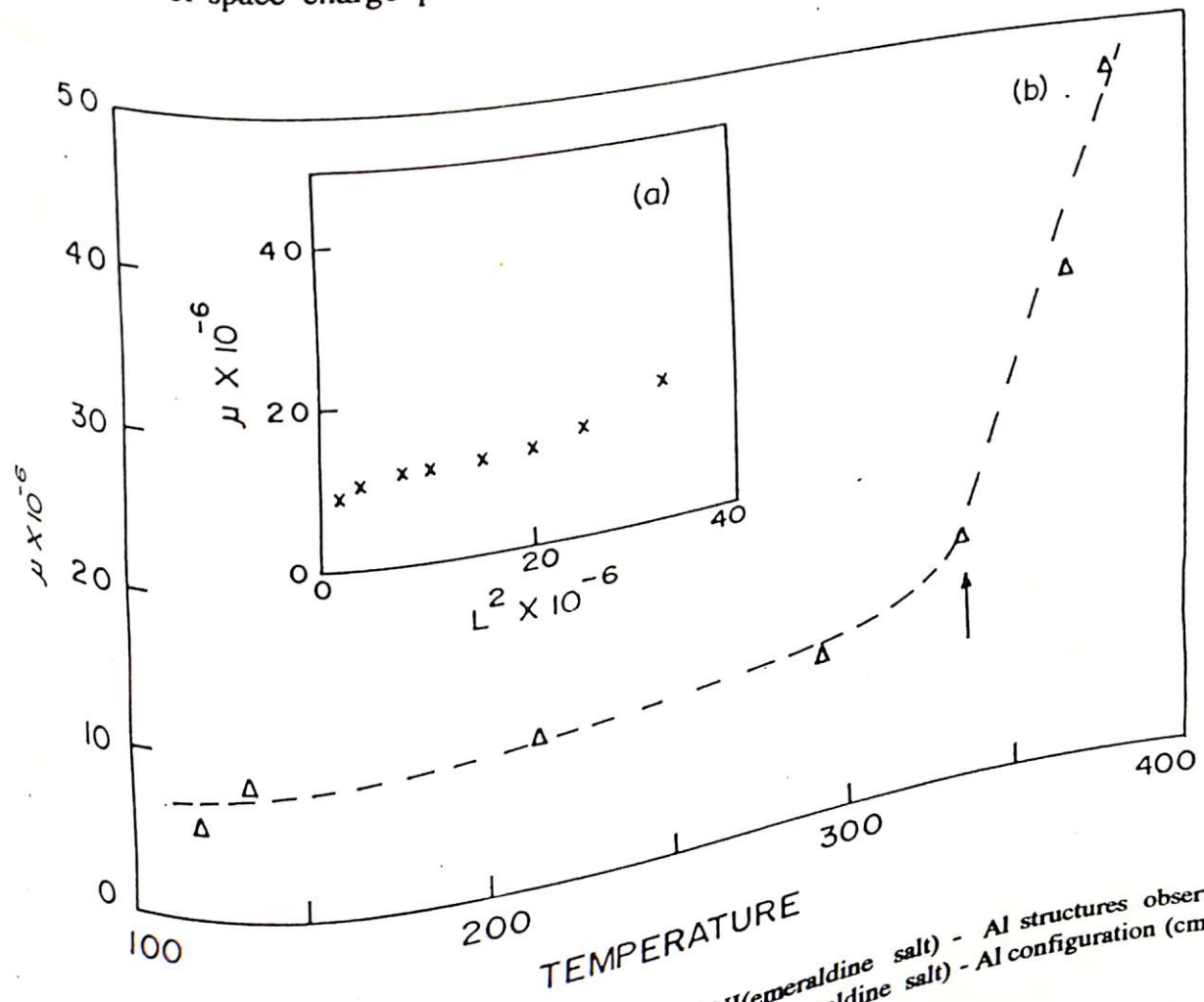

Fig. 18(a) Variation of mobility, μ (cm^2/V.sec) for Al-PANI(emeraldine salt) - Al structures observed with thickness (m^2) (a) variation of mobility, μ observed for Al-PANI (emeraldine salt) - Al configuration (cm^2/V.sec) with temperature (K)

160

The temperature (120 to 290 K) dependence of electrical conductivity as a function of measured frequency 'f' for the Al-PANI (emeraldine salt)-Al structure obeys the relation $\sigma(f, T) = B f^s$, where B is a constant and the value of S has been found to be 0.87. This result suggests once again the operation of one dimensional variable range hopping conduction mechanism in this system in the above temperature regime [44] which is consistent with the existing models. It is however, difficult to ascertain at this stage the exact mechanism that may perhaps be responsible for the observed dependence of electrical conductivity, $\sigma(f,T)$ of Al - PANI (emeraldine salt) - Al structure on frequency (f) at elevated temperatures (T > 290K).

4.3 STUDIES ON ELECTROCHEMICALLY PREPARED POLYANILINE FILMS

Electrochemically synthesized polyaniline films are generally used for the optical, electrochemical and SEM studies. The insitu polymerization, spectrochemical studies etc. have been mostly studied on electrochemically synthesized thin polyaniline films [45]. The optical properties of various electrochemically prepared polyaniline films have been investigated using UV-visible and ellipsometric measurements. The values of optical parameters in polyaniline films have been measured experimentally using the ellipsometric technique.

4.3.1. PREPARATION OF POLYANILINE FILMS USING ELECTROCHEMICAL TECHNIQUE

The thin polyaniline films have been deposited on ITO glass plates. The potential sweep from 0.2 to 1.0 V has been used at a scan rate of 20 mV/sec for obtaining thin film of polyaniline on ITO glass plate when the cell contains 0.1 M aniline in 1M HCl solution. In about 60 to 120 sec, polyaniline films (0.1 - 0.5 μm) on ITO glass plate are obtained. Polyaniline films thus obtained are, however, not self-supporting. The films are undoped in aqueous ammonia (NH$_3$) for obtaining the desired emeraldine base films. The emeraldine base film is treated for six hours with phenylhydrazine for obtaining the leucoemeraldine films. The emeraldine base film on being treated for six hours with (NH$_4$)$_2$S$_2$O$_8$ results in fully oxidized state (pernigraniline). The emeraldine base on being subsequently treated for 6 hours with 1M HCl, 1MHClO$_4$, 1M HNO$_3$ and 1 MH$_2$SO$_4$ result in emeraldine salt form, respectively.

FTIR spectra obtained for the electrochemical films are found to be similar to that of the solution cast polyaniline films.

4.3.2 UV-VISIBLE STUDIES OF ELECTROCHEMICALLY PREPARED FILMS:

Optical properties of polyaniline have been investigated as a function of both oxidation and protonation. It has been proposed that a protonic lattice structure for this polyaniline agrees with theoretical calculation [46]. Optical properties and Pauli susceptibility measurements of different forms of polyaniline such as completely oxidized (pernigraniline) to reduced (leucoemeraldine) can either be achieved by electrochemical treatment of the

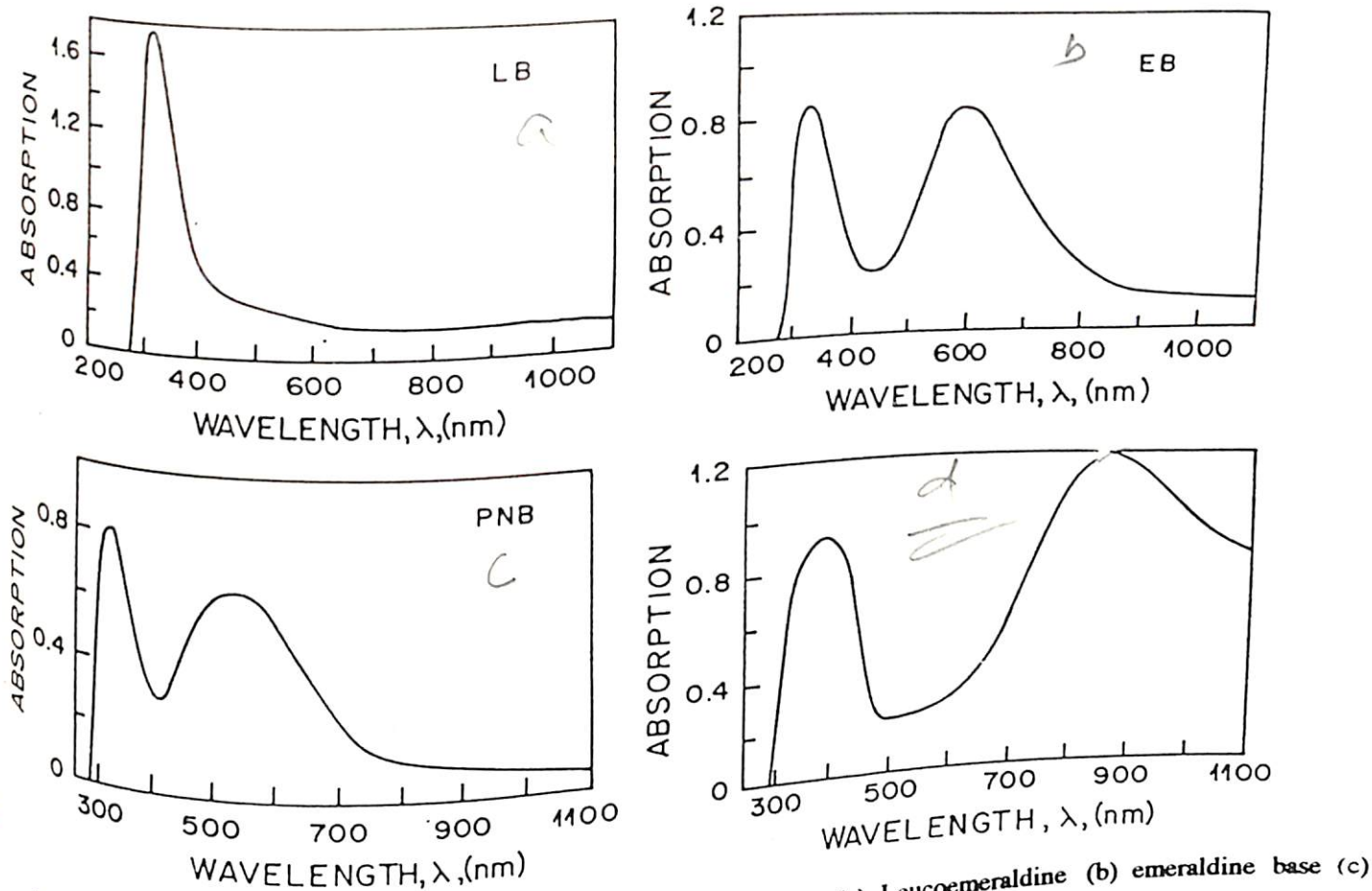film. Such electrochemical films have been used for the UV-Visible studies.

Fig.19 UV - visible spectrum for different forms of polyaniline (a) Leucoemeraldine (b) emeraldine base (c) emeraldine salt (H$_2$SO$_4$) and (d) pernigraniline.

Fig. 19 exhibits the UV-visible spectrum of leucoemeraldine form of polyaniline. It shows the π -π^* transition at 315 nm (3.94 eV) for the reduced polyaniline. This is in agreement with the 3.8 eV peak observed for the reduced polyaniline. Theoretical value obtained for polyaniline films by valence effective hamiltonian (VEH) calculation technique is 3.8 eV. The emeraldine base (fig. 19b) shows an absorption peak at 610 nm (2.03 eV) ascribed to the n-π^* transition. The 320 nm (3.88 eV)peak has been attributed to π-π^* transition . The protonation of emeraldine base with (fig. 18C) causes a lattice distortion of PANI to form a polaronic lattice which accounts for the shift of 610 nm (2.1 eV)

163

absorption to 828 nm (1,5 eV). The characteristic absorption peak of isolated quinoid imine unit at 520 nm (2.5 eV) can also be seen in this figure. Fig.19d shows the absorption bands as 590 nm (2.1 eV) and 310.5 nm (4.00 eV), respectively obtained for an electrochemically deposited polyaniline film. The absorption seen at 2.1 eV is characteristic of quinoid rings in polyaniline chain.

4.3.3 OPTICAL CONSTANTS OF ELECTRODEPOSITED POLYANILINE FILMS:

Polyaniline is a family whose electronic and optical properties can be controlled through variation of number of electrons and protons on the polymer chain. The optical response of polyaniline has been of interest since the report of steady state and picosecond photo-induced optical absorption. Judicious application of light at one wavelength can control the complex index of refraction at other wavelength. The refractive index is dependent on the frequency of the light used. It is useful that all the non-linear effects can be modified by dopant and /or substitution of polyaniline system. In this regard a theoretical model has been proposed for the calculation of optical parameters. Ellipsometric meas-urements on some of the polyaniline films have been performed to test the validity of theoretical values.

(i) THEORETICAL BACKGROUND:

The measurement of the transmission T of light through a parallel - faced dielectric film (polyaniline) in the region of transparency is sufficient to determine the real and imaginary parts of the complex refractive index [47].

$$\cap \quad = \quad n - ik \qquad \text{Eq.7}$$

		reflected energy
n_0 ↓ ↑		

$\cap = n - ik$ ↕		polyaniline film
----------		
n_1 ↓		transmitted energy

Considering a unit amplitude of the incident light in case of normal incidence the amplitude of the transmitted wave is given as:

$$A \; = \; \frac{t_1 \, t_2 \, \exp(-2\pi \, i \cap t/\lambda)}{1 + r_1 \, r_2 \, \exp(-4\pi i \cap t/\lambda)} \qquad \text{Eq.8}$$

where t_1, t_2, r_1 and r_2 are the transmission and reflection coefficients at the front and rear faces. The transmission is given below as:

$$T = \frac{n_1}{n_0} \, A^2 \qquad \text{Eq.9}$$

In the case of weakly thin absorbing film of polyaniline.

$$k^2 << (n - n_0)^2 \text{ and } k^2 << (n - n_1)^2$$

the transmission is given as:

$$A = \frac{16 \, n_0 \, n_1 \, n_2^2 \, \alpha}{C_1^2 + C_2^2 \, \alpha^2 + 2C_1 C_2 \, \alpha \, \cos(4\pi \cap t/\lambda)} \qquad \text{Eq.10}$$

Generally outside the region of fundamental absorption $hv > E_g$, thin film gap or of the free carrier absorption, the dispersion of n and k is not very large, using eq.1o can be written as:

$$C_1 = (n + n_0)(n + n_1) \text{ and } C_2 = (n - n_0)(n - n_1) \qquad \text{Eq.11}$$

and

$$\alpha = \exp(-4\pi kt/\lambda) = \exp(-kt) \qquad \text{Eq.12}$$

The maxima and minima of T can be given as $4\pi n t/\lambda = m\pi$, where m is the order number, In case of $n > n_1$, the polyaniline film on a transparent non-absorbing substrate, $C_2 < 0$, the extreme values will be as:

$$T_{max} = 16\, n_0\, n_1\, n_2^2\, \alpha\, (C_1 + C_2\, \alpha)$$

Eq.13

$$T_{min} = 16\, n_0\, n_1\, n_2^2\, \alpha\, (C_1 - C_2\, \alpha)$$

Eq.14

$$\alpha = \frac{C_1\, [\, 1 - (\, T_{max}/T_{min})^{1/2}\,]}{C_2\, [\, 1 + (\, T_{max}/T_{min})^{1/2}\,]}$$

Eq.15

The refractive index can thus be given as :

$$n = [\, N + (N^2 - n_0^2\, n_1^2)^{\frac{1}{2}}\,]^{1/2}$$

Eq.16

$$N = (n_0^2 + n_1^2)/2 + 2n_0 n_1\, (T_{max} - T_{min})\, /\, (\, T_{max}/T_{min})$$

Eq.17

The thickness can thus be calculated using the following equation:

Eq.18

$$t = M\lambda_1\lambda_2\, /\, 2(n(\lambda_2) - n(\lambda_1))$$

where M is the number of oscillations of the two consecutive maxima or minima. In λ_1, λ_2 $n(\lambda_1)$ and $n(\lambda_2)$ are the values of wavelengths and refractive indices (n). Knowing t and α the value of extinction coefficient (k) can be calculated.
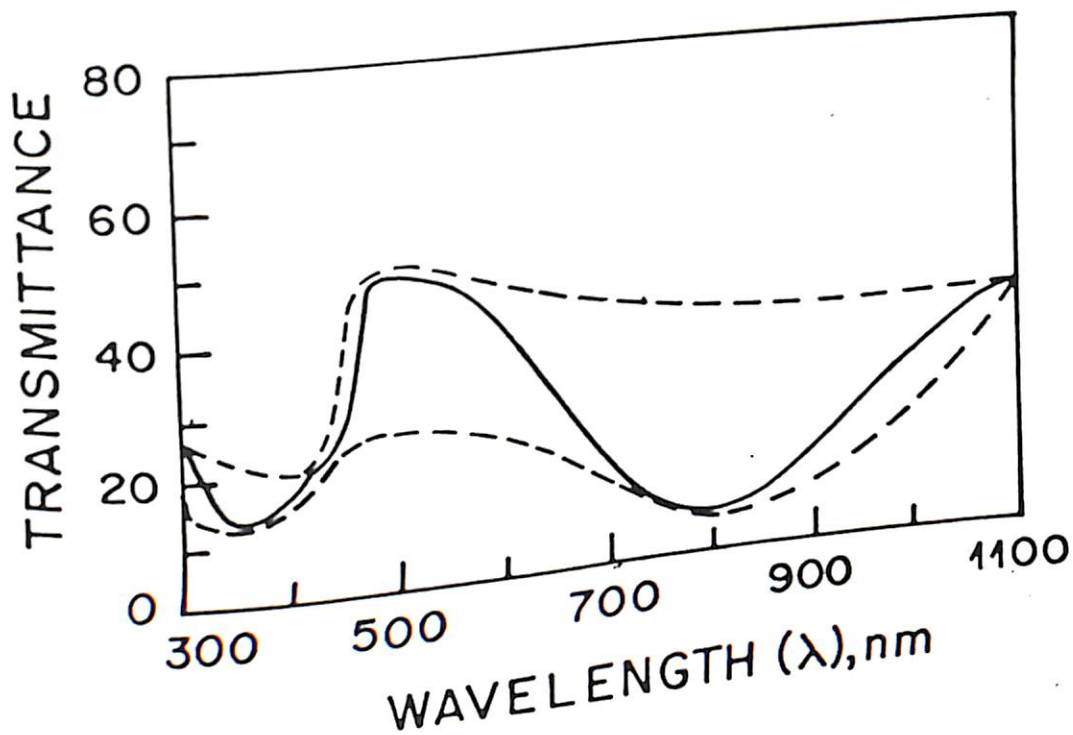
Fig.20 Variation of transmittance as a function of wavelength for H_2SO_4 doped polyaniline. The dashed line indicated the peak to peak and valley to valley connection of transmittance spectra.

Fig.20 shows the variation of transmittance obtained as a function of wavelength for the H_2SO_4 doped polyaniline. The peak-to-peak and valley-to-valley seen in transmittance spectra have been connected when the transmission is more than 60%. The optical absorption is found to occur at 3.5, 2.593 and 1.54 eV, respectively.

Fig.21a shows the variation of refractive index vs photon energy for the H_2SO_4 doped PANI films obtained by the ellipsometric measurements. The absorption peaks can be seen at 3.48, 2.8, and 1.44 eV, respectively. Fig.20b shows the variation of refractive index verses hv as a function of eV obtained theoretically.

Fig.22a shows the variation of optical dielectric constant versus photon energy (hv) as measured by ellipsometric measurements. It exhibits the maxima at 2.1, 2.7 and 3.5 eV. The highest value of real optical constant (ϵ') obtained at 2.1 eV (590 nm) has been found to be 4.4. The average value of this optical constant calculated for typical electrochemically prepared polyaniline films varies from 1.5 to 5, respectively. Table 1 gives the values of optical dielectric constant (ϵ') and imaginary (ϵ'') optical dielectric constant, refractive index (n) and extinction coefficient (k) obtained in the case of different forms of polyaniline at different wavelengths.
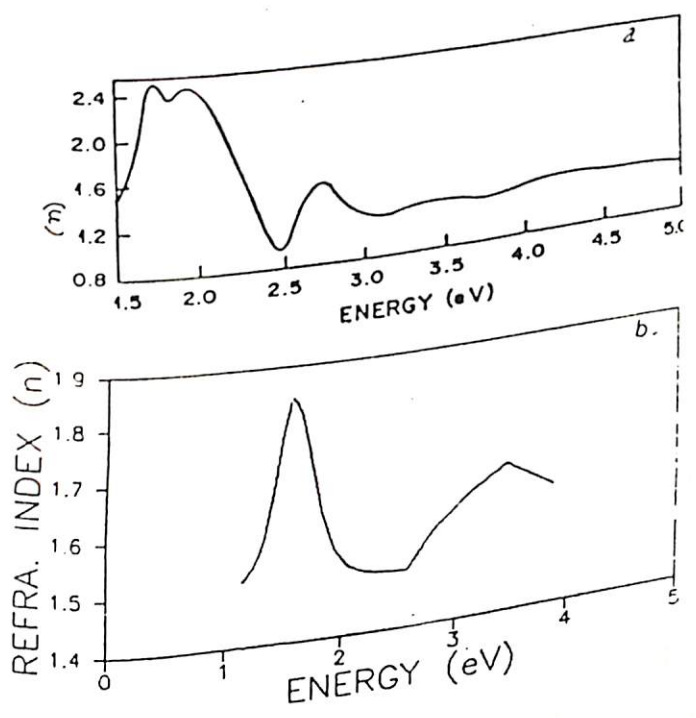
Fig.21 variation of refractive index (n) vs photon energy (eV) for H_2SO_4 doped polyaniline film (a) experimentally observed by ellipsometric measurements (b) calculated values
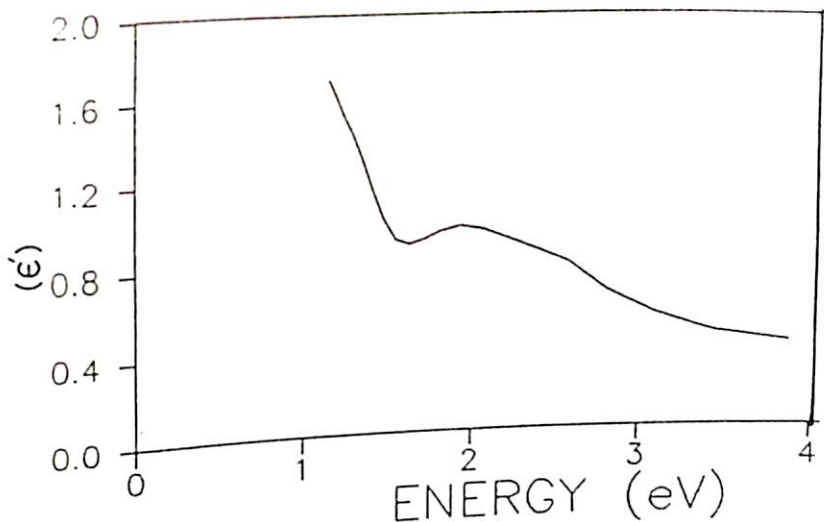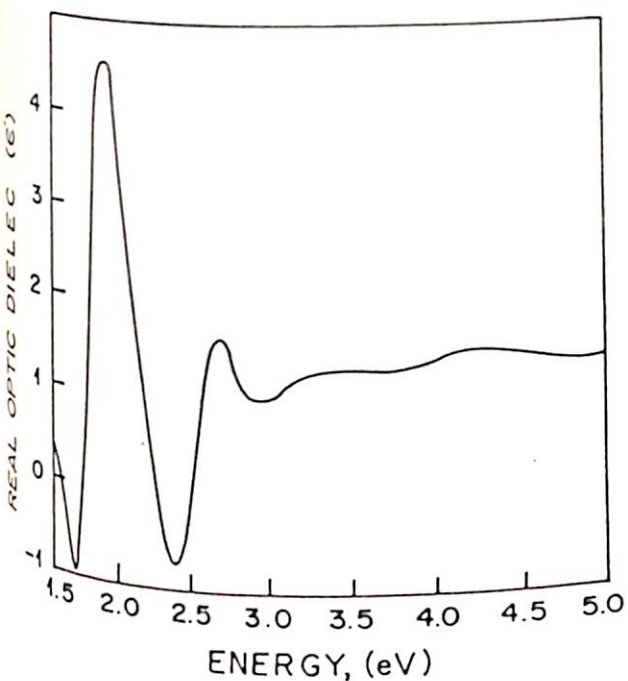
168

Fig. 22 Variation of optical dielectric constant (ϵ') vs photon energy, hv (eV) for H_2SO_4 doped polyaniline film (a) Experimentally observed by ellipsometric measurements (b) calculated values.

TABLE -1 OPTICAL CONSTANTS OBTAINED FOR DIFFERENT FORMS OF POLYANILINE:

System	λ nm	Theoretical Values				Experimental Values			
		n	k	ϵ'	ϵ''	-n	k	ϵ'	ϵ''
Leucoemeraldine	320	1.5	0.3	2.16	1.9	1.3	0.6	1.8	1.8
	520	1.51	0.93	2.08	2.29	1.64	1.14	1.7	2.1
Emeraldine base	355	1.54	0.4	2.21	1.21	1.6	0.5	2.3	1.5
	600	1.56	0.6	2.01	4.0	1.9	1.4	2.0	5.5
Emeraldine salt (H_2SO_4 Doped)	350	1.66	0.45	2.5	1.51	1.2	0.4	1.4	1.25
	800	1.84	0.91	2.57	3.34	1.42	1.4	0.2	4.45
Emeraldine salt ($HClO_4$ doped)	400	1.55	0.26	2.33	1.8	1.54	0.27	2.3	0.7
	800	1.58	0.49	2.25	1.54	1.57	0.48	2.2	1.64
Pernigraniline	400	1.58	0.2	2.32	0.7	1.46	1.69	1.7	1.8
	480	1.5	0.24	2.1	1.71	1.64	0.75	2.1	2.6

169

4.3.4 SCANNING ELECTRON MICROSCOPIC STUDIES:

The polyaniline films prepared by electrochemical method have been examined for the morphological studies by scanning electron microscope. The SEM pictures obtained for undoped PANI, H_2SO_4 doped PANI and annealed undoped polyaniline films, have been shown in fig. 23. It can be clearly seen that the polyaniline films (fig.23a) are smooth and homogeneous. When the films are doped with $1MH_2SO_4$, the growth of a microcrystalline structure can be seen with grain size of $0.5 \mu m$. Doped polyaniline films have been reported to contain 50% of crystallinity and have a pseudo-orthorombic structure [48]. Interestingly, the structure of polyaniline shows a considerable decrease in the defect density. Besides this, homogeneous smooth structure can be obtained after annealing (70 °C) for about 48 hours (fig.23c). These results indicate that a change in the surface morphology of polyaniline films occurs as a consequence of doping. This can be perhaps be understood to arise from the change in the band gap as well as the electrical conductivity as has been observed for the polypyrrole system [51].
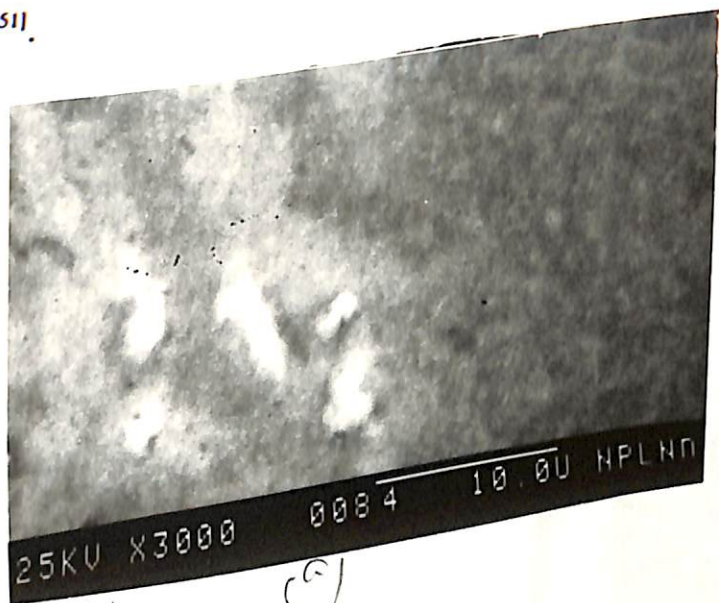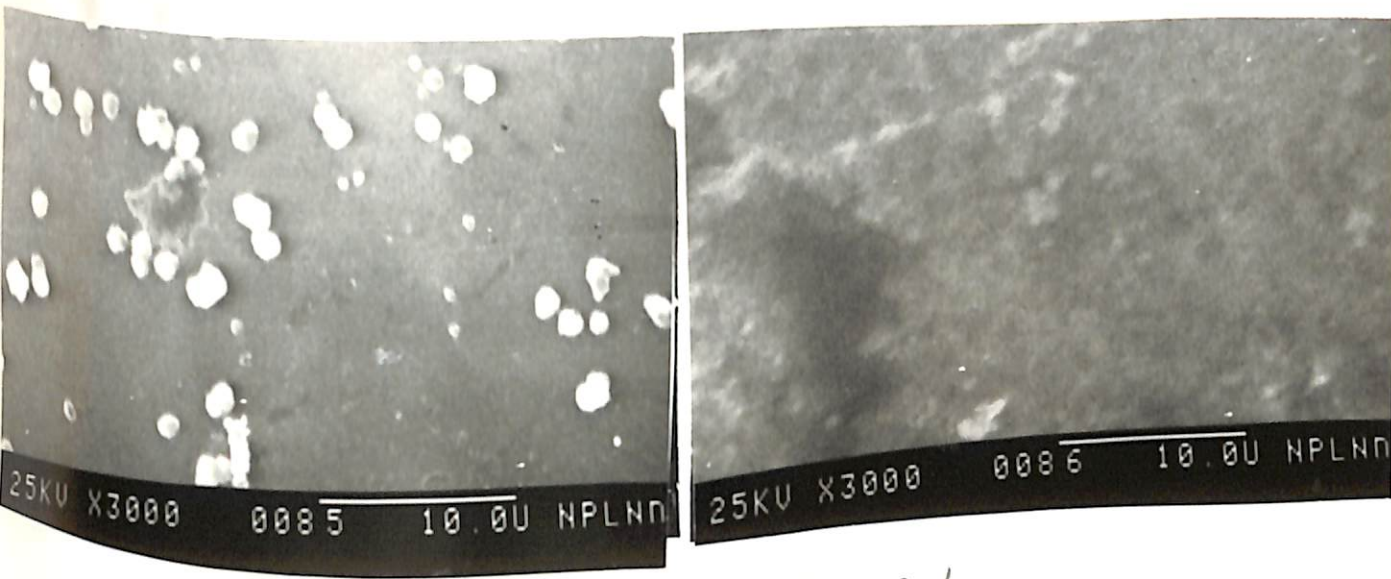

Fig.23(a)

(b)   (c)

Fig.23 SEM pictures for electrochemically deposited polyaniline films; (a) emeraldine base film, (b) H₂SO₄ doped polyaniline and (c) 48 hours annealed (70°C) emeraldine base film.

4.4 VACUUM DEPOSITED POLYANILINE FILMS

Electrically conducting polymers, including polyaniline are usually prepared by wet chemical and /or catalytic methods. These methods are usually incompatible with potential future applications of organic conducting polymers. The present section pertain to the results of preliminary studies carried out on thin films of polyaniline, namely emeraldine base, emeraldine salt fabricated by vapour deposition technique. These polyaniline films have been characterized by a UV-visible and FTIR techniques, respectively [13].

The emeraldine base (EB) powder has been used for the fabrication of vacuum deposited films on different substrates. The EB powder is kept in a boat and heated in a vacuum (10^{-6}mm Hg). Such films are further treated with aqueous ammonia for obtaining undoped films of polyemeraldine base.

171

4.4.1 FTIR STUDIES ON VACUUM DEPOSITED POLYANILINE FILMS

Fig.23 shows the FTIR spectra of freshly deposited polyaniline films and those exposed to HCl vapour. The FTIR spectra (curve a and b) correspond to that of emeraldine base and emeraldine salt. It can be seen that characteristic peaks corresponding to the backbone of polyaniline appear at 1590, 1493, 1304, 1180, 960, 870, 820 and 740 cm^{-1} respectively. The intense peaks seen at 1590 and 1493 cm^{-1} are due to C=C vibrations of quinoid benzoid rings. The peak at 1304 cm^{-1} has been attributed to a combination of C-N in quinoid and benzoid sequences. In addition there is a peak at 1170cm^{-1} attributed to the combination of C-N in quinoid and benzoid sequences. The peak at 1170 cm^{-1} has been assigned to vibrations emanating from the C=N bond. This is confirmed by a composition of IR spectra of emeraldine base and salt (fig.1).

In FTIR spectra of doped (HCl) polyaniline the 1170 cm^{-1} peak is missing. The peak at 820 cm^{-1} is due to the existence of 1-4 link in the benzene ring and the peak at 960, 870 and 740 cm^{-1} are attributed to various stretching and bending vibrations associated with C-H linkage. This indicates that the polyaniline structure corresponds to that of emeraldine base. However, it is possible that the various molecules break up during the evaporation process and a repolymerization takes place simultaneously at the substrate. The clusters (atoms, molecules and ions) arriving at the substrate have sufficient energy to intimate polymerization by bonding and diffusion of the atoms, molecules, ions to yield a polyaniline structure similar to the starting material. This appears to be the most favorable minimum energy state as confirmed by IR studies. However, the films are expected to contain a large
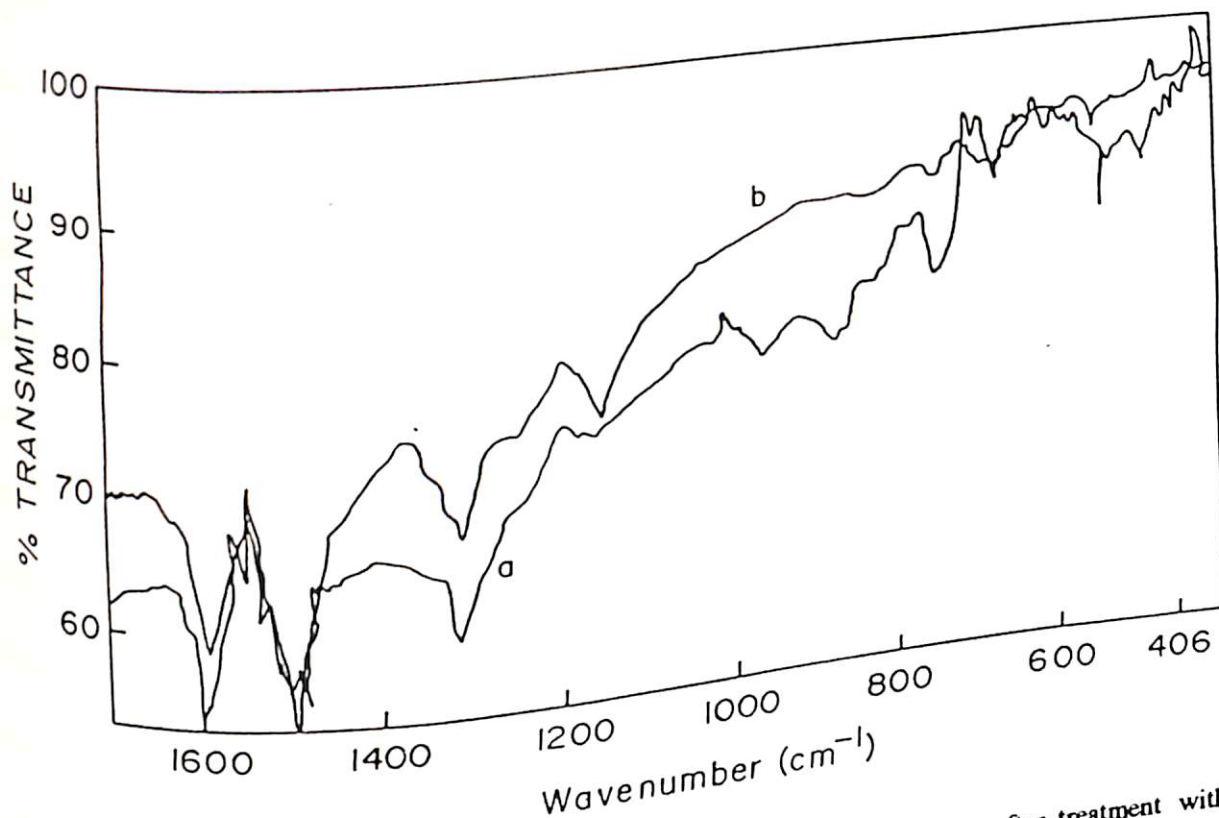
number of defects.

Fig.24 FTIR spectra of vacuum deposited polyaniline films as a deposited (b) after treatment with HCl.

4.4.2 UV-VISIBLE STUDIES OF VACUUM DEPOSITED POLYANILINE FILMS

The optical absorption spectra of various vacuum deposited polyaniline films is shown in fig.25. UV-Visible spectrum (curve 1) for the freshly vacuum deposited polyaniline films exhibits peaks at 1.34 eV and 3.9 eV. This spectrum is similar to that obtained for leucoemeraldine (100% reduced state). Besides this the UV-Visible spectrum resembles the spectra observed in films prepared by other methods and indicates that oxygen is probably drawn out during vacuum evaporation / deposition process. Curve 2 (fig.24) shows the

173

optical absorption after exposure to air. A shift in the 1.34 eV peak to 1.29 eV and the appearance of a peak at 1.64 eV is observed. This is a measure of the oxidation state of the film and the 1.64 eV corresponds to the negative polaron trapped at quinoid.

Curve 3 (fig.25) represents exposure of the film to NH_3, exhibits peaks at 1.36, 2.6 and 4 eV. This indicates that the vapour deposited polyaniline film consists of a large number of dangling bonds or reactive sites which are neutralized by NH_3 and not by N_2 upon exposure to air. This spectrum is similar to that of emeraldine base. The 2.6 eV peak may be due to over - oxidation. However, the π-π^* transition peak at about 4.0 eV does not change very much upon treatment with NH_3, HCl or oxygen, as it is an inherent characteristic of polyaniline. The conductivity of vapour deposited polyaniline film on being treated with HCl has been measured as 0.5 S/cm. The optical spectra of our HCl doped films is shown by curve 4 in fig. 24. This does not resemble the conventional emeraldine hydrochloride, instead the peaks at 3.85 eV and 1.4 eV have been observed. This indicates the effect of HCl doping on π-π^* transition peak at 4.0 eV and creates another peak at 1.4 assigned to a hole polaron trapped near a quinoid. All these possibilities like the removal/ addition of holes /electrons and bonding of various groups to the polyaniline giving rise to various distortions, twists etc., are quite possible owing to the large number in vacuum deposited polyaniline films. The energy band gap of polyaniline films has been determined from the plot of $(\alpha.h\nu)^2$ vs photon energy shown in fig.26. assuming the film to be a quasi one dimensional lattice. The optical absorption edge has been estimated to be 3.14 eV. These values correspond to those of polyaniline prepared by electrochemical and solution cast film.
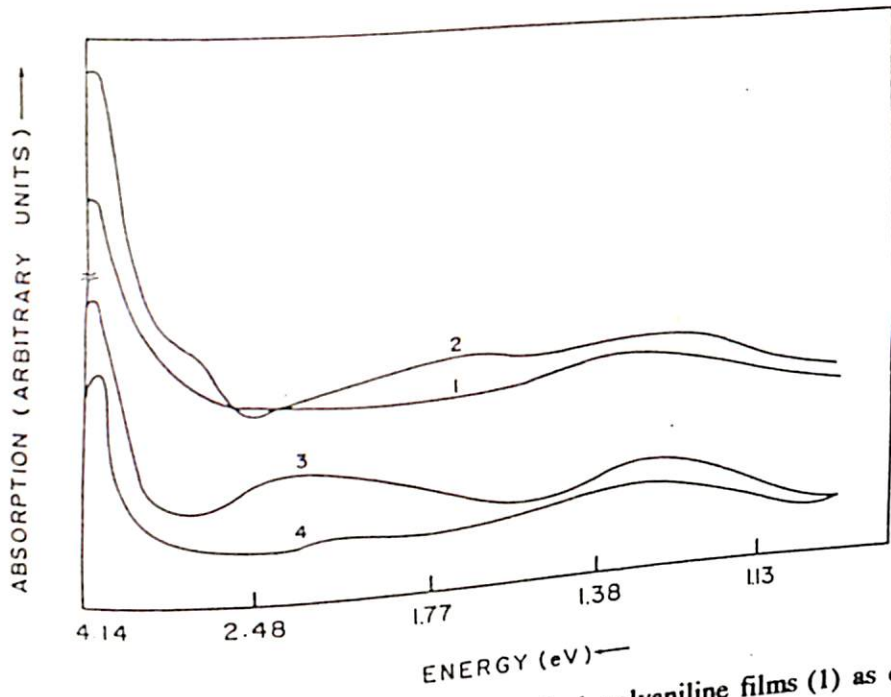
Fig.25 The UV-visible absorption spectra of vacuum deposited polyaniline films (1) as deposited (2) after 48 hours exposure to air, (3) after exposure to NH₃ and (4) after exposure to HCl
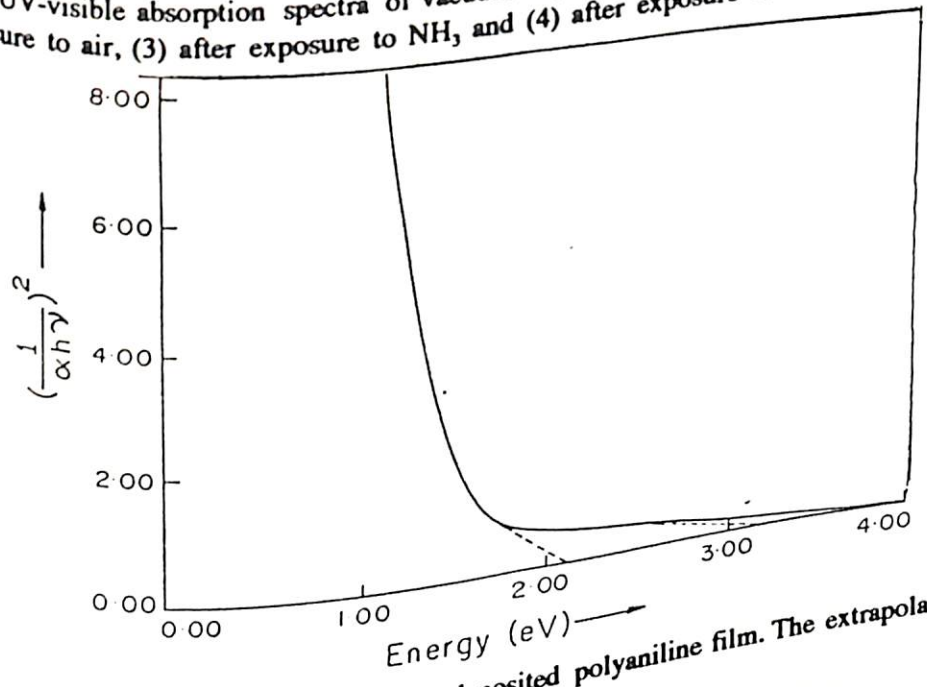

Fig.26 Plot of $(1/\alpha.h\nu)^2$ vs $h\nu$ for the vacuum deposited polyaniline film. The extrapolated value indicates the band gap.

Vacuum deposited films of emeraldine base exhibit optical spectra similar to the polyaniline films prepared by other methods. These films are close to the leucoemeraldine form but are converted to the conducting emeraldine salt on being treated with a protonic acid. The value of electrical conductivity of these vacuum deposited polyaniline films is in good agreement that of with emeraldine hydrochloride indicating that vapour deposited emeraldine films have good potential for thin application [13].

175

4.5 APPLICATIONS

4.5.1 SCHOTTKY DIODE BASED ON POLYANILINE FILMS

(i) Thin films have been found to be the best form of specimen for fabrication, study and control of characteristics of the semiconducting polymer based devices. Semiconducting polymer films suitable for device fabrication should be thin and totally oriented. In view of this metal/polymer junctions have been fabricated using chemical cast polyaniline and vacuum deposited polyaniline films.

The solution cast films of emeraldine base have been prepared as discussed in sec.4.2.1 of this Chapter. The films are subsequently protonated with MHCl(1M), $HClO_4$(1M), HNO_3 (1M) and H_2SO_4 (1M) for 24 hours. The doped polyaniline films have been vacuum dried at 100°C for 5 hours for removal of any moisture present in the film. The different metals such as Pb, In, Sn, Al and Ag have been vacuum (10^{-6} torr) deposited and the ohmic back contact of have been made using pure gold at a pressure of 10^{-6} torr. Current - voltage and capacitance - voltage characteristics have been performed by Keithley electrometer (model 617 A) and Impedance Analyzer (HP 4192 A) respectively.

The current - voltage characteristics of metal/chemical cast polyaniline HCl doped /gold with various metals such as Pb (curve 1), In (curve 2), Sn (curve 3), Al (curve 4) and Ag (curve 5) are shown in fig.27.The effective junction area is about 0.05 cm². It is apparent

that metals Pb, In, Sn and Al make the rectifying contact with polyaniline interfaces whereas Ag behaves as an ohmic contact with polyaniline interface (fig.27). The shape of the current-voltage characteristics is similar to those obtained for electrochemically deposited PPY films and indicates a build up of space charge at the metal/polyaniline junction. This has been confirmed by carrying out capacitance - voltage measurement at high frequency. In the bias region at 4V for all metal/PANI junction, the excellent rectification has been observed. It has been found that the work function of vacuum deposited polyaniline has a value of 4.12 and 4.28 eV. the current -voltage characteristics of various metal/polymer Schottky diodes are not exactly the same as those of inorganic semiconductor junction owing to fact that the structure of polyaniline semiconductor is highly defected and partial crystalline in structure (pseudo-orthorombic).
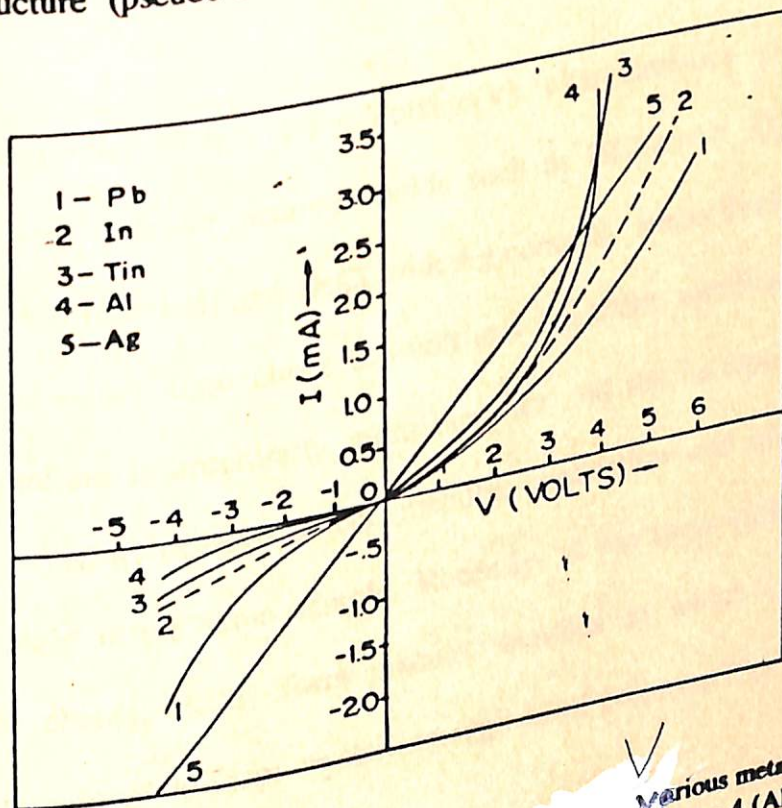

Fig.27 current(I) - voltage(V) characteristics of various metal/chemical cast HCl doped Polyaniline interfaces ; curve 1 (pb), curve 2 (In), curve 3 (Sn), curve 4 (Al) and curve 5 (Ag)

Richardson - Schottky equation has been used for a calculation of junction parameters as discussed in sec. 2.11.1 of Chapter II. Table 1 shows the dependence of barrier height and ideality factor on the metal work function. The ideality factor of 7.2 has been achieved for Al configuration. It is interesting to (not) that the Al/PANI/gold gives better rectification than with In, Pb and Sn, respectively. This is perhaps due to the more intimate contact at Al/PANI/gold interfaces, eliminating any surface irregularity which can cause deviation from Schottky behaviour. However, Al/PANI interfaces have disadvantage due to the reactivity of Al with air. Hence it is advisable to prefer the stable PANI Schottky junction.

The carrier concentration of solution cast film has been calculated using the slope of the curve obtained by plotting $1/C^2$ vs applied voltage. The slope of the observed curve can be used to calculate the magnitude of carrier concentration that has been found to be $10^{18}/cm^3$.

Fig.28 shows the current (I) - Voltage(V) characteristics of Al/polyaniline /gold Schottky diode with different protonic acids such as HCl(curve 1), H_2SO_4(curve), $HClO_4$ (curve 3) and HNO_3 (curve 4) and (HCl with Ag contact), respectively, The I-V curves show good Schottky behaviour upto about 3.5 volt and excellent rectification till 4 volts. Since, conducting polyaniline is structurally more complex and the transport of charge carriers in these materials is mainly through defect, metallic conduction and other types of conduction may perhaps coexist in the same sample. Recently, it has been reported that PANI shows coupled parallel chains which form metallic bundles in which electron wave functions extend three dimensional to form crystalline regions of polymer. This picture resembles that

of a granular metal with metallic islands separated spatially with each other. As tunneling between sites may be possible, this is also to be taken into account in interpreting the I-V data. It can be seen that in the lower range of applied voltage (4V), the slope of logJ vs V (fig.29) is about 2 for all the devices suggesting the possibility of space - charge limited current phenomenon in polyaniline.

The various electronic parameters have been calculated in Table II. It can be seen that Al shows the highest rectification with barrier height of 0.62 eV work function of 3.765 eV. The work function of Al/PANI (H₂SO₄)/gold has been found to 0.685 with a small rectification of 7.
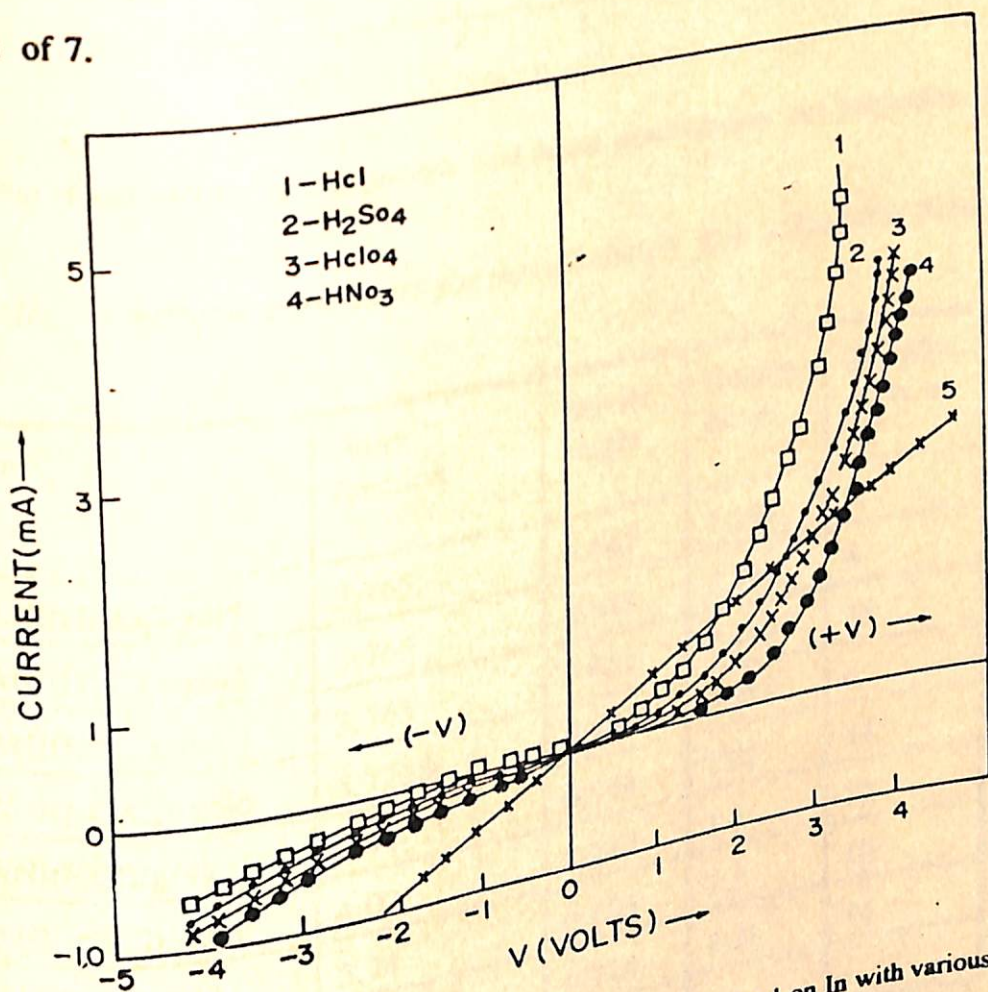
$$of\ a\ granular\ metal$$

Fig.28   Current(I) - voltage(V) characteristics of Schottky diode based on In with various protonic acids doped with solution cast polyaniline films
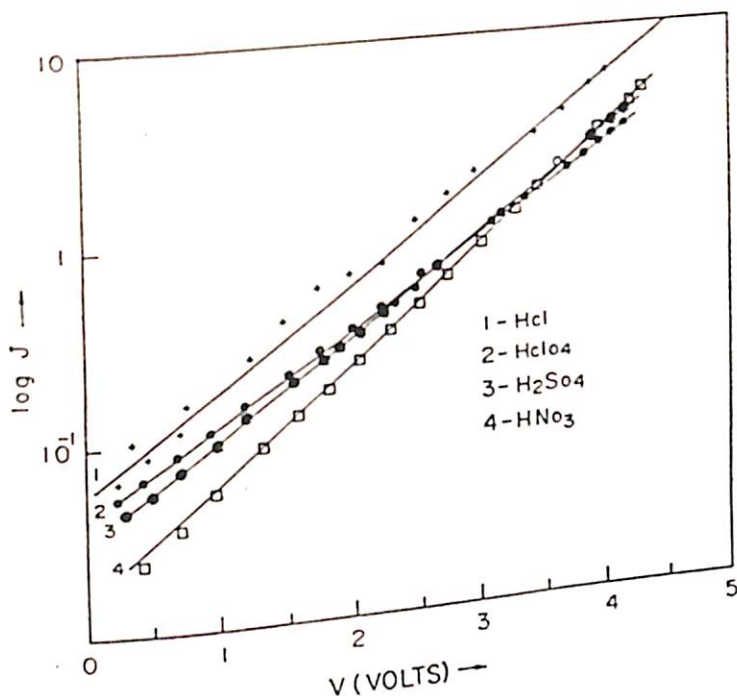
179

Fig.29   Plot of logJ vs V for various protonic acid doped metal/solution cast polyaniline interfaces

TABLE II: Electronic parameters for metal/solution cast polyaniline films

System	Work function	Barrier height	Ideality factor	Ractification at 2V
		0.645	7.140	8
Al/PANI(HNO$_3$)/gold	3.765	0.645	7.140	8
Al/PANI(H^{2}SO$_4$)/gold	3.765	0.614	7.439	15
Al/PANI(HCl)/gold	3.765	0.682	8.316	6
Al/PANI(HClO$_4$)/gold	3.7228	0.714	7.21	14
Al/PANI(HCl)/gold	4.11	0.712	7.3	12
Sn/PANI (HCl)/gold	4.02	0.685	7.5	10
Pb/PANI(HCl)/gold	3.74	0.714	7.21	14
In/PANI(HCl)/gold	4.12	-	-	-
Ag/PANI(HCl)/gold	4.28			

(ii) SCHOTTKY DIODES BASED ON VACUUM DEPOSITED POLYANILINE FILMS:

The vacuum deposited polyaniline films are initially doped with HCl(1M) before the different metals such as In, Sn, Al, Sb and Pb are vacuum deposited at a pressure of 10^{-6} Torr. The ohmic contacts have been made using the electrodag +E 502. The current(I)-voltage (V) and capacitance (C) - voltage (V) characteristics of metal/solution cast HCl doped polyaniline and metal/doped (HCl) polyaniline films have been measured using a Keithley electrometer (model 617 A) and Impedance Analyzer (HP 4192 A).

It can be seen from fig.30 that the metals In, Sn., Al, Sb and Pb make a rectifying contact while Ag/ polyaniline interface behaves as ohmic contact. The value of various electronic parameters for vacuum deposited polyaniline have been calculated (table III) using the Richardson equation. It can be seen that excellent rectification can be achieved using Al/PANI/Ag configuration as indicated by the vaule of ideality factor 1.2, which is close to that of solution cast polyaniline film. It is interesting to note that all vacuum deposited Al/PANI/Ag device shows better rectification than Al/PANI/ gold devices prepared by solution cast method. It can be tentatively concluded that this is perhaps due to a more intimate contact in the Al/PANI/Ag devices avoiding any surface irregularity which can cause deviation from the Schottky behaviour [13].

However the major problem arises due to the formation of passive aluminium oxide layer at metal/semiconductor interface which further prevents the flow of electrical current at the junction.
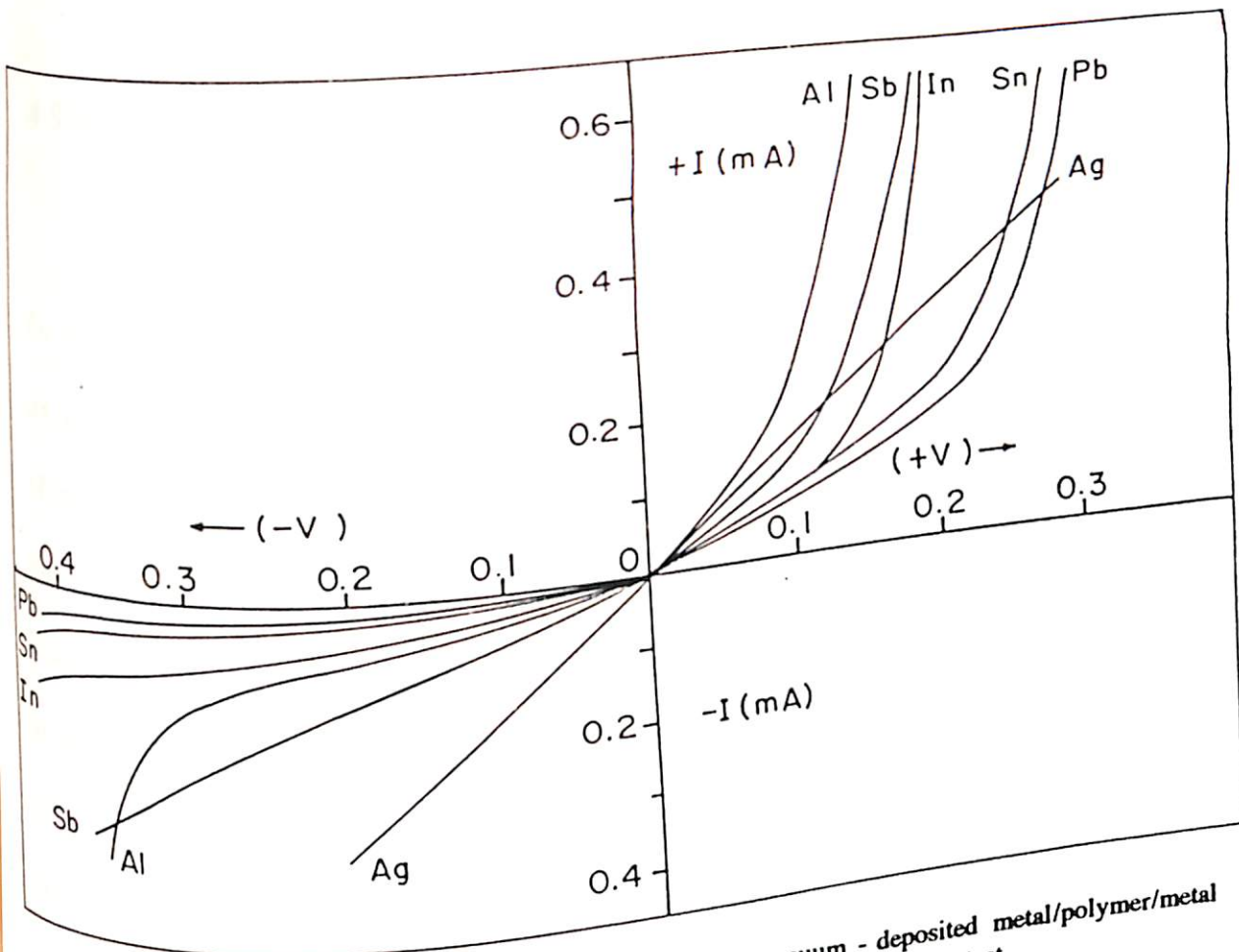
Fig.36   current(I)-Voltage(V) characteristics of the vacuum - deposited metal/polymer/metal Schottky devices with various metal rectifying electrodes and Ag or ITO as ohmic contact

TABLE III Electronic parameters of metal/vacuum deposited polyaniline films.

System	Work function (eV)	Barrier height (eV)	Ideality factor n	Rectification at 2V
In/PANI+E502	4.12	0.4	1.9	12
Al/PANI/+E502	3.74	0.4	2.8	10
Sn/PANI/+502	4.11	0.4	4.9	9
Pb/PANI/+502	4.02	0.5	6.9	8
Ag/PANI/+E502	4.28	-	-	-

4.5.2 APPLICATION OF POLYANILINE FILMS AS ELECTROCHROMIC DEVICES

Polyaniline is currently considered to have a good device potential. One of devices for which polyaniline is seriously considered is in electrochromic display. A number of studies on the electrochromism (EC) of polyaniline covering various aspects such as mechanism of the color change, effect of cell parameters on the switching time etc. have appeared [50,51]. But these and similar studies have generally been conducted in liquid media in electrochemical cells. In practical devices it is preferable to employ solid materials in order to minimize the problems of sealing in hazardous liquids. Further, EC devices are usually required to have a thin layer configuration. With these considerations in mind, an experiment has been performed with thin layer cells of polyaniline containing a supporting electrolyte such as LiClO$_4$ dissolved in polyethylene oxide (PEO) or polyvinyl alcohol (PVA).

The performance of such cells has been systematically investigated. A polymeric electrolyte such as PEO is chosen since the amorphous nature of PEO leads to good ionic conductivity and redox stability upto +3V . Further, the combination of PEO/LiClO$_4$ is known to be a very fast ionic conductor with the Li$^+$ being the mobile species [52]. Recently, reports have also appeared which describe solid state electrochromic cells of methylene blue using polyacrylamide and gels of polymethyl methacrylate in electrochromic cells of WO$_3$.

The effect of the medium on the various parameters such as switching time, cycle lifetime and applied voltage on the electrochromic display have been studied. The current transients for the switching reaction of polyaniline are analyzed to understand the influence of mass transport on the switching reaction in polyaniline.

Cells for electrochromic studies are constructed as follows. Polyaniline (nominal thickness. 1 μm) was coated on indium-tin-oxide (ITO) plate by application of alternating voltage (-0.1V to 1V) in HCl medium containing 0.1M aniline. The film is dried and dip coated with the appropriate electrolyte and then covered with another plate of ITO. The whole assembly was then sealed with wax to keep out air. The schematic of such an electrochromic cell is shown in fig.31. The experimental set up is similar to that as discussed in the chapter III (sec. 3.8.1). The only difference is that cell is illuminated at 632 nm with tungsten - halogen lamp.
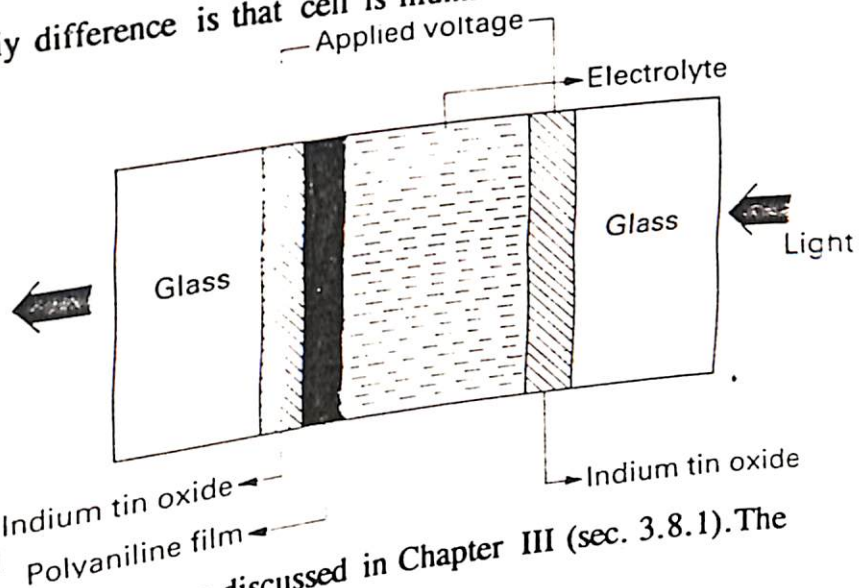

Fig.31 Configuration of electrochemical cell

The experimental set up is similar to that as discussed in Chapter III (sec. 3.8.1). The only difference is that cell is illuminated at 632 nm with tungsten - halogen lamp. In evaluating the performance of the cells listed in table IV, It is focussed on the aspects mentioned above viz. 1) switching time 2) the dependence of the switching time on mass transport which in turn is controlled by the ionic composition 3) The voltage required to be applied to the cell and 4) the stability of the cell to repeated cycling. The mechanism of polyaniline switching, which has been extensively investigated (3) has an important bearing on these aspects. The overall process involves the loss of two electrons and deprotonation by the sequence shown in Scheme 1.

184

From the mechanistic steps shown above it is clear that the rate of switching can be controlled by proton or counter ion movement into and out of the film. Which of these controls the rate is however, decided by the actual pH of the medium.
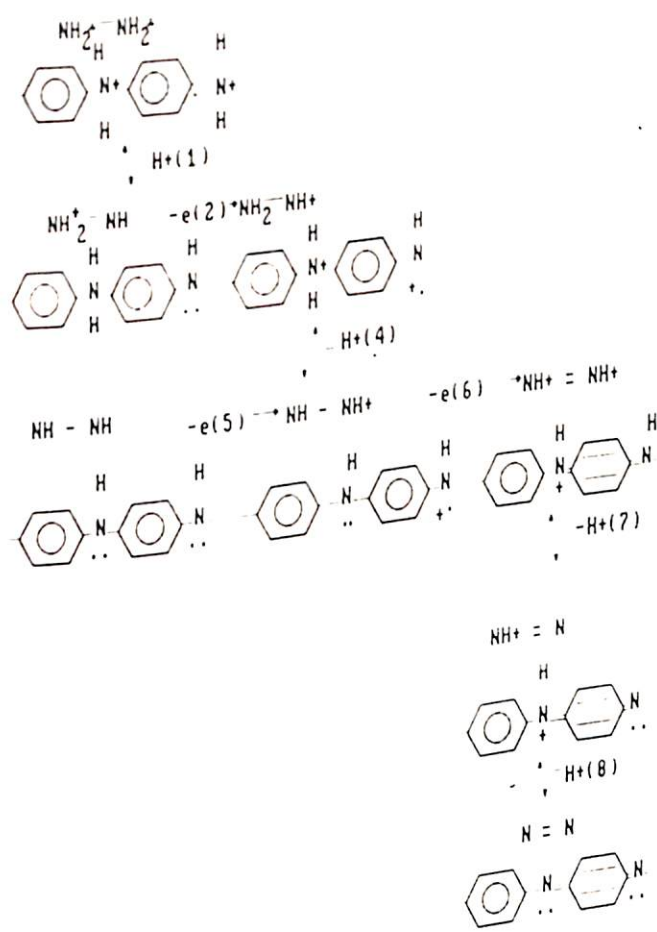
SCHEME 1

The electrochemical current transient obtained with a cell containing PANI/PTS+ urea+ Glycerol, PANI/LiClO$_4$+PANI/PTS+ PEO is shown in fig. 32. Also shown in fig.33 are the optical absorbance versus time for the same cells . As reported previously the

electrochemical and optical responses correlate directly. The half time for the colour change ($t_{0.5}$) is used to evaluate the switching speed of the film. These values are given in table 1. It is noted that the $t_{0.5}$ values vary from 330 msec. to about 1 second for the cell studied. These are much faster than electrochromic cells employing similar media where the response times are usually more than a second. Thus, polyaniline/polymeric electrolyte systems compare very favorably with other electrochromic systems including Prussian blue. A much faster response of 100 μsec is obtained earlier by Diaz in but these are in liquid cells. Comparing the switching half time ($t_{o.5}$) among cells listed in Table IV, It can be noted that the introduction of the viscous medium slows down the response. However this is offset by the convenience of handling the electrolyte. Among themselves the cells containing the polymeric electrolyte show only minor variations in $t_{o.5}$.

In order to investigate the effect of the mass transport on switching time, we consider the current transient for the redox switching. The current transients for three cells viz: PANI/urea+Glycerol+ PTS, PANI/LiClO$_4$+PEO, PANI/PTS+PEO are shown in fig.34.
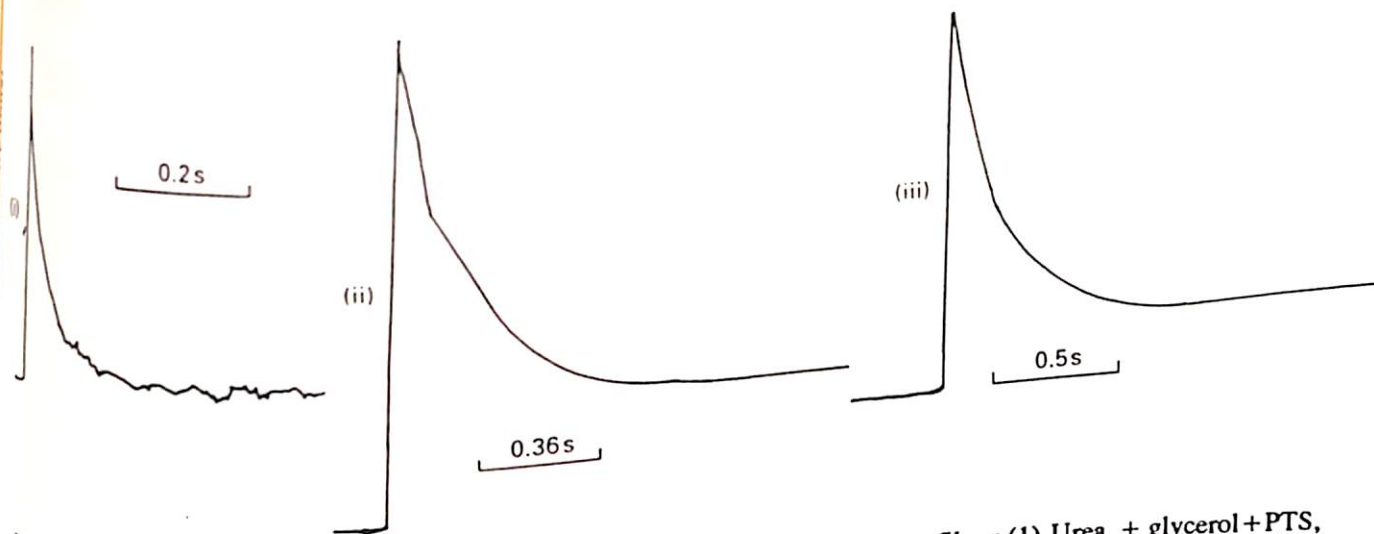
186

Fig.32 Electrochemical current transient for the colour switching of polyaniline films: (1) Urea + glycerol + PTS, (ii) LiClO$_4$ + PEO and (iii) PTS + PEO
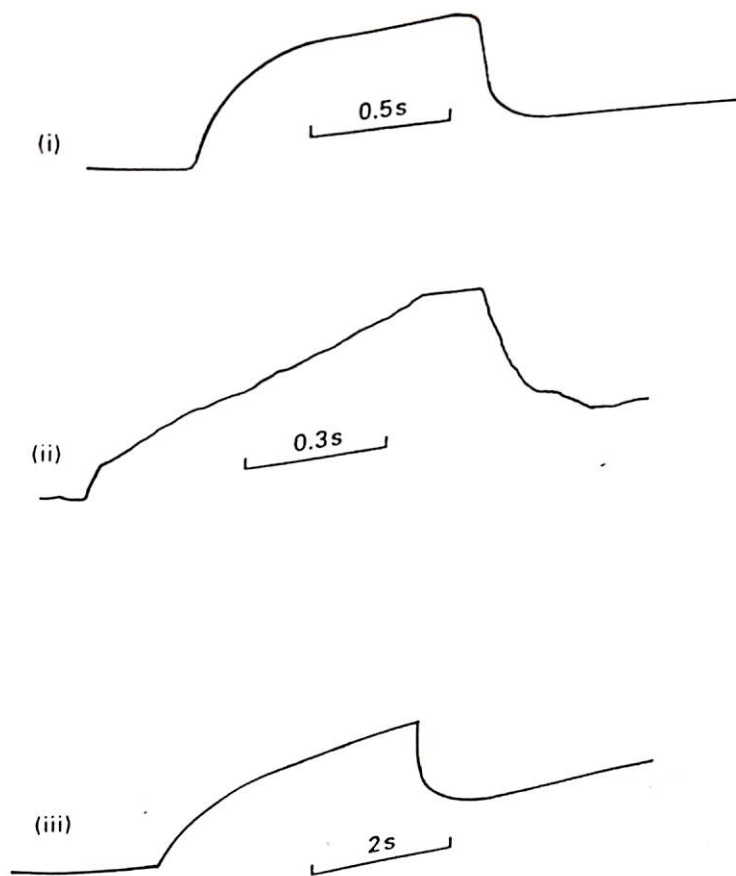

Fig.33 The optical transmittance against time for the cells in (i) Urea + glycerol + PTS, (ii) LiClO$_4$ and (iii) PTS + PEO. The ordinate is the photodiode from the Si photodiode
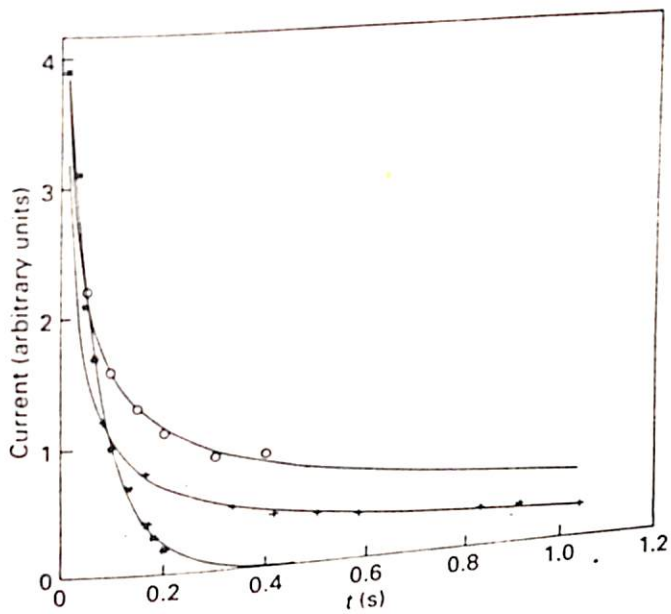
187

Fig.34 Analysis of the current transients for the polyaniline switching (1) PTS+Urea+glycerol, (2) PEO+LiClO₄ and (3) PTS+PEO

The PANI/urea+ glycerol+ PTS cell exhibits an exponential decay of current while the PANI/LiClO₄+ PEO and PANI/PTS+ PEO cells show a power of time dependence suggesting control by ionic mass transport. In the case of the urea+ glycerol cell, the exponential dependence suggests that the cell exhibits thin layer behaviour [54]. This leads to the observed faster response. The cases of the other two are in themselves different even though they both reflect the mass transport control. With the PTS cell, the dependence on mass transport is unusual since the pH < 1(8). Probably since the medium is a polymeric electrolyte and semi-viscous, mass transport dependence is observed. With the PANI/LiClO₄ + PEO cell, since proton transport will be much faster, the mass transport control is that of the cation (Li⁺). This is reflected in the value of D calculated (table IV). The slower response of the cell is also attributable in part to this control by mass transport. In calculating the diffusion coefficients of table-IV, we have used the Cottrell equation (55)

Eq. 19

$$i = [n\,F\,A\,D^{1/2}\,C]/[\pi\,t]^{1/2}$$

188

where the symbols have their usual meanings. The concentration C in the Eq.18, is that of either the anion or the cation of the supporting electrolyte in the polymer matrix. The value of 2M has been used from the value calculated by Rudzinski et al [56]. The geometric area of the film has been used in this calculation.

The life cycle of the given cells are in excess of 10^3 cycles. In comparison with the value of 10^6 cycles reported for liquid cell electrochromic devices of polyaniline film. The shorter life time of the cell is due to the higher voltages employed which in turn is due to the resistance of the electrolyte. If this parameter is optimized, it can be expected that the cell will have a longer life [57].

TABLE.IV : Parameters governing the performance of electrochromic cell

System	Half life time $(t_{1/2})$, sec	Voltage applied (V)	Diffusion coefficient (D_f) cm²/sec x 10^{-10}	Life cycle
ITO/PANI(HCl)/PTS+ PVA/ITO	0.775	-1.33 to 1.1	0.692	> 10^3
ITO/PANI(HCl)/PTS+ PEO/ITO	0.96	-1.16 to 1.12	0.11	> 10^3
ITO/PANI(HCl)+ LiClO₄/ITO	0.875	-3.1 to 1.88	1.346	> 10^3
ITO/PANI(HCl)/PEO+ HCl/ITO	1.16	-2.6 to 1.5	2.24	> 10^3
ITO/PANI(HCl)/PTS+ +glycero+ urea	0.33	-0.4 to 1.2	-	> 10^3

4.6 CONCLUSIONS:

The polyaniline films have been obtained by solution cast, electrochemical and vacuum deposited methods, respectively. The optical properties of these films have been characterized using available techniques. The band gap of polyaniline has been found to be between 3.0 to 3.2 eV. The proton acid doping with polyaniline films has been found to have significant effect on conductivity, band gap as well as in surface morphology.

The temperature dependence of electrical conductivity for the HCl doped polyaniline shows a quasi 1D- variable range hopping conduction. The electrical parameters obtained are compared with those obtained using 1D - variable range hopping [39].

The results of dielectric relaxation studies carried out on Al-PANI-Al capacitor configurations have shown that the movement of charge carriers under the influence of an electric field gives rise to interesting space charge phenomenon leading to interfacial polarization. Further, the observed shifts of Cole-Cole plot with increasing temperature indicate the presence of multiple relaxation in the Al-PANI-Al capacitor configuration. The interesting relaxation phenomenon seen in this configuration has been understood to arise from the damping of dipole oscillators arising as a result of motion of non-linear defects observed as a consequence of applications of external electric field. The observed variation of conductivity with frequency calculated for the Al-PANI-Al configuration supports the existing one dimensional hopping conduction model in literature. The mobility,'μ'of charge carriers has been calculated using the approximations to space charge theories. The increase in the mobility value both with increasing temperature and thicknesses observed for Al-PANI-Al, configuration support the formation of space charge in this system. In the light

4.7 REFERENCES

1. H. Letheby, *J. Chem. Soc.* **15** (1962) 161.

2. A. F. Diaz and J. A. Logan, *J. Electroanal. Chem.* **111** (1980) 111.

3. A. G. Green and A.E. Woodhead, *J. Chem. Soc. Trans.* **97** (1910) 2388.

4. A. G. Green and A.E. Woodhead, *J. Chem. Soc. Trans.* **101** 1912) 1117.

5. M. Jozefowicz, L. T. Yu, G. Belorgey and R. Buvet, *J. Poly. Sci. C* **16** (1967) 2943.

6. D. M. Mohilner, R. N. Adams and W. J. Argersinger Jr., *J. Am. Chem. Soc.* **84** (1962) 3618.

7. E.M. Paul, A.J. Ricco and M. S. Wrighton, *J. Phys. Chem.* **89** (1985) 1441.

8. W.S. Huang, A.G. MacDiarmid, A. J. Epstein, *J. Chem. Soc. Chem. Commun.* (1987) 1784.

9. J. J. Langner, Synth. *Metals* **36** (1990) 35.

10. A. J. Epstein and A.G. MacDiarmid, in *Electronic Properties of Conjugated Polymer*, eds. H. Kuzmany, M. Mehring and S.Roth (Springer Verlag, Berlin, 1989).

11. A. Andreatta, Y. Cao, J. C. Chiang, A. J. Heeger and P. Smith. *Synth. Metals* **26** (1988) 383.

12. Y. Cao, G. M. Treacy, P. Smith and A. J. Heeger, *Appl. Phys. Lett.* **60** (1992) 2711.

13. S.C.K. Misra, M. K. Ram, N.S. Sundaresan, B. D. Malhotra and S. Chandra, *Appl. Phys. Lett.* **61** (1992) 1219.

14. M. K. Ram, N. S. Sundaresan and B. D. Malhotra, *J. Phys. Chem.* **97** (1993) 1158.

15. T. Kobayashi, H. Yoneyama and H. Tamura, *J. Electroanal. Chem.* **177** (1984) 281.

16. Y. Cao, P. Smith and A. J. Heeger, *Synth. Metals* **32** (1989) 263.

17. N. E. Agbor, M. C. Petty, A. P. Monkman and M. Harris, *Synth. Metals* **55** (1993) 3789.

18. D. Bloor and A. Monkman, *Synth. Metals* **21** (1987) 175.

19. S. Stafstrom, J. L. Bredas, A. J. Epstein, H. S. Woo, D. B. Tanner, W.S. Huang and A.G. MacDiarmid, *Phys. Rev. Lett.* **59** (1987) 1464.

20. M. G. Roe, J. M. Ginder, P. E. Wigen, A. J. Epstein, M. Angelopoulous and A.G. MacDiarmid, *Phys. Rev. Letts.* **60** (1988) 2789.

21. R. P. McCall, M. G. Roe, J. M. Ginder, T. Kusumoto, E. M. Scherr and A.G. MacDiarmid, *Synth. Metals* **29** (1989) 29.

22. K. G. Noeh, E. T. Kang and K. L. Tan, *Synth. Metals* **40** (1991) 341; M. J. Rice, E.J. Mele, *Phys. Rev. lett.* **49** (1982) 145.

23. M. E. Jozefowicz, R. Laversanne, H. H.S. Javadi, A.J. Epstein, J. P. Pauget, X. Tang and A.G. MacDiarmid, *Phys. Rev. B* **39** (1989) 12958.

24. N. S. Sariciftci, M. Bartonek, H. Kuzmany, H. Neubegauer and A. Neckel, *Synth. Metals* **29** (1989) E193.

25. X. Tang, Private communication, A. G. MacDiarmid, A. G. Heeger and A. J. Epstein, J. Faraday Discuss. *Chem. Soc.* **88** (1989) 317.

26. W.S. Huang and A.G. MacDiarmid, *Polymer* **34** (1993) 1833. 27. H. Kuzmany, E. M. Genies and A. Sayed, *Solid State Sci.* **63** (1985) 223.

28. A. J. Epstein, J. M. Ginder, M. G. Roe, T. L. Gustafson, M. Angelopoulos and A.G. MacDiarmid, Proc. Symp. on *Nonlinear Optical Properties of Polymers* "mat. Res. Soc. Mig. Boston" (1987) 12/5/8.

29. F. Zuo, M. Angelopoulos, A.G. MacDiarmid and A. J. Epstein, *Phys. Rev. B* **36** (1987) 3475.

30. F. Zuo, M. Angelopoulos, A.G. MacDiarmid and A. J.Epstein, *Phys. Rev. B* **39** (1989) 3570.

31. M. K. Ram, R. Mehrotra, S. S. pandey and B. D. Malhotra, *J. Phys. : Conden Matter* **1** 6 (1994) 8913.

32. T. Matsunaga, H. Daifuku, T. Nakajima and T. Kawagoe, *Poly. Adv. Technol.* **1** (1990) 33.

33. G. Gustafsson, Y. Coa, G. M. Treacy. F. Klavettey, N. Colaneri and A. J. Heeger, *Nature* **357** (1992) 477; M. A. Habib, *Langmuir* **4** (1988) 1302.

34. J.J. Langer, *Mater. Sci.* **XIV** (1988) 41.

35. S.P. Armes and J.F. Miller, *Synth. Metals* **13** (1986) 193.

36. A. T. Efremova and L. D. Arsov, *J. Serb. Chem. Soc.* **57** (1992) 127.

37. D. S. Boudreaux, R. R. Chance, J. F. Wolf, L. W. Shacklett, J.L. Bredas, B. Themans, J. M. Andre and R. Silbey, *J. Chem. Phys.* **85** (1986) 4584.

38. H. S. O. Chan, M. Y. B. Teo, E. Khor and C. N. Lim, *Thermal Anal.* **35** (1989) 765.

39. P. Philips and H. L. Wu, *Science* **252** (1991) 1805.

40. A. J. Epstein and A. G. MacDiarmid, *Synth. Metals* **41** (1991) 601.

41. Q. Li, L. Cruz and P. Phillips, *Phys. Rev. B* **47** (1993) 1840.

42. M. K. Ram, S. Annapoorni and B. D. Malhotra, *Phys. letts. A* (communicated).

43. N. N. Beladakere, S. C. K. Misra, M. K. Ram, D. K. Rout, R. Gupta, B. D. Malhotra and S. Chandra, J. Phys. : *Condes. Matter*, **4** (1992) 5747.

44. H. H. Javadi, K. R. Cromack, A. G. MacDiarmid and A. J. Epstein, *Phys. Rev. B* **39** (1989) 3579.

45. B. P. Jelle, G. Hagen, S. Sunde and R. Odegard, *Synth. Metals* **54** (1993) 315.

46. R. R. Chance, D. S. Baudreau, J.F. Wolf and L.W. Shacklette, *Synth. Metals* **15** (1986) 105.

47. J. C. Manifacier, J. Gasiot and J.P. Fillard, *J. Phys. E: Scient. Instrumen.* **9** (1976) 1002.

48. J. P. Pouget, M. E. Jozefowicz and A. J. Epstein and A.G. MacDiarmid, *Macromolecules* **24** (1991) 7779.

49. S.S. pandey, S.C.K. Misra, B. D. malhotra and S. Chandra, *J. Appl. Polym. Sci.* **44** (1992) 911.

50. M. K. Ram, N. S. Sundaresan and B. D. Malhotra, *J. Mater. Sci. Lett.* **13** (1994) 1490.

51. B. P. Jelle, G. Hagen, S. Sumde and R. Odegard, *Synth. Metals* **54** (1994) 315.

52. C. A. Angelli, C. Liu and E. Sanchez, *Nature* **362** (1993) 137.

53. J. C. Lacroix, H.K. Kanazawa and A.F. Diaz, *ibid* **36** (1989) 1308.

54. E.M. Fenies, G. Bidan, A. F. Diaz, *J. Electroanal. Chem.*, **149** (1983) 101.

55. A. J. Bard, L. R. Faulkner in *Electrochemical Methods*, John Wiley, New York, 1980.

56. W. E. Rudzinksi, L. Lozano and M. Walker, *ibid* **137** (1990) 3132.

57. H. Yoneyama, S. Hirao and S. Kuwabata, *J. Electrochem. Soc.* **139** (1992) 3141.

CHAPTER V

STUDIES ON CONDUCTING COPOLYMER FILMS

5.1 INTRODUCTION

Most conducting polymers like polypyrrole, polythiophene and polyaniline have excellent electrical conductivities but have limitations in various aspects like mechanical and thermal stability and hence are not processable [1-3]. To tackle this problem various attempts have been made to synthesize conducting composites, conducting copolymers including the introduction of a long or short alkyl chain in the monomer which can be subsequently polymerized to yield processable conducting polymers [4-6]. Various conducting polymers such as poly(phenylene oxide - pyrrole), styrenes - butadiene -styrenes, polyacetylene - polypyrrole, poly (acetylene - co - methyl acetylene) etc obtained using such techniques have been found to be stable [7-10].

Amongst the various polymers polypyrole is still the most attractive material due to the high value of electrical conductivity and facile cycling between the doped and undoped states including its many projected applications in molecular electronics, biosensors and Schottky devices [11-12]. However, it has serious disadvantages in poor processibility, systematic investigations have recently shown that N - substituted pyrrole greatly influences the polymer characteristics. For example methyl substitution into pyrrole chain results in a twisted chain conformation [13]. Electrochemically prepared poly(3 - octadecyl pyrrole) has lower value of electrical conductivity (5 S/cm) and higher band gap (3.5 eV) as compared to that of polypyrrole [14]. The rough morphology and shorter conjugation length of this conducting polymer is responsible for the sharp

196

decrease in conductivity which is compensated by its processibility with an the organic solvent [14].

Conducting composites have also been found to have excellent mechanical properties. Recently, polypyrrole / poly styrenes sulphonate (PP/PPS), polypyrrole/ polyvinyl chloride and polypyrrole / methyl cellulose etc. have been found to show excellent physical properties and slightly diminished conductivity ($5 - 10^{-2}$ S/cm) over conjugated polypyrrole films [15-17]. The fact that these composites maintain charge balance via cation transport and are intractable indicates that these can be used for many applications.

To improve upon the processibility and its mechanical strength, conducting polypyrrole copolymers such poly(phenylene oxide- N- pyrrole) and poly(α - napthalene oxide pyrrole) have recently been electrochemically synthesized [17. 18]. Conducting copolymers have been found to exhibit low electrical conductivity. Like many other conducting polymers, this conducting copolymer exhibits differing electrical and optical properties as the nature of a dopant is varied. The effect of doping on electrical properties of the films obtained by electrochemical polymerization of pyrrole monomer and pyrrole on addition of dipyrine - 1 (OH) - ones has been studied [19].

Malhotra et al [20] have synthesized poly(α- napthalene oxide pyrrole) by electrochemical technique. It has been reported that poly (α- napthalene oxide - pyrrole) stores about 18% of electrical charge. The charge transport in this conducting copolymer occurs via variable - range hopping mechanism.

Conducting copolymer films such as poly (N - methyl pyrrole- pyrrole) have been fabricated for their application in Schottky diode. It has been shown that a Schottky diode exhibits excellent rectification with Al and has an ideality factor of 1.2 [21].

An attempt has been made to study the optical, electrical and thermal properties of poly(α-napthalene oxide-pyrrole) and poly (N-phenyl pyrrole-pyrrole), respectively. The insitu polymerization of these conducting copolymers has been investigated through UV-visible spectroscopic technique. The electrical characterization studies have been performed with a view to delineate charge transport phenomenon in some of these electrochemically prepared conducting copolymer films. The junction characteristics obtained for metal/poly(α-napthalene oxide-pyrrole) structures have been used to estimate the various parameters such as electron affinity and work function etc..

5.2 STUDIES ON CONDUCTING POLY (α-NAPTHALENE OXIDE - PYRROLE) FILMS :

5.2.1 ELECTROCHEMICAL SYNTHESIS

Preparation of has poly (α- napthalene oxide pyrrole)been reported using a three electrode electrochemical cell [19]. Such a cell comprises of indium-tin-oxide (ITO) as an anode, platinum as a cathode and standard calomel electrode as a reference electrode(SCE). The solution phase consists of double distilled pyrrole (0.1M), α-napthol (0.1M) in 30 ml of propylene carbonate in the cell. The solution is continuously flushed with dry nitrogen to remove traces of any dissolved oxygen so as to provide moist atmosphere for the reaction. A current density of $0.3 \, mA/Cm^2$ is drawn from a Keithley (model 160 A) current source. The current is passed through an electrochemical cell maintained at 298°C for 30 to 45 minutes for obtaining black, homogeneous and flexible poly(α-napthalene oxide pyrrole) copolymer films. The thin transparent films have been obtained on ITO glass plate for the optical measurement by varying the time period in electrochemical synthesis.

198

5.2.2 THERMAL STUDIES

Fig. 1 shows the DSC thermogram obtained for an electrochemically prepared poly (α- napthalene oxide pyrrole) film. It can be seen that the heat flow increases slowly with the rise in temperature. It can further be seen that the transition occurs at 320°C and the polymer degrades at about 460°C indicating that the conducting copolymer film remains stable upto about 320°C. From these results, it can be tentatively concluded that copolymerization of pyrrole with α- napthalene oxide results in improved stability.
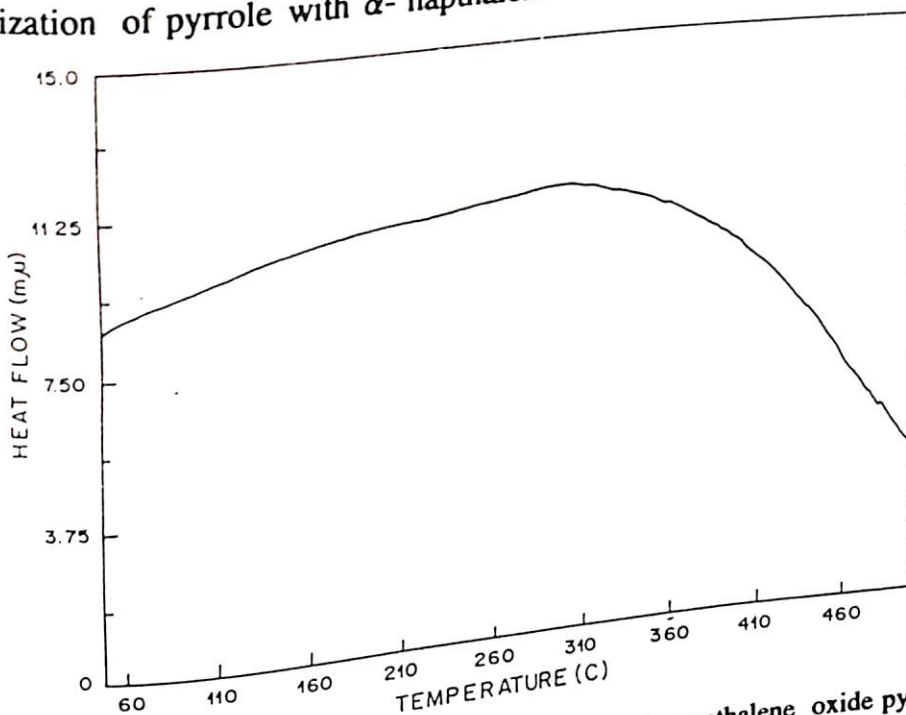
Fig.1 DSC thermogram of an electrochemically prepared poly (α-napthalene oxide pyrrole) film.

5.2.3 ELECTRICAL MEASUREMENTS

The electrical conductivity of poly(α- napthalene oxide pyrrole) has been measured to be 10-30 S/cm at room temperature (300K) using four points probe method [19]. The electrical conductivity of this conducting copolymer has been experimentally determined as a function temperature to delineate the charge conduction mechanism in this system. Fig.2 shows the variation of σ_{dc} obtained for poly (α-

napthalene oxide pyrrole) copolymer as a function of $10^3/T$ (where T is the temperature). The curve is similar to the perchlorate (ClO_4^-) doped polypyrrole system. The non-linear fit (fig.2) indicates Arrehineous type behaviour. The plot of σ_{dc} vs $T^{-1/4}$ for this conducting polymer indicates the operation of variable range hopping phenomeon at lower temperatures. The activation energy calculated for the BF_4^- doped poly (α-napthalene oxide pyrrole) copolymer has been found to be 0.0237 eV.
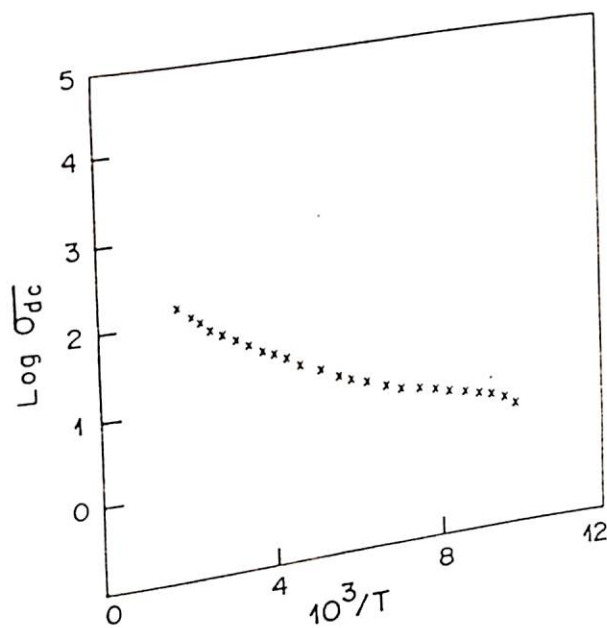
Fig.2 Variation of $\log \sigma_{dc}$ vs. $T^{-1/4}$ for BF_4^- doped poly (α-napthalene oxide pyrrole) film

5.2.4 SPECTROSCOPIC STUDIES

Fig.3 shows the FTIR spectrum of undoped poly(α-napthalene oxide pyrrole) film. It shows bands at 1569, 1484, 1305, 1215, 1100 (broad band), 1046, 970 (shoulder), 930 (strong), 790 (medium) and 685 (medium) and 530 cm^{-1} (small) bands, respectively. Fig.4 is the FTIR spectrum of BF_4^- doped poly(α-napthalene oxide pyrrole) film. The characteristic bands observed from 1800 to 1200 cm^{-1} (fig. 4) pertain to the presence of napthol in this conducting copolymer. The bands at 1569, 1484, 1305 and 1215 cm^{-1}
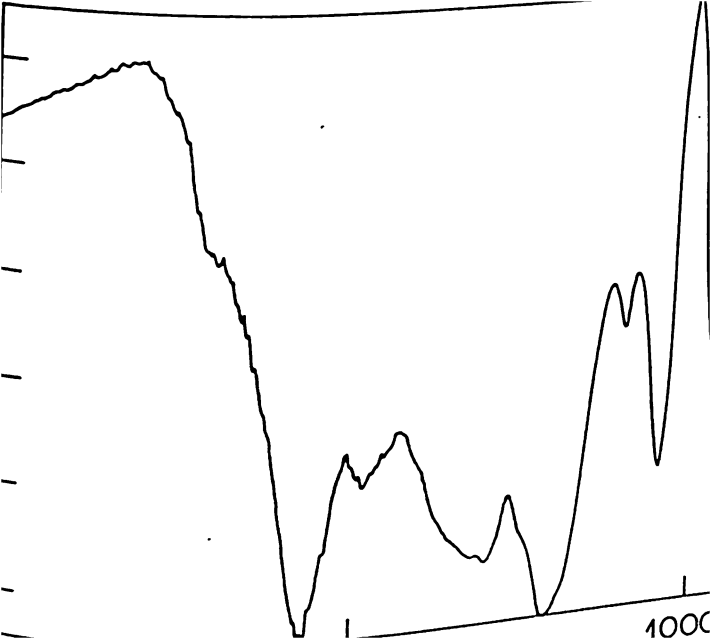
200

Fig.5 shows the results of insitu UV-visible measurements carried out using a teflon cuvette containing platinum as cathode and ITO as anode obtained for poly (α-napthalene oxide pyrrole) films. It can be clearly seen that polymerization in the case of poly(α-napthalene oxide pyrrole) films begins at about 1.75 V. The peaks seen at 425 nm and 360 nm respectively correspond to the presence of polypyrrole and α-napthol in the polymer matrix.
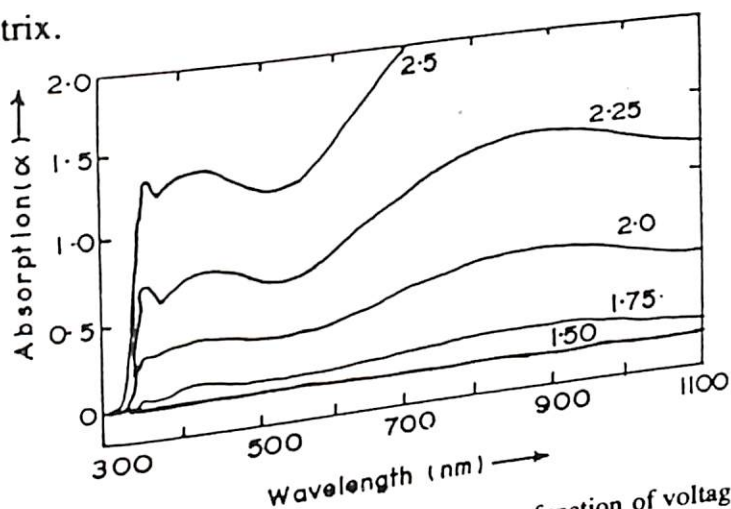

Fig.5 Variation of UV-visible absorption vs wavelength (nm) as a function of voltage obtained as a result of insitu polymerization of poly (α-napthalene oxide pyrrole) film.

Fig.6 shows UV-visible spectrum obtained as a function of wavelength (nm). It shows peaks at 330 nm and 820 nm and a slight hump at about 330 nm . The peak at 360 nm is due to the $\pi - \pi^{\bullet}$ transition whereas the peak at about 820nm is due to the n-$\pi^{\bullet}$ transition.
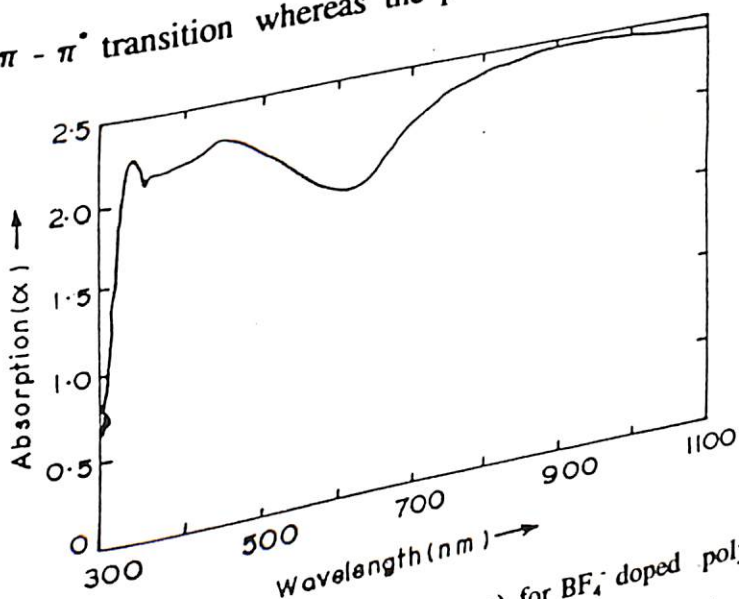

Fig.6   Variation of UV-visible absorption vs wavelength (nm) for BF_4^- doped poly (α- napthalene oxide Pyrrole) film.

202

Figure 7 shows the results of the systematic measurements of insitu polymerization of α-napthol. It shows that the polymerization of α- napthol occurs at about 1.75 V. It further reveals that there is no monomer linked with the copolymer films. Incidently, the polymerization of polypyrrole also occurs at about 1.75 V.(sec. 3.5.2, Chapter III).

An attempt has been made to calculate the band gap of this conducting copolymer from the absorption spectra shown in fig.8. The absorption coefficient for one dimensional lattice system (i.e conducting polymer) is known to be proportional to (- $E_t)^{-1/2}$ The value of band gap can be obtained by plotting $(1/\alpha.h\nu)^2$ vs the photon energy (hν) which exhibits a singularity around the band gap E_g. Fig.8 shows the variation of $(1/\alpha.h\nu)^2$ as function of . It is interesting to see that the value of the band gap of conducting polymer comes out to be 2.8 eV which is in close agreement with the theoretical reported value [23]. The observed broadening of the UV - visible curve arises due to the presence of these two structures in the conducting poly(α-napthalene oxide pyrrole) films. The first structure looks more promising as the alternate double and single bands are maintained in structures in fig. 9(a). The second structure can be speculated where oxygen lies in the chain of poly(α-napthalene oxide pyrrole) copolymer (fig.9 (b)).
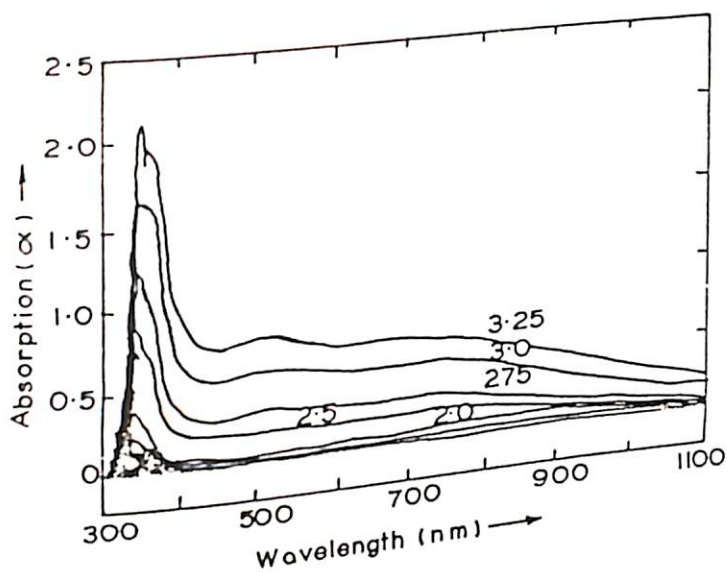
Fig.7 Variation of UV-visible absorption vs wavelength (nm) as a function of voltage in insitu polymerization of α-napthol.
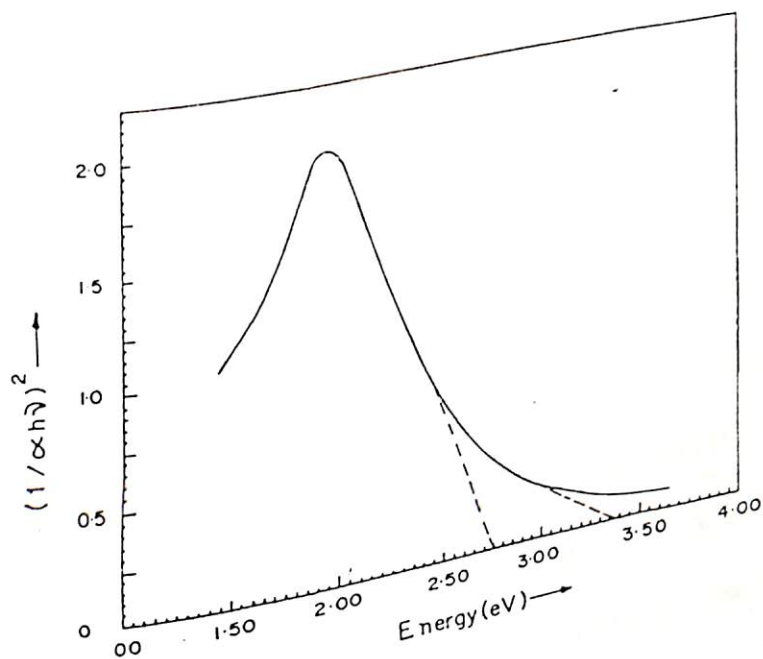

Fig. 8 Variation of $(1/\alpha.h\nu)^2$ as function of photon energy (hv) for poly(α-napthalene oxide pyrrole) film: Extrapolated value is used for the band gap calculation.
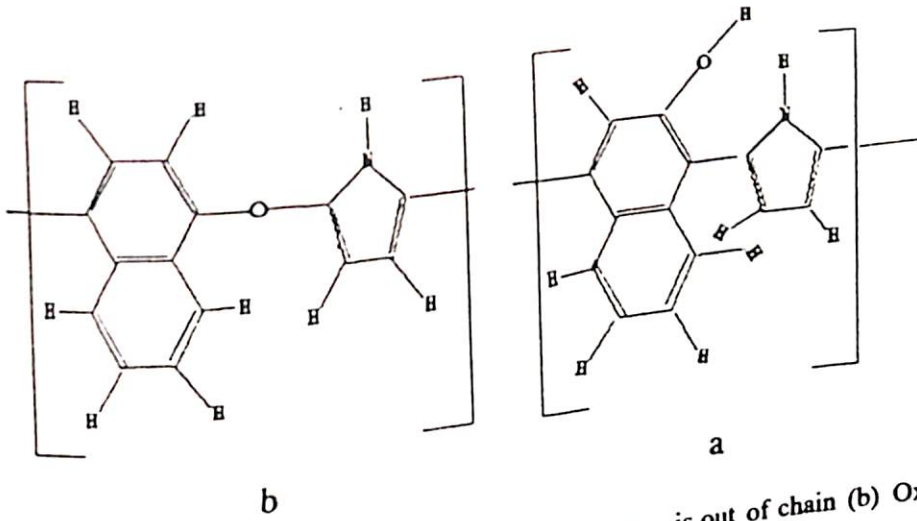
Fig.9 Structure of poly(α-napthalene oxide pyrrole): (a) Oxygen is out of chain (b) Oxygen is in chain

5.3 STUDIES ON POLY(N-PHENYLPYRROLE PYRROLE) CONDUCTING COPOLYMER

It has been shown that N-substitution in polypyrrole greatly influences the polymer characteristics. An attempt has been made to synthesize poly (N-phenylpyrrole-pyrrole), a conducting copolymer based on N-phenylpyrrole and pyrrole.

The same set up of electrodes as for the preparation of poly(α-napthalene oxide pyrrole) has been used for the synthesis of poly(N-phenylpyrrole-pyrrole) conducting copolymer films. The solution phase consists of pyrrole (0.1M) (Merck), N-phenyl pyrrole (0.2M) (Sigma) in 30ml of propylene carbonate (Aldrich) with 0.1 TEATFB maintained at about 25°C. A current density of about 0.3 mA/cm² used for 30-45 minutes to obtain free standing BF₄⁻ poly(N-phenylpyrrole pyrrole) conducting copolymer films [23].

5.3.1 THERMAL STUDIES

The results of differential scanning calorimetry experiments carried out on BF$_4^-$ doped poly (N-phenyl pyrrole) and BF$_4^-$ poly (N-phenyl pyrrole pyrrole) films are shown in fig.10. Two exothermic peaks at about 160°C and 330°C in (curve a) can be clearly seen for poly (N-phenyl pyrrole). The temperature at 160°C occurs as a result of the removal of BF$_4^-$ ions. DSC thermogram obtained for poly(N- phenyl pyrrole) shows a distinct hump (160°C) associated with melting. Thus, the inclusion of N- phenyl pyrrole in pyrrole conducting copolymer may be expected to contribute to the increased melt (450°C) processibility as is apparent in curve b (fig.10). Poly(N-phenyl pyrrole pyrrole) films are thus relatively more thermally stable than both poly(N-phenyl pyrrole) and polypyrrole films [24].
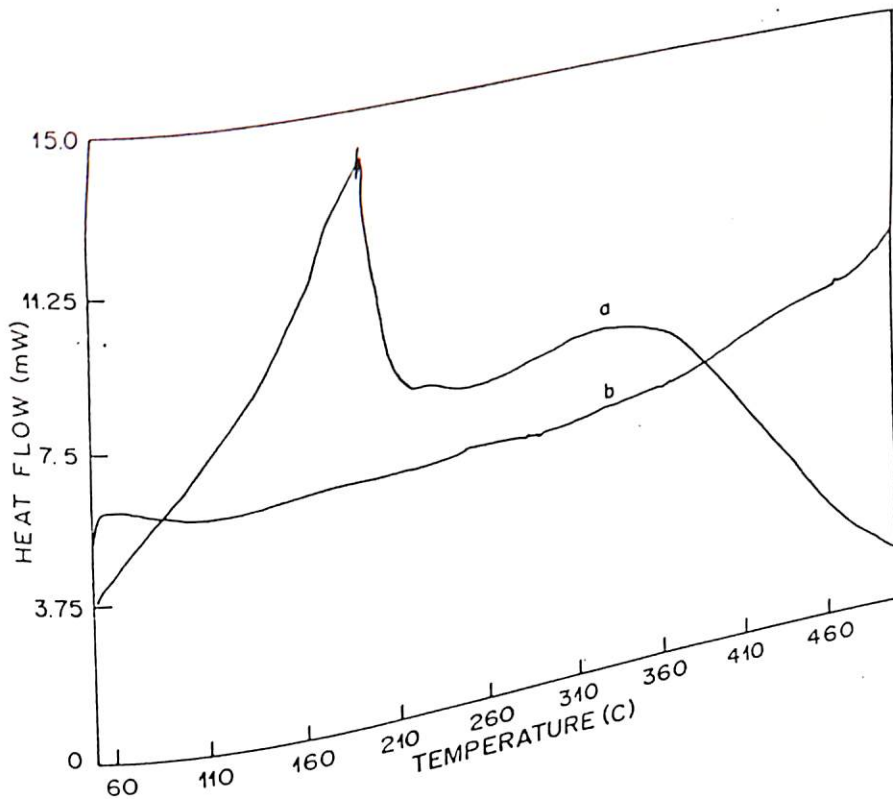

Fig.10 DSC thermogram for (a) BF$_4^-$ poly (N-phenylpyrrole) and (b) BF$_4^-$ doped poly (N-phenylpyrrole-pyrrole) films.

5.3.4 ELECTROCHEMICAL STUDIES

Cyclic voltammetry is an electroanalytical technique used to determine the electroactive and the electrochemical properties of conducting polymer films. The cyclic voltammograms obtained at small concentration (5 mM to 50mM) of pyrrole and phenylpyrrole in propylene carbonate (PC) containing 0.1M tetra(n-butyl) ammonium fluoroborate is shown in fig. 12. The broad CV peak indicates that electro-oxidation of N-phenylpyrrole occurs around a potential of 0.7 V vs quasi reference electrode.
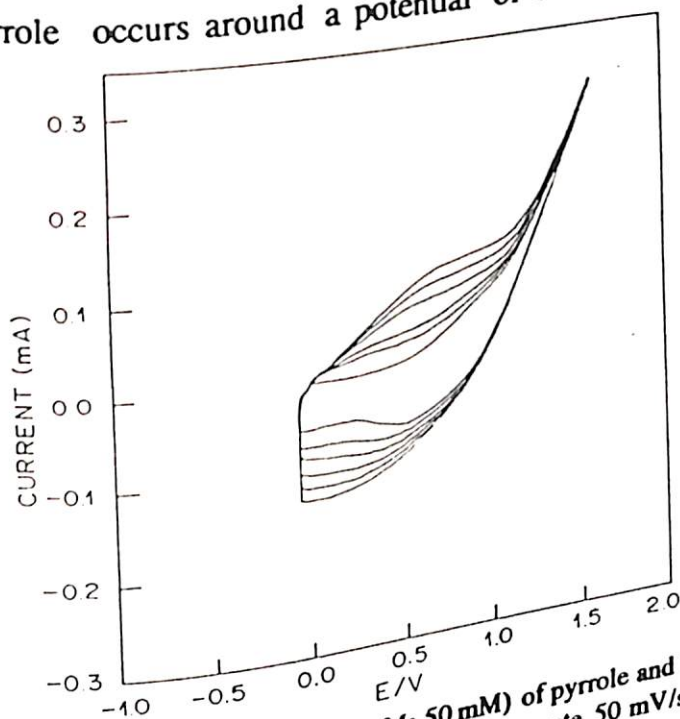

Fig.12 Cyclic voltammogram obtained (5 mM: 50 mM) of pyrrole and N-phenyl pyrrole) in 0.1M TBATFB in PC with quasi reference electrode with a scan rate 50 mV/sec
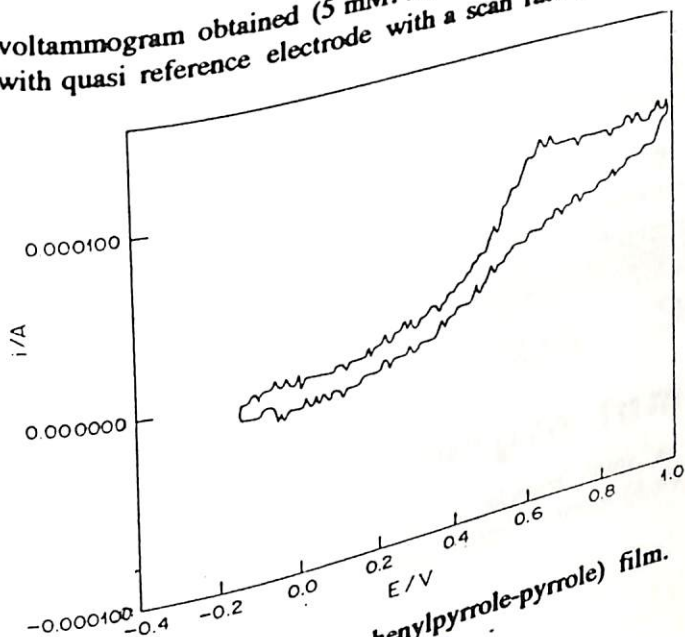

Fig.13 Cyclic voltammogram of a poly(N-phenylpyrrole-pyrrole) film.

208

5.4 SCHOTTKY DIODES BASED ON CONDUCTING POLY(α-NAPTHALENE OXIDE PYRROLE) FILMS

There is an increased interest in the possible use of molecular organic materials as the active materials in electronic or optical devices. Basic questions as to whether or not it is possible to make use of modes of operation familiar in inorganic semiconductor science remains largely unanswered. Conjugated polymers are molecular analogies of inorganic semiconductors, which exhibit high electronic mobilities in doped state. Despite the considerable progress made in the past decade towards the understanding of the electronic properties of conjugated polymers, there has been relatively little work on their active component in semiconductor device structures. There are several reasons, the most important of which is the conjugated polymers cannot be conveniently processed to the forms required in these devices. Most conjugated polymers are not readily soluble in easily handled solvents and are infusible. Conducting copolymers obtained from N-methylpyrrole and pyrrole, poly(p-phenylene vinylene) etc. have so far been used for the fabrication of Schottky diode. It has been shown that these devices show better rectification ratio including excellent electronic device parameters. Keeping these results in mind an attempt has been made to fabricate Schottky diode based on poly(α-naphthalene oxide pyrrole) with different metals.

Schottky diodes have been fabricated by depositing Ag, In, Pb and Zn on one side of the copolymer film. The ohmic contacts have been made by painting electrodag (E+502) on the other side of conducting polymer films. The effective junction area in each case is about $4.0 \times 10^{-4} cm^2$. I-V and C-V measurements have been carried out using Keithley electrometer (model 617 A) and an Impedance Analyzer (model HP 4192 A).

Similar results have been obtained in case of Zn/poly(α-napthalene oxide pyrrole) junction indicating that poly(α-napthalene oxide pyrrole) has a higher work function.
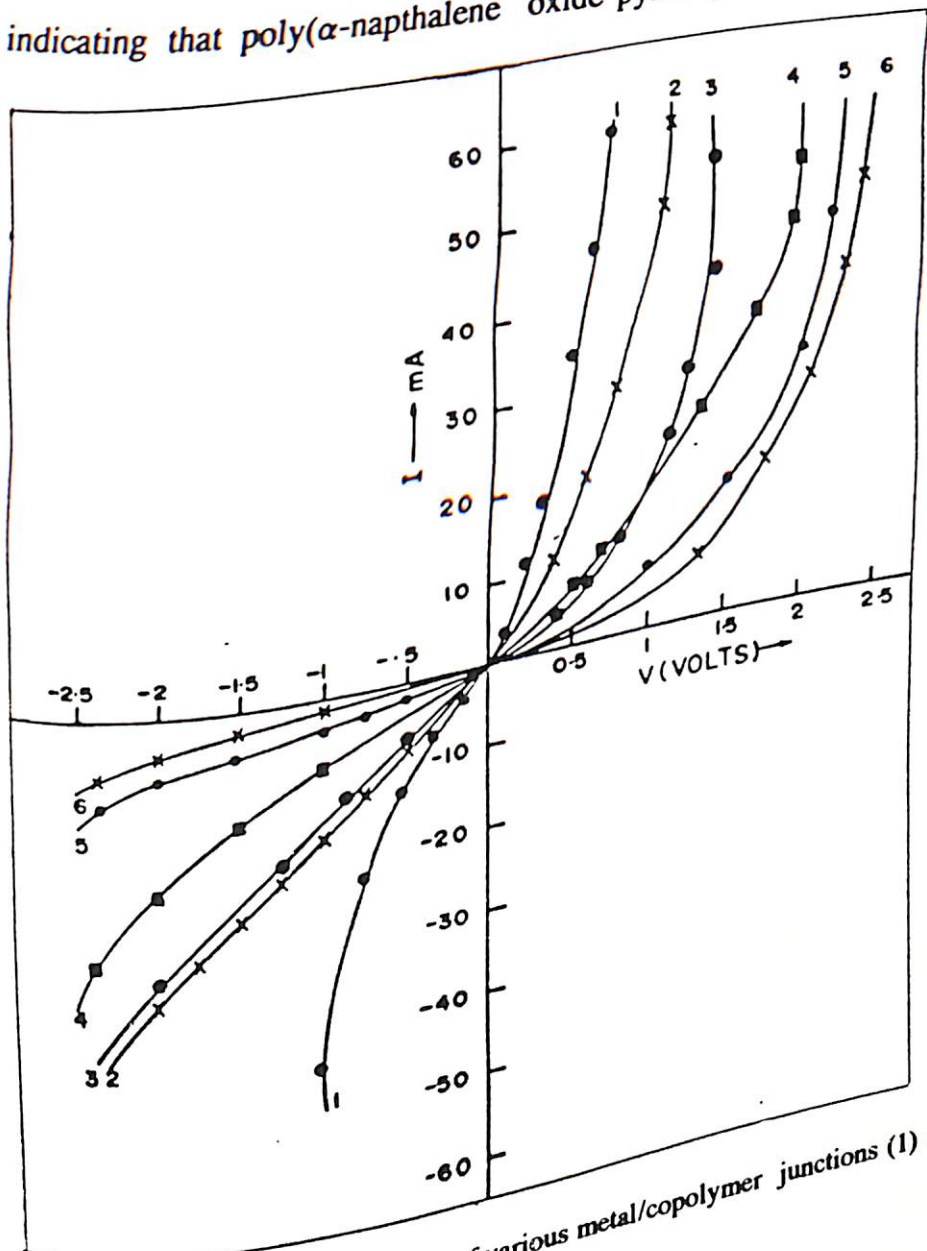

Fig.16 Current (I) - voltage (V) characteristics of various metal/copolymer junctions (1) Ag, (2) In, (3) Sn, (4) Al (5) Pb and (6) Zn

212

Fig.13 shows the results of electrochemical doping of BF_4^- in poly(N-phenyl pyrrole pyrrole) copolymer film. The oxidation peak has been obtained at 0.7V and the reduction peak at 0.6V. The appearance of redox peaks show that the composite is electroactive. Oxidation of BF_4^- anion at this electrode leads to the entrapment of products in conducting polymer matrix inhibiting further oxidation [23].

The insitu polymerization of conducting copolymer of N-phenyl pyrrole and pyrrole films have been studied via UV-visible spectroscopy. The experiments have been performed using the a two electrode cell comprising of a teflon cuvette containing pyrrole (0.1M), N-phenyl pyrrole (0.2M), in 5 ml of propylene carbonate with tetra-ethyl ammonium tetra fluroborate (0.1 M). The peak at 388 nm (3.2 eV) has been ascribed to π-π^* transition whereas the peak at 820 nm (1.51 eV) has been attributed to the n-π^* transition in doped poly(phenylpyrrole-pyrrole) copolymer films (fig.14). The change in the magnitude of absorption as a result of UV-radiation unravel the role of polymerization of poly (phenyl pyrrole pyrrole) conducting copolymer film.
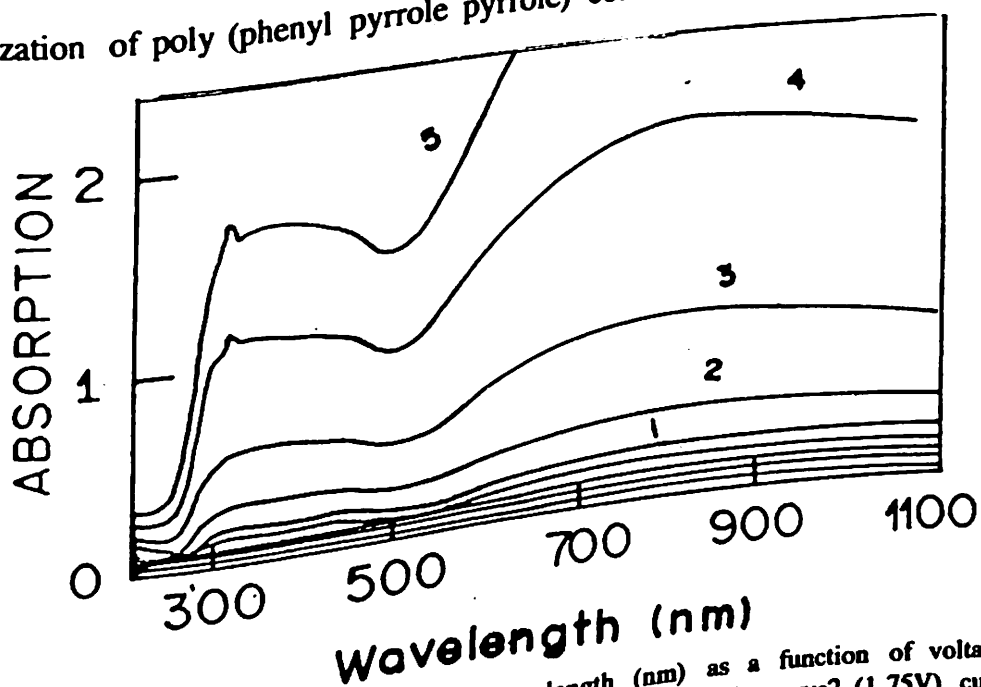

Fig.14 Variation of UV-visible absorption vs wavelength (nm) as a function of voltage in insitu polymerization of poly(N-phenylpyrrole-pyrrole): curve1 (1.5V), curve2 (1.75V), curve3 (2.0V), curve4 (2.25V) and curve5 (2.5V).

Figure 15 has been obtained by plotting $(1/\alpha.h\nu)^2$ versus photon energy (hν) for the BF$_4^-$ doped poly(N-phenylpyrrole-pyrrole) copolymer film. The optical absorption edge as determined from this figure is seen around 3.0 eV. It can be seen that the band edges are not very sharp. The optical energy band gap has been estimated to be 3.2 eV, which is very close to be value obtained for the polypyrrole films (3.0 eV). It can be remarked that the band gap of polypyrrole lies between 1.4 to 6.0 eV depending upon preparation and attached group with monomer [22].
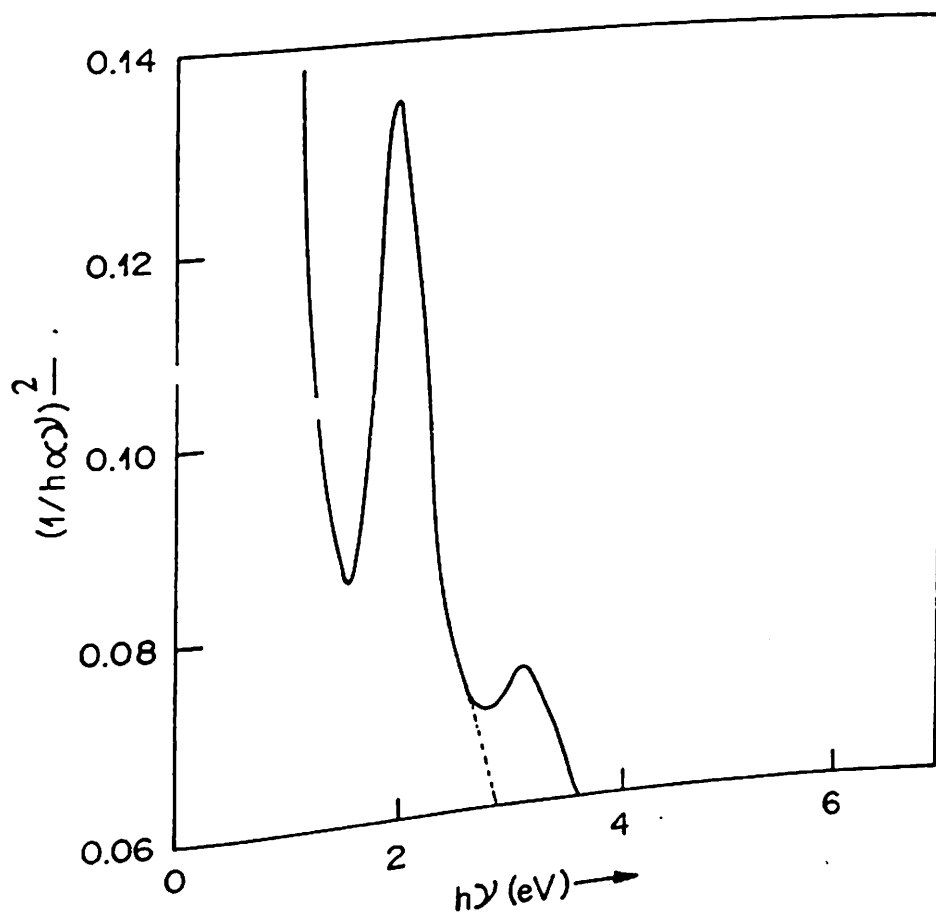

Fig.15 Variation of $(1/\alpha.h\nu)^2$ vs photon energy, hν (eV) for poly (N-phenylpyrrole-pyrrole) conducting copolymer film

From these results it can be concluded that poly (N-phenylpyrrole-pyrrole) films are both electroactive and processible[25].

5.4 SCHOTTKY DIODES BASED ON CONDUCTING POLY(α-NAPTHALENE OXIDE PYRROLE) FILMS

There is an increased interest in the possible use of molecular organic materials as the active materials in electronic or optical devices. Basic questions as to whether or not it is possible to make use of modes of operation familiar in inorganic semiconductor science remains largely unanswered. Conjugated polymers are molecular analogies of inorganic semiconductors, which exhibit high electronic mobilities in doped state. Despite the considerable progress made in the past decade towards the understanding of the electronic properties of conjugated polymers, there has been relatively little work on their active component in semiconductor device structures. There are several reasons, the most important of which is the conjugated polymers cannot be conveniently processed to the forms required in these devices. Most conjugated polymers are not readily soluble in easily handled solvents and are infusible. Conducting copolymers obtained from N-methylpyrrole and pyrrole, poly(p-phenylene vinylene) etc. have so far been used for the fabrication of Schottky diode. It has been shown that these devices show better rectification ratio including excellent electronic device parameters. Keeping these results in mind an attempt has been made to fabricate Schottky diode based on poly(α-naphthalene oxide pyrrole) with different metals.

Schottky diodes have been fabricated by depositing Ag, In, Pb and Zn on one side of the copolymer film. The ohmic contacts have been made by painting electrodag (E+502) on the other side of conducting polymer films. The effective junction area in each case is about $4.0 \times 10^{-4} cm^2$. I-V and C-V measurements have been carried out using Keithley electrometer (model 617 A) and an Impedance Analyzer (model HP 4192 A).

Results of I-V measurement carried out on metal/poly(α-napthalene oxide pyrrole) junction with different metals (Sn, Pb, Al, Ag, and Zn) have been shown in fig. 16. It can be seen that all metals used for the fabrication of these junctions form blocking contacts. The striking asymmetry in the case of reverse bias conditions in the case of poly(α-napthalene oxide pyrrole) indicates complete blocking of charge carriers. Similar results have been obtained in case of Zn/poly(α-napthalene oxide pyrrole) junction indicating that poly(α-napthalene oxide pyrrole) has a higher work function.
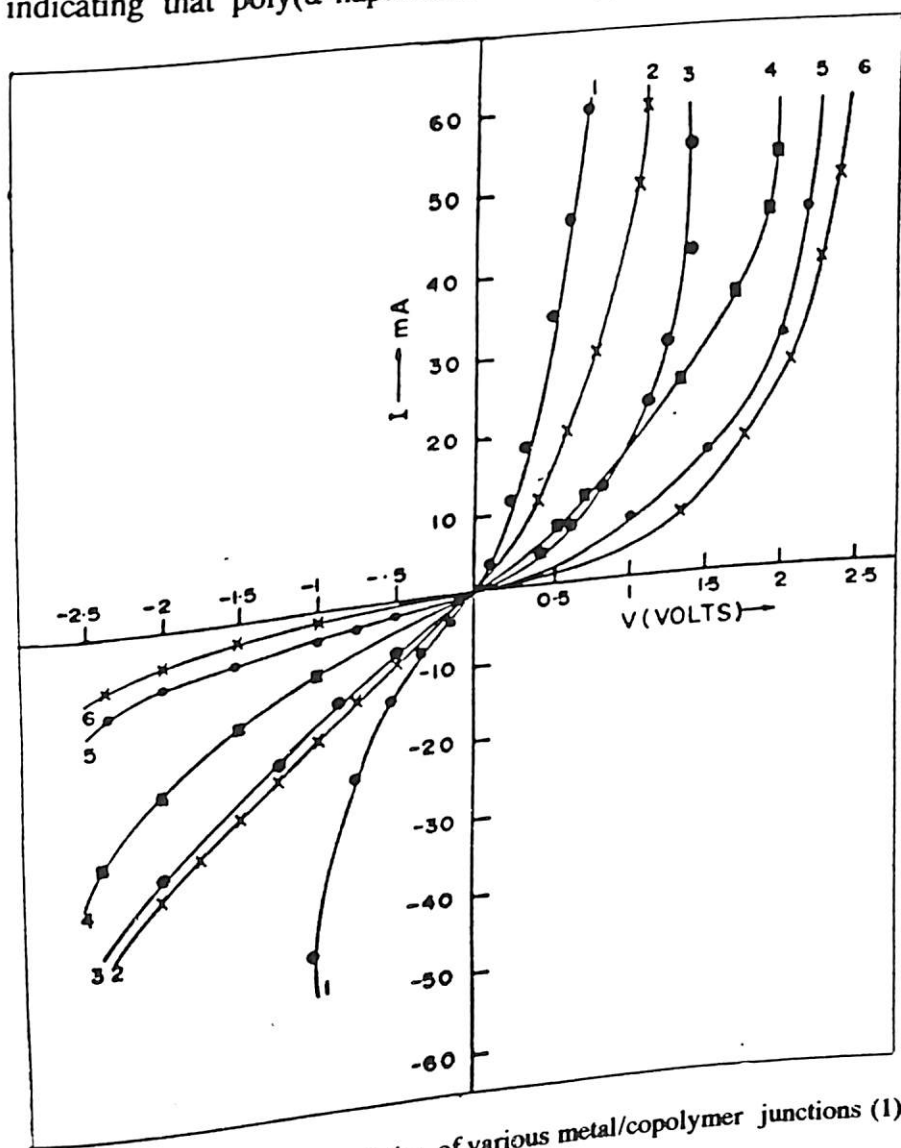

Fig.16 Current (I) - voltage (V) characteristics of various metal/copolymer junctions (1) Ag, (2) In, (3) Sn, (4) Al (5) Pb and (6) Zn

212

Fig. 17 shows the variation of lnJ as a function of voltage for Pb/poly(α-napthalene oxide pyrrole) and Zn/poly(α-napthalene oxide pyrrole) junctions when these are forward biased. The observed linear behaviour between lnJ and V at low fields (≤ 0.2V) points out to the presence of Schottky type emission (fig. 17). At higher fields (≥ 0.2V), lnJ vs V characteristics are found to be highly nonlinear. It can be seen that Schottky barrier disappears beyond 0.2V (the threshold voltage) and the current is limited by the bulk resistance. The various junction characteristics can be obtained using the Schottky emission equation for Pb and Zn/poly(α-napthalene oxide pyrrole) interface. The results have been given in Table 1. A low value of ideality factor obtained as 1.2 compared to that of polypyrrole indicates the excellent Schottky behaviour of this conducting copolymer. The estimated barrier height estimated from (fig.17) lnJ Vs V characteristics lies in 0.45 - 0.5 V range [26].

TABLE 1: Estimates for the junction parameters for some metal /poly(α -napthalene oxide pyrrole) junctions.

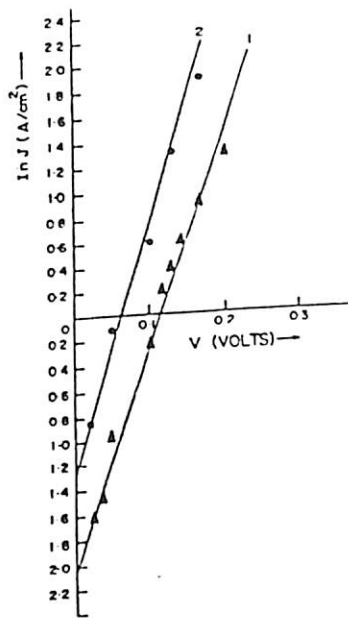| System	Ideality factor n	Barrier height (eV)	Work function (eV)
Zn	1.5	0.46	4.33
Pb	1.5	0.47	4.24
In	1.2	0.60	4.12

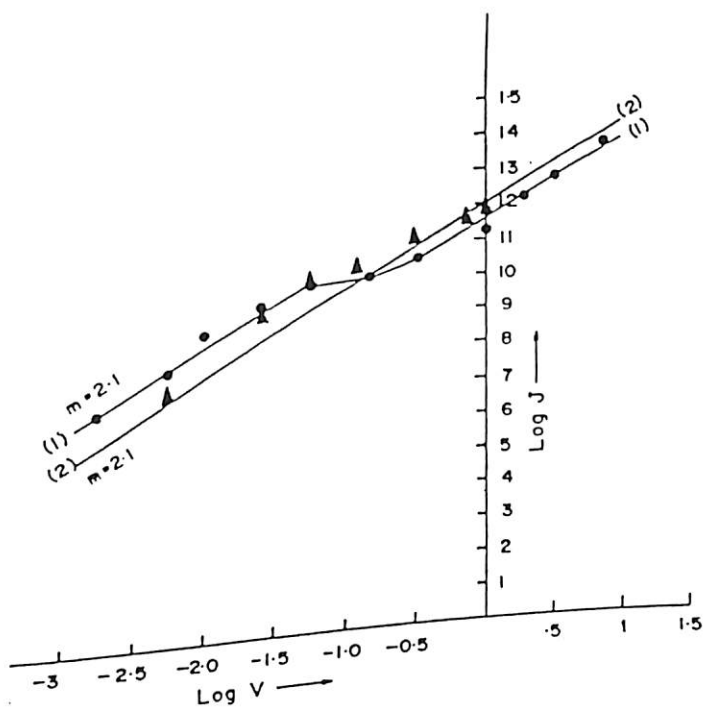Fig. 17 ln J vs V characteristics of (1) Pb/copolymer junction and (2) Zn/copolymer junctions

Fig. 18 Variation of logJ vs logV for metal/poly (α-napthalene oxide pyrrole) (1) In and (2) Zn.

Figure 18 shows the plot of logJ vs logV for different junctions in the forward direction for the flat band states. Such a plot yields the relationship, $J \propto V^n$, indicating he existence of space charge limited current (SCLC). The observed value of $m \geq 2$ ndicates the operation of space charge limited current mechanism behaviours with a ;iven energy range. It can be concluded that SCLC is perhaps caused by the presence

214

of traps at interfacial region comprising of metal and the poly(α - napthalene oxide pyrrole) conducting copolymer.
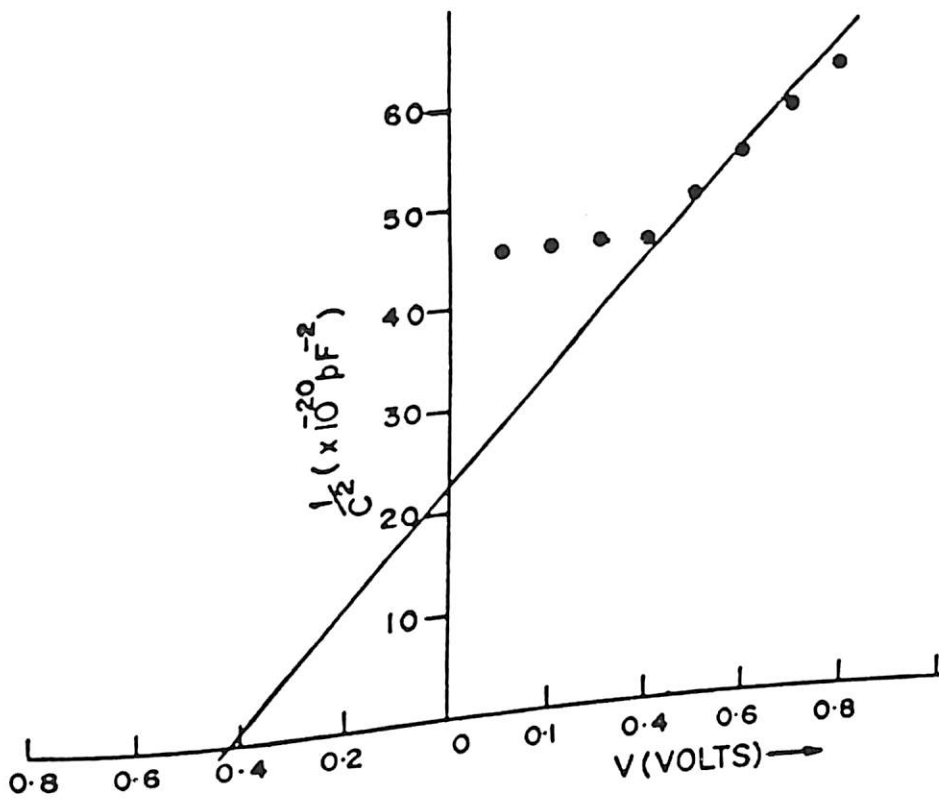

Fig. 19 $1/C^2$ vs voltage (V) for In/poly(α-napthalene oxide pyrrole) junction

Capacitance(C)-Voltage(V) measurements have been made on indium / poly(α-napthalene oxide pyrrole) junction. Variation of $1/C^2$ with voltage(V) follows the following equation (fig.19) [27].

$$1/C^2/(V_c - V) = 2/Nq \ \epsilon_s 2A^2 \qquad\qquad \text{Eq. 1}$$

where C is the junction capacitance, V is the voltage across the junction, C_s is the dielectric constant of a given material, A is the area of the electrode and V_c is the contact potential. It can be seen that a linear behaviour from 0.4 V to 0.8 V is observed. The carrier concentration has been estimated to be $2x10^{15}/cm^3$. This value of concentration is four orders of magnitude less than the value observed for a polypyrrole

215

film. The observed behaviour from 0 to 0.4V is perhaps due to the charges trapped in local band of the indium/poly(α-napthalene oxide pyrrole) junction. The junction capacitance C can be expressed as:

$$C = \epsilon_0 \epsilon_s A / w \qquad \text{Eq.2}$$

where w is the depletion width, A is the area of the sample and ϵ_s is the dielectric constant of the material used. The value of ϵ_s has been calculated to be 13.6 and the depletion width for indium/poly(α-napthalene oxide pyrrole) junction has been estimated to be of the order of 300 Å.

It can be seen that the values of various electronic parameters such as ideality factors and rectification ratio, etc. are considerably improved than those of metal/polypyrrole junctions [26].

5.5 CONCLUSIONS

It has been shown that the processibility of conjugated polymer can be enhanced by copolymerization techniques. The thermal characteristics of polypyrrole can be increased by copolymerizing it either with α-napthol or N-phenyl pyrrole, respectively. The copolymeric systems have been shown to be less conducting than polypyrrole. It has been further shown that polymerization of poly(α-napthalene oxide pyrrole) and poly (N-phenylpyrrole-pyrrole) starts at the same potential as that of polypyrrole.

Copolymerization has been studied by insitu UV-visible spectroscopy. The band gap for both poly(α-napthalene oxide pyrrole) and poly (N-phenylpyrrole-pyrrole have been found to be 3.2 eV. The charge transport in poly(α-napthalene oxide pyrrole) and poly (N-phenylpyrrole-pyrrole) occurs via variable range hopping conduction mechanism. -V characteristics of different metal/ poly(α-napthalene oxide pyrrole) junctions have

been found to exhibit excellent Schottky behaviour with low ideality factors. Both the junction characteristics and electronic parameters for metal /poly(α-napthalene oxide pyrrole) have been estimated. The excellent ideality factors obtained for such a junction using Schottky device indicates that this important conducting copolymer can be used for technological applications.

Next chapter describes the result of the optical and electrical measurements including some such applications of the Langmuir - Blodgett films based on cadmium stearate and polyemeraldine base, respectively.

5.6 REFERENCES

1. R. Ansari and G. C. Wallace, *Polymer* **35** (1994) 2371.

2. M. K. Ram, R. Mehrotra, S.S. Pandey and B. D. Malhotra, *J. Phys.: Condens. Matter* **6** (1994) 8913.

3. M. Ito, H. Shida and K. Tanaka, *J. Polym. Sci.; Polym. Lett. Eds.* **24** (1986) 147.

4. H. Masuda, S. Tanaka and K. Kaeriyama, *J. Chem. Soc., Chem. Commun.* (1989) 725.

5. O. Inganas, M. Sundberg, G. Gustafsson, J.O. Noilsson, S. Stafstrom and B. Sjogren, *Springer Ser. Solid State Sci.* **91** (1989) 336.

6. A. Assadi, C. Svensson, M. Wilander and O. Ignanas, *Appl. Phys. Lett.* **53** (1988) 195.

7. G. Ahlgren and B. Krische, *J. Chem. Soc., Chem. Commun.* (1984) 946.

8. M.A. D. Paoli, R. J. Waltman, A.F. Diaz and J. Bargon, *J. Polym. Sci.: Polym. Chem. Eds.* **23** (1985) 1687.

9. B. Zinger and D. Kijel, *Synth. Metals* **41** (1991) 1013.

10. N. Kumar, B. D. Malhotra and S. Chandra, *J. Polym. Sci.: Polym. Lett. Eds.* **23** (1985) 571.

11. R. Gupta, S.C. K. Misra, B. D. Malhotra, N. N. Beladakere and S. Chandra, *Appl. Phys. Lett.* **58** (1991) 51.

12. N.C. Foulds and C.R. Lowe, *J. Chem. Soc., Faraday Trans I* **82** (1986) 1259.

13. G. R. Mitchell, F. J. Davis and A. Geri, *British Polym. J.* **23** (1990) 157.

14. H. Masuda, *J. Polym. Sci.: Part A: Polym. Chem.* **28** (1990) 1891.

15. R. E. Noftle and D. Pletcher, *J. Electroanal. Chem.* **227** (1987) 229.

16. R. B. Bjorklund and B. Liedberg, *J. Chem. Soc. Chem. Commun.* (1986) 1293.

17. G. Ahlgren and B. Krische, *J. Chem. Soc. Chem. Commun.* (1989) 946.

18. W. Huang and J.M. park, *Chem. Soc. Chem. Commun.* (1987) 856.

19. Y. Nagasaki, M. Taniuchi and T. Tsuruta, *Makromol. Chem.* **189** (1988) 723.

20. B. D. Malhotra, N. Kumar, S. Ghosh, H. K. Singh and S. Chandra, *Synth. Metals* **31** (1989) 155.

21. H. Koezuka and S. Etoh, *J. Appl. Phys.* **54** (1983) 2511.

22. N. N. Beladakere, M. K. Ram, S. Annapoorni, S. S. pandey and B. D. Malhotra, F.L. Pratt and W. Hayes, *Indo-US Workshop of Perspective in New Materials*, New Delhi, India, (1991).

23. M. K. Ram, S. Annapoorni, N. S. Sundaresan, S. Kumar and B. D. Malhotra, *Indo-US Workshop of Perspective in New Materials*, New Delhi, India, (1991).

24. M. Salmon, E. Carbajal, J. F. Reed, *Mol. Cryst. Liq. Cryst.* **118** (1985) 403.

25. In *Absorption Spectroscopy*; R.P. Bauman, (John Wiley New York) 1962.

26. N. N. Beladakere, M. K. Ram, S. Annapoorni, S. S. pandey and B. D. Malhotra, F.L. Pratt and W. Hayes, *Phys. Lett. A* (communicated).

27. S. M. Sze, *Physics of Semiconductor Device* (Wiley, 2nd Eds. (1982).

CHAPTER VI

STUDIES ON LANGMUIR - BLODGETT FILMS

6.1 INTRODUCTION:

It has known for many centuries that ripples or waves in water can be reduced by pouring natural oil on its surface. Benjamin Franklin has performed such experiments at Clapham in a pond and has concluded that as soon as oil touches water, it spreads instantaneously to many feet around the surface of water. This has been attributed to repulsion between the water and oil drop [1,2]. Lord Rayleigh [3] has concluded the maximum extension of oil on the surface of water can be 1 nm thick. Later Agnes Pockel [4] has performed experiment for direct measurements pertaining to molecular size for the spreading material in its elucidation of the size, shape and orientation of molecules at air - water interface.

Irving has investigated the pressure- area isotherm of stearic acid $(CH_3(CH_2)_{16}COOH)$ and different fatty acids during the years, 1917 - 1920 [5]. Studies relating to sequential transfer of monolayers on the glass substrate have been carried out by Katherine Blodgett in 1920 [3]. These built up monolayer assemblies on the substrate are now referred to as Langmuir - Blodgett films whereas the floating monolayer is termed as Langmuir monolayer [6]. Due to the second world war, the research on LB films has not made much progress till 1960. Gaines [7] has found some of the applications of LB films and reviewed the work of monolayer properties in 1966. Fukuda et al [8] and Lauda et al [8] have successively deposited highly ordered monolayers on solid supports with a view to explore possibilities of their applications in molecular electronics.

Malcom et al [9] and Daniel et al [9] have carried out a number of investigations pertaining to contact angles and the energy transfer ratio of molecules that form LB films. Physical characteristics of Langmuir-Blodgett monolayers have been examined by respective measurements of pressure, surface potential and viscosity as a function of area per molecule.

Half a century after the pioneering work by Langmuir - Blodgett (LB), in the science and technology of LB films has been regenerated [10]. The field of LB films has received a major research thrust with the recognition that such multilayers being ordered at the molecular level, can have applications in molecular electronics and opto - electronics [11]. The LB technique is an elegant means of depositing organic multilayers onto solid substrates. Most classic materials, which are used for LB film deposition are cylindrically shaped surface active molecules possessing both hydrophilic and hydrophobic chemical groups (e.g fatty acids and fatty acid salts).

In the past about few years, there have been a number of reports of non-polar macromolecules being deposited by the method. Examples include fullerenes (C_{60}), metallophthalocyanines, macrocyanine dyes, conducting polymers such as poly (methoxy aniline), polyaniline etc. [12]. Aiming towards the application of conducting LB films, generally a lipophilic fatty acid tail is attached to the monolayer to facilitate the deposition of an oriented layer. These monolayers are polymerized by suitable methods such as UV-vis radiation or electrochemical techniques, respectively. Polyalkyl thiophenes, octadecyl pyrrole and a variety of alkyl substituted thiophenes have been used for fabrication of conducting LB films [13]. Besides this, LB films have been obtained from mixed monolayers comprising of cadmium stearate and a given conjugated polymer. The resultant mixed monolayers are then transferred as Y-type LB films and when desired

can be rendered electrically conductive by a suitable doping technique such as solution dipping or electrochemical supramolecular structure of LB films.

Langmuir-Blodgett films can be characterized by a number of available techniques. In this context, ellipsometry, UV -visible, interferometery, low angle X - ray diffraction, etc. are used to measure the thickness and uniformity of freshly prepared LB films. Contact angles with different liquids (ie water or glycerol) are measured to evaluate wetting properties, surface free energy and uniformity. Fourier transform infrared (FTIR) spectroscopy in both grazing angle and attenuated - total - reflection (ATR) modes, have been used to learn about the direction of transition dipoles and to evaluate dichroic ratios, molecular orientation, packing and coverage of LB films [13]. Raman spectroscopy is used as a tool for the quantitative analysis of molecular orientation which contributes to the understanding of ordered processes, order - disorder transition and organic films. Neutron diffraction is used to study the monolayers of molecules containing bulky groups in an alkyl chain. Neutron diffraction studies of partially deuterated chains are studied to provide additional structural information that together with electron and X-ray diffraction can be helpful for understanding the contribution of different parts to the overall packing and orientation scheme [14].

Langmuir - Blodgett films of cadmium stearate have been deposited on electrochemically prepared conducting polypyrole films [15]. UV - visible and scanning electron micrographs have been used to study the uniformity and the surface morphology of the of these film. Besides this, LB films of polyaniline have been fabricated on desired substrates and characterized by UV-visible, FTIR, SEM and cyclic voltammetry techniques, respectively. Cadmium stearate LB films have been used for the fabrication of metal - insulator - semiconductor devices.

6.2 PREPARATION AND CHARACTERIZATIONOF SOME LANGMUIR - BLODGETT (LB) FILMS

6.2.1 CADMIUM STEARATE LB FILMS

Stearic acid (procured from Merck) (10 - 20 μg) is dissolved in chloroform and is dropped on the surface of water (pH 5.6) contained in a Joyce Loebl trough (model 4). The pressure - area isotherm has been recorded at a barrier speed of 0.3 mm/ min. The cadmium stearate monolayers are formed at air -water interface in this trough at a surface pressure of 25 mN/m. Polypyrrole films deposited on ITO glass are inserted / withdrawn at a rate of 1 mm/min in the LB trough resulting in the deposition of the CdSt$_2$ mono/multilayers onto the substrates. UV-visible spectra of such cadmium stearate monolayers have been recorded on the Shimadzu (model 160 A) spectrophotometer. The surface morphology of such cadmium stearate LB films has been investigated using Joel 35 CF scanning electron microscope.

A number of distinct regions are immediately apparent on examining the pressure - area isotherm curve. The compressibility in the solid phase transition is found to be the same as reported in literature. The value of 22 A$^{\circ 2}$ at 25 mN/m of cadmium stearate per molecule is close to that occupied by stearic acid molecules in single crystals, thus confirming the interpretation of a compact film as a two dimensional solid. Fig.1 shows the results of UV - visible studies carried out in reflection mode on various monolayers of cadmium stearate deposited on the annealed (70° C) polypyrrole films. The magnitude of absorption increases with increase in the number of monolayers indicating uniform nature of these cadmium stearate LB films on polypyrrole surface.
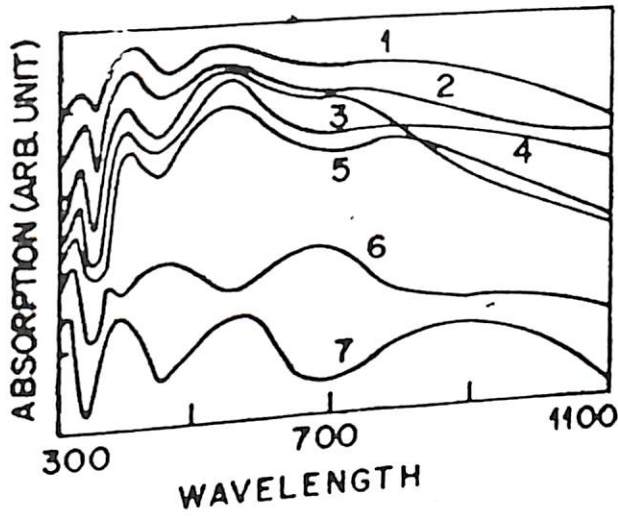
Fig. 1 UV-visible spectra recorded as a function of wavelength (nm) for various monolayers of cadmium stearate on polypyrrole surface of 30 layers (curve 1), 20 layers (curve 2), 15 layers (curve 3), 10 layers (curve 4), 8 layers (curve 5)), 6 layers (curve 6), 4 layers (curve 7)

SEM pictures (fig. 2 a & b) of cadmium stearate LB films (9 and 20 monolayers) deposited on annealed polypyrrole films indicate the absence of any pinholes. SEM pictures obtained for 9 and 20 monolayers demonstrate that CdSt$_2$ layers are uniform on the polypyrrole surface and hence can be used the for fabrication of a desired solid state device.
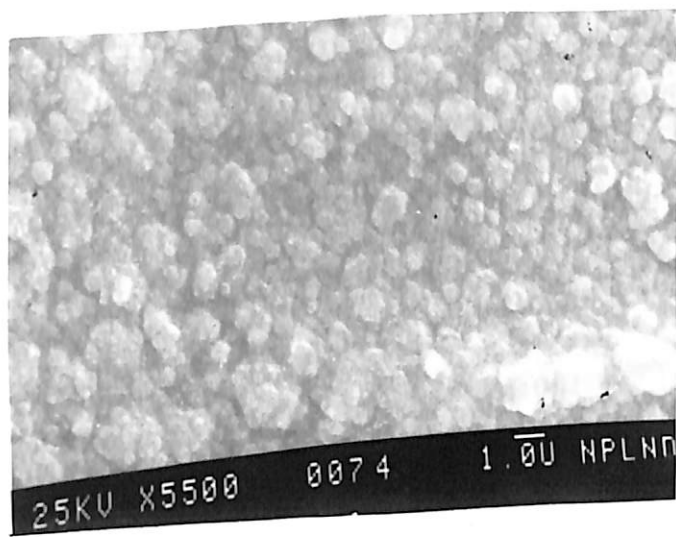

Fig.2(a)

Fig.2(b)

Fig.2 SEM pictures recorded for (a) 9 and (b) 20 monolayers of Cd stearate on polypyrrole surface.

6.2.2 POLYANILINE LB FILMS

The LB films of polyaniline have been earlier fabricated by Agbor et al [16] and Rosner et al [16] with known amount of polyaniline in N- methyl pyrrolidinone (NMP) /CHCl₃ and acetic acid solution. An attempt has been made to fabricate polyaniline LB film without using acetic acid and characterized with a view for their application in molecular electronics.

Polyaniline used for the preparation of LB film is in the deprotonated form (emeraldine base). The emeraldine base powder is chemically synthesized as discussed in Sec 4.2.1 of the fourth Chapter. The emeraldine base powder, is washed with water and acetone before its use for the preparation of an LB film. Emeraldine base is dissolved by varying the percentage (30%, 40%, 50%, 60%, 80% and 100%) of CHCl₃ in N- methyl pyrrolidinone. The solution is shaken thoroughly before filtration. The Joyce Loebl LB trough has been used for the LB film deposition.

The pressure - area isotherms of polyaniline in various mixture of CHCl₃ and NMP have been obtained at the barrier compression speed of 0.5 mm/min during the desired temperature range (9.2°C to 40°C). The LB films of polyaniline have been

225

deposited at a surface tension of 25 mN/m and the barrier speed of 0.5 mm/min [17]. The deionized water from Millipore (model RTS - 10) water purification system of is used for filling the Langmuir trough and the pH of water is maintained at 7. The speed of the dipping head is maintained at 3 mm/min and the temperature of the subphase is kept at 22°C by circulating the water in trough using a refrigerated recirculator (Bio Rad model No. E 4870).

LB films have been deposited on glass plates, quartz plates and indium-tin-oxide (ITO) glass plates and silver coated glass plates, respectively. The area displaced from the trough is recorded from time to time for obtaining the plot of area displaced from the trough vs the number of strokes. The different monolayers of polyaniline are coated on the various substrates that are annealed for 10, 20, 50, 72 and 90 hours, respectively for the desired structural and optical studies. The LB film of polyemeraldine base are doped in 1M H_2SO_4, 1M HCl, 1M HNO_3, 1M HF and 1M $HClO_4$, respectively to make these electrically conducting. The Y- type LB films of polyaniline have been deposited on the above substrates. The UV -visible and FTIR spectroscopic measurements have been carried out using Shimazdu (model 160 A) UV - visible spectrophotometer and Nicolet FTIR spectrophotometer (model 510 P), respectively. Cyclic voltammograms have been recorded by Schlumberger Electrochemical Interface (Model SI 1286).

(i) PRESSURE - AREA ISOTHERMS

Fig. 3 shows the pressure - area (π - A) isotherm at 22° C of polyaniline film when emeraldine base is dissolved in chloroform ($CHCl_3$). It shows two distinct liquid phases indicated in fig.3 as L_1 and L_2, respectively. It may be mentioned that both these liquid phases (L_1 and L_2) also referred to expanded phases are more pronounced at the

molecular area of $10\mathring{A}^2$ and $8\mathring{A}^2$, respectively. The solid phase transition occurs at about the molecular area of $6.5 \mathring{A}^2$. From this curve, it can be seen that phase compressibility of both these phases lies between 0.004 to 0.016 and the solid phase compressibility lies between about 0.0005 to 0.001.

Fig.4 shows the pressure - area isotherm obtained at 22°C of polyaniline dissolved in a mixture of NMP and $CHCl_3$. The liquid gas (LG) condensation begins at about the molecular area of $36 \mathring{A}^2$. From fig. 4, it can be seen that there is only one liquid phase (L_2). The solid phase condensation of polyaniline molecules can be seen at a surface pressure of 25mN/m and molecular area of $16 \mathring{A}^2$.
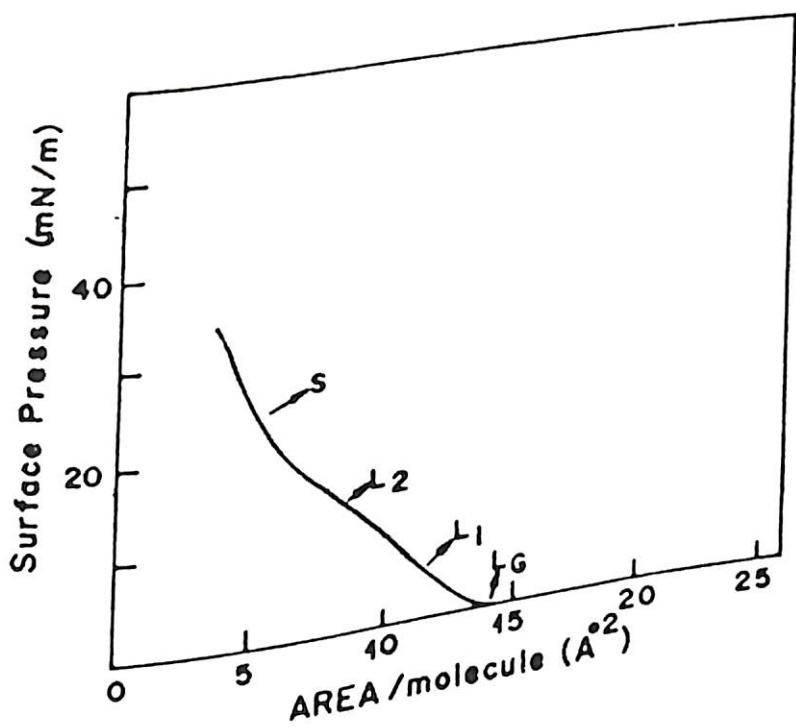

Fig.3 Pressure - area isotherm for polyemeraldine base with polyaniline dissolved in $CHCl_3$
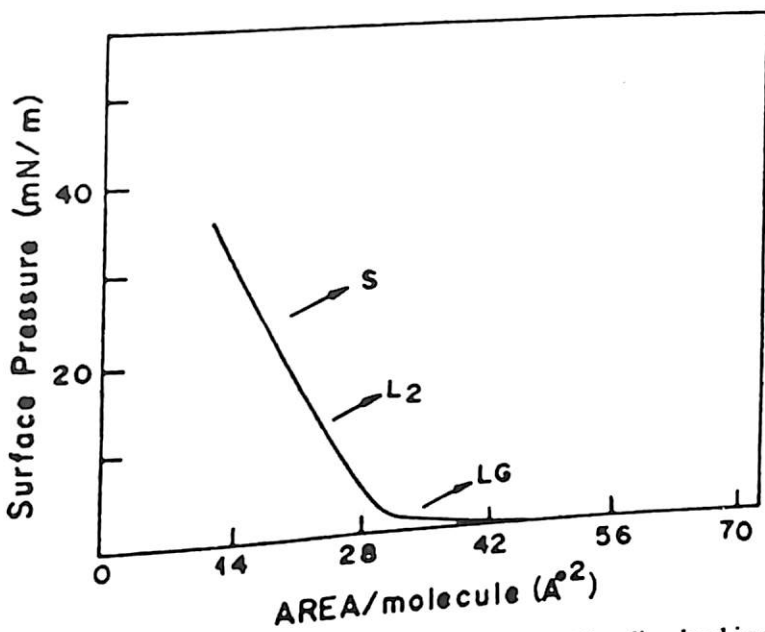
Fig.4 Pressure area isotherm of polyemeraldine base with polyaniline dissolved in a mixture of NMP+CHCl$_3$ (60% CHCl$_3$).

Fig.5 has been obtained by plotting the molecular area of the solid phase at a pressure of 25 mN/m as a function of polyaniline dissolved in NMP + (60%) CHCl$_3$ solution. It has been seen that the molecular area at solid phase is 16 Å when CHCl$_3$ is 60% in the NMP + CHCl$_3$ solution. It has been calculated that minimum area of aniline repeating unit is 18 Å, which is in close proximity with the molecular area of 16Å for 60% CHCl$_3$ in the NMP + CHCl$_3$ solution. Polyaniline has two liquid phases L$_1$ and L$_2$ when it is dissolved in CHCl$_3$. It can be seen that the area occupied by the molecule is only 6.5 A^2 in comparison to the value of 18 Å for the aniline repeating molecule. The value of molecular area estimated as 23 -26 A^{o2} for the substituted aniline suggests that monolayers are stable at air - water interface for the mixture of CHCl$_3$ + NMP containing 60 % CHCl$_3$ in the solution.

Fig.5 is the pressure area (π-A) isotherm of polyaniline, covering a wide range of temperatures from 9.2 to 40°C when polyaniline is dissolved in a mixture of NMP + CHCl$_3$, containing 60% CHCl$_3$ in the solution. It can be seen that liquid gas (LG) phase is obtained upto the molecular area of 27 Å to 35 Å. The solid phase condensation area also changes from 15.91 to 17.0Å from 9.2°C to 40°C. The observed temperature varia-

228

tion of molecular area is similar to that obtained for pressure - area isotherm which shows the stability of the monolayers on the surface of water. It is interesting to observe that there is dispersion in the pressure - area isotherm with a wide range of temperature (9.2°C to 40°C). The stability of monolayers on the subphase with the rise in temperature indicates that polyemeraldine base LB films can be deposited at the elevated temperature.
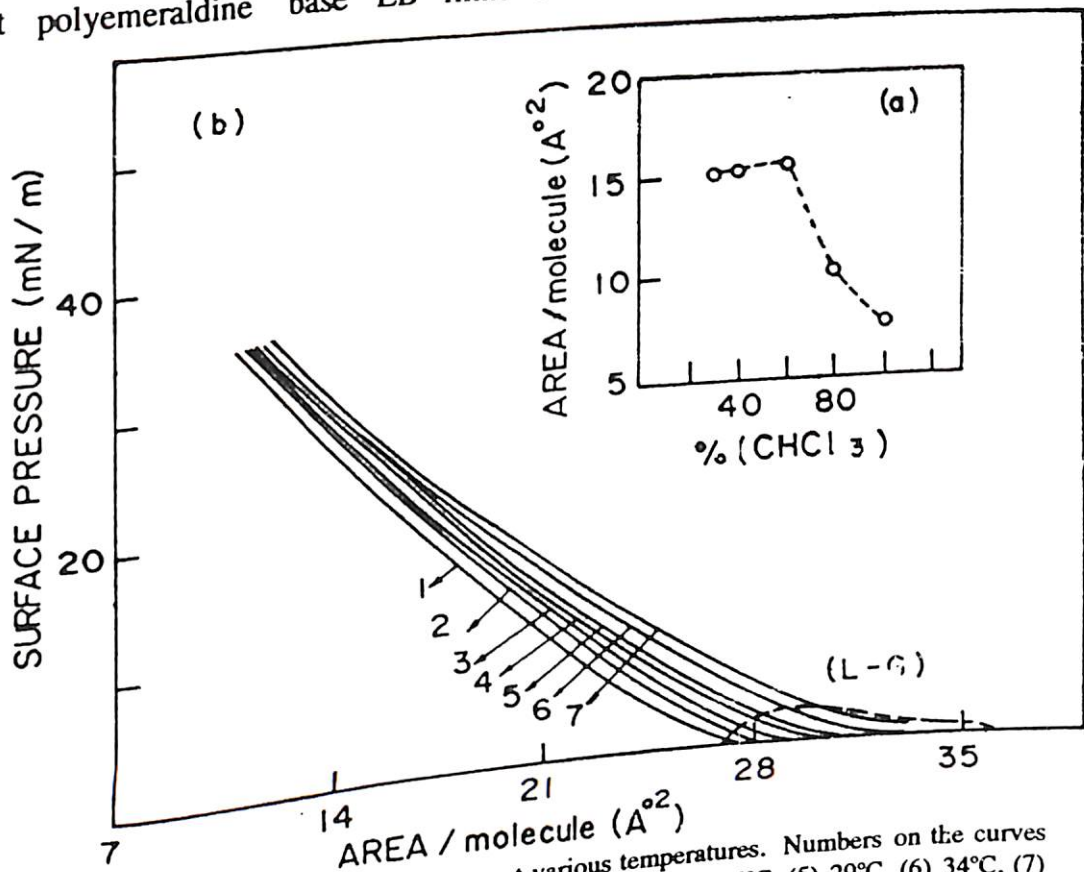

Fig.5 Pressure - area isotherm for polyemeraldine base at various temperatures. Numbers on the curves indicate the various temperatures, (1) 9.2°C, (c) 15°C, (3) 22°C, (4) 26°C, (5) 29°C, (6) 34°C, (7) 40°C
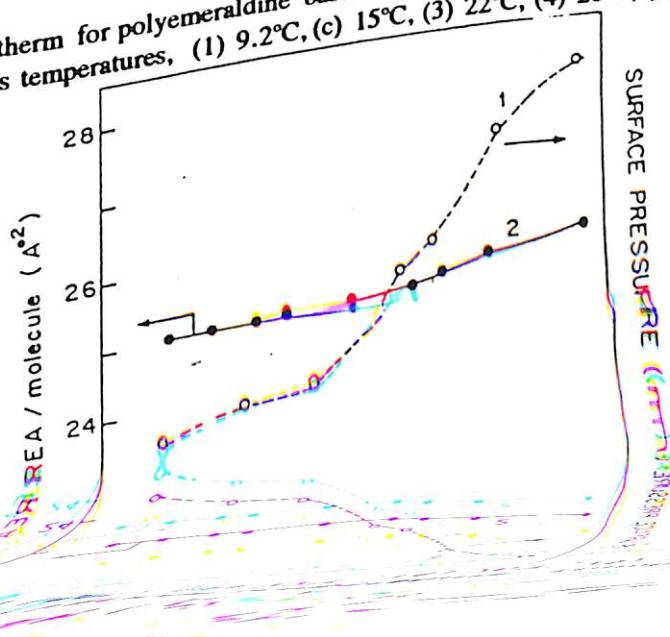
Fig.6 (curve 1) shows the variation of surface pressure of the solid phase obtained as a function of temperature. As the temperature increases from 9.2 to 40°C the surface pressure increases from 28.2 to 27.5 mN/m. Curve 2 in fig.6 is the observed variation of molecular area at solid phase at a pressure of 25mN/m as a function of temperature (9.2 to 40°C). It can be seen that there is not much change in the molecular area at solid phase with rise in temperature of the subphase.

Fig. 7 shows the number of strokes per cm² area displaced from the trough after the LB film is deposited on the quartz substrate. It can be seen that up to 20 numbers of monolayers, the equal area has been displaced from the trough. It can be seen that after twenty strokes, the mode of deposition changes from Y to X type. This type of transition has earlier been obtained in fatty acid molecules [18].
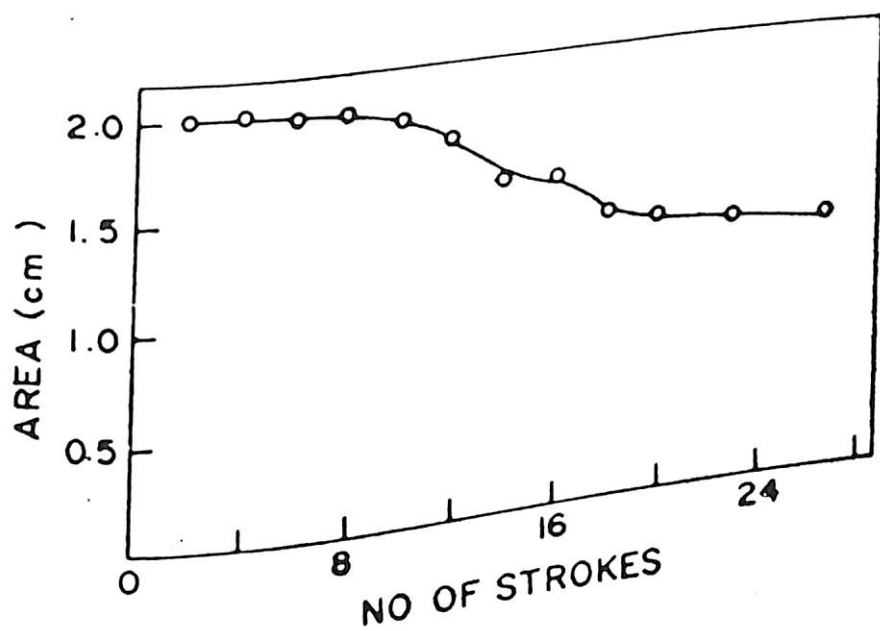

Fig.7 Area displaced from the LB trough as a function of number of deposition strokes. Area of the ITO glass substrate used for deposition of LB films is 2 cm².

(ii) UV - VISIBLE STUDIES

UV-visible spectroscopy has been performed on a number of polyaniline LB films. Fig.8 shows two absorption peaks at about 390 nm (3.35 eV) and 610 nm (2.041 eV). The

230

absorption peak observed at 390 nm can be understood to arise from $\pi - \pi^*$ bond and

the peak at 610 nm arises due to a $n-\pi^*$ transition centered on the benzoid the ring [19,20].

These results bring out that the magnitude of absorption increases uniformly with the

increase of number of monolayers indicating that the deposition of LB films of PEB base
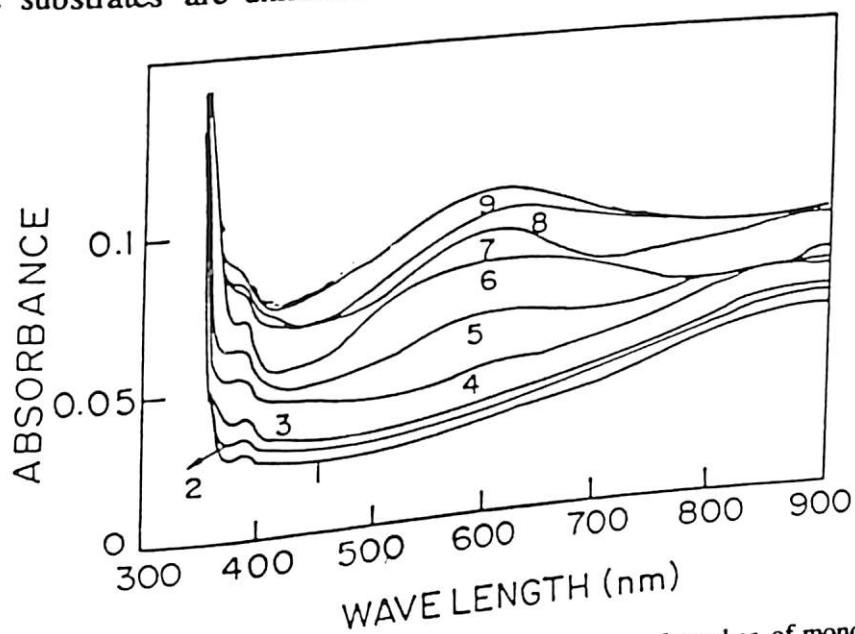
on quartz substrates are uniform.

Fig.8 UV-visible absorption of polyaniline LB films as a function of number of monolayers. Curves 1 to 10 are respectively for 2, 4, 6, 8, 10, 14, 16 and 20 monolayers
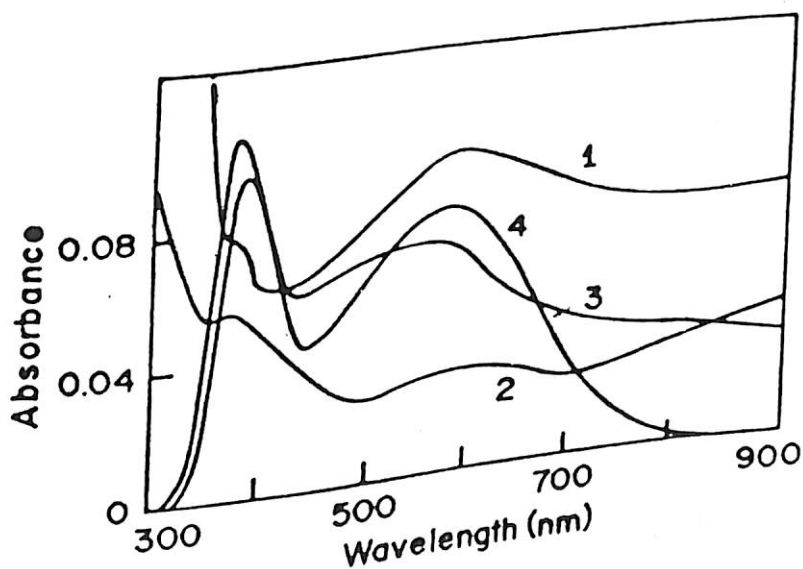

Fig.9   UV - visible spectrum of freshly prepared 20 monolayers of PEB. Curve 1 shows the spectra of PEB LB films and Curves 2,3 and 4 are obtained as a consequence of annealing (50°C) of LB films for 10, 24, and 48 hours, respectively.

231

The deposition of successive layers of polyemeraldine base are monitored by the change in the value of optical absorption at 360 nm as shown in Fig. 10. The near linear variation in the initial stage is an indication of the deposition of ordered layers while the non-linear response with multilayers is indicative of irregular deposition.
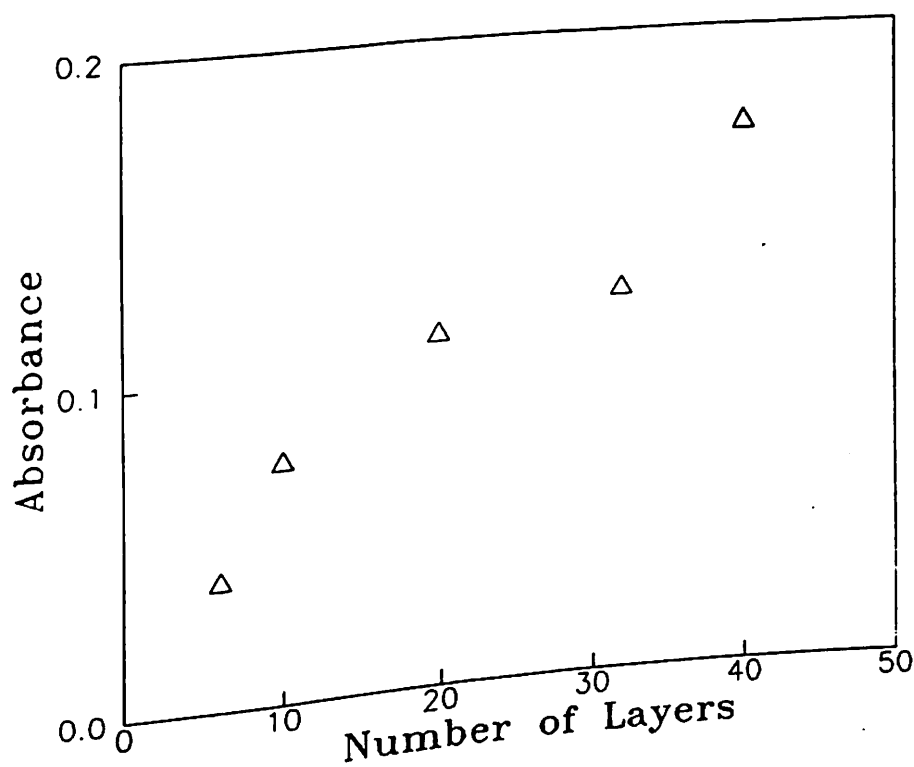

Fig. 10 Plot of absorbance at 360 nm for the polyaniline LB films as a function of the number of layers deposited.

The effect of different dopants on PEB has been investigated through UV - visible spectroscopic studies. Fig. 11 shows the UV - visible absorption spectrum of 20

monolayers of LB films obtained as a function of different protonic acids such as 1M H₂SO₄, (curve 1), 1M HNO₃ (curve 2) and 1M HCl₄ (curve 3), respectively. The absorption peaks for each of the dopants occurs at about 400 nm. However, in case of HCl doped PEB LB films, 550 nm peak is also obtained. The peaks at 850 - 900 nm (1.2-1.3eV) attributed to the metallic absorption, are obtained with each protonic acids. The lowest band at 550 nm (2.02 eV) can be understood to arise from the presence of bipolarons formed as a result of doping [19, 21].

Fig. 12 shows the UV-visible absorption obtained as a function of monolayers of polyaniline HCl doped films. The intensities of the absorption bands seen at 400, 530 and 850 nm have been found to be increasing uniformly with the increase in the number of monolayers. It shows that the orderliness in of polyaniline LB films is maintained even after it is doped with 1M HCl [22].
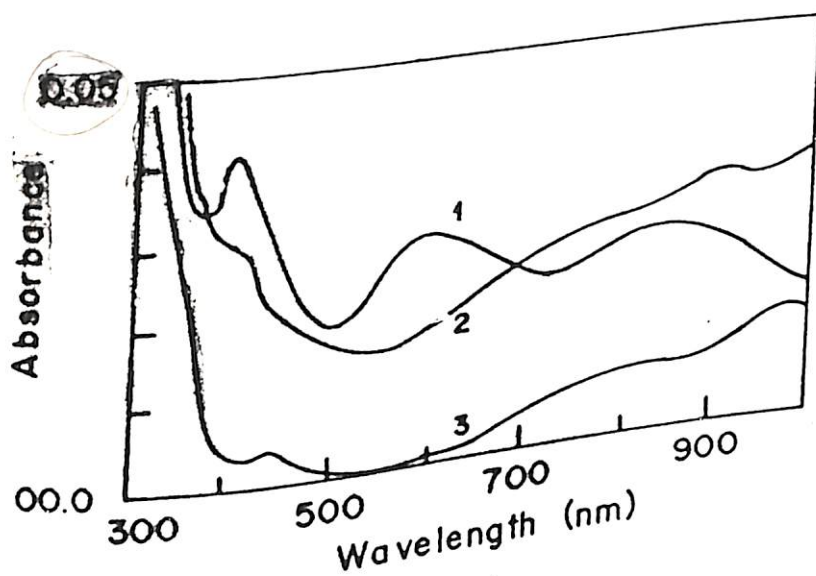

Fig. 11 UV - visible absorption spectrum of 20 monolayers of LB films obtained as a function of different protonic acid such as 1M H₂SO₄ (curve 1), 1M HNO₃ (curve 2) and 1M HCl₄ (curve 3)
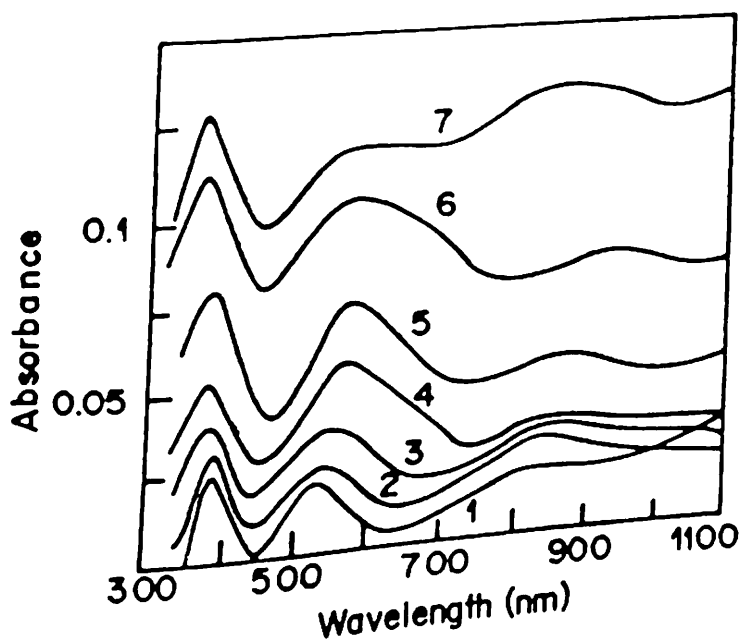
233

Fig.12   UV - visible absorption spectra of HCl doped LB films as a function of number of layers of PEB Curve 1 to 7 are respectively for 4, 8, 16 , 20 ,28,32, and 41 monolayers.
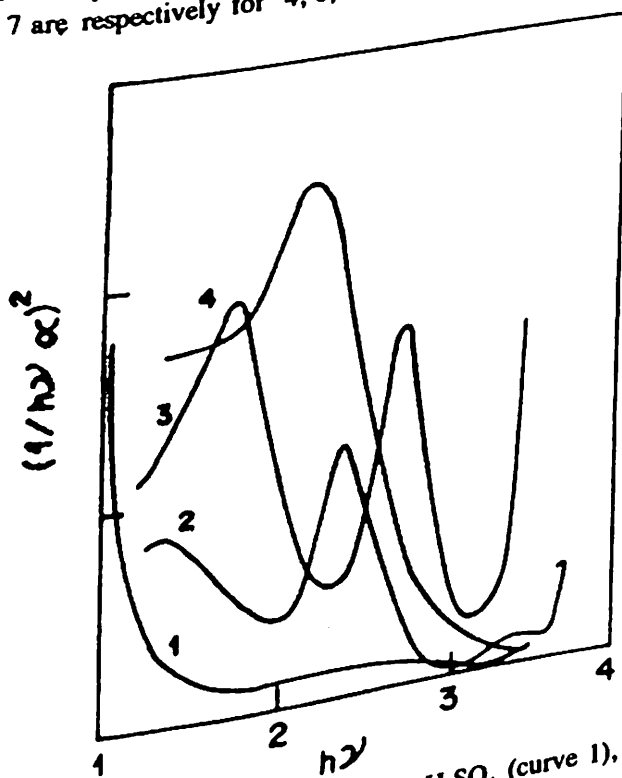

Fig.13 Plot of $(1/\alpha h\nu)^2$ vs hν (photon energy) for 1M H_2SO_4 (curve 1), 1M HCl (curve 2) and 1M $HClO_4$ (curve 3) and HCl doped PEB LB films (curve 4).

An attempt has been made for the calculation of band gap of polyaniline LB films using the one dimensional extrapolated curve obtained by plotting $(1/\alpha h\nu)^2$ vs $h\nu$ (photon energy. Fig.13 shows such plots observed for 1M H_2SO_4 (curve 1), 1M HCl (curve 2), and 1M $HClO_4$ (curve 3) doped PEB LB films. The values of band gap for polyaniline LB films after being doped with different acids such as 1M H_2SO_4, 1M HCl and 1M $HClO_4$ have been obtained to be 3.0, 3.2, and 3.25 eV, respectively. Interestingly, the band gap of polyemeraldine LB films (curve 4 in fig.13) has been calculated to be 4.0 eV. These values of band gaps are in reasonable agreement with those obtained for the electrochemically prepared, solution cast and vacuum deposited polyaniline films, respectively [22].

(iii) FTIR STUDIES

Fig.14 shows the FTIR spectra of freshly deposited LB films of PEB obtained as a function of number of monolayers. FTIR spectra of monolayers of LB films of PEB contains absorption peaks at 1780, 1715, 1590, 1468, 1270, 925, 800, 700, 604, 530 and 516 cm^{-1}, respectively. The peak at 1715cm^{-1} arises due to C=C vibration of quinoid benzoid rings. The peak seen around 1270cm^{-1} has been attributed to the combination of C-N linkage. There is an additional peak at 1032 cm^{-1} that may arise from a C=N bond. The peak found at 925cm^{-1} can be attributed to the 1-4 linkage of benzene ring. The various peaks found at 925, 703, 530 and 516 cm^{-1} have been assigned to various stretching and bending modes associated with C-1 linkage with benzene ring [23]. The intensities of the various peaks seen in the various FTIR spectra have been found to be decreasing with the increase in the number of monolayers.
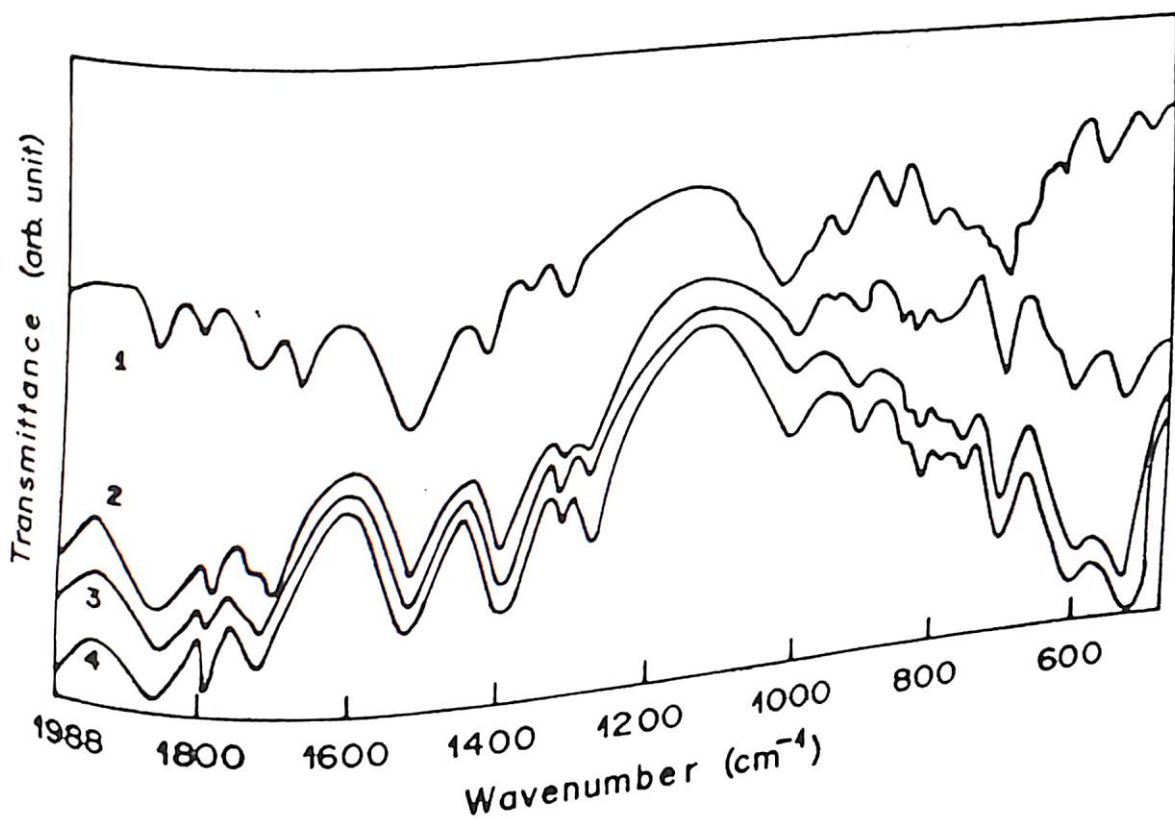
Fig.14 FTIR spectra of PEB LB films of varying thickness. Curves 1 to 4 are respectively for 20, 24, 32 and 40 monolayers.

Fig.15 shows the FTIR spectra of 20 monolayers of undoped and HCl doped polyaniline films. The various peaks seen (fig.14) for the undoped polyaniline LB films are clearly visible in fig.15. The peaks such at 703, 530, 450 cm^{-1} have been assigned to the various stretching and bending modes associated with the C-1 linkage. The additional peak at 1325 cm^{-1} (curve 2, fig.15) is due to the additional HCl in polyaniline.

236

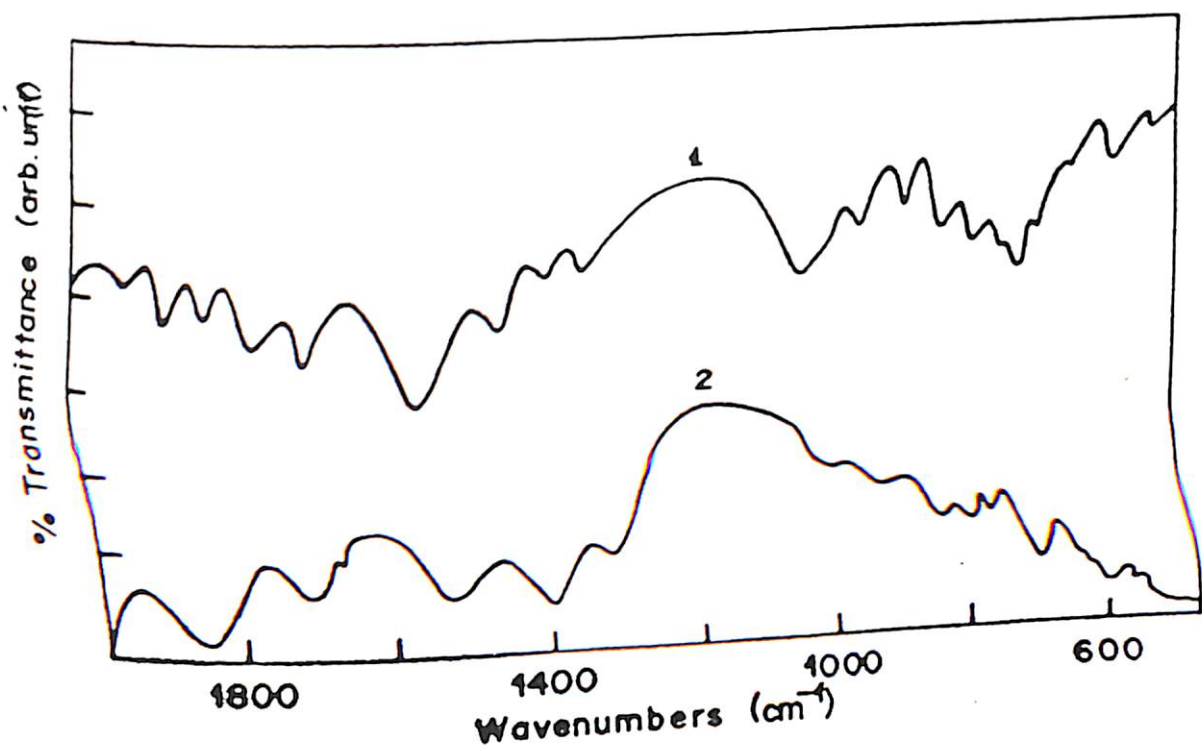Fig.15 FTIR spectra of 20 monolayers of PEB LB films (curve 1) and HCl doped LB films (curve 2)

(iv) SEM STUDIES

An attempt has been made to carry out the structural studies of LB films of PEI using scanning microscope. Fig. 16 a, b, c, d and e are the SEM pictures obtained both for freshly prepared and annealed (50°C) LB films of PEB for various durations of time (24, 48, 72 and 90 hours). Fig. 16 clearly shows the uniform structure with formation o a small distribution of pore sizes on the surface of the PEB LB films. In fig. 16b, one can see that the surface of PEB film has become smoother without the increase of pore size. It can also be noticed that the uniform structure of PEB LB films has been obtained (fig. 16C) due to annealing for 48 hours. Further, a consequence of prolonged heating (72 and 90 hours), the ordered structure of PEB LB film collapses (Fig. 16d and 16e) resulting in the formation of new pores (0.5 μm). These studies have clearly revealed that extended (48 hours) heating results in the collapse of uniform structure in LB films.

237

25KV X10000 1783 1.0U NPI Nn

25KV X10000 1779 1.0U NPI Nn

25KV X10000 1784 1.0U NPI Nn
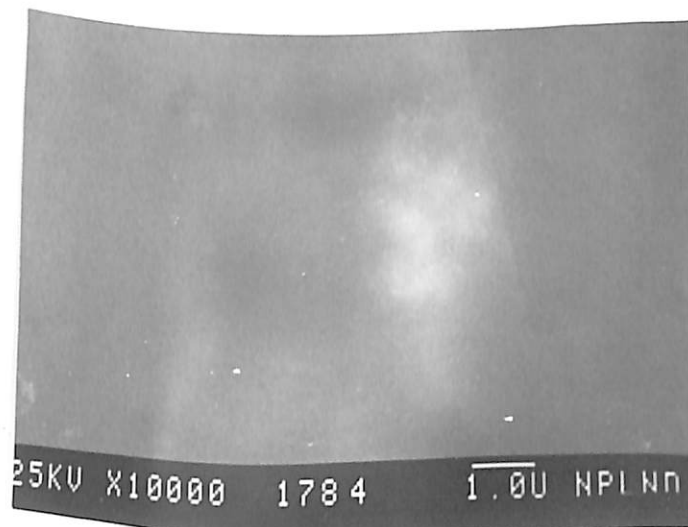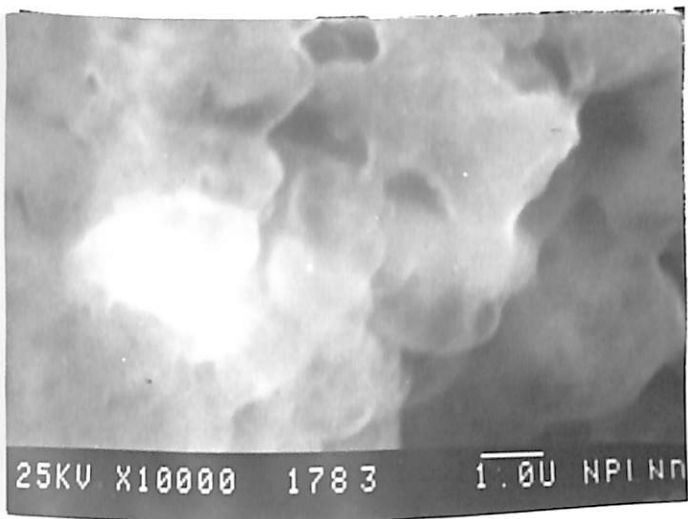
25KV X10000 1782 1.0U NPI Nn

Fig. 17 shows the scanning electron micrograph of 20 monolayers polyaniline LB films treated with 1M protonic acid. When the LB films are doped with 1M HCl there is a slight deviation from the uniformity of the film indicating segregation at some stage resulting in the formation of pores (0.05 μm). It is interesting to observe that when it is doped with slightly bigger anion such as HSO_4^- (fig. 17b) the uniformity of the films gets destroyed resulting in larger pores (1 μm). Further, doping effect can be observed with ClO_4^- doping (fig. 17c). The pores of (1 μm) can be seen to be developed throughout the LB films of polyaniline. These results indicate that the bigger size of the anions create inhomogenities in the PEB LB films. The uniform doping has only been observed in the 1M HCl (protonic acid) doped polyaniline films.

Fig. 17(a)

Fig. 17(b)

238

Fig.17(c)

Fig.17 Scanning electron micrograph of polyaniline LB films of 20 monolayers treated with (a) 1M HCl, (b) 1M H$_2$SO$_4$, (c) 1M HClO$_4$.

6.3.6 CYCLIC VOLTAMMETRY

The electrochemical studies of PEB LB films have been investigated using cyclic voltammetry (CV) studies. The cyclic voltammetry studies on various PEB LB films (6, 20, 38 and layers) have been performed containing 1M hydrochloric acid medium using the platinum as a reference electrode. The voltage scan rate has been made at 100mV/sec cycling -0.5 to 0.8 V.

The deposition of ordered monomolecular layers of conducting polymers by the Langmuir Blodgett (LB) technique is an important goal in this connection. Conventionally, a lipophilic fatty acid tail is attached to the monomer to facilitate the deposition of an oriented layer and subsequently, the monomer is polymerized by suitable means or the preformed polymer (e.g. polyalkylthiophene) mixed with stearic acid is dissolved in a suitable solvent and is deposited [11,24]. The former however, usually requires a difficult chemical manipulation and in addition, the polymeric films thus produced tend to crack.

Recently, in an attempt to obviate the above difficulties, Agbor et al [25] have reported the deposition of preformed polyemeraldine base (PEB) by the LB technique. In their method, polyaniline dissolved in N-methyl pyrrolidinone (NMP)/CHCL$_3$ can be

239

cast as a film with an aqueous subphase containing acetic acid. However, it has been found that an LB film can be deposited without acetic acid and can be subsequently doped.

Multi-layer films with varying number of layers have been deposited in an attempt to study the changes in surface upon going from monolayers to multilayers and to compare the results with a theoretical studies which predict the development of an irregular surface after a certain number of layers. Additionally, the deposited films have been examined using cyclic voltammetry in an acid medium in order to assess the effect on the redox characteristics of changes in surface morphology in going from thin films to thick multilayers. Indeed, visually smooth films have been deposited as expected from the nature of the pressure-area isotherm. It is employed to effect Y type deposition with a drying time of 4 minutes between successive dips. The linear variation in the initial stage is an indication of the deposition of ordered layers while the nonlinear response with multilayers is indicative of irregular deposition [25].

The electrochemistry of the LB films prepared as above has been investigated using cyclic voltammetry. The cyclic voltammogram (CV) of an LB film of PEB containing 6 monolayers in 1M hydrochloric acid medium is shown in Figure 18. The peak currents scale linearly with sweep rate indicating surface confined species, though the peaks are broader than expected for such a situation. In the same figure is shown the CV of an LB film of PEB of 38 layers which exhibits only a broad hump from -0.5V to about 0.8V. In an attempt to understand this behaviour, the CV of different films containing varying number of layers has been recorded and the half peak width ($E_{p/2}$) is plotted as a function of the number of layers as shown in Figure 19. It is seen that the change is gradual as we go from 6 layers to 38 layers indicating the slowing down of the

240

electron transfer as we go to multilayer films. The use of half peak width for evaluating charge transfer is well established. Slow electron transfer has often been seen with electroactive species immobilized on electrodes.

In an attempt to explain the results obtained with the LB films in the frame work of these earlier studies the redox behaviour of polyaniline deposited electrochemically has been well studied previously including such aspects as its dependence on the pH of the bathing solution and its relation to the method of preparation whether by pulsed or by potentiodynamic and potentiostatic methods [26,27]. The effect of the acid used in the synthesis has also been investigated. These studies suggest that better quality films exhibiting good CV response are obtained for pulsed and potentiodynamic methods of preparation probably due to a growth activation during the earlier stages of film formation leading to well ordered films. It is important to note that though good CV response has been observed for fairly thick films (1 μm), much broader CV peaks have also been observed for films of comparable thickness underlining the notion that the redox kinetics is probably controlled by the degree of order in the film rather than ohmic effects due to thickness. Though, it may seem anomalous that electrochemically prepared films thicker than the multilayer LB film described here should show good CV response, it is emphasized that such a situation is seen only with those electrochemical films which are regular. The key factor that determines CV response is surface regularity. This effect of order and surface regularity on redox behaviour is well illustrated by the CV of electrochemically prepared polyaniline films deposited by two different electrochemical techniques e.g controlled potential (CP) and potential pulse shown in Figure 18(a & b). In the CV of the CP deposited film the first pair of redox peaks of polyaniline is seen only as a broad rise while the second couple exhibits broader peaks, though both the

241

films have similar thickness as estimated from their optical transmittance. It might be mentioned that the peak broadening observed with the multilayer LB film of polyaniline (e.g. 38 layers) is reminiscent of the behaviour of redox polymer modified electrodes[29] where slowness of electron transfer between the metal electrode and one of the layers leads to a large E_p value.
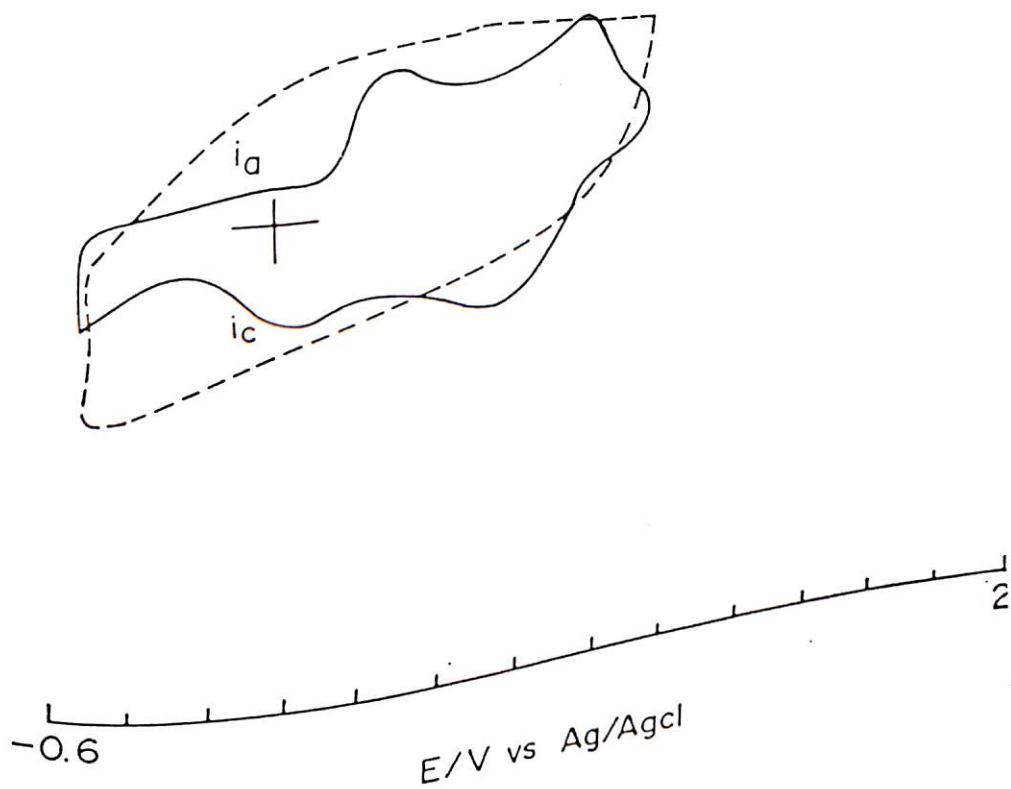

Fig. 18 Cyclic voltammogram of LB films of polyemeraldine on ITO in hydrochloric acid (1M) medium: six - layers LB films (—), and 38 layers LB film (...).
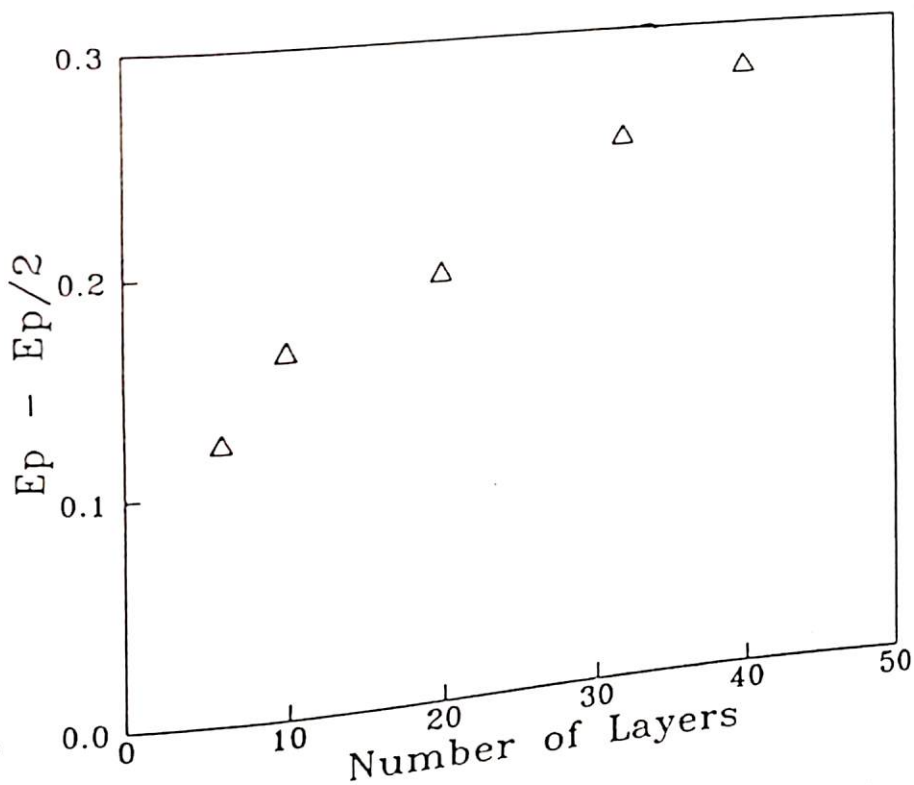
Fig. 19 Plot of $E_p - E_{p/2}$ verses the number of layers. A voltage ramp of 100 mV/s has been employed

Chronopotentiometric studies of polyaniline indicating that the rate of oxidation of the leucoemeraldine is kinetically limited support of conclusion for slowness of electron transfer in multilayer films [29]. Anisotropy in conductivity is ruled out as being a probable cause, since it has been shown in polypyrrole LB films that solution doping yields much less anisotropy in conductivity. A recent theoretical treatment has been discussed for the effect of domain size in altering the kinetics and the shape of cyclic voltammograms [12]. Changes in domain size can be brought about by a number of factors including molecular disarray during LB film deposition. Thus, it may be expected that the inhomogeneous 38 layer film to display poor kinetics leading to the broad hump in the CV. This result has important implication for the performance of eletroactive devices fabricated using polyaniline LB films.

243

6.3 APPLICATIONS OF SOME LANGMUIR-BLODGETT FILMS

Langmuir- Blodgett films have been projected to have a large number of applications in the field of microelectronics and biosensors including insulation, adhesion and encapsulation [30,31]. The Langmuir - Blodgett films of various fatty acids such as stearic acid, arachidic acid and w-tricosenoic acid etc. show good insulating behaviour and dielectric loss. These attractive properties of LB layers suggest that these may find application as a dielectric layer in metal - insulator - semiconductor (MIS) and metal - insulator - metal (MIM) devices, respectively [32]. The next section describes the application of polyemeraldine base LB film as an insulator in MIM and MIS devices, respectively.

6.3.1 METAL - INSULATOR - METAL (MIM) DEVICES BASED ON POLYEMERALDINE (PEB) LB FILMS

The continued minituarization of microelectronic elements based on inorganic semiconductors has resulted in a large number of displays. However, the feature size of these devices are based on large molecules [33,34]. Question of the ultimate size has stimulated discussions on the use and possible advantages of organic materials in devices where dimensions would be that of single molecule. A driving force in molecular electronics device (MED) research is the potential use of molecular properties rather than bulk material. For obtaining a molecular electronics device and also supramolecular structure, Langmuir - Blodgett technique is an elegant means of deposition of organic multilayers onto the various solid supports.

Many investigations pertaining to metal - LB layers - semiconductor and metal - insulator - metal have been conducted. Metal -insulator - metal (MIM) is a convenient insulator - metal have been conducted. Metal -insulator - metal (MIM) is a convenient

device for understanding the phenomenon of charge transport as well as the interfacial properties. MIM devices based on fatty acids as insulators have already been fabricated [35]. It has also been found that there are numerous studies on rectification in organic molecule and polymeric solids. In this regard various methods wherein PEB LB films sandwiched between metal such as silver, indium and indium-tin-oxide (ITO) with metal such as silver for base electrode have respectively been used. The band diagram for an MIM configuration has been shown in fig.20.
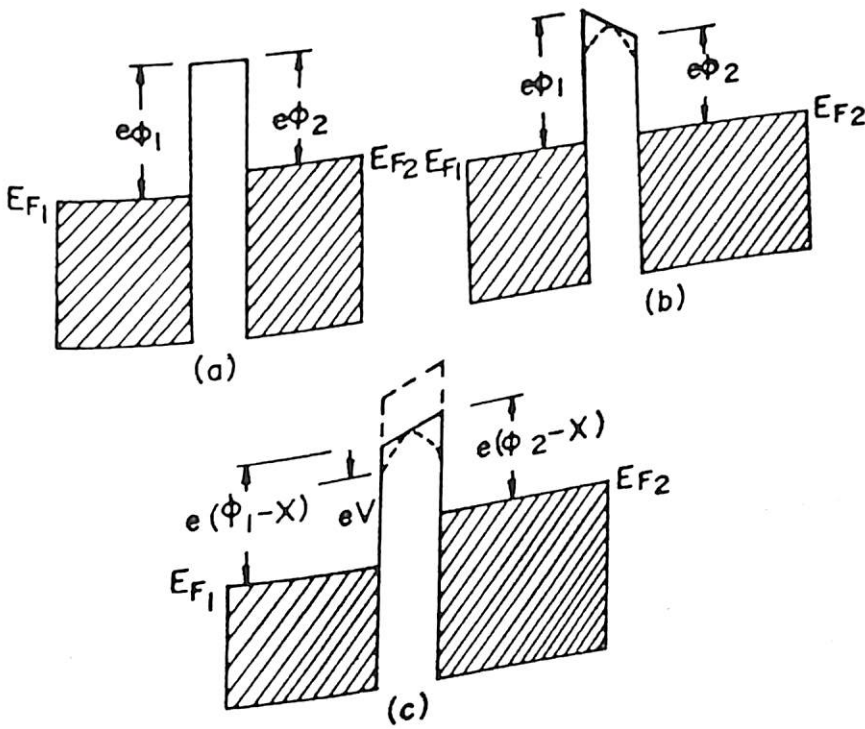

Fig.20 (a) MIM structure with vacuum level and different metal (b) MIM structure with insulator with different metal.(c) MIM structure with insulator with bias voltage V. Where Φ_1, Φ_2, F_{F1} and E_{F2} are work functions and Fermi energy levels and eX is the barrier height.

The transfer of an electron from the metal into the insulator requires less energy than its removal to the free space. The height of barrier is correspondingly reduced by the eX. If V is applied to the metals, there is a slight displacement of Fermi level by an amount eV and electrons tunnel from one metal to another (fig. 20C). The current density can be expressed as:

$$J = - (2\pi \, e/ \, h) \; T_{12}^{\;2} \; N_2(\Sigma) \qquad\qquad \text{Eq.1}$$

where T_{12} is transition matrix from 1 to 2 state, $N_2(\Sigma)$ is the carrier density of wave vector near Fermi level [36]. So the mechanism of charge conduction with respect to barrier can be investigated in metal - insulator - metal (MIM) device.

The PEB LB films comprising of 41 layers have been deposited on different vacuum deposited silver, indium-tin-oxide and glass plates, respectively. The effective electrode area of vacuum deposited metal (Ag) electrode onto PEB film is about 10^{-3} cm^2. Current(I) - voltage (V) and capacitance(C) - voltage(V) measurements have been conducted using a Keithley electrometer (model 617) and impedance analyzer (model HP 4192 A), respectively.

Initially, dc conductivity measurements have been made on the undoped polyaniline LB films. The in-plane conductivity of emeraldine base (EB) has been estimated to be about 5×10^{-8} S/cm at room temperatures using measured thickness of 8.0 Å [16]. This value is significantly higher than that of undoped polyaniline cast film and of polyaniline pellets suggesting some degree of protonation in molecular level attributed to its dissolution in chloroform. In contrast the dc conductivity of the doped LB film is calculated to be 0.15 S/cm at room temperature. The value is small compared to that obtained for the doped form of polyaniline in pellet or the solution cast film. Fig. 21 (inset) shows current(I) - voltage (V) characteristics of MIM device at the

voltage scan rate of 20 mV/sec for silver (Ag) /PEB LB layer/ silver (Ag) structure. It can be seen that the curve is both linear and symmetric indicating tunneling of electrons on application of voltage. It is known that silver makes ohmic contact with polyaniline. Fig. 21 shows the I-V characteristics obtained at 20 mV/sec for ITO/PEB LB layers/Ag (curve 1) and In/ PEB LB layers/Ag (curve 2) devices, respectively.
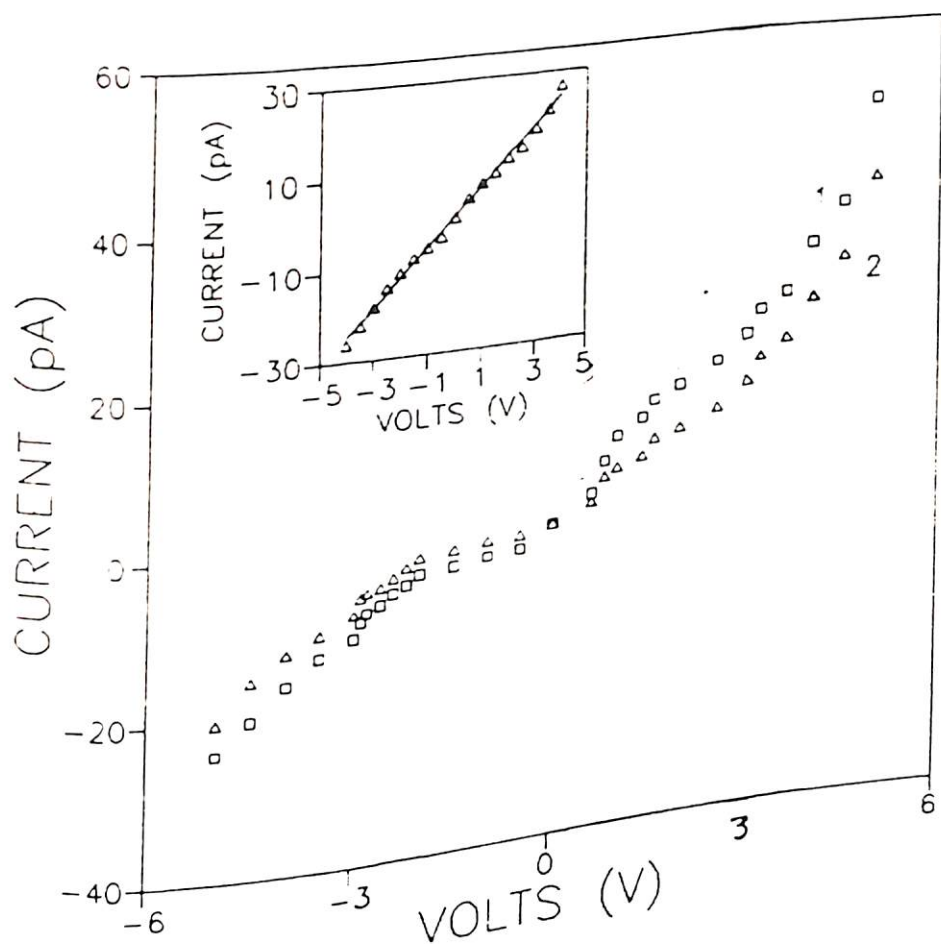

Fig.21 Inset shows current(I) vs voltage (V) characteristics for Ag/41 layers PEB LB films/Ag; (curve 1) In/ 41 layers PEB LB films/ PEB LB films/Ag and (curve 2) ITO/ 41 layers PEB LB films/Ag structures

I - V characteristics obtained are asymmetric and non-linear in nature. The non-linear behaviour seen beyond 0.5V has earlier been observed for MIM devices when fatty acids (salts) are used. It has been associated with some form of tunneling through

the LB film where the insulating barrier has been lowered by the image force. This cannot however be considered as-simple tunneling because the thickness of the LB film is greater than the usual thickness of barrier.

Fig.22 and fig.23 show the variation of logI as a function of V^n for In/ 41 layers LB films/ LB films/Ag and ITO/ 41 layers LB films/Ag. It can be seen (fig. 22) that at lower voltage the logI vs $V^{1/4}$ plot shows a linear indicating simple tunneling at low voltage. Besides this, two different values of slope (fig.23) In/ 41 layers LB films/ LB films/Ag (curve 1) and ITO/41 layers LB films/Ag (curve 2) for structures have been observed at higher voltages. It reveals that the simple tunneling is perhaps not predominant at higher voltages. Value of n has been taken to be 3 indicating space charge limited phenomenon in the medium at voltage greater than 1.2V.
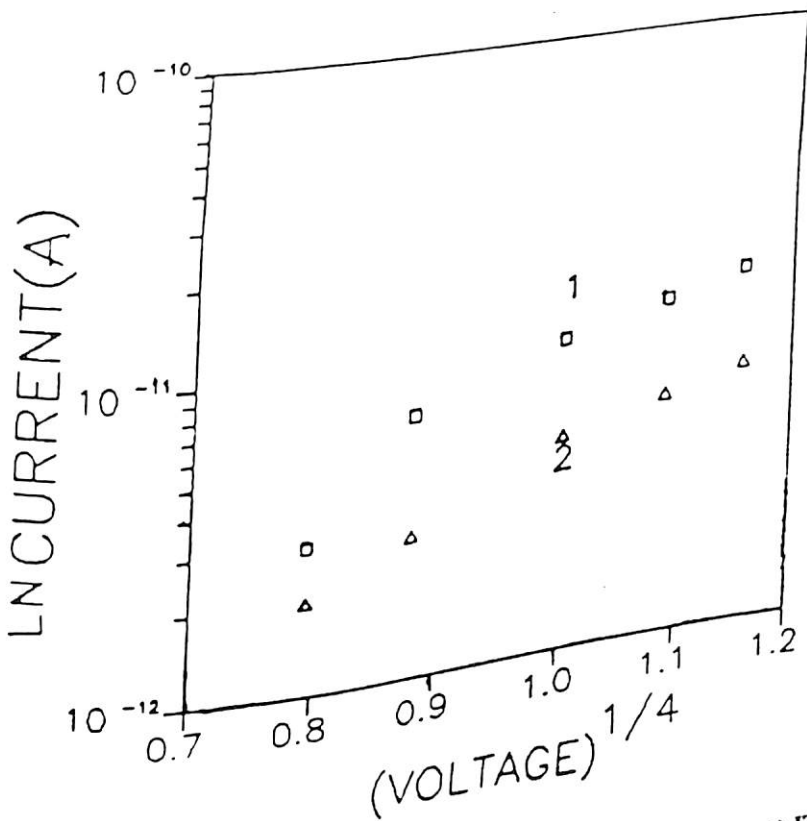

Fig.22 Variation of log current (I) vs (voltage)$^{1/4}$ characteristics for (curve 1) ITO/41 PEB LB films/Ag and (curve 2) In/ 41 layers PEB LB films/Ag structures
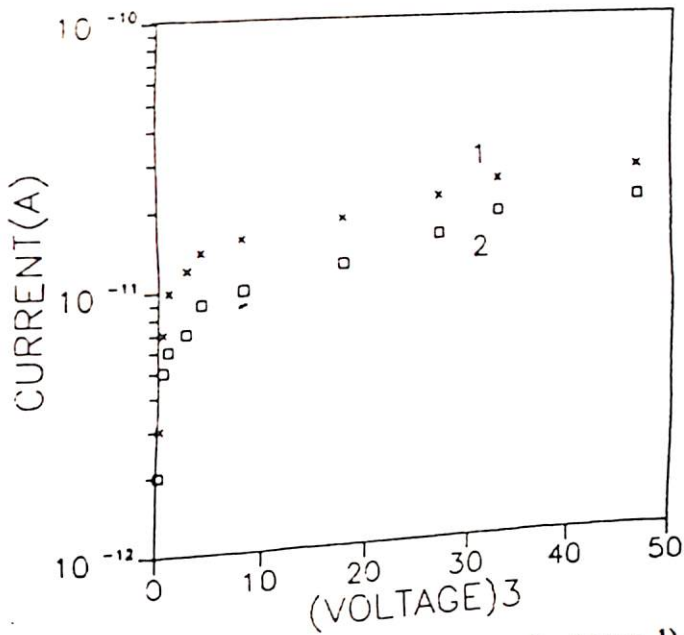
248

Fig.23 Variation of log current (I) vs (voltage)³ characteristics for (curve 1) ITO/41 layers PEB LB films/Ag and (curve 2) In/ 41 layers PEB LB films/Ag structures.

Fig. 24 shows the capacitance (C) - voltage (V) plot obtained for In /41 PEB LB layers/Ag and for Ag/PEB LB layers/Ag (curve 1), In/ LB PEB LB layers/Ag (curve 2) and ITO/PEB LB layers/Ag (curve 3) structures, respectively. It can be seen that in each of these value, the capacitance decreases upto 2 volts whereas it reaches to saturation. The exception lies in the case of ITO/PEB LB layer/Ag structures where capacitance decreases sharply from 0 to 1 volts and remains constant upto about 2 volts, whereafter it decreases and saturates. At this voltage there may be formation of space charges. Further, each device shows the saturation capacitance at 2V perhaps due the formation of depletion region.

Fig.25 shows the capacitance (C) vs frequency (Hz) plot obtained for Ag/41 layers PEB LB films/Ag (curve 1); In/ 41 layers PEB LB films/Ag (curve 2) and ITO/ 41 layers PEB LB films/Ag (curve 3) structures, respectively. The variation of capacitance with frequency is in agreement with the behaviour reported in literature. At low frequency (100< f <1 kHz), ITO/ PEB LB layers/Ag structure shows Max - Wagner polarization arising due to the contact effect. The ac conduction mechanism in M/LB/M
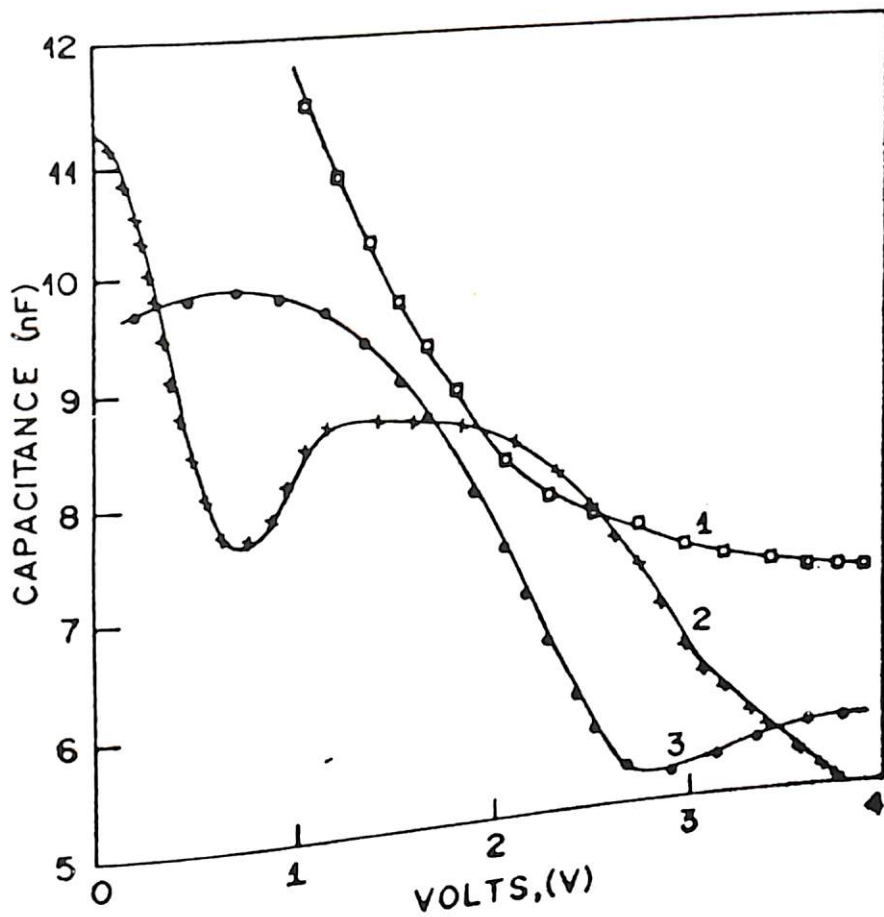
249

Fig. 24 Variation of Capacitance (nF) vs. Voltage (V) of Ag/41 layers of LB PEB films/ Ag (curve 1), In/41 layers PEB LB films/ LB films/ Ag (curve 2) and ITO/41 layers of LB PEB films/ Ag (curve 3) structures.

junction is assumed to be due to the hopping of charge carriers. Under the low bias condition conductance (G) is proportional to w^n, where value of n lies between 0 and 1. This dependence is also in agreement with a hopping model that describes the low bias ac conduction for redox active organic molecular compound as reported by N. J. Geddes et al [40]. The lower values of both the conductivity and capacitance than those expected from an extrapolation of the results of silver electrodes, once again suggest that silver deposited on the PEB LB film perhaps gets oxidized [36].
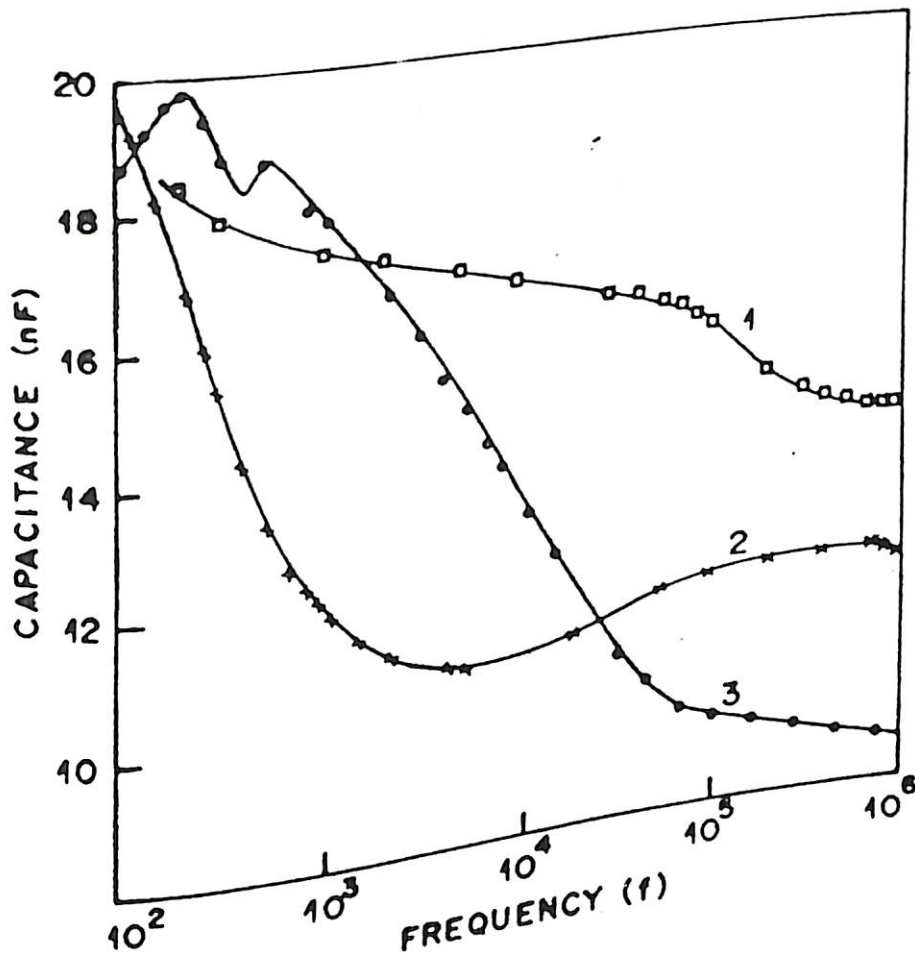

Fig. 25 Variation of capacitance (C) vs frequency (f) of Ag/41 layers LB PEB films / Ag (Curve 1), In/41 layers PEB LB films /LB films /Ag (curve 2) and ITO/41 layers of LB PEB films/ Ag (curve 3) structures.

Fig. 26 shows the observed variation of dielectric loss factor (tan δ) obtained for PEB LB layers at various frequencies for Ag/ 41 layers PEB LB film/Ag, In/ 41 layers PEB LB film/ Ag and ITO/ 41 layers PEB LB film/ Ag structures, respectively. The low dispersion seen in tan δ vs frequency indicates the absence of inhomogeneity and barrier effect. However, the dielectric loss factor does not show the usual trend. It is significant to see the ITO/ PEB LB layers/ Ag structures show the loss peaks at 500 kHz, which has also earlier been seen in the case of the polyaniline film. The motion of charge carriers (e.g polarons/bipolarons) results in the formation of dipoles in the PEB.
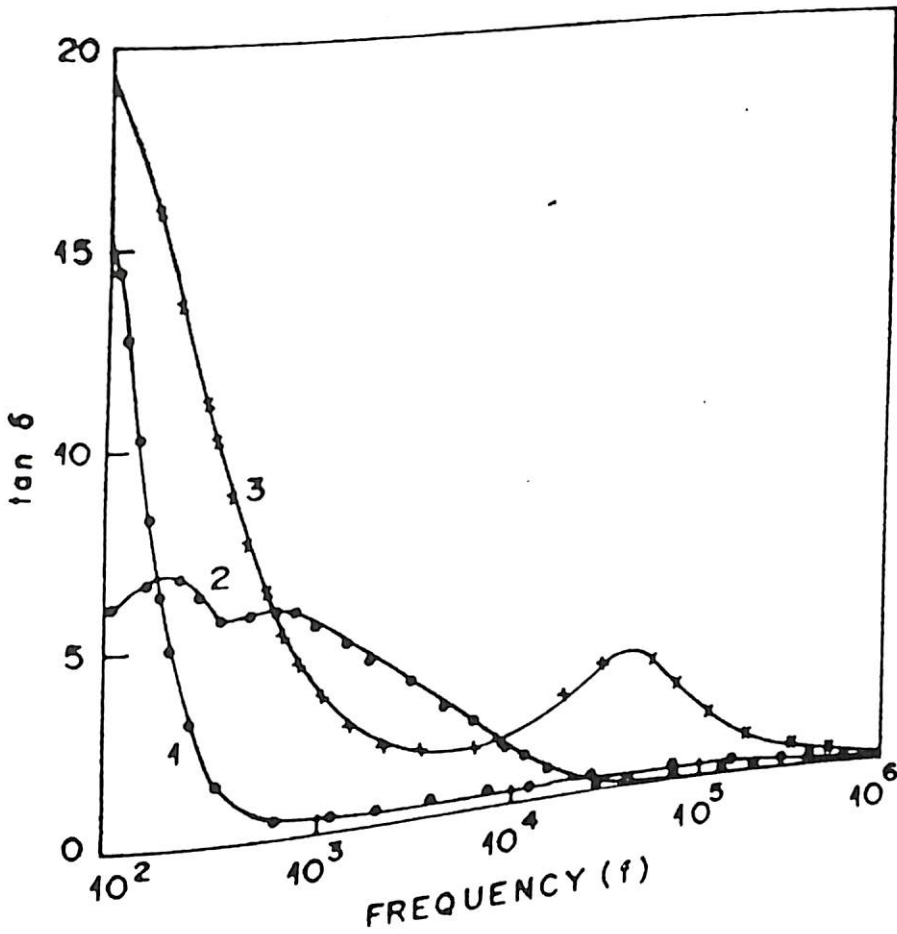
Fig.26 Variation of dielectric loss factor (tan δ) vs frequency (f) in (curve 1) Ag/41 layers PEB LB films/Ag; (curve 2) In/ 41 layers PEB LB films/Ag and (curve 3) ITO/ 41 layers PEB LB films/Ag structure

It can be tentatively concluded that In /PEB LB films /Ag structures show tunneling phenomenon whereas the ITO/PEB LB film/Ag and In/PEB LB film /Ag show the space charge limited current in the insulating medium. At higher voltage , I α V³ dependence for an MIM structure with metal oxide (ITO) and metal (In) indicate

251

rectification across a distance due to the PEB barrier. The Max Wagner polarization has been seen for MIM device with ITO metal. These results bring out that the ac conduction in ITO/PEB LB layers/Ag structures is due to the hopping of charge carriers (polarons /bipolarons) which result in the formation of dipoles in PEB.

6.3.2 METAL - INSULATOR (CdSt₂ LB LAYER) - SEMICONDUCTOR (PPY) DEVICES (MIS)

Metal - insulator - semiconductor (MIS) is a convenient device for the characterization of an insulating layer and a semiconductor - insulator interface [37]. Schottky devices based on electrochemically deposited PPY and desired metal (Ag,Sn, Al and In) have been shown to exhibit interesting electrical characteristics. The Langmuir - Blodgett (LB) technique is an excellent method for the deposition of ultra - thin uniform insulating layers comprising of fatty acids, the salts of fatty acids and polymeric materials with controllable thickness for fabrication of MIS devices [38]. Many investigations pertaining to metal - LB layers - semiconductor configuration based on silicon, amorphous silicon and compound semiconductors have been conducted. MIS devices based on PPY have been reported to have ideality factors ranging from 10.11 to 10.67 [39]. The passivation of PPY with an insulating layer has been predicted to result in improvement of the junction characteristics of such a device. The use of an LB film as a gate dielectric for the fabrication of MIS devices have been reported [40].

The systematic studies have been performed on Ag-cadmium stearate (CdSt₂) LB layer-PPY, Sn-CdSt₂ LB layer-PPY, Al-CdSt₂ LB layer-PPY and In-CdSt₂ LB layer-PPY devices, respectively.

The Langmuir - Blodgett film of cadmium stearate (CdSt₂) have been deposited

on PPY films as described in sec. 6.2.1 of this Chapter. MIS structures have been fabricated by thermally evaporating pure (99.99%) metals (Ag, Sn, Al and In) of about 0.5 μm thickness on CdSt$_2$ LB films/PPY structures using a vacuum evaporation (10^{-6} torr). Effective junction area in each case is about 10^{-3} cm^2. Gold contacts have been made after carefully removing various metal/CdSt$_2$ LB layer/PPY structure from respective ITO glasses.
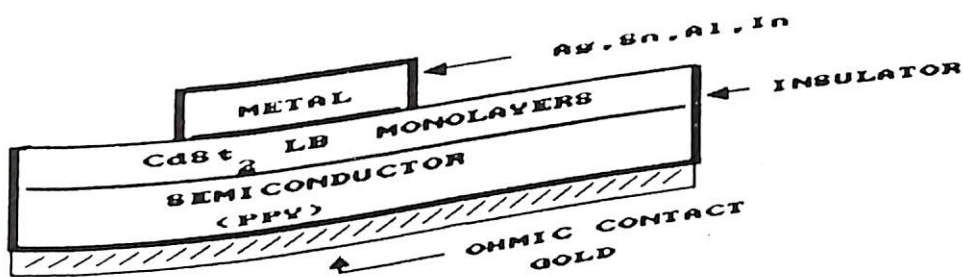
Fig. 27 Schematic diagram showing cross - section of such an MIS device

A schematic diagram showing cross - section of such an MIS device has been given in Fig. 27. Current (I) - voltage (V) measurements of various MIS devices have been conducted using Keithley electrometer (model 617 A). Capacitance (C) - voltage (V) measurements on In/CdSt$_2$ LB layer/PPY devices have been carried out using an Impedance Analyzer (HP 4192 A).

253

A distinct shift in the I-V curves seen in this figure points out to the improved junctions characteristics of In/LB layer/PPY devices.

The values of the junction parameters shown in Table 1 for various MIS devices have been calculated using the following Schottky equation [40]:

$$J = J_o \exp(qV/nkT) \qquad \text{Eq.2}$$

where Jo is the saturation current density that can be obtained from

$$J_o = A^*T^2 \exp(-q\,\chi_b/nkT) \qquad \text{Eq.3}$$

where A^* is the Richardson's constant $(1.2 \times 10^{-6} \text{ m}^2 \text{ T}^2)$, n is the ideality factor, χ_b is the barrier height and k_B is the Boltzmann constant. Values of rectification ratio obtained for each of the devices has been measured at 2V.

TABLE - I : Electronic Parameters of MIS Diode Based on Conducting Polypyrrole Films.

METAL	METHOD	BARRIER HEIGHT (χ_b) (eV)	IDEALITY FACTOR (n)	WORK FUNCTION (eV)
Ag	I-V	0.406±0.001	7.729	4.74
Sn	I-V	0.381±0.001	6.430	4.42
Al	I-V	0.398±0.001	6.570	4.28
In	I-V	0.393±0.001	6.630	4.12

The values of rectification ratio, barrier height and ideality factor determined as 2, 0.406 eV and 7.729, respectively for Ag / 10CdSt₂ LB monolayers / PPY devices point out to its non-ohmic behavior resulting due to application of a CdSt₂ LB monolayer.

A decrease in the value (6.63) of ideality factor determined for Sn/10CdSt₂ LB monolayers/PPY device over a value (8.85) for Sn/PPY device once again demonstrates the role played by the CdSt₂ LB monolayers. However, the observed lower value (5.0) of rectification ratio limits its application as a Schottky diode.

The values of rectification ratios both for Al/10CdSt₂ LB monolayers/PPY and

In/10CdSt$_2$ LB monolayers/PPY devices have been determined as 10 and 8, respectively. Moreover, the lower values of the ideality factors coupled with the higher values of barrier heights found for both these MIS devices clearly indicate that these devices can be used as excellent Schottky diodes. Short term stability of Al/10CdSt$_2$ LB monolayers/PPY device compared to that of In/10CdSt$_2$ LB monolayers/PPY has been attributed to the oxidation of aluminium in air.
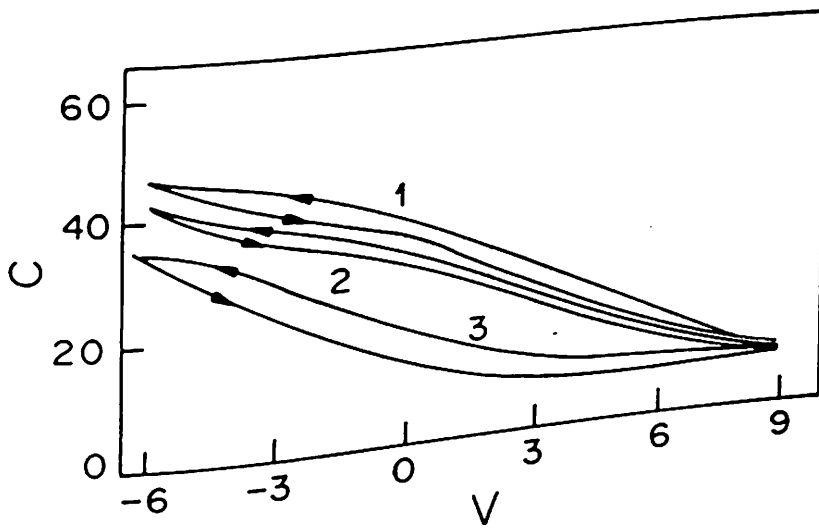

Fig.29 Variation of capacitance, C(pF) with voltage, V (volts) for In/CdSt$_2$ LB film (15 monolayers)/PPY structure obtained at 10 kHz (curve 1), 100 KHz (curve 2), 1 MHz (curve 3)

Fig. 29 shows the results of capacitance measurements carried out as a function of monolayer on various In/15CdSt$_2$ LB monolayers/PPY device obtained at 10 Hz, 100 kHz and 1 MHz, respectively. It can be seen that the interface comprising semi-conducting PPY and CdSt$_2$ LB layer undergoes a transition from accumulation to depletion as the voltage is swept (20 mV/s) from negative to positive values. Fig.30 shows the results of C-V measurements carried out on annealed (50°C) and unannealed devices comprising of indium/LB film (Cd stearate, 15 layers)/ semiconducting

256

polypyrrole structures. From these results, it can be tentatively concluded that the magnitude of hysteresis observed in the above samples shows a significant decrease as a consequence of annealing. The decrease in the magnitude of hysteresis can be understood to arise from the annealing of this device resulting in a reduced trap density at the semiconducting PPY/CdSt$_2$ LB film interface.
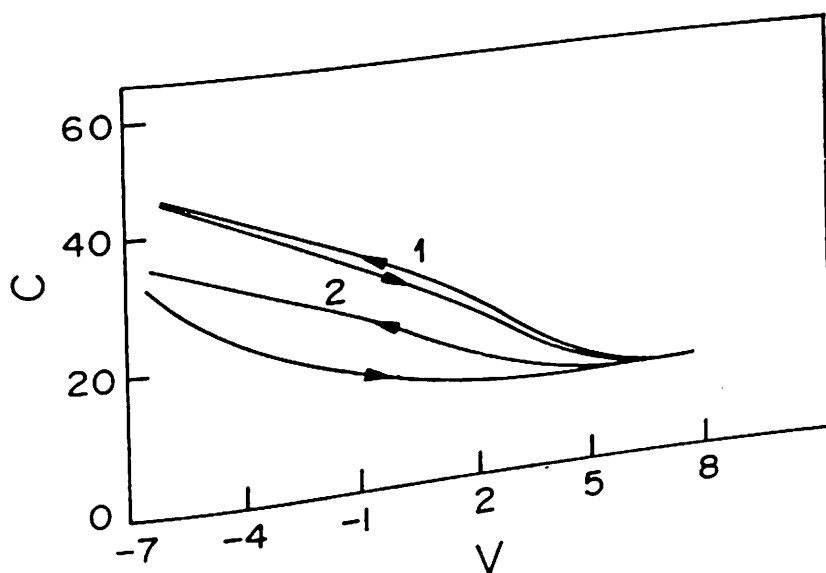

Fig.30 Variation of capacitance, C(pF) with voltage, V(volts) for In/CdSt$_2$ LB film (15 monolayers)/PPY structure obtained at 1 MHz for annealed (curve 1) and unannealed (curve 2) structure.

Fig. 31 is the 1 MHz C-V plot of such a device containing 9 and 15 CdSt$_2$ monolayers. These results demonstrate that the decrease in the number of CdSt$_2$ LB monolayers results in the higher value of the capacitance, which is likely to lead to the improved functioning of such MIS device. Fig. 32 shows the variation of capacitance of In/CdSt$_2$ LB monolayers/PPY device with increase in the number of CdSt$_2$ LB monolayers. The decrease in the value of capacitance with the increase in the number of CdSt$_2$ LB monolayers can be attributed to the variation in the dielectric characteristics of CdSt$_2$ that have been shown to be a function of its thickness. The inset in Fig.31 shows

257

variation of the reciprocal film capacitance with number of LB monolayers. From the results shown in inset of Fig. 31 and employing the relationship :

$$C = C_a \ Co \ A/W \qquad\qquad eq.4$$

where W is the thickness of the material, A is the area, Co is the space charge permitivity; the value of effective dielectric constant, C_a of CdSt$_2$ LB layer has been estimated to be 1.84. This is in reasonable agreement with the reported value (2.13).
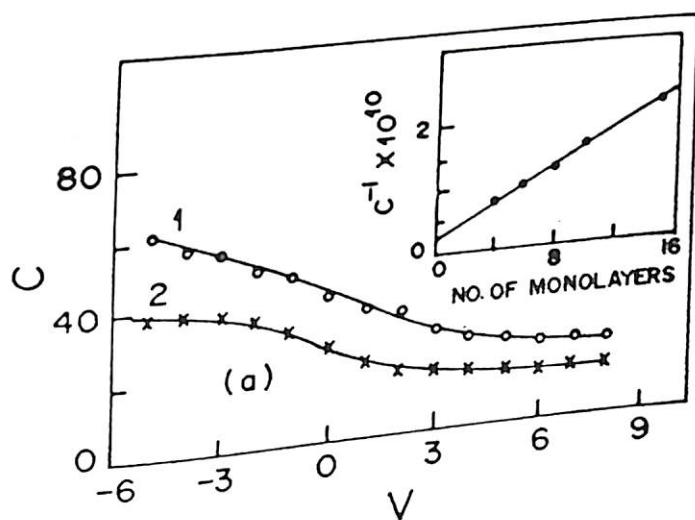

Fig. 31 Variation of C-V plot of 9 and 15 CdSt$_2$ monolayers (inset) shows variation of reciprocal film capacitance with number of LB monolayers.
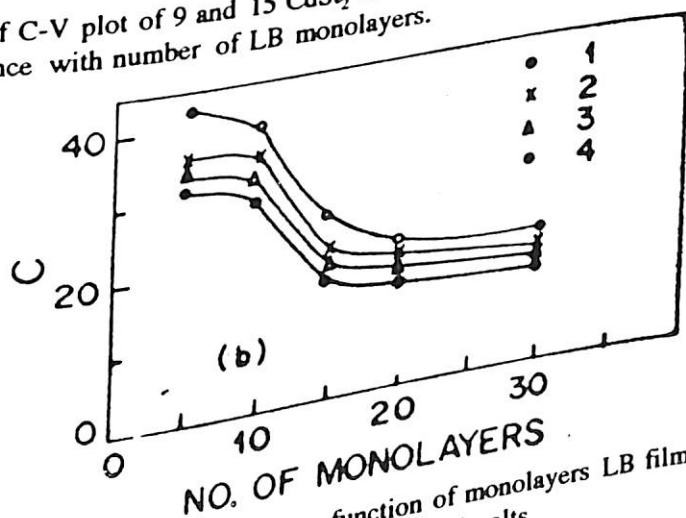

Fig.32 Variation of capacitance, C (pF) a function of monolayers LB film/PPY Structure obtained for dc bias (V). Curves 1 to 4 for respectively for 0,1,2and 4 volts.

258

6.4 CONCLUSIONS

It has been shown that Y-type cadmium stearate Langmuir - Blodgett films can be deposited on annealed polypyrrole surface. Further, Langmuir - Blodgett films of polyemeraldine base can be deposited on different substrates such as glass, quartz and ITO glass plates from NMP containing varying amount of $CHCl_3$. It has been revealed that monolayers of PEB are thermally stable over a wide range of temperature (9.2 to 40°C).

The results of characterization studies based on FTIR, UV - visible and SEM studies conducted on LB films of PEB obtained from a mixture of NMP containing 60% $CHCL_3$ indicate the ordered nature of such LB films. In order to further verify this result, the effect of annealing on various PEB LB films has been investigated. Results show that prolonged annealing (72 to 90 hours) of polyaniline LB films results in the collapse of emeraldine structure.

The effect of various different protonic acids such as HCl, H_2SO_4, HNO_3 and $HClO_4$ on various PEB LB films has been demonstrated. It has been shown that HCl doping of LB films does not result in the loss of any order. The band gap of polyaniline LB films doped with different protonic acid lies between 3.1 eV to 3.4 eV. These results are in agreement with those observed for the vacuum deposited, solution cast and electrochemically prepared polyaniline films. Besides this, when PEB LB films are treated with different acids, it is seen that morphologies of various PEB LB films undergo significant changes.

In the deposition of Langmuir - Blodgett film with the increase of number of monolayers, irregularity begins to be formed in the film and the ordered nature of LB films is lost. After deposition of certain number of layers, Y - type films are deposited

259

and it has been shown that the area is displaced with each stroke. The results of UV - visible absorption spectra obtained at 360 nm also show irregularities after many layers of deposition. This has been also confirmed by cyclic voltammogram of the 38 monolayers of PEB LB film, which shows poor electroactivity with the increase in number of monolayers.

The presence of Max Wagner polarization has been noticed in MIM structure with ITO metal. The ac conduction mechanism in MIM structure based on polyaniline LB film is due the to hopping of charge carriers based on (polarons and bipolarons) resulting in the formation of dipoles in PEB in ITO/PEB LB film/Ag structure. The simple tunneling in PEB has been found to occur at low voltages but the space charge limited region occurs at higher voltages.

Metal - insulator - semiconductor structures have been fabricated by thermal evaporation of various metals (Sn, Al, In and Ag) onto LB films of Cd stearate deposited onto electrochemically deposited semiconducting polypyrrole films. The results of I-V measurements carried out on such structures have been used for the estimation of various junction parameters such as barrier height, work function and ideality factors of various metal (Sn, Al, In and Ag)/ LB layer (Cd stearate)/ semiconducting polypyrrole devices. The capacitance - voltage measurements have been used to compute the value of the effective dielectric constant of insulating LB film (Cd stearate).

In view of the improved junction characteristics, it should be interesting to conduct studies in relation to the applications of such MIS devices in electroluminicent displays, photovoltaic and photonic devices.

6.5 REFERENCES

1. G. Gabrelli, G.G. Gurani and E. Ferroni, *J. Colloid. Interface. Sci.* **54** (1976) 424.

2. J. C. Earnshaw, *Thin Solid Films* **99** (1985) 189.

3. K. B. Blodgett and I. Langmuir, *Phys. Rev.* **51** (1937) 965.

4. K. Fukuda, H. Nakahara and T. Kato, *J. Colloid Interface Sci.* **54** (1976) 430.

5. V. K. Agarwal, *Phys. Today* **41** June (1988).

6. R.H. Tredgold, *Rep. Prog. Phys.* **50** (1987) 1609.

7. G.L. Gaines Jr., *The Insoluble Monolayers at Liquid Gas Interfaces*, Interscience, New York (1960).

8. T. Kato, *Jap. J. Appl. Phys.* **27** (1988) L2188.

9. S. Kuroda, K. Ikegami, K. Saito, Y. Tabe, M. Saito and M. Sugi, *Bulletin of the Electrochemical Lab.* **54** (1990) b 227.

10. G. G. Roberts, *Sensors & Actuators*, **4** (1983) 131.

11. P. Hodge, F. Davis and R.H. Tredgold, *Phil. Trans. R. London A*, **330** (1990) 153.

12. M. K. Ram, N. S. Sundaresan and B. D. Malhotra, *J. Phys. Chem. Letters*, **97** (1993)

13. K. Hong, R. B. Rubner and M.F. Rubner, *Chem. of Materials* **2** (1990) 82; Y.P. Song, J. Yarwood, J. Tsibouklis, W. J. Feast, J. Cresswell and M. C. Petty, *Langmuir*, **8** (1992) 263.

14. K. Kjaer, J. Als. Nielsen, C.A. Helm, L.A. Laxhauber, H. Mohwald, *Phys. Rev. Lett.* **58** (1987) 2224.

15. M. K. Ram, S. Annapoorni and B. D. Malhotra, *Appl. Phys. Lett.* (communicated).

16. N. E. Agbor, A. P. Monkman, M. C. Petty, M. Harris, *Extended Abstracts of International Conference on Science and Technology of Synth. Metals*, Goteborg, Sweden (1992) 442.

17. A. P. Monkman and P.Adams, *Synth. Metals* **40** (1991) 87.

18. M. K. Ram and B. D. Malhotra, *Langmuir* (communicated).

19.   Y. Cao, P. Smith, A. J. Heeger, *Synth. Metals* **32** (1989) 263.

20.   K. G. Neo, K. L. Tani, T. C. Tan, E. I. Kung, *J. Macromol. Sci. Chem.* **23** (1990) 347.

21.   M. Bartonek, N.S. Sariciftci and H. Kuzmany, *Synth. Metals* **36** (1990) 83.

22.   S. C. K. Misra, M.K. Ram, S. S. Pandey, B.D. Malhotra and S.Chandra, *Appl. Phys. Lett.* **74** (1992) 2109.

23.   N. S. Sariciftci, M. Bartonek, H. Kuzmany, H. Neugebauer and A. Neckel, *Synth. Metals.* **29** (1989) E193.

24.   I. A. Skotheim, X. G. Yang, J. Chen, T. Tnagaki, M. Denbuer, S. Tripathy, L. Samuelson, M. F. Rubner, K. Hong, I. Watanabe, Y. Okamoto, *Thin Solid Films* **178** (1993) 233.

25.   R. B. Rosner, J. H. Cheng, BM. F. Rubner, 4th Int. *SAMPE Elec. Conf.*, June 12-14 (1990) 346.

26.   C. Qui, L. H. Long, T. C. Tan and J. Y. Lee, *J. Electroanal. Chem.* **346** (1993) 477.

27.   A. F. Diaz, J. A. Logan, *J. Electroanal. Chem.* **111** (1980) 111.

28.   M. Fukui, C. Degrand, L. L. Miller, *J. Am. Chem. Soc.*, **104** (1982) 28.

29.   M. Kalaji, L. Nyholm, L.M. Peter, *J. Electroanal. Chem.*, **325** (1992) 269.

30.   A. S. Deva, C. D. Fung, E. P. Dipoto and E. E. Rickert, *Thin Solid Films* **132** (1985) 27. 31. M. T. Fowler, M. C. Petty, G. G. Roberts, P. J. Wright and B. Cockayne, *J. Mol. Elect.* **1** (1985) 93.

32.   ST. Los and ST. Kochowski, *Thin Solid Film* **165** (1988) 21.

33.   M. Schmelzer, M. Burghard, C. M. Fischer, S. Roth and W. Gopel, *Proceeding of ICMS' 94 Seoul* (to be published in Synth Metals).

34.   A. Desormeaux, J. J. Max and R. M. Lablanc, *J. Phys. Chem.*, **97** (1993) 6670.

35.   Molecular Electronics Devices, edited by F.L. Carter (Dekker New York, 1983), *Molecular Electronics Devices II*, Edited by (Dekker New York 1987).

36.   N. J. Geddes, J. R. Sambles, D. J. Jarvis and W. G. Parker and D. J. Sandman, *J. Appl. Phys.*, **71** (1992) 756.

37.   D. Vuillaume, P. Fontaine, J. Collet, D. Deresmes, M. Garet and F. Rondelez, *Microelectronic. Engg.*, **22** (1993) 101.

38.	M. T. Fowler, M. C. Petty, G. G. Roberts, P. J. Wright and B. Cockayne, *J. of Mol. Electronics* **1** (1985) 93.

39.	R. Gupta, S. C. Misra, B. D. Malhotra, N. N. Beladakere and S. Chandra, *Appl. Phys. Lett.* **58** (1991) 51.

40.	N. J. Geddes, W. G. Parher, J. R. Sambles and D. J. Jaruis, *Thin Solid Films*, **168** (1989) 151.

41.	M. C. Petty, J. Batley and G. G. Roberts, *IEE Proceedings* **132** pt. I no (3) (1985) 133.

APPENDIX

SUMMARY

SUMMARY

It has been shown that conducting polymer films of polypyrrole, polyaniline, poly(α-naphthalene oxide pyrrole) and poly(N-phenyl pyrrole) can be electrochemically obtained on indium-tin-oxide (ITO)/platinum. Further, it has been revealed that both solution cast and vacuum deposition technique can be used to obtain conducting polyaniline films.

It has been found that optical and electrical properties of conducting polymer films based on polypyrrole, polyaniline, poly(α-naphthalene oxide pyrrole) and poly(N-phenyl pyrrole) can be investigated using UV-Visible, FTIR, ellipsometry, dielectric relaxation, conductivity and cyclic voltammetry techniques, respectively. Besides this, SEM, DSC techniques have been used to investigate the various physical characteristics of some of these conducting polymers.

Application of polypyrrole, polyaniline and poly(α-naphthalene-oxide pyrrole) as Schottky devices have been systematically studied. Junction parameters of all such devices have been experimentally determined. Besides this, operational characteristics of electrochromic displays based on polypyrrole and polyaniline have been investigated in detail.

Langmuir Blodgett film technique has been used to obtain mono/multilayers of polyemeraldine base. It has been shown that irregularities and inhomogenieties begin to

form after deposition of about 38 monolayers of PEB on ITO/ quartz substrate. These results have indicated a transition from Y-type to X-type mode of deposition in polyemeraldine base LB films. Besides this, it has been shown that metal-insulator-semiconductor (MIS) devices can be fabricated by deposition of cadmium stearate LB films onto electrochemically deposited polypyrrole films deposited on ITO glass. A distinct improvement in the ideality factor and barrier height has been found to occur in each of these devices.

LIST OF PUBLICATIONS:

1. **M.K. Ram**, N.S. Sundaresan and B.D. Malhotra, Langmuir-Blodgett films of processable polyaniline, *J. Phy. Chem.*, 1993, **97**, 1158.

2. S.C.K. Misra, **M.K. Ram**, S.S. Pandeyy, B.D. Malhotra and Subhas Chandra, Vacuum deposited metal/polyaniline Schottky devices, *Appl. Phys. Lett.*, 1992, **61**, 1219.

3. N.N. Beladakere, S.C.K. Misra, **M.K. Ram**, R. Gupta, D.K. Rout, B.D. Malhotra and Subhas Chandra, The space charge polarization in thin polypyrrole films, *J. Phy. Cond. Mat.*, 1992, **4**, 5747.

4. S.C.K. Misra, N.N. Beladakere, S.S. Pandey, **M.K. Ram**, T.P. Sharma, B.D. Malhotra and Subhas Chandra, Optical and Electrical characteristics of the electrodeposited polypyrrole films, *J. Appl. Poly. Sci.*, 1993, **50**, 411.

5. **M.K. Ram**, R. Mehrotra, S.S. Pandey and B.D. Malhotra, A.C. Conductivity of polyemeraldine base, *J. Phys. Cond. Mat.*, 1994, **6**, 8913.

6. **M.K. Ram**, N.S. Sundaresan and B.D. Malhotra, Performance of electrochromic cells of polyaniline in polymeric electrolytes, *J. Mater. Sci. Lett.*, 1994, **13**, 1490.

7. **M.K. Ram**, S. Annapoorni, S.S. Pandey and B.D. Malhotra, Dielectric relaxation in thin polyaniline films, *Phys. Lett. A.*, 1994, (in press).

8. **M.K. Ram**, S. Annapoorni and B.D. Malhotra, Electrical properties of metal/ 1B layer/ semiconductive polymer device, *Appl. Phys. Lett.*, 1994, (communicated).

9. N.N. Beladakere, S.S. Pandey, **M.K. Ram**, S.C.K. Misra, B.D. Malhotra and Subhas Chandra, Field effect in the metal/ semiconducting polyaniline junction, *Synth. Met.*, 1994, (communicated).

10. N.N. Beladakere, **M.K. Ram**, S. Annapoorni, S.S. Pandey and B.D. Malhotra, Optical and electrical properties of electro-deposited copolymer films having pyrrole and α-naphthalene oxide, *J. Appl. Phys.*, 1994, (communicated).

11. **M.K. Ram** and B.D. Malhotra, Preparation and characterization of Langmuir-Blodgett films of polyemeraldine base, *Langmuir*, 1994, (communicated).

12. Kumaran Ramanathan, **M.K. Ram**, M.M. Verghese and B.D. Malhotra, Dielectric relaxation studies of polypyrrole glucose oxidase films, *Thin solid films*, 1994, (communicated).

13. **M.K. Ram**, S.K. Dhawan and B.D. Malhotra, Novel tunable charge transfer chromism in polyaniline film, *J. Am. Chem. Soc.*, 1994, (communicated).

PAPERS PRESENTED IN CONFERENCES:

1.   **M.K. Ram**, S. Annapoorni and B.D. Malhotra, Electrical properties of metal-insulator- semiconducting structure based on conducting polypyrrole and Langmuir-Blodgett films of stearic acid, *Indo-US workshop on perspectives in new materials*, Dec. 17, 1991 (New Delhi, India).

2.   **M.K.Ram**, S. Annapoorni, N.S. Sundaresan, Sanjay Kumar and B.D. Malhotra, Poly-1-(phenyl-pyrrole) -pyrrole, A new conducting polymer, *Indo-US workshop on perspective in New Materials*, Dec. 17, 1991 (New Delhi, India).

3.   N.N. Beladakere, **M.K.Ram**, S. Annapoorni, S.S. Pandey, B.D. Malhotra, F.L. Pratt and W. Hayes, Optical and electrical properties of electrodeposited copolymer films having pyrrole and α-Naphthol units, *Indo-US workshop on perspective in New materials*, Dec. 17, 1991 (New Delhi, India).

4.   S.C.K. Misra, S.S. Pandey, **M.K. Ram**, B.D. Malhotra and S. Chandra, Polyaniline a new material, *Molecular electronics conference*, 1992 (Meerut, India).

5.   **M.K. Ram** and B.D. Malhotra, Electrical properties of metal sandwiched Langmuir-Blodgett layers of emeraldine base, *International conference on molecular electronics and biocomputing*, 1994 (Goa, India).

6.   R. Mehrotra, **M.K. Ram** and B.D. Malhotra, Optical properties of electrodeposited polyaniline films, *International conference on molecular electronics and biocomputing*, 1994 (Goa, India).

7.   Kumaran Ramanathan, **M.K. Ram**, B.D. Malhotra and A.Surya N. Murthy, Application of Langmuir-Blodgett films of polyaniline as glucose biosensor, *International conference on molecular electronics and biocomputing*, 1994 (Goa, India).

8.   S.S. Pandey, **M.K. Ram** and B.D. Malhotra, Schottky devices based on polyanilines, *International conference on molecular electronics and biocomputing*. 1994 (Goa, India).